PHOSPHORYLATION OF MYB75 TRANSCRIPTION FACTOR BY MAP KINASES IN *ARABIDOPSIS THALIANA*

by

ANNA EVGENYA KREYNES

B.Sc., The University of Toronto, 2006.

M.Sc., The University of British Columbia, 2008.

A THESIS SUBMITTED IN PARTIAL FULFILMENT OF THE REQUIREMENTS FOR THE DEGREE OF

DOCTOR OF PHILOSOPHY

in

The Faculty of Graduate and Postdoctoral Studies

(Botany)

THE UNIVERSITY OF BRITISH COLUMBIA

(Vancouver)

July 2018

The following individuals certify that they have read and recommend to the Faculty of Graduate and Postdoctoral Studies for acceptance, the dissertation entitled: "Phosphorylation of MYB75 transcription factor by MAP kinases in *Arabidopsis thaliana."*

Submitted by **Anna E. Kreynes**, in partial fulfilment of the requirements for the degree of

Doctor of Philosophy, in **Botany.**

Examining committee:

Dr. Brian Ellis, Land and Food Sciences, University of British Columbia
Supervisor

Dr. Juergen Ehlting, Biology, University of Victoria
Supervisory committee member

Dr. Christine Scaman, Land and Food Sciences, University of British Columbia
University Examiner

Dr. David Kitts, Land and Food Sciences, University of British Columbia
University Examiner

Additional supervisory committee members:

Dr. Leonard Foster, Proteomics, University of British Columbia
Supervisor

Dr. Shawn Mansfield, Forestry, University of British Columbia
Supervisory committee member

ABSTRACT

The *Arabidopsis* transcription factor MYB75 has been described in the literature as a positive transcriptional regulator of anthocyanin biosynthetic genes. More recently, MYB75 was shown to also negatively regulate lignin and other secondary cell wall biosynthetic genes. MYB75 has two canonical MAP kinase phosphorylation sites, at threonines 126 and 131; we wanted to explore the possibility that MYB75 is regulated post translationally through phosphorylation by MPKs.

In our lab, Dr. Yonge found that MYB75 could be phosphorylated *in vitro* by MPK3, MPK4, MPK6 and MPK11, almost exclusively at threonine 131. Subsequently, I demonstrated that MYB75 interacts *in vitro* with a large number of *Arabidopsis* MAP kinases, suggesting that it could be a target for multiple MPKs. We decided to explore how phosphorylation affects MYB75 function, in terms of protein-protein interaction, protein turnover and localization, and describe the impact of this putative phosphorylation event on the ability of MYB75 to drive transcription of target genes. For this purpose we used point mutants, $MYB75^{T131A}$ and $MYB75^{T131E}$ to mimic permanently non-phosphorylated and phosphorylated versions of MYB75, respectively.

While protein localization and protein-protein interactions of MYB75 were not strongly impacted in the point mutants, several *in vivo* experiments indicated that $MYB75^{T131E}$ is more labile than either $MYB75^{WT}$ or $MYB75^{T131A}$, suggesting that phosphorylation at T-131 negatively affects protein stability.

Over-expressor lines, *35Spr:3xHA:MYB75 gene*, as well as inducible *DEXpr:3xHA:MYB75 gene* lines were used, to analyze MYB75 protein dynamics *in vivo* and to assess the ability of each phosphovariant to drive anthocyanin production. *Arabidopsis* plants over-expressing $MYB75^{WT}$, $MYB75^{T131A}$ or $MYB75^{T131E}$ displayed increased anthocyanin production, compared to Col-0 WT, suggesting that phosphorylation status at T-131 does not affect this aspect of MYB75 function. However, HPLC analysis revealed quantitative differences between the biochemical species of anthocyanins and flavonols that accumulate in different phosphovariant over-expressing plants.

Transcriptome analysis revealed that $MYB75^{T131E}$ is a more potent regulator of gene expression. This finding, along with distinct developmental differences between MYB75 phosphovariants, suggest that phosphorylation at T-131 could affect the ability of MYB75 to drive the expression of a broader spectrum of genes than previously described in the literature.

LAY SUMMARY

My research project is part of a larger body of work, aimed at understanding how plants sense their environment, respond to stress and ultimately adapt to unfavourable conditions. My project is focused in particular on a gene that controls production of anthocyanins and flavonoids, which are antioxidant compounds that help plants cope with different stresses and are of interest to humans as medicinal and nutritional supplements. My findings suggest that certain environmental signals can alter the types of flavonoids and anthocyanins that the plants produce, through regulation of my gene of interest (MYB75). Additionally, I found that this gene has additional roles in development, which should be explored further. My findings can help us understand how plants change their biochemical composition in response to specific environmental stimuli. This knowledge can be used for growing medicinal plants as well as antioxidant rich crops, where the desired biochemical output is achieved through manipulation of environmental factors rather than genetic engineering.

PREFACE

This dissertation is based on original experimental work performed primarily in the laboratory of Dr. Brian Ellis, in the Michael Smith Laboratories. The text in this dissertation is original work, not taken from previous publications or collaborative written products.

Experiments described in Ch2 which were performed by other lab members, include *in vitro* phosphorylation assay, described in section 2.3. These experiments were initially designed and performed by a post-doctoral fellow, Dr. Zhenhua Yonge, and were repeated by another post doctoral fellow, Dr. Xiao Min Liu. Dr. Liu also performed the intracellular localization experiments described in section 2.4.1 of Ch2.

Dr. Zhenhua Yonge performed site-directed mutagenesis on *MYB75* cDNA, to generate the phosphovariants MYB75^{T126A}, MYB75^{T131A}, MYB75$^{T126/131A}$, MYB75^{T126E}, MYB75^{T131E}, MYB75$^{T126/131E}$. Dr. Yonge then cloned these cDNA versions of MYB75 into a binary vector behind an endogenous MYB75 promoter to generate *MYB75pr:MYB75 cDNA* constructs which she transformed into *Arabidopsis* plants, that I subsequently analysed for anthocyanin production in Ch 3. I performed the yeast two-hybrid experiments described in Ch2 (sections 2.2 and 2.4.2) and was responsible for cloning all the constructs required for these experiments, with the exception of MPK3-DBD, MPK4-DBD, and MPK6-DBD, which were cloned by Dr. Liu.

I conducted site-directed mutagenesis on the full gene version of MYB75, to create MYB75^{T131A} and MYB75^{T131E}, which I subsequently cloned into binary vectors generating *35Spr:3xHA:MYB75 gene* and *DEXpr:3xHA:MYB75 gene* constructs. I transformed these constructs into *Arabidopsis* plants, to obtain transgenic lines. I performed all experiments

pertaining to MYB75 turnover *in vivo*, anthocyanin quantification and analysis of developmental phenotypes.

I processed tissue samples from *35Spr:3xHA:MYB75 Arabidopsis* plants which I submitted for HPLC analysis, conducted by Dr. Lina Midilao. Anthocyanin and flavonol profiles obtained from HPLC analysis were processed and quantified by Dr. Simone Castellarin. I also processed tissue samples from *35Spr:3xHA:MYB75 Arabidopsis* plants to submit to the Brain Research Centre at UBC, for transcriptome analysis by next generation sequencing. The raw data was processed by Dr. Darren Wong, from the Castellarin lab. I subsequently conducted detailed analysis and classification of the genes up- and down-regulated in each phosphovariant over-expressor line.

TABLE OF CONTENTS

LIST OF TABLES

LIST OF FIGURES

LIST OF SUPPLEMENTARY MATERIALS

LIST OF ABBREVIATIONS

ABA	abscisic acid
ABCB/PGP (1,19)	ATP-binding cassette B protein, auxin transport channel / P-glycoprotein
ACS (4,5, 11)	1-aminocyclopropane-1-carboxylate synthase 4
AD	activation domain
Ade	adenine
Ala	alanine
ANS/LDOX	anthocyanidin synthase/leucoanthocyanidin dioxygenase
ARF	auxin response factor
ARR (5,15)	*Arabidopsis* response regulator 15
AS1	asymmetric leaves 1
ATBLU10	*Arabidopsis thaliana* anthocyanin 3-O-6-O-coumaroylglucoside: glucosyltransferase
ATEXP	*Arabidopsis thaliana* expansin
ATHB8	*Arabidopsis thaliana* homeobox gene 8
ATMAT	*Arabidopsis thaliana* anthocyanin 5-glucoside malonyltransferase
ATP	adenosine triphosphate
ATSBT1	*Arabidopsis thaliana* subtilisin-like serine protease
AT3AT (1,2)	*Arabidopsis thaliana* anthocyanidin 3-O-glucoside coumaroyl CoA transferase
AUX/IAA	auxin/indole acetic acid repressors
BEE3	brassinosteroid enhanced expression 3
bHLH	basic helix-loop-helix
BIFC	bimolecular fluorescence complementation
BSA	bovine serum albumin

CAMKK	constitutively active mitogen activated kinase kinase
CA-MPK	constitutively active mitogen activated protein kinase
CAMV35S	cauliflower mosaic virus 35S promoter
CCR	cinnamoyl-CoA reductase
cDNA	complementary DNA
CDS	coding sequence
CFP	cyan or cerulean fluorescent protein
CHI	chalcone Isomerase
CHIP	chromatin immunoprecipitation
CHS	chalcone synthase
CHX	cycloheximide
CO-IP	co-immunoprecipitation
Col-0	Columbia *Arabidopsis* ecotype
COMT	caffeic acid O-methyl transferase
COP1	constitutive photomorphogenic 1
COV1	continuous vascular ring 1
CRF2 or TMO3	cytokinin response factor2 or target of Monopteros3
CRY (1,2,3)	cryptochrome photoreceptors
CSLA1	cellulose synthase-like A1
CSLG3	cellulose synthase-like G3
CYP	cytochrome P-450
C4H	cinnamate 4-hydroxylase
DAPI	4’6-diamino-2-phenylindole
DBD	DNA binding domain

DEX	dexamethasone
DFR	dihydroflavonol reductase
DIN (2,11)	dark inducible
DNA	deoxyribonucleic acid
DPBA	diphenylboric acid 2-aminoethyl ester
ECL	enhanced chemiluminescence
EGL3	enhancer of glabra 3
ELF4	early flowering 4
EMS	ethyl methylsulfonate
FRET	fluorescent resonance energy transfer
ERF	ethylene response factor
ESI	electrospray ionization
FKF	flavin-binding kelch repeat F-box photoreceptor
FLA (1,13)	fasciclin-like arabinogalactan
FLAG tag	epitope tag with the amino acid sequence DYKDDDDK
FLC	flowering locus C
FLS	flavonol synthase
FLS2	flagellin-sensitive 2
F3’H/TT7	flavonol 3’-hydroxylase
F3H/TT6	flavonone 3’-hydroxylase
GA	gibberellic acid
GAL4	yeast transcription factor driving galactose-induced gene expression
GASA	gibberellic acid-stimulated protein
GA3OX1	gibberellin 3-oxidase 1

GFP	green fluorescent protein
Glc	glucose
Glu	glutamic acid
GL3	glabra 3
GO	gene ontology
GMO	genetically modified organism
GST	glutathione S-transferase
GUS	β-glucoronidase
HA-tag	hemagglutinin-tag
HCA2	high cambial activity 2
HCl	hydrochloric acid
His	histidine
HPLC	high performance liquid chromatography
HRP	horseradish peroxidase
HsfA2	heat stress factor A2
HY5	elongated hypocotyl 5
IAA	indole-3-acetic acid
IAN	Indole-3-acetonitrile
IPTG	isopropyl 1-thio-ß-galactopyranoside
JAZ	jasmonate ZIM-domain proteins
kDa	kilodaltons
KNAT7	knotted *Arabidopsis thaliana* protein 7
LAC (2 and 7)	laccase 7
LB	Luria broth

LBD38	lateral organ boundary domain 38
LC	liquid chromatography
Ler	Landsberg *Arabidopsis* ecotype
Leu	leucine
LKP2	Lov kelch repeat protein 2 photoreceptor
MADS	MCM1 agamous, deficiens srf
MAF5	MADS affecting flowering
MAPK/MPK	mitogen activated protein kinase
MAPKK/MAP2K	mitogen activated protein kinase kinase
MAPKKK/MAP3K	mitogen activated protein kinase kinase kinase
MES	2-(N-Morpholino) ethanesulfonic acid
MG-ProtoIX	magnesium-protoporphyrin IX
MP	monopteros
½ MS	½ Murashige and Skoog basal media
MS	mass spectrometry
MYB	myeloblastoma
NCBI	national centre for biotechnology information
NDPK2	nucleotide diphosphate kinase 2
NES	nuclear export signal
NGS	next generation sequencing
NLS	nuclear localization signal
NPA	N-1-naphthylphthalamic acid
NPC	nuclear pore complex
OMT1	flavonol-3-O-methyltransferase

ORF	open reading frame
OSR1 or NAC3	organ size related 1
OX	over-expressor
PA	proanthocyanidin
PAP1-D	production of anthocyanin pigment-1 dominant
PAL	phenylalanine ammonia-lyase
PCR	polymerase chain reaction
PHY (A-E)	phytochrome photoreceptors
PIF	phytochrome interacting factors
PIN	pin formed, auxin transport channel
PVDF	polyvinylidene fluoride
qPCR	quantitative reverse transcription polymerase chain reaction
RAM	root apical meristem
RBCS1A/RUBISCO	ribulose-1,5-bisphosphate carboxylase/oxygenase
RNA	ribonucleic acid
ROS	reactive oxygen species
RP-HPLC	reverse phase high performance liquid chromatography
RT-PCR	reverse transcription polymerase chain reaction
SAM	shoot apical meristem
SAQR	senescence-associated and qua-quine starch-related
SAT	sinapoyl-glucose: anthocyanin acyltransferase
SD	standard deviation
SD (-trp-leu-ade-his)	synthetic defined media without one or more amino acid or base; tryptophan, leucine, adenine and histidine.

SDS-PAGE	sodium dodecyl sulphate polyacrylamide gel electrophoresis
SE	standard error
Ser	serine
SPA (1,3 and 4)	suppressor of PHYA-105
SPL9	squamosa promoter binding protein-like 9
TAIR	the *Arabidopsis* information resource
TCP3	teosinte branched 1, cycloidea and pcf transcription factor 3
Thr	threonine
TT (2,3,4,5,6 and 8)	transparent testa
TTG (1 and 2)	transparent testa glabra
T (0,1,2 etc…)	generation of plants after genetic transformation, where T0 is the parent plant that was transformed by floral dip, and T1 plants are the progeny of the transformed parent
UDP	uridine diphosphate
UFGT	UDP flavonoid-glucosyltransferase
UGT71B5	quercetin 3-O-glucosyltransferase
UGT73C6	flavonol-7-O-glucosyltransferase
UGT75C1	anthocyanidin 5-O-glucosyltransferase
UGT78D1	flavonol-3-O-rhamnosyltransferase
UGT78D2	flavonoid-3-O-glycosyltransferase
UGT78D3	flavonol-3-O-arabinosyltransferase
UGT84A2	sinapic acid:UDP-glucose glucosyltransferase
UGT89C1	flavonol-7-O-rhamnosyltransferase
UV	ultraviolet
UVR-8	ultraviolet receptor 8

WDR	tryptophan (W) aspartic acid (D) repeat
WT	wild type
XCP2	xylem cysteine peptidase
Y2H	yeast two-hybrid
ZTL	zeitlupe photoreceptor
3AT	3-amino 1,2,4-triazole
4CL	4-coumarate-CoA ligase
4-OH-ICN	4-hydroxyindole-3-carbonyl nitrile
6xHis-tag	polyhistidine tag, containing 6 consecutive histidine residues

ACKNOWLEDGEMENTS

First, I would like to thank my supervisor, Dr. Brian Ellis, for his extraordinary patience, compassion and support through all the challenges I faced in my academic career, during my PhD. I want to thank my co-supervisors, Dr. Carl Douglas and Dr. Leonard Foster as well as my committee members, Dr. Shawn Mansfield, and Dr. Juergen Ehlting, for their guidance and scientific advice.

I want to thank the Canadian Army Reserves, particularly Vancouver's Infantry regiment, the Seaforth Highlanders of Canada, not only for financial support, but for being my family all these years, and a brotherhood that I could lean on in difficult times. I also want to thank Vancover's 6 intelligence company and the 39 Brigade, for providing me with employment opportunities during the last few years.

I want to thank my mom Tatyana, and my brother Arseny for their continued encouragement and for pushing me to succeed, as well as my partner Sean, for being there for me through all my challenges. I also want to thank my good friend and mentor, Dr. Wenzislava Ckurshumova for shaping my early scientific career and encouraging me to carry on in science.

I also want to thank everyone in the Ellis, Douglas and Samuels labs, for sharing this challenging experience and assisting me in accessing different tools that enriched my research. Finally, I want to thank UBC graduate studies, and particularly the Department of Botany and the Michael Smith Laboratories.

CHAPTER1 General Introduction

1.1 Phenylpropanoid metabolism

Plant secondary metabolism is a vast network of biochemical pathways producing thousands of different classes of phytochemicals. Although, by definition, secondary metabolites are not essential for survival under optimal conditions, these compounds are vital for the plants' ability to cope with biotic and abiotic stress, and thus play a pivotal role in plant ecology, species distribution and adaptation to unique niches. Phenylpropanoids comprise one of the largest groups of secondary compounds with over 8000 different phytochemicals known to date (Tohge *et al*.,2013). Phenylpropanoid compounds are largely restricted to land plants, with the exception of a few phenolics and early phenylpropanoid biosynthetic enzymes found in algae and prokaryotes, believed to be the evolutionary precursors of the complex phenylpropanoid metabolism found in vascular plant (Tohge *et al*.,2013). The diversification of phenylpropanoid compounds is believed to be a key evolutionary adaptation in land plants. The production of soluble phenolics such as coumarins and flavonoids, improved plant resistance to increased UV light exposure in terrestrial environments and the evolution of lignin in vascular plants, imparted physical strength, allowing organisms to reach colossal sizes, and develop a vascular system for long-distance transport of water and nutrients.

Despite its small genome and relative simplicity *Arabidopsis thaliana* is emerging as a model for the study of secondary metabolism, as research in recent years revealed this small plant to have many of the same classes of compounds as other plant taxa (D'Auria and Gershenzon, 2005; Kliebenstein, 2004.). While plant-environment interaction has been an

established role for many secondary compounds, increasing evidence in recent years has demonstrated that some of these phytochemicals have an impact on primary plant functions.

Phenylpropanoid metabolism branches off the primary shikimate pathway, which leads to the synthesis of aromatic amino acids in plants, bacteria and fungi. The first step of phenylpropanoid metabolism is the conversion of the amino acid phenylalanine to cinnamic acid, catalyzed by a highly conserved enzyme, phenylalanine ammonia lyase (PAL1-4 in *Arabidopsis*). This step is followed by hydroxylation, catalyzed by coumarate 4-hydroxylase (C4H), and formation of CoA thioester 4-coumaroyl-CoA, mediated by 4-coumarate-CoA ligase (4CL). 4-coumaroyl-CoA is a key branching point in phenylpropanoid biosynthesis, as it can be converted to *p*-coumaroyl-shikimate, the entry point to biosynthesis of lignin and sinapate esters. Alternatively 4-coumaroyl-CoA can be combined with three malonyl-CoA units to produce naringenin chalcone, in a condensation reaction mediated by chalcone synthase (CHS), which marks the entry point into flavonoid biosynthetic branch of phenylpropanoid metabolism (reviewed in Fraser and Chapple, 2011; Vogt, 2010). Naringenin chalcone is then converted to naringenin by chalcone isomerase and to dihydroflavonol by flavonol 3-hydroxylase (F3H). Dihydroflavonol represents another key branching point in flavonoid metabolism, as it can be converted to flavonols by flavonol synthase (FLS) or to anthocyanins by dihydroflavonol reductase (DFR) (Fig 1.1).

Flavonoids are a diverse group of soluble end products of phenylpropanoid metabolism, which comprise several major subgroups including aurones, flavones, chalcones, flavandiols, isoflavones, flavonols, anthocyanins and proanthocyanidins. With over 6000 flavonoid

compounds identified in different plant species, these phytochemicals display immense functional diversity. In the roots of legumes, flavonoids (mainly flavonols and flavones) are essential for nodulation (Abdel-Lateif *et al.,* 2012; Wasson *et al*., 2006; Zhang *et al.,* 2009). They also play an important role in protection against pathogen attacks, as many of these compounds are toxic to insect herbivores (reviewed in Simmonds, 2003). Flavonoids (particularly anthocyanins) are responsible for bright flower colour in many species, which attract pollinators (Grotewold, 2006; Winkel-Shirley, 2001). In vegetative tissues anthocyanins act as sunscreens, shielding the photosynthetic machinery and other cell components from harmful UV radiation and excess light. Anthocyanins and other flavonoids are well known for their antioxidant properties, as these compounds can chelate free radical-generating metal ions, and reduce harmful reactive oxygen species (ROS) (Deng *et al.,* 1997). Apart from protecting plants from oxidative stress, antioxidant properties of flavonoids have made them a central topic in plant medicine, with anti-allergic, anti-inflammatory and anti-microbial properties in mammalian systems, and showing promising results in treatment of neurodegenerative disease and cancer (reviewed in Kumar and Pandey, 2013; Sandhar *et al*., 2011). The widespread roles in plant and human health, has made flavonoid biosynthesis a hot topic in plant biology. Having only three classes of flavonoids, (flavonols, anthocyanins and proanthocyanidins) *Arabidopsis* is a simple model for understanding flavonoid chemistry and biosynthesis, and has been vital in elucidating the flavonoid biosynthetic pathway and the regulatory networks that control flavonoid biosynthesis (reviewed in Saito *et al*., 2013).

1.2 Transcriptional regulation of flavonoid and anthocyanin biosynthesis

MYB (MYEOLOBLASTOSIS) family of proteins is a group of transcription factors found across eukaryotic species. Initially discovered in avian myeloblastosis virus, MYBs have been established as key players in cell growth, development, and homeostasis in mammalian systems (reviewed in Oh and Reddy, 1999). In the plant kingdom this protein family has undergone significant expansion and functional diversification, resulting in MYBs controlling a broad spectrum of functions (Dubos *et al.,* 2010; Stracke *et al*., 2001).

The MYB family is defined by their characteristic DNA binding domain; an imperfect helix-turn-helix repeat of about 50 amino acids. Subfamilies of MYB transcription factors can be categorized as R1, R2R3 and R3, according to the number adjacent repeats in their MYB domain (Stracke *et al*., 2001). Members of the R2R3 subfamily of MYB transcription factors participate in a range of plant-specific processes, including development, tissue differentiation, cell fate determination and secondary metabolism (Dubos *et al.,* 2010; Stracke *et al.,* 2001).

Plant MYBs are key transcriptional regulators of phenylpropanoid biosynthetic genes. MYB11, MYB12 and MYB111 are positive regulators of early flavonoid biosynthesis enzymes, driving expression of CHS, CHI, FLS and F3H (Mehrtens *et al.,* 2005; Stracke *et al*., 2007). Late flavonoid and anthocyanin biosynthesis genes on the other hand are positively regulated by MYB75, MYB90, MYB113 and MYB114 (Gonzalez *et al*., 2008; Borevitz *et al*., 2000). Among these latter MYBs, MYB75 appears to be the most important player in driving flavonoid and anthocyanin production, showing higher levels of expression than MYB90, MYB113, or MYB114 in developing seedlings and adult plants. Furthermore, the *myb75*$^{-}$*null* mutant (Nossen ecotype)

fails to accumulate anthocyanins even in the presence of sucrose, a known driver of anthocyanin production (Gonzalez *et al*., 2008).

MYB75 was initially identified in an activation-tag screen, where its over-expression induced a purple colouration in *Arabidopsis*, resulting from the accumulation of anthocyanins throughout the plant. For this reason, it was initially given the name *PAP1-D* for Production of Anthocyanin Pigment-1 Dominant (Borevitz *et al.,* 2000). Since its initial discovery, MYB75 has been widely studied in the context of anthocyanin biosynthesis and has been of great interest as a target for metabolic engineering. A study by Tohge *et al*., (2005) combined transcriptome analysis with metabolomics to reveal details of gene-expression and biochemical changes in *PAP1-D* plants compared to WT *Arabidopsis*. The authors demonstrated that 11 species of anthocyanins (A1-A11) which accumulated in *Arabidopsis* leaves are more abundant in *PAP1-D* plants than in WT *Arabidopsis*. While different plant organs showed distinct molecular profiles (for instance roots only accumulated five anthocyanins; A1-A3, A5 and A8), *PAP1-D* plants consistently showed at least ten-fold increase in abundance for each molecular species compared to WT plants (Tohge *et al*., 2005). Over-expression of *MYB75* in *PAP1-D* plants also had an apparent impact on flavonol profiles. Among kaempferol derivatives (F1-F3), the usually abundant kaempferol dirhamnoside (F1) was slightly reduced in leaves of *PAP1-D* plants, while quercetin glycosides (F4-F6) showed a 10 fold increase. Interestingly, there was no significant shift in flavonol profiles in roots under the conditions tested (Tohge *et al*., 2005). As expected, transcriptome analysis revealed up-regulation of genes involved in anthocyanin biosynthesis (*ANS*, *DFR*, *F3H*, *F3'H* and *GST*) as well as early flavonoid biosynthesis genes (*4CL*, *CHI*, and *CHS*). Additionally, a number of flavonoid glycosyltransferases and acyltransferases were upregulated

in *PAP1-D* plants, suggesting that expression of flavonoid-modifying enzymes is also influenced by MYB75 expression (Tohge *et al*., 2005).

In a different study, several direct targets of MYB75 were identified, along with a promoter consensus sequences required for MYB75-mediated transcriptional activation (Dare *et al*., 2008). The authors showed that MYB75 was able to drive reporter expression from the promoters of dihydroflavonol reductase (*DFR*), glutathione S-transferase (*GST*), leucoanthocyanidin dioxygenase (*LDOX*) also known as anthocyanidin synthase (ANS), UDP flavonoid 5-O-glucosyltransferase (*UFGT*), chalcone synthase (*CHS*), MYB114 and flavonone-3-hydroxylase (*F3H*). The analysis of these reporters identified the essential consensus sequence, YCN**C/TCAC**RWK, which was termed *PAP1* cis-element (*PCE*; Dare *et al.,* 2008). The conserved **C/TCAC** core in the *PCE* is consistent with previously described type I MYB-regulatory elements (Feldbrugge *et al*., 1997; Berendzen *et al*., 2012). Genes showing the highest level of upregulation by MYB75 encode enzymes required for anthocyanin biosynthesis (DFR, LDOX, UFGT and GST), while enzymes required for earlier steps of flavonoid biosynthesis (CHS, F3H), showed more moderate induction by MYB75 (Dare *et al.,* 2008) (Fig 1.1). These data agree with earlier studies which showed MYB75 to be primarily a positive regular of anthocyanin biosynthesis (Gonzalez *et al.,* 2008; Teng *et al.,* 2005). Although recent evidence suggests that MYB75 may influence other branches of phenylpropanoid metabolism, such as lignin biosynthesis, as well as biosynthesis of other components of the secondary cell wall (Bhargava *et al.,* 2010).

1.3 MYB75 transcription-regulatory complexes required to drive flavonoid and anthocyanin biosynthesis

While MYB11, MYB12, and MYB111 are sufficient to drive transcription of genes involved in flavonol biosynthesis, transcriptional regulation of anthocyanin biosynthetic genes by MYB75 typically requires the formation of regulatory complexes with other transcription factors. In vegetative tissues, MYB75 forms a complex with the WD repeat protein TTG1 and either one of the bHLH proteins, GL3, EGL3 or TT8 (Gonzalez *et al*., 2008) to drive anthocyanin biosynthesis (Baudry *et al*., 2004; Zimmerman *et al*., 2004). The MYB/bHLH/WD transcriptional complexes, highly conserved in plants, are also implicated in epidermal cell differentiation and cell fate determination (Bernhardt *et al.,* 2004, Schellmann and Hulskamm, 2005; Serna, 2005; Serna and Martin 2006; Ramsay and Glover; 2005, Song *et al*.,2011). While bHLH and WD repeat proteins can have a broad spectrum of functions, the MYB transcription factors convey specificity to the MYB/bHLH/WDR complex (Ramsay and Glover, 2005); in the case of MYB75 this specificity is thought to be restricted to flavonoid and anthocyanin biosynthetic genes (Fig 1.1)

1.4 Role of MYB75 in cell wall biosynthesis and lignin deposition

In addition to regulating anthocyanin production within MYB/bHLH/WDR complexes, MYB75 has also been shown to interact with KNAT7 (Bhargava *et al., 2010*), a member of the *Knotted Arabidopsis Thaliana Protein* family. KNAT7 activity negatively affects lignin deposition and secondary cell wall thickness in interfascicular fibers (Bhargava *et al*., 2013; Li *et al*., 2012), and appears to act synergistically with MYB75 in inflorescence stems and the seed coat by down-regulating lignin biosynthesis (Bhargava *et al.*, 2013). MYB75 by itself is a weak

transcriptional activator, while KNAT7 has transcriptional repressor activity (Bhargava *et al.*, 2013). The *myb75*$^{-}$ null mutants have thicker secondary cell walls in interfascicular fibers of *Arabidopsis* stems, whereas *PAP1-D* plants (over-expressing *MYB75*) have thinner cell walls in both interfascicular fibers and vessels (Bhargava *et al.*, 2010). Lignin content was significantly greater in *myb75*$^{-}$ mutants and lower in *PAP1-D* plants, as determined by Klason analysis of mature stems. Lignin composition analysis by thioacidolysis revealed that *myb75*$^{-}$ plants had lower levels of syringyl (S) lignin monomers while *PAP1-D* plants had higher levels of syringyl and lower levels of guaiacyl (G) lignin in their stems (Bhargava *et al.*, 2010). The changes in total lignin content, and the shift in the S/G ratio in both mutants, implicate MYB75 in the regulation of gene expression important for lignin biosynthesis and composition.

The impact of MYB75 on gene expression varies in different tissues. Earlier studies performed on either seedlings or adult vegetative leaves showed that MYB75 is a positive regulator, not only of genes responsible for anthocyanin biosynthesis, but also of early flavonoid (*CHS, F3H, F3'H)* and phenylpropanoid (*4CL*, and *PAL)* genes, which contribute to lignin accumulation (Gonzalez *et al.,* 2008; Borevitz *et al.,* 2000). In contrast, when examining specifically the lower portion of *Arabidopsis* stems, where secondary cell wall deposition is prominent, MYB75 emerges as a negative regulator of the lignin branch of phenylpropanoid metabolism (Bhargava *et al.,* 2010). Although neither *PAP1-D* nor *myb75*$^{-}$ mutants showed significant changes in cell wall carbohydrate content or composition, *myb75*$^{-}$ mutants showed an increase in expression of genes responsible for synthesis of cellulose and hemicellulose in secondary cell walls, implicating MYB75 in regulation of plant cell wall development, beyond phenylpropanoid metabolism (Bhargava *et al.,* 2010). Most importantly, these studies bring to

light additional roles of MYB75 in developmental and biochemical processes, in different tissues and at different stages of the *Arabidopsis* life cycle, highlighting the importance of spatial and temporal regulation of MYB75 activity.

Fig 1.1

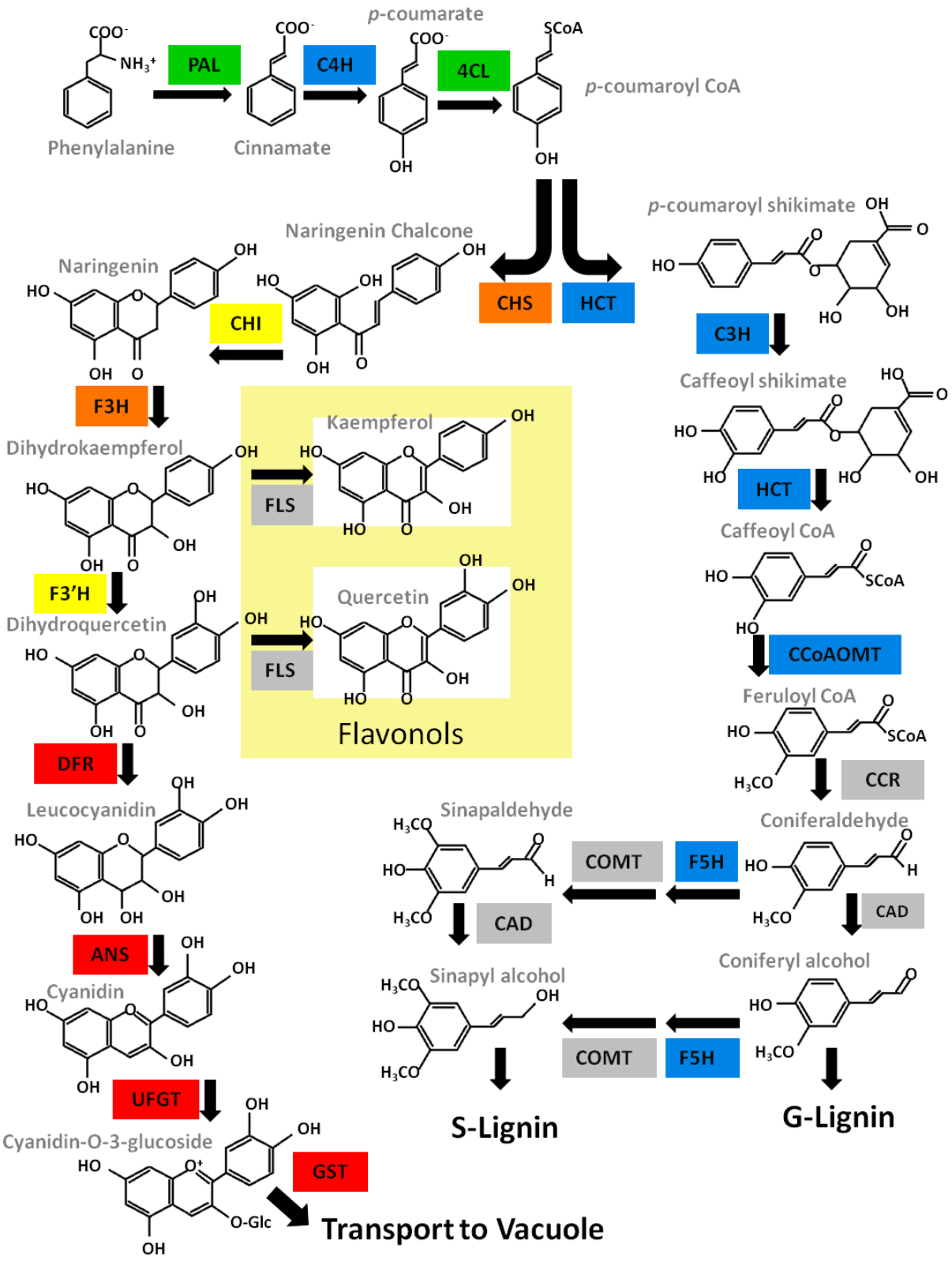
p-coumarate
PAL
C4H
4CL
p-coumaroyl CoA
Phenylalanine
Cinnamate
CHS
HCT
p-coumaroyl shikimate
C3H
Naringenin Chalcone
Naringenin
CHI
F3H
Caffeoyl shikimate
HCT
Caffeoyl CoA
CCoAOMT
Feruloyl CoA
CCR
Kaempferol
FLS
Dihydrokaempferol
F3'H
Quercetin
FLS
Dihydroquercetin
Flavonols
DFR
Leucocyanidin
ANS
Cyanidin
UFGT
Cyanidin-O-3-glucoside
GST
Transport to Vacuole
Sinapaldehyde
COMT
F5H
Coniferaldehyde
CAD
CAD
Coniferyl alcohol
Sinapyl alcohol
COMT
F5H
S-Lignin
G-Lignin

Fig 1.1 Simplified diagrammatic representation of the phenylpropanoid biosynthetic pathway in *Arabidopsis*, depicting key biochemical compounds within the flavonoid and lignin branches of the pathway, as well enzymes required to catalyze their biosynthesis. Enzymes required for biosynthesis of different compounds within the phenylpropanoid pathway are indicated in coloured boxes, colour-coded according to their responsiveness to transcriptional regulation by MYB75. Flavonoid and anthocyanin biosynthesis enzymes highlighted in red and orange are very strongly and moderately upregulated by MYB75 respectively, while those highlighted in yellow are weakly upregulated by MYB75. Genes highlighted in green have been reported to be upregulated by MYB75 in some studies, but not in others. Genes highlighted in blue are downregulated by MYB75. Transcription of genes highlighted in grey is not known to be affected by MYB75. (Based on combined data from: Borevitz *et al.,* 2000; Teng *et al.,* 2005; Dare *et al., 2008;* Gonzalez *et al.,* 2008; Bhargava *et al.,* 2010, 2013).

1.5 MYB75 protein-protein interactions; additional layers of regulation

Recent work has unveiled additional players which regulate MYB75 function through direct interaction with MYB75 or its bHLH partners. Light intensity, photoperiod length, and circadian rhythm influence the levels of regulatory and biosynthetic genes of phenylpropanoid metabolism, including MYB75 (Rogers *et al*., 2005; Shi and Xie, 2010). High light intensity and longer days typically lead to an increase in accumulation of anthocyanins and flavonoids (Shi and Xie, 2010). This can be, in part, accounted for by increased sucrose availability resulting from greater photosynthetic activity under abundant light conditions. However, an independent signalling mechanism through photoreceptors allows light to directly influence gene expression and levels of certain proteins, through post-translational regulation, that contribute to anthocyanin accumulation, independently of sucrose response (Chang *et al*., 2008; Shin *et al.,* 2007; Rogers *et al.,* 2008). MYB75 protein accumulates in the light and is degraded in the dark. Accumulation of MYB75 under high light conditions is partly dependent on HY5, a bZIP family transcription factor which plays a central role in photomorphogenesis,

and positively regulates *MYB75* expression, by directly binding to the *MYB75* promoter and driving its transcription (Chang *et al.*, 2008). In the dark MYB75 is targeted for degradation by a tetrameric complex of COP1 and SPA proteins which are E3 ubiquitin ligases, known to target transcription factors for degradation by the 26S proteasome (Maier *et al.,* 2013). SPA1, SPA3 and SPA4 (which form a complex with COP1) are able to directly bind MYB75 in the dark, leading to its degradation, thus regulating MYB75 levels post translationally. In the light, the COP/SPA complex is de-stabilized, and therefore unable to drive protein turnover, which allows MYB75 to accumulate (Maier *et al.,* 2013). Anthocyanins are known to accumulate during senescence and in response to various abiotic stresses: this process is in part be driven by the phytohormone jasmonic acid (Shan *et al.,* 2009). Jazmonate-ZIM-Domain (JAZ) proteins are transcriptional repressors that can bind the MYB75/bHLH/WDR complex and block its ability to drive transcription of target genes. The degradation of these JAZ proteins triggered by jasmonate hormone, leads to the release of the MYB75/bHLH/WDR complex, allowing it to drive transcription of anthocyanin biosynthetic genes (Qi *et al.,* 2011). JAZ1 and JAZ8 have been shown to specifically bind to MYB75, blocking anthocyanin biosynthesis (Qi *et al.*, 2011).

MYBL2 and SPL9 are two negative regulators of anthocyanin biosynthesis which can disrupt the MYB/bHLH/WDR complex, or prevent it from binding to target promoters through competitive protein-protein and protein-DNA interactions, respectively. MYBL2 is a single repeat MYB lacking the C-terminal transcriptional activation domain that can bind to bHLH proteins, preventing the formation of functional complex with MYB75 and TTG1 (Dubos *et al*., 2008). Similarly, *SPL9* (*SQUAMOSA PROMOTER BINDING PROTEIN LIKE 9*) can disrupt the MYB/bHLH/WDR complex by binding to R2R3 MYBs, including MYB75 and MYB113.

Additionally, SPL9 can compete with MYB75 for binding sites in the promoters of anthocyanin biosynthetic genes (Gou *et al.,* 2011).

On the other hand, TCP3 is a transcription factor that positively regulates complex-formation between MYB75, TT8/GL3/EGL3 and TTG1, leading to increased anthocyanin biosynthesis. TCP3 is also able to bind MYB11, MYB12 and MYB111, and appears to enhance their ability to drive transcription of early flavonoid biosynthetic genes (Li and Zachgo, 2013). Interestingly, both SPL9 and TCP3 have been implicated in developmental processes connected to the hormone auxin. In *Arabidopsis* plants over-expressing TCP3, increased levels of flavonols coincide with inhibition of auxin-response, resulting in widespread developmental abnormalities such as altered vessel development, organ shape, root growth and reduced apical dominance (Li and Zachgo, 2013). According to Gou *et al*., (2011), the spatial-temporal distribution of SPL9 modulates the proportion of anthocyanins to flavonols in developing stems. The authors demonstrated that SPL9 over-expression promotes flavonol and inhibits anthocyanin accumulation. Since flavonols and anthocyanins are made from the same dihydroflavonol precursor, their accumulation is competitive. Therefore, the relative proportions of these classes of compounds in *Arabidopsis* stems can affect certain aspects of development, such as time of floral transition, in which SPL proteins have been implicated (Gou *et al.,* 2011, Wang *et al.,* 2009).

Growing evidence suggests a high degree of interconnectedness between secondary metabolism and primary developmental functions. Until recently MYB75 was primarily thought to regulate a restricted number of genes controlling anthocyanin biosynthesis, with possible

indirect impact on other flavonol compounds through metabolic channeling. The findings of Bhargava *et al*., (2010) demonstrated that MYB75 is involved in lignin production in mature stems, demonstrating that this gene may have a broader spectrum of functions in plants than previously described. Thus, we cannot exclude the possibility that MYB75 may have additional roles, and other transcriptional targets that have not yet been identified, in tissues and/or developmental contexts that are yet to be explored.

1.6 Plant hormones and flavonoid biosynthesis

Plant hormones constitute a diverse group of small molecules that mediate signals important in plant growth and development as well as secondary metabolism and response to stress. These molecules are vital for systemic signal transduction between distant plant organs, but can also participate in localized cell to cell communication. Many physiological stresses and developmental cues, which induce flavonoid and anthocyanin accumulation, are under the influence of hormonal regulation. In turn, flavonoids can influence hormone signalling in plants; perhaps the most prominent example of this is the modulation of auxin flow by flavonols. An in-depth analysis of how flavonoids impact auxin-regulated developmental processes was done by Buer *et al.,* (2013), where the entire collection of *transparent testa* mutants, defective in enzymes required for different steps of flavonoid biosynthesis was examined. The authors describe the perturbations among *tt* mutants, in terms of accumulation and tissue-specific distribution of individual flavonoid compounds, and correlate these changes with perturbations in auxin flow, as well as specific developmental defects. Various *transparent testa* mutants showed alterations in root architecture, gravitropic response and aerial tissue development, which coincided with blockage of shootward (acropetal) and rootward (basipetal) flow of auxin

(Buer *et al*., 2013). Flavonols, including quercetin, kaempferol and their glycoside derivatives, can negatively impact auxin flow (Buer *et al*., 2013; Brown *et al.,* 2001) by directly binding to auxin ABCB1 and ABCB19 transporters (Bouchard *et al*., 2006; Bailly *et al*.,2008). Additionally, flavonols can influence the localization of PIN efflux channels, which mediate directional auxin transport, and drive auxin canalization required for vascular differentiation (Michniewicz *et al*., 2007; Heinrich *et al*., 2012).

The relationship between MYB75, development and the hormone auxin is intuitive, yet not well defined. Accumulation of MYB75 in cyanic cells of the plant epidermis leading to anthocyanin production has been most widely studied. Only the most recent work began to expose additional roles of MYB75 in cell wall deposition; a process typically coupled with vascular development, which is largely an auxin driven process. Interaction between MYB75 and transcription factors such as KNAT7 and TCP3, implicated in cell wall development and auxin response respectively, suggests that MYB75 may have different roles depending on the cellular, environment and developmental contexts. Uncovering these additional roles will require fine tuning our understanding of how plants integrate different signals controlling development and response to the environment, and how these signals affect MYB75 function.

1.7 MAP kinase signalling in plants

MAP kinase signalling pathways are highly conserved among eukaryotes and are essential for relaying messages from outside to inside the cell, and in crosstalk between parallel and antagonistic signalling pathways, which allows for integration of multiple stimuli. MAP kinase signalling typically starts with the activation of a cell-surface receptor-kinase, triggered

by binding of a ligand to its extracellular domain or a change in the extracellular environment. Such cell surface receptors have either tyrosine or serine/threonine kinase activity. Upon activation, they can recruit downstream signalling components such as adaptor proteins and members of the MAP kinase phosphorelay (Gomez-Gomez *et al.*, 2000; Schulze *et al.,* 2010). The core components of the MAP kinase cascade include MAP kinase kinase kinase (MAP3K), MAP kinase kinase (MAP2K) and MAP kinase (MAPK). MAP3Ks can be phosphorylated and activated by the receptor itself or by associated kinases. MAP3K's are serine/threonine kinases, which can activate MAP2Ks by phosphorylation of their activation loop. Activated MAP2K can phosphorylate and activate MAP kinases on specific threonine and tyrosine residues. Once activated MAP kinases can phosphorylate serine and threonine residues on a wide spectrum of targets, including enzymes, transcription factors and cytoskeletal proteins (reviewed in Rodriguez *et al.,* 2010; Colcombet and Hirt, 2008). Phosphorylation typically causes a topological or conformational change in the target protein and this process can affect one or more aspects of protein function, including protein-protein interactions, protein localization and stability and susceptibility to proteolytic degradation. In the case of transcription factors phosphorylation can affect transcriptional activity and the ability to bind to target promoter sequences (reviewed in Whitmarsh and Davis, 2000). A given target can have multiple phosphorylation sites, which can be phosphorylated by different kinases, affecting different aspects of its function, and sometimes having antagonistic effects on the target protein (Yoo *et al.*, 2008).

In the *Arabidopsis* genome 20 MAP kinases, 10 MAP2Ks and 80 MAP3Ks have been identified, on the basis of homology to analogous families in animals and fungi (Ichimura *et al.,*

2002). In plants, some of the best studied MAP kinase-regulated pathways are involved in responses to a variety of abiotic stresses (reviewed in Rodriguez *et al.,* 2010), including ozone (Lee and Ellis, 2007; Miles *et al.,* 2009), drought, heat (Rizhsky *et al.,* 2004), oxidative stress (Kovtun *et al.,* 2000, Nakagami *et al*., 2006), salt, cold (Teige *et al.,* 2004; Mizoguchi *et al.,* 1996), touch, water stress (Mizoguchi *et al.,* 1996), UV radiation (González Besteiro *et al.,* 2011), heavy metals (Jonak *et al.,* 2004), and nutrient deprivation (Wang *et al.,* 2002). MAP kinase signalling pathways also play a crucial role in plant responses to biotic stresses such as herbivory (Heinrich *et al.,* 2011) and pathogen attack, as MAPK activity is vital for mounting a defense response (Petersen *et al.,* 2000; Asai *et al.,* 2002; Del Pozo *et al.,* 2004; Andreasson *et al.,* 2005; Jones and Dangl, 2006; Chinchilla *et al.,* 2007, Boller and Felix, 2009). In *Arabidopsis*, MAP kinases MPK3, MPK4 and MPK6 have been most widely studied. Interestingly, many of the stresses, which are known to activate MAP kinase signalling are also known to trigger anthocyanin accumulation.

MAP kinases are also implicated in growth, development and differentiation (Ohashi-Ito and Bergmann, 2006; MacAlister *et al.,* 2007; Wang *et al.,* 2007; Kanaoka *et al.,* 2008, Lampard *et al.,* 2008.). Many MAP cascades exhibit significant crosstalk with phytohormone signalling pathways, creating a complex network which allows for the integration of multiple stimuli (reviewed in Rodriguez *et al.,* 2010). While some MAP kinase modules are highly specific for a small subset of cellular targets, others are more promiscuous. For instance MPK3 and MPK6 are implicated in a variety of biotic and abiotic stress responses (reviewed in Rodriguez *et al.*, 2010), in hormone signalling (Yoo *et al.*, 2008) as well as development and cell differentiation (Lampard *et al.*, 2008). MAP kinases activation in response to auxin has been demonstrated in

Arabidopsis roots. The authors found that kinase activation was reduced in auxin-insensitive mutants, and auxin-inducible marker expression was abolished in the root elongation zone upon chemical inhibition of MAP kinase activation, implicating MAP kinase signalling in auxin-driven developmental processes (Mokaitis and Howell, 2000).

1.8 MYB transcription factor phosphorylation by MAP kinases

Regulation of MYB transcription factor-function by phosphorylation has been well documented in animals (Miglarese *et al.,* 1996; Bessa M., *et al.,* 2001; Cesi *et al.,* 2002), and more recently in plants (Ito *et al.,* 2001, Haga *et al.,* 2007, Popescu *et al.,* 2009). Recent work in *Pinus taeda* revealed that the xylem-specific R2R3-MYB transcription factor PtMYB4, is phosphorylated by PtMPK6 (Morse *et al.,* 2009). The authors showed that PtMPK6 was able to phosphorylate PtMYB4 at a serine residue found in its activation domain, which has a negative impact on the transcriptional activity of PtMYB4, without affecting its ability to bind the target DNA sequence (Morse *et al.,* 2009). The Arabidopsis homologues most closely related to PtMYB4 are AtMYB46 and AtMYB83, both of which are global regulators of secondary cell wall development (Zhong and Ye, 2012), while the closest *Arabidopsis* homologue of PtMPK6 is AtMPK6.

MYB75 has two threonine residues (T126 and T131) that appear as canonical MAP kinase phosphorylation sites, where the threonine residue is followed by a proline. Unlike other global regulators in the MYB family, MYB75 has a relatively restricted number of target genes and a predictable set of functions defined to date; neither the over expression nor deletion of the gene have severe consequences that would compromise plant survival. These features of MYB75 make it good candidate for connecting MAP kinase signalling to stress response and

secondary metabolism, and to uncover how phosphorylation can impact this transcription factor family, and the biological functions they regulate.

In living cells protein phosphorylation is an ongoing and dynamic process, with kinetics of target phosphorylation ranging from seconds to minutes of stimulation with an elicitor of kinase activation (Peck, 2006; Leoni *et al.,* 2013). Protein phosphorylation events can be cyclical: for example, proteins responsible for cell cycle checkpoints and progression are often activated by phosphorylation at specific stages of cell growth (Pearce and Humphreys, 2001). Alternatively, phosphorylation can occur in response to an external or intracellular stimulus. Some prominent examples in plants include activation of FLS2 receptor by flagellin (flg22), which initiates an immune response (Gomez-Gomez and Boller, 2000; Shulze *et al*., 2010), and the activation of a MAP kinase signalling cascade in response to an oxidative burst (reviewed in Liu and He, 2017). In all of these cases, by altering the function of existing proteins, phosphorylation can elicit a rapid response, localized in a specific cell or tissue that would otherwise require significant transcriptional reprogramming. Additionally, phosphorylation signalling cascades are kept in check through the antagonistic action of protein phosphatases which de-phosphorylate proteins (Lee *et al.,* 2008; González Besteiro *et al.,* 2011; Bhalla *et al.,* 2002), making this form of post-translational modification reversible and transient, and therefore challenging to capture and study. Point mutations have been routinely used to simulate phosphorylated and un-phosphorylated protein forms. Serine and threonine residues are commonly mutated to alanine, creating a form of the protein that can no longer be phosphorylated. Replacing a serine with an aspartic acid, or a threonine with a glutamic acid residue creates another non-phosphorylatable form of the protein, however, the large

electronegative groups present in aspartic and glutamic acids simulate the presence of a phosphate group on the serine or threonine respectively, as they mimic the steric and electrostatic properties of phosphoserine and phosphothreonine. Throughout this work phosphomutants are employed to describe the impact of phosphorylation on MYB75 protein function. Initially, threonines 126 and 131 were replaced with alanine or glutamic acid residues creating phosphomutant and phosphomimic versions of MYB75, respectively. The point-mutants used in our analysis initially included $MYB75^{T126A}$, $MYB75^{T126E}$, $MYB75^{T131A}$ and $MYB75^{T131E}$ as well as the double mutants, $MYB75^{AA}$ and $MYB75^{EE}$, however, as my focus shifted towards threonine 131, $MYB75^{T131A}$ and $MYB75^{T131E}$ were primarily used in my final experiments.

1.9 Role of MAP kinases in ROS and light signalling

An overwhelming volume of literature on MAP kinases implicates these signalling cascades in responses to a wide variety of biotic and abiotic stresses. A common feature of many such stress responses is the burst of reactive oxygen species (ROS) which accompanies the initial perception of the stress elicitor. Reactive oxygen species include hydroxyl radicals ($HO^{\cdot}$), singlet oxygen ($^1O_2$), superoxide anions ($O_2^{\cdot-}$), and hydrogen peroxide H_2O_2. These molecular species can cause severe oxidative damage to cell components, but they also play an important role in stress perception and response (reviewed in Liu and He, 2017).

The vast majority of knowledge on how MAPK kinase phosphorelay is involved in ROS signalling comes from analyses of various null mutants of *mkkk, mkk* and *mpk* genes (reviewed in Liu and He, 2017). The precise mechanism of how MAP kinase cascades affect ROS-driven changes in gene expression is far from being fully elucidated, however, several lines of evidence

suggest that phosphorylation of transcription factors is an important part of this regulation (Wang *et al.,* 2013, reviewed in Liu and He, 2017). MPK3 and MPK6 are the best described regulators of ROS signalling. These MAP kinases are activated by H_2O_2 and can modulate expression of genes, such as ROS-scavenging enzymes, that enable plants to cope with oxidative stress (Xing *et al*., 2007;2008;2013), supporting previous data which showed that MAP kinase cascade activation enhances stress tolerance and acclimation (Kovtun *et al*., 2000).

ROS signalling is not only part of stress response, but is an ongoing monitoring system of cell and organelle redox status. Chloroplasts are major hubs for ROS production, generated as byproducts of photosynthesis (reviewed in Asada, 2006; Pospisil, 2009). Excess light can cause overexcitation of chlorophyll and excess reduction of the photosynthetic apparatus, leading to generation of reactive oxygen species (Tipathy and Oelmüller, 2012). Because of this direct connection between light and ROS signalling, it is not surprising that MAP kinases are emerging as important players in light-dependent stress signals, connected to photomorphogenesis.

Recent work has demonstrated the involvement of plastid signals in activation of MPK6, when plants were shifted from low to high light (Vogel *et al*., 2014). Although the authors suggest that metabolites exported from the chloroplast act as signals that lead to MPK6 activation, an earlier study showed that MKK4 can localize to the chloroplast, suggesting that the plastid can also be a site of MPK cascade initiation (Samuel *et al*., 2008). In another study MKK3 was shown to be necessary for acclimation when plants were shifted from dark to light (Lee, 2015), consistent with previous findings showing that MKK3-MPK6 modules play an important role in seedlings photomorphogenesis (Sethi *et al*., 2014). Since increased exposure to light is accompanied by increased light stress (including ROS accumulation), these recent

findings reinforce the role of MAP kinases in managing stress response and maintenance of homeostasis.

1.10 Light and plant development

As autotrophs, plants rely on light for growth, development and reproduction. It is therefore not surprising that light has a profound influence on every aspect of plant physiology. Plants are able to perceive light quality and quantity, and adjust to suboptimal lighting conditions. Photomorphogenesis is plant development shaped by light, aimed at maximizing photosynthesis, ultimately ensuring survival and reproduction. Photomorphogenesis is most commonly used to describe changes in early plant development, when a seedling transitions from heterotrophy (relying on nutrients stored in the seed) to photosynthesis. Key events in this transition include chloroplast development and establishing of stem cell populations in the apical meristems, which initiate organ differentiation. Additionally, photomorphogenesis can shape the plants' later stages of development, and has been shown to affect core processes, including seed germination, hypocotyl de-etiolation, organ expansion, stem elongation, apical dominance, chloroplast biogenesis, as well as floral initiation and flowering time (reviewed in Arsovski *et al*., 2012). At the genetic and cellular levels, photomorphogenesis involves large scale reprogramming of gene expression, leading to visible morphological and developmental changes. Prominent examples of this light-dependent reprogramming include seedling etiolation in the dark and de-etiolation upon exposure to light. Besides shaping the early plant-developmental stages, photomorphogenesis is also important in driving shade avoidance of plants under a canopy. The molecular components which control these processes comprise vast signalling networks, where light perception is intertwined with hormonal signals, the circadian

clock and various environmental cues. The comprehensive description of all molecular components of light signalling and their relationships is beyond the scope of this thesis. This work will focus on describing only key developmental trends and global regulators of photomorphogenesis that may be pertinent to the role of MYB75 in light-dependent developmental processes.

1.11 Plant photoreceptors

Plants have several classes of photoreceptors which allow them to perceive light quantity and quality. Some of the best studied light signalling pathways are associated with phytochromes (PHYA-E), which absorb red and far-red light (600-750nm) (reviewed in Li *et al.*, 2011) and cryptochromes (CRY1, CRY2 and CRY3) which absorb blue light and UV-A (320-500nm) (reviewed in Lin, 2002; Yu *et al*., 2010). Other classes of blue-light and UV-A photoreceptors discovered in recent years include phototropins (PHOT1-2) (reviewed in Lin 2002), ZEITLUPE (ZTL) (Kim *et al,* 2007)., FLAVIN-BINDING KELCH REPEAT F-BOX (FKF) (Nelson *et al.,* 2000) and LOV KELCH REPEAT PROTEIN 2 (LKP2)(Baudry *et al.,* 2010). Additionally, UVR-8 was a recently described UV-B photoreceptor, shown to mediate UV-B stress response (280-315nm) (Rizzini *et al*., 2011; Tilbrook *et al*., 2013). Together red and blue light photoreceptors monitor light in the spectrum that is required for photosynthesis, and can work synergistically and antagonistically to relay highly detailed light information to the plant cell.

Phytochromes and cryptochromes are the best described photoreceptors in terms of structure and function. They consist of a protein linked to distinct types of chromophores, which absorb specific wavelengths of light and trigger a conformational change in the protein portion, essential to initiate the light signalling cascade downstream of that photoreceptor.

In the case of phytochromes photoactivation-driven transition from the inactive conformation (P_r) to the active form (P_{fr}), leads to relocation of the photoreceptor from the cytosol to the nucleus, where it can impact gene expression. Cryptochromes on the other hand are predominantly found in the nucleus; their activation requires both photoexcitation and phosphorylation, which promotes their interaction with downstream signalling components, inducing blue-light driven developmental changes (Reviewed in Lin ,2002; Liu *et al*., 2011, Gyula *et al*., 2003).

Phytochromes and cryptochromes influence light-driven gene expression in several ways. They can bind directly to distinct transcriptional regulators, and target them to specific promoters. These photoreceptors can also trigger phosphorylation of transcription factors and other regulatory proteins, altering their stability or the ability to drive gene expression, due to altered protein-protein and/or protein-DNA interactions (reviewed in Lin, 2002; Gyula *et al*., 2003., Schepens *et al* 2004., Liu *et al*., 2011., Li *et al.,* 2011., Wang and Wang 2015). Perhaps the best described function of phytochromes and cryptochromes is their ability to disrupt COP1/SPA ubiquitin ligase complexes, which target photomorphogenic transcription factors for degradation. In this manner photoreceptors can lead to global changes in gene expression, through stabilization of light responsive transcriptional regulators.

Phytochromes and cryptochromes have unique and overlapping functions. Most of these photoreceptors are able to drive seedling de-etiolation and photomorphogenesis during early development, when exposed to appropriate wavelengths of light. PHYA is important for mediating far-red light responses, while the remaining phytochromes (PHYB-PHYE) predominantly drive red light-activated processes (Li *et al., 2011*). In *Arabidopsis* PHYA

promotes flowering, while PHYB inhibits floral initiation, along with PHYD and PHYE (Schepens *et al*., 2004; Wang and Wang ,2015; Li *et al*., 2011). Blue light has also been shown to induce flowering, through CRY1 and CRY2. Additionally CRY1 can mediate hypocotyl de-etiolation and chloroplast biogenesis, thus having overlapping functions with phytochromes. Years of research have unveiled increasing complexity and connectivity between different photoreceptors and their downstream signalling components; in recent years this complexity has increased, as researchers discovered the involvement of plastid signals in light perception and response.

1.12 Plastid-derived signals

In addition to photoreceptors, chloroplasts can act as monitors of light quality and quantity as well as cell redox status. Plastids can communicate with the nucleus, optimizing gene expression to coordinate development with energy output from photosynthesis, and protect the plant from photooxidative damage. A recent study demonstrated that the chloroplast controls approximately half of light-regulated genes (Ruckle *et al*., 2012). The authors used lincomycin antibiotic (a plastid-specific translational inhibitor), in conjunction with global transcriptional analysis, to show that of ~6400 genes whose expression changed in response to increased light intensity, over 3000 genes depended on a functional chloroplast. The major classes of genes dependent on plastid integrity included those required for photosynthesis, plastid biogenesis and maintenance, as well as stress response and photoprotection. Interestingly, expression of chalcone synthase (*CHS)* was increased in seedlings treated with lincomycin, indicating that flavonoid biosynthesis can be influenced by plastid-derived signals (Ruckcle *et al*., 2012, Hills *et al* ., 2015).

Although our understanding of chloroplast to nucleus communication is still limited, the overall emerging view is that various metabolites (such as chlorophyll biosynthetic intermediates) generated as a result of damage or disruption of chloroplast function, activate signalling cascades that can affect nuclear gene expression. For instance, MG-protoporphyrrin IX (MG-ProtoIX), a precursor in chlorophyll biosynthesis, acts as a signalling molecule that can impact nuclear gene expression (Mochizuki *et al*., 2001, Kindren *et al*., 2012). In turn, chloroplast function is tightly linked to light signalling through phytochromes and cryptochromes, and is heavily reliant on the function of nuclear genes, regulated by these photoreceptors (Susek *et al.,* 1993; Kohchi *et al.,* 2001). Recently, a direct link between plastid signals mediated by MG-ProtolIX were shown to negatively affect expression of photosynthesis-associated nuclear genes, through HY5 - a global regulator of light signal transduction and photomorphogenesis, and a direct regulator of MYB75 expression.

1.13 Global regulators of light-driven gene expression

Two classes of global gene-expression regulators controlled by photoreceptor activity include a group of bHLH proteins called phytochrome interacting factors (PIFs) and the bZIP-family transcription factor LONG HYPOCOTYL 5 (HY5). In the dark HY5 is targeted for degradation by COP/SPA ubiquitin ligase complexes (Osterlund *et al.,* 2000; Saijo *et al.,* 2003). Exposure to light and photoreceptor activation, allows HY5 to accumulate and drive light-dependent development. During seedling development HY5 acts as a positive regulator of photomorphogenesis in the light, inhibiting hypocotyl elongation, while promoting cotyledon expansion and chloroplast biogenesis, leading to greening of plant tissues and establishment of autotrophy (Oyama *et al.,* 1997). Conversely, PIFs are important in driving processes such as

skotomorphogenesis (plant development in the dark), and shade avoidance in suboptimal light conditions. PIFs accumulate in the dark and act primarily as negative regulators of light-driven developmental programs: PIFs can inhibit seed germination (Piskurewicz *et al*., 2009), cotyledon expansion, chlorophyll biosynthesis (Huq *et al.,* 2004; Chen *et al.,* 2013) and plastid development (Barnes *et al.,* 1996; Stephenson *et al.,* 2009), while promoting hypocotyl elongation (Reviewed in Castillon *et al.,* 2007 and Leivar and Monte, 2014). In the dark PIFs accumulate and drive global changes in gene expression. In the light, activated phytochromes (P_{fr}) can bind and phosphorylate PIFs, leading to their degradation (Al-Sady *et al.,* 2006), or, in some cases, disruption of transcriptional activity or binding to target promoters (reviewed in Leivar and Monte, 2014). Overall, PIFs have a growth-promoting function in plants, which drives the rapid extension of the hypocotyl during etiolation and stem growth during shade avoidance, as well as growth and development throughout the lifecycle of the plant.

Although initially PIFs and HY5 were defined by their light-responsive functions, the last two decades of research have unveiled their participation in a broad range of developmental processes. HY5 has been linked to the action of different hormones, including ethylene (Yu *et al.,* 2013), brassinosteroids (Li and He, 2016; Shi, 2011), auxin and cytokinin (Cluis *et al.,* 2004), and as a result is implicated in a broad spectrum of developmental functions throughout the life of the plant.

PIFs have been shown to act as communication lines between light signals and circadian clock (reviewed in Hayama and Coupland, 2003; Shin *et al.,* 2013). The ability of PIFs and HY5 to regulate a wide spectrum of genes depends largely on their ability to form complexes with other transcriptional regulators (reviewed in Castillon *et al*., 2007; Gangappa and Botto, 2016).

Both HY5 and PIF3 can positively regulate anthocyanin biosynthesis on exposure to light, by binding to promoters of anthocyanin biosynthetic genes, in a HY5-dependent manner (Shin *et al.,* 2007). Crucially, HY5 was shown to positively regulate MYB75 expression by directly binding to its promoter (Shin *et al*., 2013).

1.14 Possible role of MYB75 in light signalling

MYB75 is already known to be part of the light signalome as it is a direct transcriptional target of HY5, and is turned over in the dark, through ubiquitination mediated by COP/SPA complexes, which are known to promote degradation of various light-responsive transcription factors, including HY5 (Osterlund *et al.,* 2000; Saijo *et al.,* 2003; Maier *et al.,* 2013). The participation of MYB75 in light responses is intuitive, as anthocyanins provide a photoprotective screen for the photosynthetic machinery and other cellular components by absorbing excess photons. Regulation of anthocyanin production through MYB75 is therefore an important dimmer switch that dictates how much light reaches the photosynthetic machinery. A recent publication demonstrated that MYB75 phosphorylation by MPK4 at threonines 126 and 131 is necessary to stabilize MYB75, enabling it to drive anthocyanin biosynthesis (Li *et al.,* 2016). The study showed that far red light was responsible for MPK4 activation, which also appeared to activate MPK3 and MPK6. While our data contradicts some of their conclusions (to be addressed later in this thesis), activation of multiple MAP kinases by far red light, is congruent with our findings that MYB75 phosphorylation status may help define additional roles of MYB75 in developmental processes connected to light signals.

The Ellis lab has pioneered the idea that MYB75 participates in developmental processes beyond anthocyanin production by demonstrating that MYB75 can negatively impact secondary

cell wall biosynthesis (Bhargava *et al*., 2010). This discovery is in stark contrast with dozens of papers that type-cast MYB75 as solely a regulator of anthocyanin production, and demonstrates an ongoing paradigm shift in science, where increasing connectivity between different biological processes reveals increasing multi-functionality of their regulators.

1.15 Research Objectives

The main research goal in this thesis is to determine how phosphorylation of MYB75 affects its function and describe the impact of this phosphorylation event on plant growth and development. The primary tools used in this body of work are the phosphovariant mutants described earlier. The first part of the project required determining that MYB75 can in fact bind to and be phosphorylated by one or several of the 20 *Arabidopsis* MAP kinases. The second part of the project focused on determining how phosphorylation affects various aspects of MYB75 function in different phosphorylation states, using MYB75 phosphovariants. MYB75 protein localization, stability, and interaction with known binding partners were tested. Subsequently, I set out to describe the impact of MYB75 phosphorylation on its function *in-vivo*, using *Arabidopsis* plants expressing different MYB75 phosphovariants from the endogenous MYB75 and constitutive 35S promoters. Functionality of each phosphovariant was primarily evaluated with respect to anthocyanin biosynthesis, however, notable changes in development were also observed and recorded.

CHAPTER 2 MYB75 interaction with *Arabidopsis* MAP kinases, *in vitro* phosphorylation, and differences in protein function among MYB75 phosphovariants

2.1 Introduction

In depth exploration of how phosphorylation affects MYB75 function, requires prior demonstration that MYB75 is in fact phosphorylated, and determining which of the 20 *Arabidopsis* MAP kinases are able to phosphorylate each putative target site. MYB75 has two canonical MAPK phosphorylation sites at threonines 126 and 131; the phosphopeptide containing these residues has been identified by mass spectrometry (Li *et al*., 2016). In this chapter I demonstrate that MYB75 is a target for phosphorylation by several *Arabidopsis* MAP kinases *in vitro.* This chapter will also explore how this phosphorylation can impact the function of MYB75, in terms of subcellular protein localization, the physical interaction of MYB75 with known binding partners, and the protein's stability. A recent paper, which was published while I was completing this thesis, demonstrated that MYB75 was phosphorylated by MPK4. The authors showed that both threonines T126 and T131 were target sites for phosphorylation by MPK4 and that phosphorylation at these residues stabilized MYB75 protein *in vivo* (Li *et al*, 2016). The results presented by Li *et al.,* (2016) contradict some our findings; these differences as well as possible explanations for such discrepancies will be addressed in the discussion.

2.2 MYB75 interaction with *Arabidopsis* MAP kinases in yeast

Phosphorylation events catalyzed by MAP kinases require a physical interaction between the MAP kinase and its intended target protein. In order to determine which MAP kinases might be involved in phosphorylating MYB75, a directed yeast two-hybrid screen was

conducted, testing the interaction between MYB75 and each of the 20 *Arabidopsis* MAP kinases. The results of the Y2H screen indicated that MYB75 was able to interact with several MAP kinases *in vitro* (Fig 2.1). Interestingly, a few MAP kinases, particularly MPK4 and MPK11 displayed background reporter gene activation in yeast; yeast colonies in the control lanes for these MPKs appear light pink rather than red when growing on SD-trp-leu culture medium and they survived on medium without histidine containing up to 1mM 3AT. Despite this background signal, the strength of MYB75's interaction with each MAP kinase could be assessed on selective media with higher stringency (higher 3AT concentration). Survival of yeast cells on drop-out media lacking histidine, under higher concentrations of 3AT (2.5mM-10mM), as well as on medium lacking adenine, indicated that the strongest interacting partners of MYB75 were MPK3, MPK10, MPK11, MPK13, MPK14 and MPK20. Moderate interaction strength was observed for MPK6, MPK10, MPK18 and MPK19, while weak binding was seen in MPK1, MPK2, MPK4, MPK7 and MPK17. MYB75 did not interact with MPK5, MPK8, MPK9, MPK12, MPK15 or MPK16 in this assay.

This apparent MYB75 binding promiscuity made it difficult to narrow down the search for possible pathways that might connect MAP kinase signalling with MYB75 function. While biological functions have been demonstrated for some of the strong or moderate interactor MPKs (e.g MPK3, 6, 18), for others (e.g. MPK13, 14, 19 and 20) there is little or no information in the literature. Since preliminary experiments in our laboratory had demonstrated that a small subset of the strong/moderate interacting MPKs (3, 4, 6 and 11) might directly phosphorylate recombinant MYB75 *in vitro*, further experiments focused on these MAP kinases. Although MPK4 showed only a weak interaction with MYB75 in my yeast 2-hybrid screen, it was

included in the more detailed *in vitro* phosphorylation assays because it is a very close paralog of MPK11 (a strong interactor). Furthermore, much like MPK3 and MPK6, MPK4 has been relatively well studied, and implicated in signalling, in response to biotic and abiotic stress (reviewed in Rodriguez *et al.,* 2010).

Fig 2.1

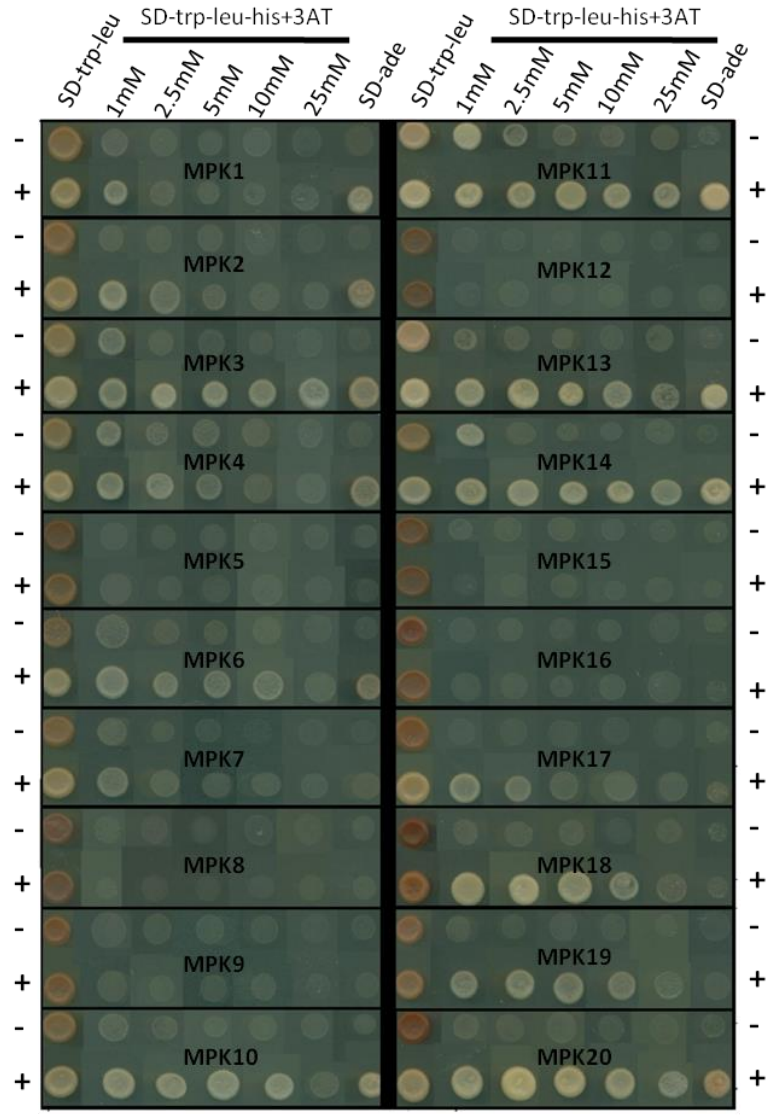

Interaction strength	
strong	MPK3, MPK11, MPK13, MPK14, MPK20
moderate	MPK6, MPK10, MPK18, MPK19
weak	MPK1, MPK2, MPK4, MPK7, MPK17
none	MPK5, MPK8, MPK9, MPK12, MPK15, MPK16

Fig. 2.1 MYB75 interacts with several *Arabidopsis* MAP kinases in yeast. MYB75 interaction with each of the 20 *Arabidopsis* MAP kinases was tested in a yeast two-hybrid system, using *MYB75* cDNA fused to GAL4-AD and each MAP kinase fused to GAL4-DBD. The interaction strength was evaluated visually, based on colony colour when grown on medium lacking leucine and tryptophan, and by evaluating survival on media lacking histidine, with addition of 1-25mM 3-aminotriazole (3AT), and on medium lacking adenine. Negative control rows (-) display results of MPK-DBD co-transformed with the empty pGADT7 (AD) vector. Rows (+) are results from co-transformation of MYB75-AD and MPK-DBD. MYB75 displays a strong interaction with MPK3, MPK11, MPK13, MPK14, and MPK20, moderate strength interaction with MPK6, MPK10, MPK18, and MPK19, and only a weak interaction with MPK1, MPK2, MPK4, MPK7 and MPK17.

2.3 *In vitro* phosphorylation of MYB75 by MPK3, MPK4, MPK6 and MPK11

Among the 20 *Arabidopsis* MPKs the best studied family members are MPK3, MPK4 and MPK6. These three MPKs, are known to be involved in signalling responses to biotic and abiotic stresses, and such stresses are often accompanied by increased anthocyanin accumulation in stressed plant tissues. This correlation made these members of the MPK family plausible candidates for MYB75-modifying kinases. MPK3 and MPK6 are closely related paralogs that often (but not always) share the ability to mediate the same signalling responses (reviewed in Rodriguez *et al*., 2010). MPK4 and MPK11 form another pair of closely related paralogs, however, despite sharing 87% amino acid sequence similarity, there is little evidence that the biological roles of MPK4 and MPK11 overlap. While *mpk4* mutants display severe developmental defects, including dwarfism and partial male sterility, *mpk11* mutants appear relatively normal (Petersen *et al*., 2000; Zeng *et al.,* 2011). Furthermore, expression of the *MPK11* coding sequence under the control of an *MPK4* promoter in an *mpk4* knock-out background failed to complement the *mpk4* loss-of-function phenotype, indicating that there is no apparent functional overlap between these MAP kinases (Zeng *et al.,*2011). Nevertheless, the strong amino acid sequence similarity between MPK4 and MPK11 suggests that some similarities in terms of function or target specificity may exist. When Dr. Zhenhua Yonge in our laboratory began to explore the possibility that MYB75 might be phosphorylated by *Arabidopsis* MAP kinases, she conducted a directed yeast two-hybrid screen using the Invitrogen Proquest® kit. With this system, she found that MPK11 was the only MAP kinase able to interact with MYB75. She then tested four MAP kinases (MPK3, 4, 6 and 11) to determine if they a) can

phosphorylate recombinant MYB75 *in vitro,* b) whether phosphorylation is occurring at one or both of the two canonical PXT sites in MYB75, and c) whether there was any evidence for a preferential phosphorylation by each MPK for either of the two target site threonines.

Dr. Yonge showed that recombinant GST-tagged MYB75 can indeed be phosphorylated by all four MAP kinases tested (Fig 2.2). In addition, when mutated forms of MYB75 were tested, in which either the T126 or T131 residue, or both, were replaced with alanine, it was apparent that T131 was the preferred site of phosphorylation for all four MAP kinases (Fig 2.2). With the knowledge that MYB75 can interact physically with MPKs and can serve as an *in vitro* substrate for MPK phosphorylation, my next goal was to understand the impact of such a phosphorylation event on MYB75 function.

Fig 2.2

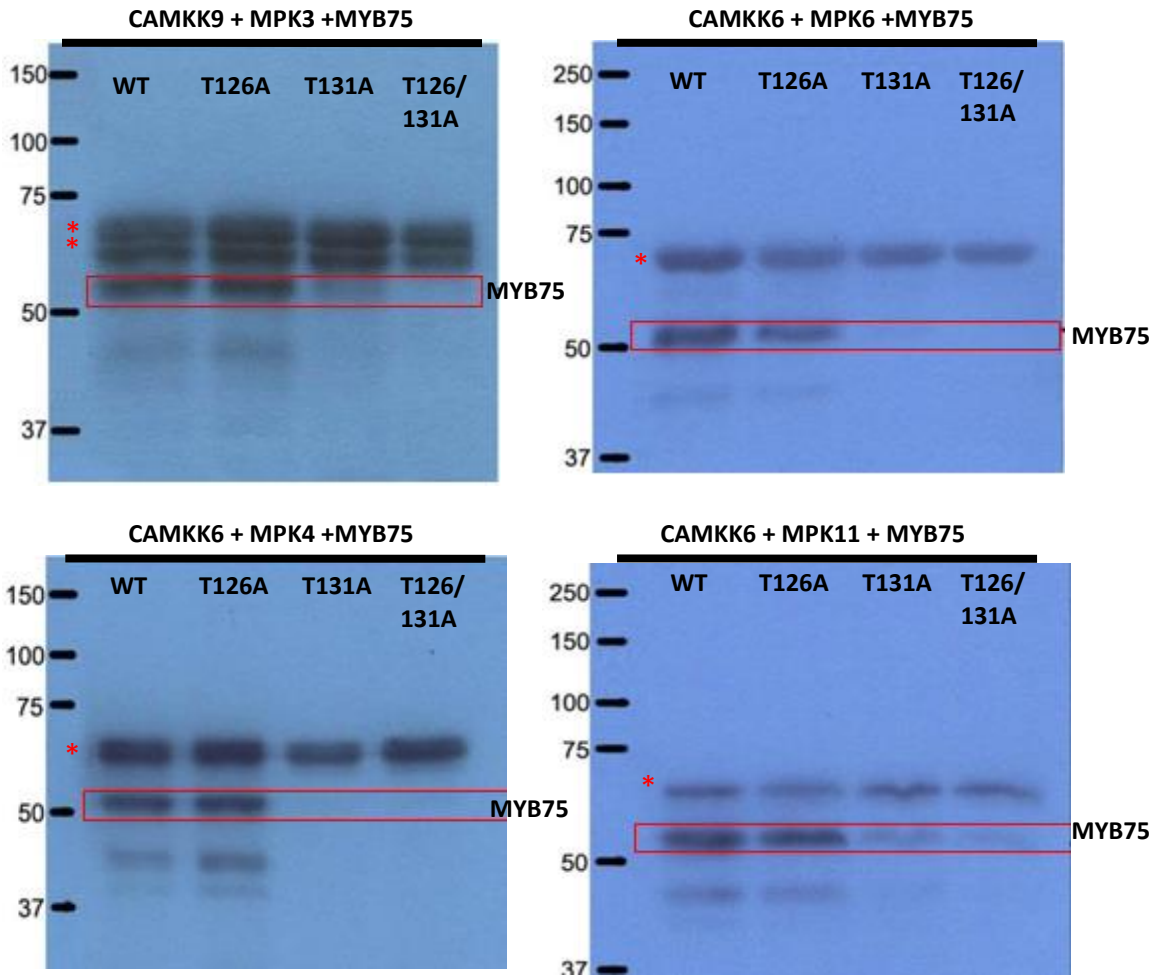

Fig. 2.2 *In vitro* phosphorylation of MYB75 by *Arabidopsis* MPK3, MPK4, MPK6 and MPK11. Recombinant proteins with a GST tag (MYB75, MAP kinases 3,4,6 and 11, as well as CAMKK6 and CAMKK9) were expressed in *E. coli* (BL21) and recovered from bacterial cell extracts using glutathione-sepharose® 4B beads. The *in vitro* phosphorylation assay was performed by combining each MPK with MYB75 in the presence of radiolabelled [Y-32P] ATP, and a 'constitutively active' MAP kinase kinase (CAMKK). Wild type MYB75 was used, along with point mutants where threonine 126, threonine 131, or both, was replaced with alanine, preventing phosphorylation at this site. X-ray film was used to detect signal from radiolabelled phosphate. The pattern of autoradiogram signals indicates prominent phosphorylation by all four MAP kinases, of wild type MYB75 and of $MYB75^{T126A}$, with only negligible signal in lanes with the $MYB75^{T131A}$ mutant forms. Red * indicate background bands present in all samples.

2.4 Impact of MYB75 phosphorylation on protein function

Post translational modification through phosphorylation can affect many different classes of proteins, including enzymes, membrane receptors, ion channels, structural and regulatory proteins (reviewed in Ranjeva and Boudet, 1987; Johnson, 2009; Nishi *et al.,* 2011). At the molecular level, phosphorylation results in the addition of a large electronegative phosphate group to a specific site, which leads to topological and electromagnetic changes near that site. Phosphorylation can also result in large-scale conformational changes in the protein, ranging from localized shifts in secondary structure to dramatic, long range conformational changes, such as disorder-to-order and order-to-disorder transitions (Groban *et al.,* 2006; Nishi *et al*., 2011; Bah *et al.,* 2015). In summary, phosphorylation impacts protein function by modifying the physiochemical properties of the target site, and/or by causing a conformational change that leads to the exposure or blockage of features important for the functionality of the protein.

The impact of phosphorylation on a particular aspect of protein function can potentially be either positive or negative, while the type of functions which phosphorylation can affect are as diverse as the classes of proteins subject to this form of post translational regulation. In transcription factors, phosphorylation plays an important role in nucleocytoplasmic shuttling, by mediating exposure or blockage Nuclear Localization and/or Nuclear Export Signal sequences (NLS and NES respectively). Phosphorylation can affect NLS and NES exposure through inducing intrinsic conformational changes in the transcription factor itself, or by promoting or inhibiting interactions of the modified protein with binding partners that affect accessibility of these sequences (reviewed in Whitmarsh and Davis 2000; Endt *et al* 2002). In this manner, by

inducing nuclear translocation or cytosolic sequestration, phosphorylation can control the ability of a transcriptional regulator to reach target promoters and modify gene expression. In addition to altering target protein localization, the DNA binding activity of transcription factors can also be affected by phosphorylation. Typically, if the phosphorylation site is directly located in the DNA binding domain, addition of a negatively charged phosphate group has an adverse effect on the protein-DNA interaction (Smykowski *et al*., 2015; reviewed in Meshi and Iwabuchi, 1995; Whitmarsh and Davis, 2000; Endt *et al*., 2002). However, in many cases phosphorylation has been shown to have a positive impact on DNA-binding activity of transcriptional regulators, enhancing the interaction between the transcription factor and a specific *cis*-element in the target promoter sequence (Menke *et al.,* 2005; reviewed in Ishimara and Yoshioka, 2012). Phosphorylation can also directly impact transcriptional activity. An example of this is the xylem-specific PtMYB4, found in pine, which is phosphorylated on a serine residue located in its transcriptional activation domain. The ability of recombinant phosphomimic mutant PtMYB4 to drive transcription of reporter genes, in yeast, was reduced compared to a wild type version of the recombinant protein, while the DNA-binding activity of the MYB was not affected (Morse *et al.,* 2009).

In some cases phosphorylation affects protein stability, indirectly, by influencing protein-protein interactions. Some protein-protein interactions can have a stabilizing effect on one or both interacting partners, whereas others promote degradation. For instance, Ubiquitin ligases bind their target proteins; this interaction is necessary for target protein polyubiquitination and subsequent degradation by the 26S proteasome (reviewed in Whitmarsh and Davis, 2000; Endt *et al.,* 2002). Prominent examples of this mode of regulation

in plants include the phosphorylation of light-regulated components, HY5 and phytochrome interacting factors (PIFs). In the case of HY5, phosphorylation was shown to interfere with the binding of HY5 to COP1 protein (Hardtke *et al.,* 2000). Since the interaction with COP1 leads to HY5 polyubiquitination and degradation (Osterlund *et al.,* 1999), phosphorylation has a stabilizing effect on HY5 (Hardtke *et al.,* 2000). Conversely, light induced PIF1 phosphorylation promotes its binding to the CUL4 $^{COP1\text{-}SPA}$ E3 ubiquitin ligase complex, which leads to polyubiquitination and rapid degradation of PIF1 (Zhu *et al.,* 2015).

Protein-protein interactions can thus influence multiple aspects of protein function while in turn, phosphorylation can significantly impact protein-protein interactions (reviewed in Whitmarsh and Davis, 2000; Endt *et al.,* 2002; Ishimara and Yoshioka, 2012; Johnson, 2009; Nishi *et al.,* 2011). For transcription factors that participate in combinatorial control of gene expression, phosphorylation can define which transcriptional complexes form, by enhancing or suppressing interactions between specific transcriptional complex components, thus influencing the ability of the complex to drive the expression of a specific subset of genes (Shen *et al*., 2003; reviewed in Nishi *et al.,* 2011; Chi *et al.,* 2013). In addition, phosphorylation can modulate the interaction between transcription factors and other regulatory proteins, such as binding partners that block the ability of a transcriptional regulator to bind to target promoters or initiate transcription (reviewed in Whitmarsh and Davis, 2000; Endt *et al.,* 2002; Ishimara *et al.,* 2011; Chi *et al.,* 2013).

The goal of the experiments described below was to better understand how phosphorylation might affect MYB75, in terms of the localization of the protein, its turnover,

and its ability to bind known interacting partners. In these experiments phospho-analogues of MYB75 (phospho-null MYB75^{T131A}, and phosphor-mimic MYB75^{T131E}) were used to model unphosphorylated and permanently phosphorylated MYB75 protein, respectively.

2.4.1 Impact of phosphorylation status on MYB75 localization

The main function of transcription factors is to drive expression of target genes from specific promoters. Accessing these target promoters requires localization of the transcription factor to the appropriate cellular compartment. In the case of MYB75, whose known target genes are found in the nuclear genome, localization of the protein to the nucleus is essential for performing its main function. In eukaryotes, the selective import of proteins into the nucleus requires active transport through the Nuclear Pore Complex (NPC), which begins with the physical interaction between the protein designated for nuclear import and the NPC (reviewed in Hicks *et al.,* 1993; Lange *et al.,* 2006; McGonigle *et al.,* 2017). In order to bind to parts of the cellular machinery that mediate nuclear import, a cargo protein must possess a nuclear localization signal (NLS). Unlike some transport-related signal peptides, NLSs are not cleaved upon translocation to the nucleus, which means that the signal sequence can be located anywhere in the protein sequence. Animals, plants and fungi use similar NLS signal peptides. In plants, three main NLS types that have been well characterized, a) SV40-like sequences consisting of a single short stretch of basic amino acids (e.g. PKKKRKV); b) bipartite sequences, which contain two short stretches of basic amino acids (R/K) separated by ~10 undefined residues, and c) MAT α2-like NLS (K/RIPIK/R) which contains basic residues within a short stretch of hydrophobic amino acids (reviewed in Raikhel, 1992; Varagona *et al.,* 1992; Carrington *et al.,* 1991; Smith *et al.,* 1997). In addition, six other classes of NLS types have been

identified which bind importin-α, a key component of nuclear import machinery found in plants, animals and fungi (Smith *et al.,* 1997; Hübner *et al.,* 1999; Kosugi *et al.,* 2009). However, nuclear localization can be challenging to predict simply by looking at the amino acid sequence, as NLSs are loosely conserved, defined largely by the presence of short stretches of basic amino acids. Furthermore, nuclear localization of a protein is thought to involve multiple protein-protein interactions (for an example in plants, see McGonigle *et al.,* 2017). MYB75 contains several NLS's, including two classical bipartite sequences and two importin-α binding sites (Fig 2.3 A and B). None of these NLS sequences-overlap with the proposed phosphorylation sites, threonine 126 or 131, although one of bipartite NLSs is very close, ending at amino acid 123 (Fig 2.3 A and B).

Nuclear localization of wild type MYB75 has been previously demonstrated in *Arabidopsis* protoplasts (Bhargava *et al.,* 2010). However, little is known about the mechanism of MYB75 nuclear localization, or how that process is regulated. In order to assess whether the phosphorylation status at threonine 131 can affect MYB75 protein localization, each MYB75 phosphovariant was fused C-terminally to Green Fluorescent Protein (GFP) and introduced into *N. benthamiana* epidermal cells using *Agrobacterium*-mediated infiltration, for transient expression. This experiment was performed by Dr. Xiaomin Liu. Visualization of the transformed cells by fluorescence microscopy revealed that WT, T131A and T131E versions of MYB75 all localized to the nuclei of the epidermal cells, as is evident from the co-localization of the green GFP signal with DAPI nuclear label (Fig 2.3). While this was only a preliminary experiment, conducted at relatively low resolution, Dr. Liu's data suggest that phosphorylation at threonine 131 does not have any obvious effect on MYB75 subcellular localization.

Fig 2.3

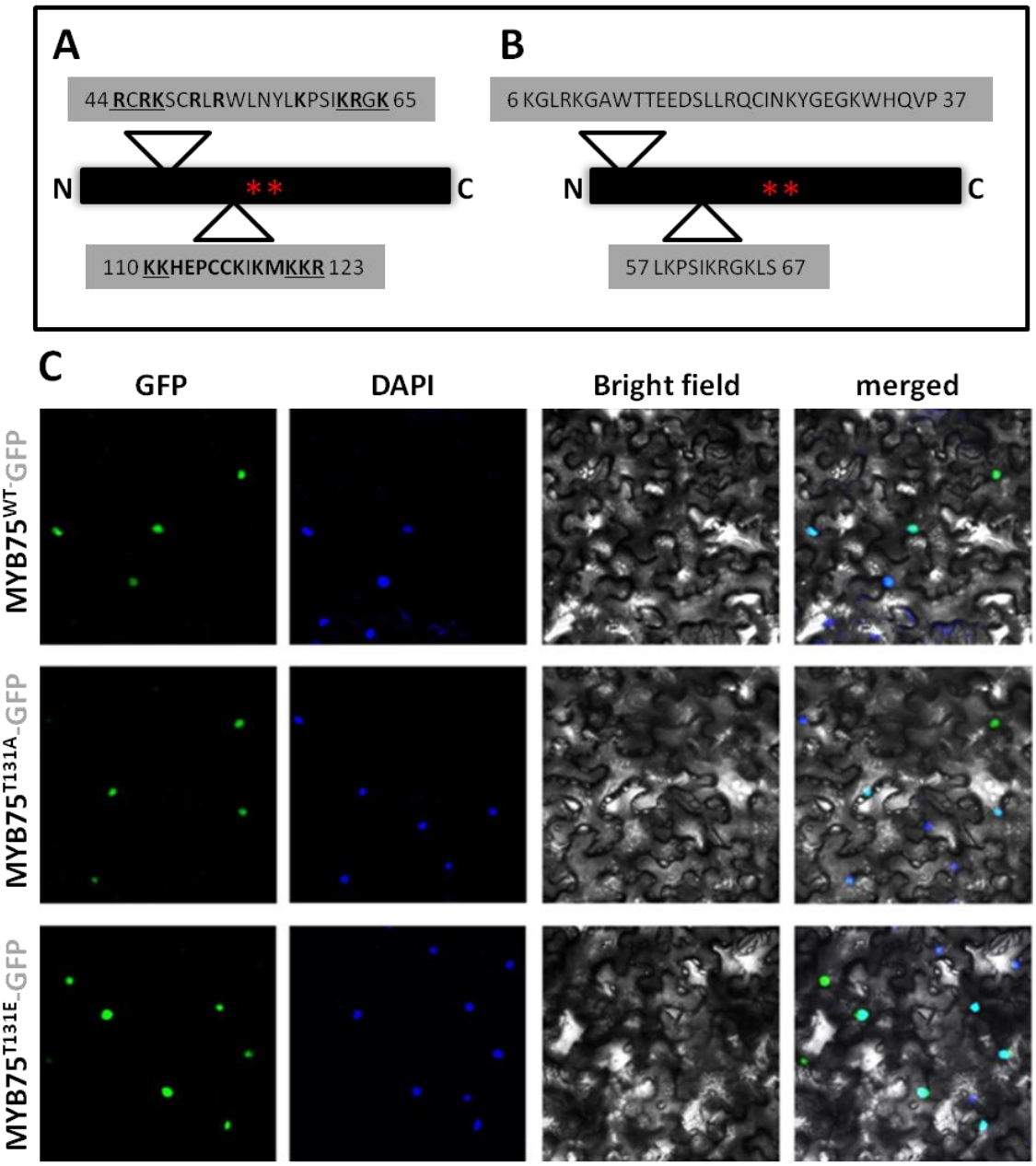
A
44 RCRKSCRLRWLNYLKPSIKRGK 65
N
C
110 KKHEPCCKIKMKKR 123
B
6 KGLRKGAWTTEEDSLLRQCINKYGEGKWHQVP 37
N
C
57 LKPSIKRGKLS 67
C
GFP
DAPI
Bright field
merged
MYB75WT-GFP
MYB75T131A-GFP
MYB75T131E-GFP

Fig 2.3 Nuclear localization of MYB75^{WT}, MYB75^{T131A} and MYB75^{T131E} in *N. benthamiana* epidermal cells. MYB75 has several nuclear localization sites, including two bipartite sequences (A), and two α–importin binding sites (B). Each of the MYB75 phosphovariants was C-terminally fused to GFP and introduced into *Agrobacterium tumefaciens* strain GV3103. Mature leaves of 3-week old *N. benthamiana* plants were infiltrated with *A. tumefaciens* culture carrying each of the GFP-fused MYB75 phosphovariants. Two days after infiltration, the leaves were mounted in water and visualized using Zeiss Pascal Scanning confocal microscope. MYB75^{WT}, MYB75^{T131A} and MYB75^{T131E} all show nuclear localization, as GFP signal co-localized with DAPI nuclear stain (C).

2.4.2 Impact of MYB75 phosphorylation on protein-protein interactions with known binding partners

MYB75 function *in vivo* is thought to be largely defined by its protein interaction network which includes the formation of regulatory complexes with several bHLH partners and TTG1, to drive expression of flavonoid biosynthetic genes (Gonzalez *et al.,* 2008). Interaction between MYB75 and TCP3 promotes the formation of the MYB/bHLH/WDR complex and enhances transcription of flavonoid biosynthetic genes (Li and Zachgo, 2013), while binding to JAZ1 and JAZ8 proteins has the opposite effect (Qi *et al.,* 2011). MYB75 also interacts with KNOX-homeodomain transcription factor, KNAT7, to negatively regulate secondary cell wall biosynthesis (Bhargava *et al.,* 2013). Finally, *MYB75* transcript turnover is diurnally regulated (Pan *et al,m* 2009) and it can be hypothesized that the size of the intracellular pool of MYB75 protein is therefore also likely to oscillate. Indeed, turnover of MYB75 in the dark has been shown to be mediated by its interaction with SPA1, SPA3 and SPA4, which leads to polyubiquitination of MYB75 by the COP-SPA complex and degradation by the 26S proteasome (Maier *et al.,* 2013).

The domains of MYB75 which participate in different types of protein-protein interaction have been defined for some, but not all of its known binding partners (Fig 2.4). For

instance, a detailed characterization of MYB-bHLH interaction has led to the identification of a specific motif and key residues, within the R3 domain of several MYB proteins (including MYB75), that are vital for interaction with bHLH transcription factors. (Fig 2.4 B) (Zimmermann *et al.,* 2004). Interestingly, the R3 domain was also shown to be important for interaction of MYB75 with KNAT7 (Bhargava *et al.,* 2013). JAZ1 and JAZ8 proteins were reported to bind to the C-terminal half of MYB75 (Fig 2.4 C), but in this case, the authors did not narrow down this interaction down to a specific domain (Qi *et al.,* 2011). The specific domain(s) of MYB75 required for interaction with TCP3, SPA1, SPA3 and SPA4 are unknown.

Fig 2.4

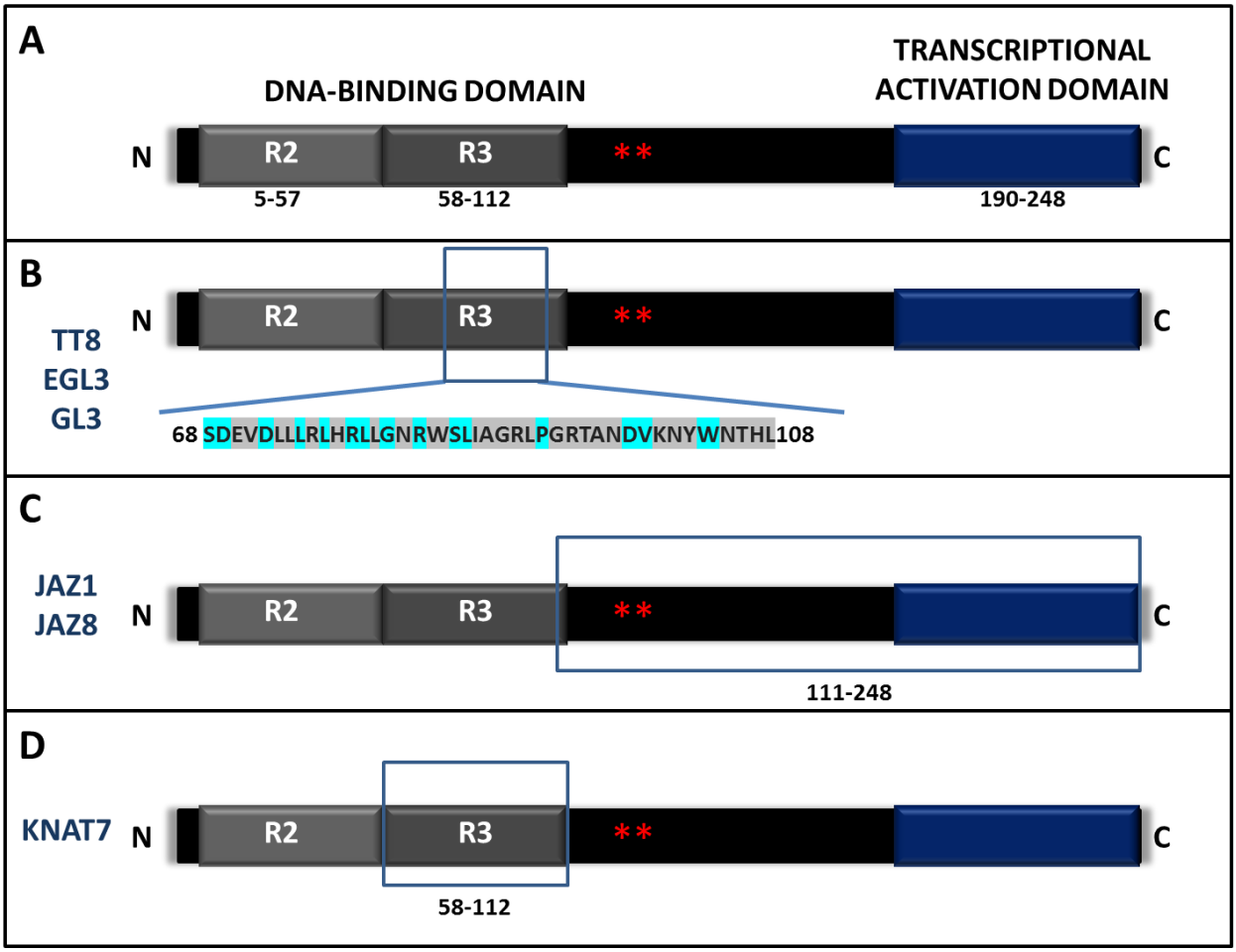

Fig 2.4 Linear representation of MYB75 amino acid sequence depicting different domains. The DNA binding domain is located near the N-terminus, and contains the R2R3 repeats, while the transcriptional activation domain lies in the last 58 amino acid of the C-terminus (A). The sequence required for binding to bHLH partners lies in the R3 domain of MYB75; the consensus sequence essential for the interaction with these partners is indicated, with key residues highlighted in blue (Zimmermann *et al.,* 2004) (B). (C). JAZ1 and JAZ8 are known to bind broadly to the C-terminal portion of MYB75, amino acids 111-248 (Qi *et al.,* 2011) (C). The R3 repeat region is required for interaction with KNAT7 (Bhargava *et al.,* 2013). Red asterisks indicate the location of the phosphorylation sites T126 and T131 (D).

To assess whether MYB75 phosphorylation status affects any of the known MYB75 protein-protein interactions, a directed yeast two-hybrid screen was conducted, using each of the MYB75 phosphovariants as prey and most of the MYB75 interacting partners as bait. The

only known interacting partner that was not included in the screen was SPL9; it was ultimately omitted due to time constraints and technical difficulties in cloning this gene into the pGBKT7 vector. The results of the yeast two-hybrid screen indicated that the interacting partners tested can bind all phosphovariants of MYB75 with equal affinity, with the exception of TCP3, which appeared to have a slightly weaker interaction with MYB75^{T131E} (Fig 2.5). Since TCP3-DBD displayed a high level of auto-activation in yeast, the strength of its interaction with MYB75 had to be assessed in higher stringency medium. Fig 2.5 (B) shows reduced growth of yeast colonies where TCP3-DBD was co-transformed with MYB75^{T131E}-AD compared to those co-transformed with MYB75 ^{WT}-AD, in drop out medium lacking histidine, but supplemented with 25mM 3AT. These data suggest that phosphorylation at T131 may weaken the ability of MYB75 to bind TCP3, an effect that may, in turn, interfere with the ability of TCP3 to induce the formation of the MYB-bHLH-WDR complex.

Fig 2.5

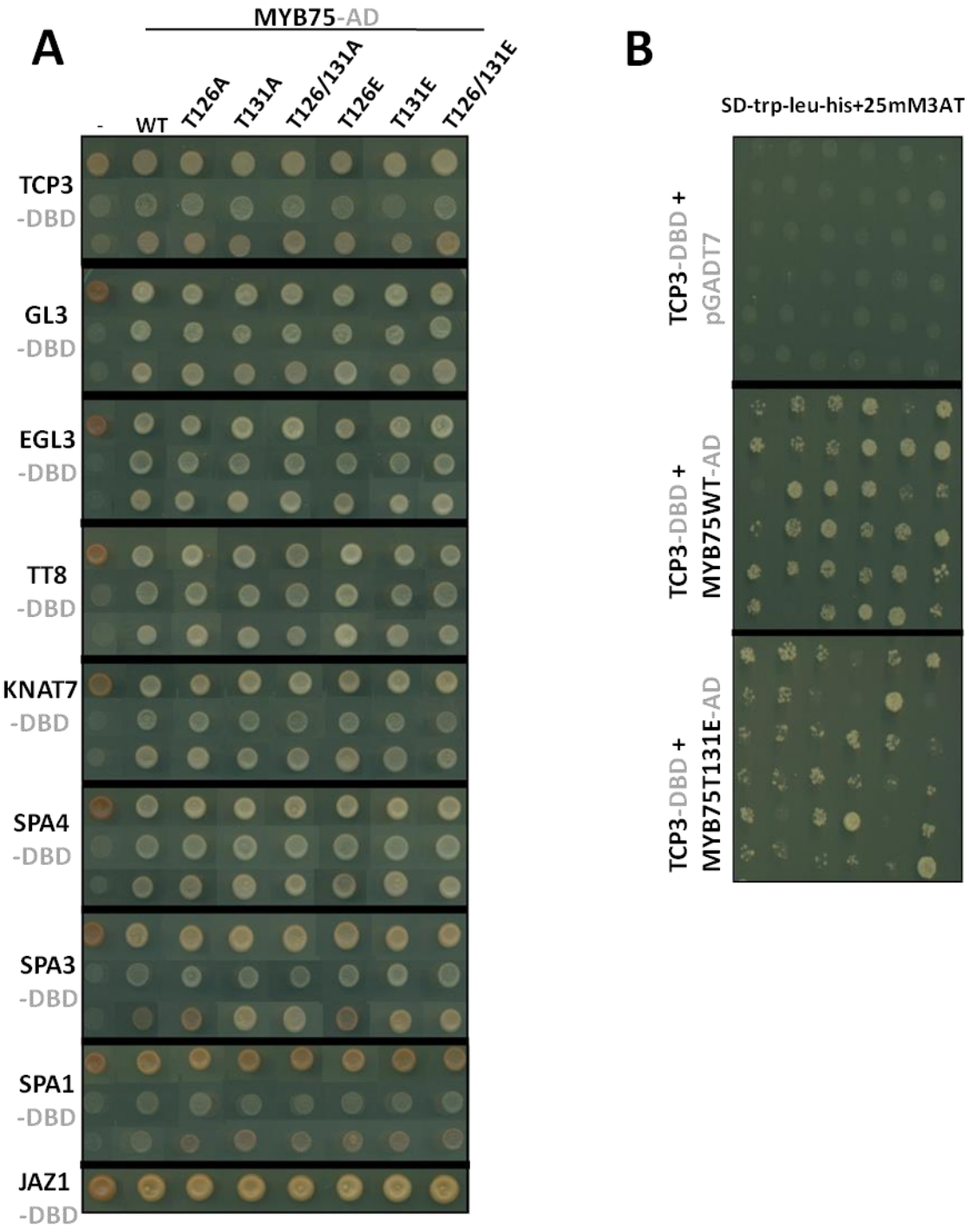
A
MYB75-AD
-
WT
T126A
T131A
T126/131A
T126E
T131E
T126/131E
TCP3 -DBD
GL3 -DBD
EGL3 -DBD
TT8 -DBD
KNAT7 -DBD
SPA4 -DBD
SPA3 -DBD
SPA1 -DBD
JAZ1 -DBD
B
SD-trp-leu-his+25mM3AT
TCP3-DBD + pGADT7
TCP3-DBD + MYB75WT-AD
TCP3-DBD + MYB75T131E-AD

Fig 2.5 Interaction between different phosphovariants of MYB75 and its known binding partners, in yeast. MYB75 interaction with previously described binding partners was assessed in a Y2H screen, using *MYB75* cDNA (WT and all phosphovariants) fused to GAL4-AD and each MYB75 binding partner fused to GAL4-DBD. The results in panel (A) indicate that the majority of partner proteins interact with all phosphovariant forms of MYB75 with equal affinity, except TCP3, which displayed a weaker interaction with $MYB75^{T131E}$. Panel (B) shows additional TCP3 test colonies growing on drop-out medium without histidine and with 25mM 3AT added, where yeast in which TCP3 was co-transformed with $MYB75^{T131E}$ displays reduced growth compared to TCP3 co-transformation with $MYB75^{WT}$.

2.4.3 Impact of MYB75 phosphorylation on protein turnover in *Arabidopsis* seedlings

In eukaryotes, several mechanisms of protein turnover exist which differ in terms of target specificity and method of degradation; three of the major pathways are autophagy, proteasomal degradation of polyubiquitinated proteins and cleavage by specific proteases.

Autophagy is a recycling system, involved in turnover of cellular debris, multi-molecular complexes, organelles and proteins, primarily for nutrient remobilization. In plants and yeast this process involves sequestration of cytosolic components destined for degradation in small membrane-bound vesicles called, autophagosomes, which deliver their contents to the central vacuole where they are degraded by hydrolases (reviewed in Araújo *et al.,* 2011; Li and Vierstra, 2012; Izumi *et al.,* 2013). Proteins destined for degradation by autophagy can also be targeted to the vacuole by chaperones, with a higher degree of target specificity. However, although this mechanism has been established in animals, it has not yet been described in plants (reviewed in Li and Vierstra, 2012).

Polyubiquitination and degradation of proteins by the 26S proteasome is a mechanism that plays a vital role both in recycling of misfolded proteins and in degradation of specific

protein targets (reviewed in Moon *et al.,* 2004; Vierstra, 2009). Ubiquitin is a 76 amino acid polypeptide that can be polymerized into polyubiquitin chains by E1 and E2 ubiquitin ligases, and covalently linked to a target protein by E3 ubiquitin ligases. The specificity displayed by this pathway depends on the ability of a particular E3 ubiquitin ligase to bind to a specific target protein. As previously described, SPA1, SPA3, and SPA4 are E3 ubiquitin ligases that bind to MYB75 and mediate its degradation in the dark (Maier *et al.,* 2013).

Plant proteases constitute another major mechanism of target-specific protein cleavage and degradation. Over 600 proteolytic enzymes have been identified in *Arabidopsis*, and many have been functionally characterized, although determination of *in vivo* target specificity remains a challenge. Proteases play a vital role in different aspects of development as well as response to environmental stimuli and stress, with perturbations in the expression of some proteases leading to lethal consequences for the plant (reviewed in Schaller, 2004; Van der Hoorn, 2008). Proteases recognize short peptide sequences and cleave the substrate proteins at specific amino acids within that site. The affinity of a protease for a particular target site can be affected by charge, polarity, pH, hydrophobicity and steric properties of the proteolytic substrate (Gu and Walling, 2000; Galiullina *et al.,* 2015). Furthermore, the substrate specificity of many proteases is ensured through their localization to specific cellular compartments where their targets are present (reviewed in Gu and Walling, 2000; Schaller, 2004; Van der Hoorn, 2008). To date, the only specific proteolytic mechanism known to be associated with MYB75 turnover is polyubiquitination of MYB75 by COP-SPA complexes in the dark.

To determine if phosphorylation can affect MYB75 turnover, a time-course protein degradation assay was conducted, using *Arabidopsis* seedlings transformed with either wild type MYB75 or the phosphomimic *MYB75*^{T131E} gene, both with an N-terminal 3xHA tag, expressed under the control of a DEX-inducible promoter. The assay was performed using small pools of seedlings incubated in 24 well plates, (~20-40 seedlings per well), containing liquid ½MS medium. To maximize protein accumulation, 11-day old seedlings were incubated for 24 hours in medium containing dexamethasone (DEX), which induced expression of the transgene, plus the MG132 proteasome inhibitor, which would prevent degradation of the newly synthesized 3xHA:MYB75 protein. After a period of induction, further protein translation was blocked via subsequent treatment with cycloheximide (CHX), and total protein was extracted from pooled samples of ~20-40 seedlings at different time points. The level of recombinant 3xHA:MYB75 protein in each pool of seedlings was assessed using western blot analysis and ImageJ quantification of the blot signals.

The results revealed a distinct difference in stability between the wild type and the T131E versions of 3xHA:MYB75, where MYB75^{T131E} was degraded much faster than its wild type counterpart (Fig 2.6). Both versions of the protein accumulate to comparable levels at the time of cycloheximide application (Fig 2.6 A, 0 hours), but after four hours MYB75^{T131E} was no longer detectable in the western blot, while the wild type protein remained abundant. The assay was repeated at least three times (see appendix for additional western blots), and while the absolute levels of protein detected could vary from one experiment to another at most time points, the pattern of more rapid degradation of the 3xHA:MYB75^{T131E} was observed in all replicates. Since the degradation experiment was performed under conditions of continuous

light, it is unlikely that COP-SPA complexes are involved in this differential degradation of MYB75^{T131E}. That interpretation is supported by the yeast two-hybrid data which demonstrated that the strength of interaction between MYB75 and SPA1, SPA3 or SPA4 is not affected by the phosphorylation status of the MYB75 protein (Fig 2.5). Together these data indicate that another protein turnover mechanism may be acting on MYB75, and that, at least under these conditions, MYB75^{T131E} is more susceptible to this type of degradation.

Fig 2.6

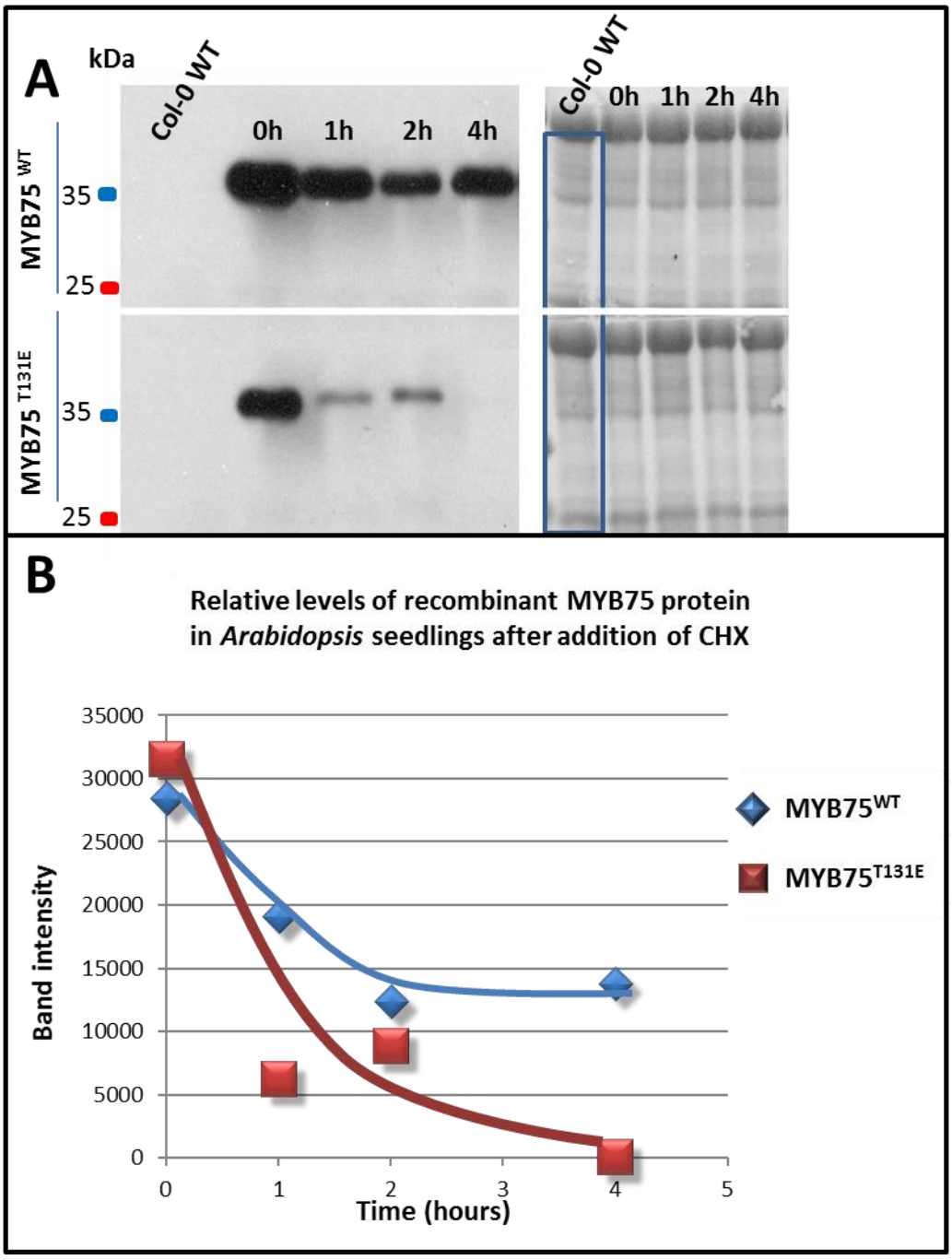
A
kDa
Col-0 WT
0h
1h
2h
4h
MYB75 WT
35
25
MYB75 T131E
35
25
Col-0 WT
0h
1h
2h
4h
B
Relative levels of recombinant MYB75 protein in Arabidopsis seedlings after addition of CHX
Band intensity
35000
30000
25000
20000
15000
10000
5000
0
0
1
2
3
4
5
Time (hours)
MYB75WT
MYB75T131E

Fig 2.6 Degradation of MYB75^{WT} and MYB75^{T131E} in *Arabidopsis* seedlings. MYB75^{T131E} is degraded more rapidly than MYB75^{WT}, in 12-day-old *Arabidopsis* seedlings, treated with cycloheximide (CHX), in liquid ½MS medium under continuous light. The protein degradation assay was performed using heterozygous *Arabidopsis* seedlings expressing N-terminal, 3xHA-tagged MYB75 (WT or T131E), under the control of a DEX-inducible promoter. Seedlings were grown on ½MS agar medium with 30µg/ml Hygromycin, under light fluence of ~35 µmol m^{-2} s^{-1}, and 16h light/8h dark photoperiod. Ten days after germination, hygromycin-resistant seedlings were transferred to 24 well plates, containing liquid ½MS medium, with ~20-40 seedlings per well. Recombinant MYB75 protein expression was induced by addition of 30µM DEX, with overnight incubation under continuous light, in the presence of 50µM MG132 proteasome inhibitor, to prevent protein degradation. The following day, the DEX/MG132-containing medium was removed and replaced with liquid ½MS containing 1mM CHX. Each well was harvested at a specific time point, immediately before (0h) and after (1h, 2h, 4h and 8h) addition of CHX. The seedlings were ground in liquid nitrogen and resuspended in a proportional amount of 2xSDS loading buffer. Western blot analysis was performed to detect the relative amount of recombinant MYB75 protein, present in the seedlings at each time point. Recombinant MYB75 was detected with anti-HA antibody (left panel), and the Ponceau-stained membrane was used to evaluate relative amounts of total protein loaded in each well (right panel) (A). Plot of MYB75 protein levels overtime, quantified using band intensities generated in western blots and analyzed with ImageJ software, with each western blot signal normalized to Ponceau background signal in the corresponding lane (B). Additional replicates displayed in the appendix Fig S2.2.

Fig 2.7

Fig 2.7 Heterozygous *Arabidopsis* lines (T2) carrying *DEXpr:3xHA:MYB75* constructs, 48 hours after application of DEX. Heterozygous lines carrying recombinant *MYB75* gene tagged with a 3xHA tag, under the control of a DEX-inducible promoter, were selected from a pool of T1 plants which displayed anthocyanin production 24-48 hours after DEX application. Four independent lines were isolated for each *DEXpr:3xHA:MYB75*^{WT} and *DEXpr:3xHA:MYB75*^{T131E}, all of which displayed patches of bright purple color after DEX application and abundant accumulation of recombinant MYB75 protein. *DEXpr:3xHA:MYB75*^{T131A} could not be isolated.

The DEX-inducible lines used in this assay were initially isolated based on visible anthocyanin accumulation in T1 plants after application of DEX to adult transformants growing on soil. These T1 plants showed anthocyanin accumulation in rosette leaves, manifested as purple colouration, approximately 48h after application of DEX (Fig 2.7). Plants showing this purple phenotype had MYB75 protein expression levels which could be readily detected by western blot. Curiously, none of these lines showed visible signs of anthocyanin accumulation after DEX induction in the seedling stage, i.e. under the conditions used in this protein degradation assay, despite expressing substantial amounts of recombinant MYB75 protein. It therefore appears that the experimental conditions employed in this degradation assay somehow prevented anthocyanin accumulation in seedlings, whereas DEX-induced MYB75 expression in soil-grown mature plants, led to abundant anthocyanin production. This observation prompted further exploration of how MYB75 protein stability and function might be affected by different environmental conditions *in vivo,* and the resulting consequences for anthocyanin production.

2.5 Discussion

In discussing the experimental results presented above, it is important to address the details of the recently published work on MYB75 phosphorylation by MPK4 (Li *et al.,* 2016), particularly the differences between their results and ours. Many of the differences between our findings and those of Li *et al.,* (2016) can probably be attributed to the tools employed in the two studies, starting with their use of a mutant 'constitutively active' form of MPK4 (CA-MPK4), which contains two amino acid substitutions (D198G/E202A). The authors initially identified MYB75 as a possible target of MPK4 phosphorylation by conducting a yeast two-

hybrid screen using the CA-MPK4 protein as bait and an *Arabidopsis* cDNA library as prey. According to their data, and contrary to ours, the native form of MPK4 did not interact with MYB75 in yeast. While yeast two-hybrid screening is a powerful tool for identifying putative protein-protein interactions, it can display a great deal of variability, as stringency and sensitivity of the assay differs between different yeast two-hybrid kits, and between the yeast strains used in a given experiment. We observed this in our own work: when Dr. Zhenhua Yonge initially started working on this project, she conducted a directed yeast two-hybrid screen using the Invitrogen *Proquest* ® kit. In this system, only MPK11 could interact with MYB75 (unpublished observations). When I repeated the directed yeast two-hybrid experiment using the Clontech Matchmaker® system, I was able to corroborate Dr. Yonge's data, showing that MYB75 interacted strongly with MPK11. However, I also observed that MYB75 interacted very strongly with MPK3, MPK13, MPK14 and MPK20, and showed a moderate level of interaction with MPK6, MPK10, MPK18 and MPK19. In the work reported by Li *et al*., (2016), the yeast two-hybrid experiments were conducted using Clontech Matchmaker® Gold kit, which is an updated version of the Matchmaker® kit used in my work. While the basic constructs employed by Clontech kits are the same, the yeast strains and the selectable markers have distinct differences. In my work, I used histidine and adenine deficiency as the primary selectable markers to identify interactions, and increasing stringency of selection using 3AT to evaluate interaction strength. In contrast, the authors of Li *et al.,* (2016) used serial dilutions of their yeast cultures to demonstrate interaction strength. Furthermore, the Y2HGold yeast strain, employed in their study contains an additional selectable marker, namely resistance to Aureobasidin antibiotic, which is activated upon positive bait-prey interaction. Together, these

technical differences could potentially explain why I was able to identify a broad range of MYB75 interacting partners, among the 20 native *Arabidopsis* MAP kinases.

A major information gap in my work is the lack of *in vivo* data to corroborate our yeast two-hybrid results. Li *et al.,* (2016) demonstrated that MYB75 could interact in *N. benthamiana* epidermal cells with both CA-MPK4 and native MPK4, but not with a mutated kinase-inactive form of MPK4 (T201A/Y203F), using a Bimolecular Fluorescence Complementation (BIFC) assay and co-immunoprecipitation (CO-IP) of MPK4 using HA-tagged MYB75 (Li *et al.,* 2016, Fig 1 B and C). Their results suggest that either *N. benthamiana* can activate some of the transgenic MPK4 from *Arabidopsis*, or that MYB75 has some affinity for native MPK4 *in vivo*.

Our data also differ from the findings reported by Li *et al.,* (2016) with respect to the *in vitro* phosphorylation of MYB75 by MAP kinases. According to the data generated by Dr. Zhenhua Yonge, and subsequently corroborated by Dr. Xiaomin Liu in our lab, MYB75 phosphorylation by MPK3, MPK4, MPK6 and MPK11 occurs almost exclusively at threonine 131 (Fig 2.2). In contrast, Li *et al*., (2016) demonstrated that both threonine 126 and 131 are phosphorylated by CA-MPK4 in *vitro* (Li *et al*., 2016, Fig 5A). Once again, there are several technical differences between our experiments and those described by Li *et al*., (2016). In our lab, MYB75 was N-terminally fused to glutathione S-transferase (GST). The protein was produced in *E. coli* and purified *in vitro*, then combined with each recombinant MAPK in the presence of radiolabelled ATP and a constitutively active recombinant MKK (see Material and Methods). In Li *et al.,* (2016), MYB75 was fused to a smaller, affinity tag (6xHis), and the *in vitro* phosphorylation was performed using recombinant CA-MPK4. The advantage of our approach is

that it involved a genuine MPK activation by CAMKKs, while Li *et al.,* (2016) used a mutant form of MPK4, one which imitated the activated form of the MAP kinase. One major shortcoming of our approach is the use of a large GST tag on the recombinant MYB75 construct. While GST is a commonly used and proven tool, this tag is ~24kDa in size, which could present significant steric hindrance for a relatively small protein like MYB75 (~28kDa), possibly blocking access to some sites. If the large N-terminal GST tag happened to shield threonine 126 in our assay, leaving only threonine 131 to be phosphorylated by MPKs, this steric hindrance would be one possible explanation for the divergence between our *in vitro* phosphorylation data and the results presented by Li *et al*., (2016).

The authors of Li *et al*., (2016) also did not address the impact of MYB75 phosphorylation on protein-protein interactions with known MYB75 binding partners, whereas I conducted a comprehensive yeast two-hybrid screen of all known binding partners of MYB75 (except SPL9), against all MYB75 phosphovariants, and found that $MYB75^{T131E}$ displayed reduced binding affinity to TCP3. I next intended to corroborate this yeast-based observation *in vivo*, using BIFC in plant cells. Demonstrating that the interaction between $MYB75^{T131E}$and TCP3 had been reduced compared to $MYB75^{WT}$, but not eliminated, required at least a semi-quantitative method. For this purpose, I designed a multi-colour BIFC assay, where TCP3 was fused to a C-terminal portion of a cyan fluorescent protein; $MYB75^{WT}$ was fused to the N-terminal portion of Venus (a variant of yellow fluorescent protein); and $MYB75^{T131E}$ was fused to the N-terminal portion of cerulean (a variant of blue fluorescent protein). The experiment was designed as a competitive binding assay, whereby the final colour detected by fluorescence

microscopy of the protoplast population would be indicative of which variant of MYB75 (WT or T131E) had greater affinity for TCP3 (Fig 2.8).

Unfortunately, the transformation efficiency I obtained in *Arabidopsis* protoplasts was not high enough to allow me to perform this assay in a quantifiable fashion. Co-transformation of each TCP3 and individual MYB75 variants (WT or T131E) yielded a fluorescence signal in each case, but only 1-3 nuclei were showing fluorescence for each interaction pair tested. However co-transformation of three constructs (N-VENUS:MYB75^{WT}, N-CERULEAN:MYB75^{T131E} and C-CFP:TCP3), for the final competitive fluorescence assay did not yield any signal. Despite several attempts, I was unable to improve the protoplast transformation efficiency, and I concluded that alternative approaches to testing the interaction strength between TCP3 and each variant of MYB75 will be required. One such alternative would be transient co-infiltration of all three constructs into *N. benthamiana* epidermal cells, or *Arabidopsis* seedlings, which typically yields a higher transformation efficiency. This approach, however, would have required the transfer of existing BIFC constructs into binary vectors, for *Agrobacteria-mediated* infiltration and transient expression, which would have demanded more time than was available at this point.

Fig 2.8

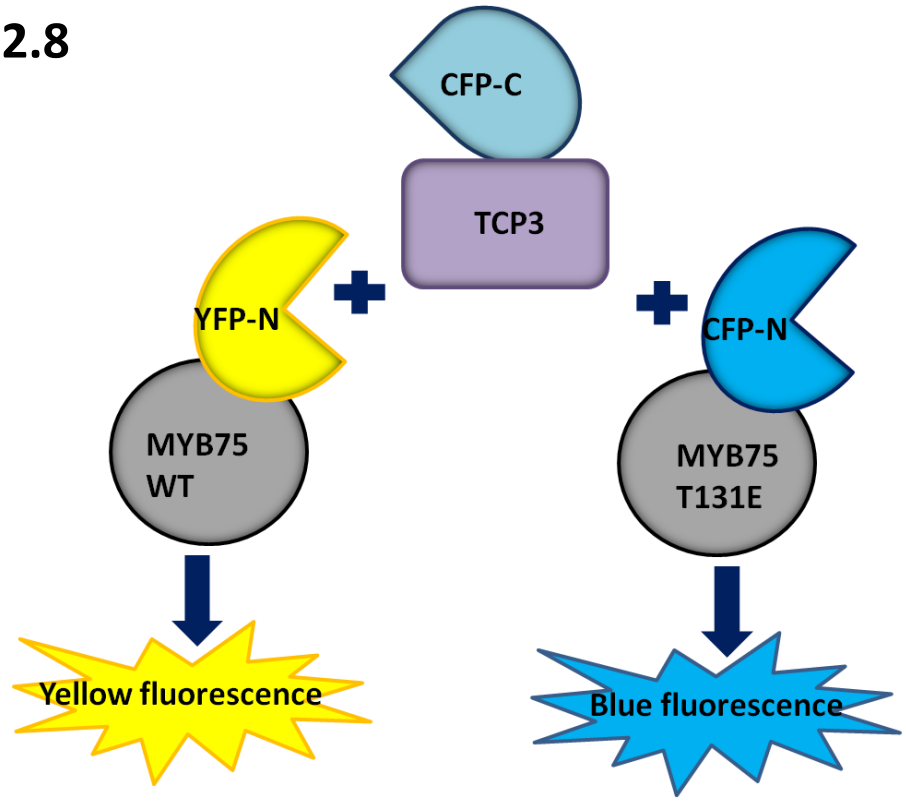

Fig 2.8 Experimental design for MYB75-TCP3 competitive binding assay. Each MYB75 ORF (either WT or T131E) was cloned into pSAT4-nVENUS-N and pSAT4-nCERULEAN-N, creating fusion proteins where each MYB75 phosphovariant was N-terminally fused to the N-terminal portions of either VENUS or CERULEAN florescent proteins respectively. TCP3 was cloned into pSAT4-cCFP-C, fusing TCP3 to the C-terminal portion of CFP. The competitive binding assay was conducted by co-transforming all three constructs displayed above into *Arabidopsis* protoplasts, for transient expression. The ability of TCP3 to interact with one or both phosphovariants of MYB75 should be assessed by observing the predominant colour of fluorescence in the nuclei of the protoplasts, using a fluorescent microscope. If TCP3 has equal affinity for both phosphovariants, yellow and blue fluorescence should be observed in equal proportion, however, if MYB75^{T131E} has a reduced affinity for TCP3, only yellow (or mostly yellow) but little or no blue fluorescence should be observed.

Since Dr. Yonge and Dr. Liu demonstrated that *in vitro* phosphorylation of MYB75 by MPK3, MPK4, MPK6 and MPK11 occurs predominantly at threonine 131 (Fig 2.2), I chose to focus my subsequent experiments on phosphovariants T131A and T131E. Li *et al*., (2016), on the other hand used double mutants, T126/131A (AA) and T126/131D (DD). For unknown

reasons they chose to use aspartic acid instead of glutamic acid to replace threonines 126 and 131 in their phosphomimic form of MYB75, although most phosphomimic studies have used glutamate to replace threonine. A detailed discussion on multi-site phosphorylation of target proteins will be postponed until Chapter 3; here, I will address how different experimental conditions in the protein degradation assays performed in our lab and those performed by Li *et al*., (2016) could have led to opposing results.

My data indicates that phosphomimic MYB75^{T131E} is degraded more rapidly *in vivo* than MYB75^{WT} (Fig 2.6), while Li *et al*., (2016) found that phosphomimic MYB75 was more stable than WT (or AA mutant). In my protein degradation experiment, I used DEX inducible lines expressing 3xHA-tagged MYB75 (WT and T131E), and the degradation assay was performed as a time course experiment (0-8 hours) under continuous light, in liquid ½MS (see Materials and Methods). Li *et al.,* (2016) evaluated degradation of MYB75 in dark-adapted seedlings grown on solid medium after a period of 24 hours. Some of the factors that could have affected MYB75 turnover rate in our experiment include prolonged immersion in liquid medium and incubation in small wells which could possibly limit gas exchange. Notably, anthocyanin accumulation was not observed in these seedlings, despite incubation under continuous light for over 48 hours, and induction of substantial levels of recombinant MYB75 protein expression by DEX treatment. Anthocyanins have been shown to accumulate in various plant species, (including *Arabidopsis*) in response to drought (reviewed in Chalker-Scott, 2002). Excess water, on the other hand, can suppress accumulation of flavonoids and anthocyanins in submerged plant tissues (Nanjo *et al.*, 2011), which could explain why seedlings floating in liquid media did not show purple colour despite over-expressing MYB75. Additionally, ethylene gas can have a negative impact on

anthocyanin production, and ethylene has been shown to prevent anthocyanin accumulation under conditions of poor gas exchange (Craker and Wetherbee, 1973; Jeong *et al.,* 2010).

The differences between the experimental conditions I used and those used by Li *et al.,* (2016) make it very challenging to compare our data. Since little is known about post-translational regulation of MYB75, it is possible that there are undiscovered mechanisms of MYB75 protein turnover that are specific to particular environmental conditions. Our data suggest that, in seedlings immersed in liquid for a period over 48 hours, $MYB75^{T131E}$ undergoes a faster turnover than $MYB75^{WT}$, despite being continuously exposed to light. These striking differences between my results and those of Li *et al.,* (2016) may provide a starting point for investigation of the interaction between light, gas exchange (ethylene), and other aspects of the plant physical environment in controlling turnover of MYB75.

Protein degradation experiments conducted by Li *et al*., (2016) suggest that the action of the 26S proteasome plays a key role in MYB75 turnover, since addition of MG132 led to significant increase in protein levels of $MYB75^{AA}$ and $MYB75^{WT}$, as well as moderate increases in the levels of $MYB75^{DD}$ protein (the levels of this phosphomimic form were relatively high prior to addition of MG132) (Li *et al.,* 2016 Fig 7B). In my experiments MG132 was primarily used, in conjunction with DEX, to induce accumulation of recombinant MYB75 protein: both DEX and MG132 were removed prior to addition of cycloheximide, at the beginning of the time course experiment (0h), and thus protein turnover was monitored in the absence of MG132. Although both my data and that of Li *et al.,* (2016) show that 26S proteasome plays an important role in MYB75 turnover, we cannot exclude the possibility that other protein degradation mechanisms

participate in MYB75 protein degradation. To answer this question it is worthwhile repeating my time-course experiments with MG132 included in the cycloheximide-containing media in order to monitor protein turnover rates in the absence of 26S proteasome function, which could help uncover additional MYB75 protein degradation mechanisms, and determine how phosphorylation affects this process.

Perhaps the biggest challenge in studying MYB75 dynamics is the fact that anthocyanin production, and therefore MYB75 expression respond rapidly to multiple environmental stimuli. Environmental condition had to be considered carefully in designing each experiment, with the understanding that those particular conditions would inevitably influence the outcome, and hence my interpretation of the results. My data indicates that MYB75 phosphorylation at threonine 131 has a negative impact on protein stability under certain conditions and has a reduced affinity towards TCP3 *in vitro*. Both of these outcomes would be anticipated to have a negative effect on anthocyanin accumulation *in vivo*. While some of our data contradicts the conclusions presented by Li *et al.,* (2016), these discrepancies can potentially reflect the technical differences between the two studies. It is also important to bear in mind that the scope of my study differed from that of the Li group; they focused on delineating the impact of MPK4 phosphorylation on MYB75 (at T126 and T131), while my focus was on understanding how phosphorylation of MYB75 by one of several MPKs (at T131 alone) impacts flavonoid biochemistry and plant development *in vivo*.

2.6 Materials and Methods

2.6.1 Yeast two-hybrid screen

2.6.1.1 Cloning constructs for Yeast two-hybrid screen

To test the interaction between MYB75 and 20 *Arabidopsis* MAP kinases, and between different MYB75 phosphovariants and known MYB75 binding partners, a directed Yeast two-hybrid screen was conducted using the Clontech Matchmaker® yeast two-hybrid kit. To create bait and prey constructs, the full length CDS of each gene was amplified by PCR from total *Arabidopsis* cDNA (Col-0 ecotype), using Phusion® polymerase (New England Biolabs) and primers listed in tables 2.1 and 2.2. Purified PCR products were digested with corresponding restriction enzymes and ligated into pGBKT7 or pGADT7 vector, using T4 DNA ligase (Invitrogen), creating bait and prey constructs respectively. For cloning of MYB75 phosphovariants, cDNA clones provided by Dr. Zhenhua Yonge were used as templates: these were generated by Dr. Yonge, through site-directed mutagenesis, using QuickChange II kit (Agilent Technologies). I created all the constructs listed in tables 2.1 and 2.2, with the exception of MPK3, MPK4 and MPK6 in pGBKT7, which were cloned by Dr. Xiao Min Liu. MYB75 and GL3 display transcriptional activity in yeast, which resulted in strong false positives when either of these proteins was fused to the GAL4 DNA-binding domain. To test the interaction between MYB75 and GL3, a truncated version of each MYB75 phosphovariant (MYB75-58aa), lacking the transcriptional activation domain, was cloned into pGBKT7, while GL3 was cloned into pGADT7.

Table 2.1 Primers for cloning constructs for the directed yeast two-hybrid screen between MYB75 and 20 *Arabidopsis* MAP kinases.

cDNA	PRIMER SEQUENCES	Restriction sites	VECTOR
MPK1	F-5' GGCGAATTCGCGACTTTGGTTGATCCTCC R-5' GCCGGATCCGTCAGAGCTCAGTGTTTAAGGTTG	**EcoRI/BamHI**	**pGBKT7**
MPK2	F-5' GGCGAATTCGCGACTCCTGTTGATCCACCTAATGG R-5' GCCGGATCCGTCAAAACTCAGAGACCTCATTG	**EcoRI/BamHI**	**pGBKT7**
MPK3	F-5' CGCGAATTCATGAACACCGGCGGTGGCC R-5' GCGGATCCCTAACCGTATGTTGGATTGAG	**EcoRI/BamHI**	**pGBKT7**
MPK4	F-5' CGCGAATTCATGTCGGCGGAGAGTTGTTTC R-5' GCGGATCCTCACACTGAGTCTTGAGG	**EcoRI/BamHI**	**pGBKT7**
MPK5	F-5' GGCCCATGGAGGCGAAGGAAATTGAATCAGCGACAG R-5' GGCGTCGACG TTAAATGCTCGGCAGAGGATTGAACTTC	**NcoI/SalI**	**pGBKT7**
MPK6	F-5' CGCCATATGATGGACGGTGGTTCAGGTC R-5' GCGGATCCCTATTGCTGATATTCTGGATTG	**NdeI/BamHI**	**pGBKT7**
MPK7	F-5' GGCGAATTCGCGATGTTAGTTGAGCCACCAAATGG R-5' GCCCTGCAGCTTAGGCATTTGAGATTTCAGCTTCAGG	**EcoRI/PstI**	**pGBKT7**
MPK8	F-5' GGCCATATGGGTGGTGGTGGGAATCTCGTCGACG R-5' GGCCCATGGGCTTAAGAATTGTGAAGAGAAGCAACTTTATC	**NdeI/NcoI**	**pGBKT7**
MPK9	F-5' GGCGAATTCGATCCTCATAAAAAGGTTGCACTGG R-5' GCCCTGCAGCTCAAGTGTGGAGAGCCGCGACCTTTTGAGAC	**EcoRI/PstI**	**pGBKT7**
MPK10	F-5' GGCGAATTCGAGCCAACTAACGATGCTGAGAC R-5' GCCGGATCCGTCAATCATTGCTGGTTTCAGGGT	**EcoRI/BamHI**	**pGBKT7**
MPK11	F-5' GGCCCATGGAG TCAATAGAGAAACCATTCTTCGGTGATG R-5' GGCGTCGACGTTAAGGGTTAAACTTGACTGATTCACGA	**NcoI/SalI**	**pGBKT7**
MPK12	F-5' GGCGAATTCTCTGGAGAATCAAGCTCTGGTTCTACCG R-5' GCCGGATCCGTCAGTGGTCAGGATTGAATTTGACAG	**EcoRI/BamHI**	**pGBKT7**
MPK13	F-5' GGCGAATTCGAGAAAAGGGAAGATGGAGGGA R-5' GCCGGATCCGTTACATATTCTTGAAGTGTAAAGACTC	**EcoRI/BamHI**	**pGBKT7**
MPK14	F-5' GGCGAATTCGCGATGCTAGTTGATCCTCCAAATG R-5' GCCGGATCCGTTAAGCTCGGGGGAGGTAATGAAGC	**EcoRI/BamHI**	**pGBKT7**
MPK15	F-5' GCCGGATCCGTGGTGGTGGTGGCAATCTCGTCGACGG R-5' GCCCTGCAGCCTAAGAATTGTGTAGAGATGCAACTTTCAC	**BamHI/PstI**	**pGBKT7**

Table 2.1 (continued) Primers for cloning constructs for the directed yeast two-hybrid screen between MYB75 and 20 *Arabidopsis* MAP kinases.

MPK 16	F-5' GGCCCATGGAGCAGCCTGATCACCGCAAAAAGTCATCAG R-5' GGCGTCGACGTTAATACCAGCGACTCATTGCAGTATCTTG	**NcoI/SalI**	**pGBKT7**
MPK17	F-5' GGCCCATGGAGTTGGAGAAAGAGTTTTTCACGGAGTATGG R-5' GGCGTCGACGCTATGACACTGCAGAGGAGACACCAACAC	**NcoI/SalI**	**pGBKT7**
MPK18	F-5' GGCGAATTCCAACAAAATCAAGTGAAGAAGGGC R-5' GCCGGATCCGCTATGATGCTGCGCTGTAACTAATTGTGC	**EcoRI/BamHI**	**pGBKT7**
MPK19	F-5' GGCGAATTCCAAAAAACTCAGGAGAAGAAGAACATGAAAGAGATGG R-5' GCCGGATCCGCTAAGACATGCCATACCCAACAGCTCC	**EcoRI/BamHI**	**pGBKT7**
MPK20	F-5' GCCGGATCCGTCAGCAAGATAATCGCAAAAAGAATAATCTG R-5' GGCGTCGACGCTAGTACATCTTTGACATACCGTACCG	**BamHI/SalI**	**pGBKT7**
MYB75	F-5' GGCGAATTCGAGGGTTCGTCCAAAGGGCTG R-5' GCCGGATCCGCTAATCAAATTTCACAGTCTCTCC	**EcoRI/BamHI**	**pGADT7**

Table 2.2 Primers for cloning constructs for the directed yeast two-hybrid screen between MYB75 phosphovariants and previously characterized interacting partners of MYB75.

cDNA	PRIMER SEQUENCES	Restriction sites	VECTOR
MYB75	F-5' GGCGAATTCGCGACTTTGGTTGATCCTCC R-5' GCCGGATCCGTCAGAGCTCAGTGTTTAAGGTTG	**EcoRI/BamHI**	**pGADT7**
MYB75-58aa	F-5' GGCGAATTCGCGACTCCTGTTGATCCACCTAATGG R-5' GCCGGATCCGCTATTGGTCTTTCTTCTTATCTTTGTTG	**EcoRI/BamHI**	**pGBKT7**
EGL3	F-5' GGCGAATTCGCAACCGGAGAAAACAGAACG R-5' GCCGGATCCGTTAACATATCCATGCAACCCTTTG	**EcoRI/BamHI**	**pGBKT7**
GL3	F-5' GCCGAATTCGCTACCGGACAAAACAGAACAACTG R-5' GCCGGATCCGTCAACAGATCCATGCAACCCTTTG	**EcoRI/BamHI**	**pGADT7**
TT8	F-5' GGCGAATTCGATGAATCAAGTATTATTCCGGC R-5' GGCGGATCCGCTATAGATTAGTATCATGTATTATGACTTG	**EcoRI/BamHI**	**pGBKT7**
TCP3	F-5' GGCGGATCCGTGCACCAGATAACGACCATTTC R-5' GCCCTGCAGCTTAATGGCGAGAATCGGATGAAGC	**BamHI/PstI**	**pGBKT7**
JAZ1	F-5' GGCGAATTCTCGAGTTCTATGGAATGTTCTG R-5' GCCGGATCCGTCATATTTCAGCTGCTAAACCGAGC	**EcoRI/BamHI**	**pGBKT7**

Table 2.2 (continued) Primers for cloning constructs for the directed yeast two-hybrid screen between MYB75 phosphovariants and previously characterized interacting partners of MYB75.

JAZ8	F-5' GGCCCATGGAGAAGCTACAGCAAAATTGTGAC R-5' GCCCTGCAGCTTATCGTCGTGAATGGTACGGTG	**NcoI/PstI**	**pGBKT7**
SPA1	F-5' GGCCCATGGAGCCTGTTATGGAAAGAGTAGCTG R-5' GCCCTGCAGCTCAAACAAGTTTTAGTAGCTTCATG	**NcoI/PstI**	**pGBKT7**
SPA3	F-5' GGCGAATTCGAAGGTTCTTCAAATTCTAACTCTAGGG R-5' GCCGGATCCGTCAAGTCATCATCTCCAGAATT	**EcoRI/BamHI**	**pGBKT7**
SPA4	F-5' GGCGAATTCAAGGGTTCTTCAGAATCTAGTTCC R-5' GCCGGATCCGTCATACCATCTCCAAAATCTTGATA	**EcoRI/BamHI**	**pGBKT7**
KNAT7	F-5' GGCGAATTCCAAGAAGCGGCACTAGG R-5' GCCGGATCCGTTAGTGTTTGCGCTTGGAC	**EcoRI/BamHI**	**pGBKT7**

2.6.1.2 Yeast transformation and screen for protein-protein interactions by yeast two-hybrid

Yeast strain AH109 (Clontech), which has the phenotype -leu-trp-his-ade, was used for the directed yeast two-hybrid screen. Competent AH109 cells were co-transformed with 1-2µg of each prey and bait constructs, plated on agar plates containing dropout media without leucine and tryptophan (SD-trp-leu), and incubated for three-four days at 30˚C. Successful transformations (plates with at least 100 colonies), were used for replica plating on different selective media as shown in Fig 2.6. Interaction strength was determined based on colony colour, on the medium SD-trp-leu (red= no interaction, white= strong, pink= weak-moderate), and on survival on dropout media without histidine (SD-trp-leu-his) with either 1mM, 2.5mM, 5mM, 10mM or 25mM 3-aminotriazole (3AT), as well as on medium lacking histidine and adenine (SD-trp-leu-his-ade). A total of eight representative colonies were replica plated per bait-prey combination.

Fig 2.9

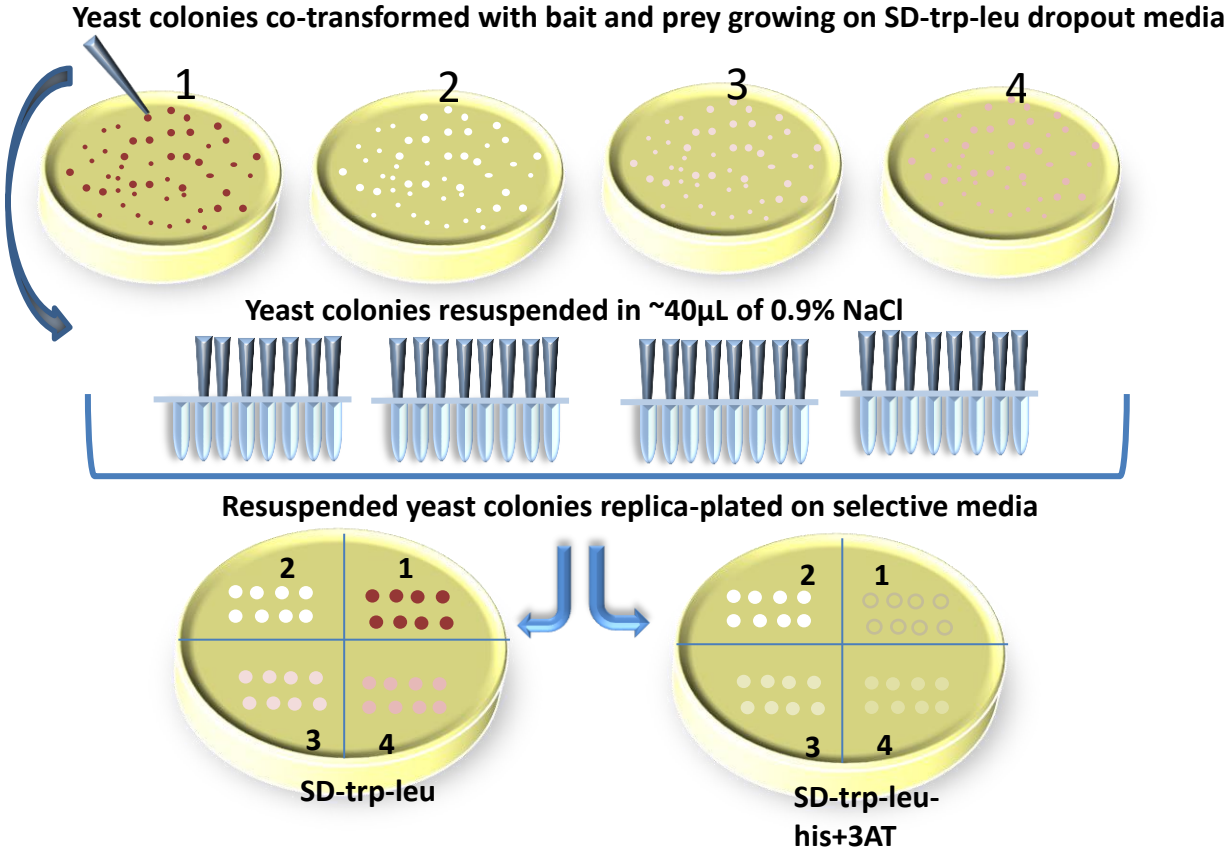

Fig. 2.9 Replica plating procedure used in the directed yeast two-hybrid screen. Yeast colonies co-transformed with bait and prey constructs, growing on SD-trp-leu plates were replica-plated on different selective media to test the strength of interaction between the fusion proteins. A total of eight colonies were used per bait-prey combination. Each colony was resuspended in 40µL of 0.9% NaCl, and 2µL of cell suspension were pipetted unto each selection plate. The media used in the screen included SD-trp-leu, SD-trp-leu-his-ade and SD-trp-leu-his+3AT with 3AT concentrations of 1mM, 2.5mM, 5mM, 10mM and 25mM. The replica plates were incubated for 3 days at 30°C, and the resulting colonies were photographed. Interaction strength was determined based on colour on SD-trp-leu, and colony survival on SD-trp-leu-his+3AT, and SD-trp-leu-his-ade media.

2.6.2 *In vitro* phosphorylation of MYB75 by MAP kinases

This experiment was performed by Dr. Zhenhua Yonge and Dr. Xiao Min Liu

2.6.2.1 Cloning and recombinant protein purification

Constitutively active MKK6 and MKK9 (CAMKK6 and CAMKK9) were previously created by Dr. Jin Suk Lee, by replacing serine and threonine residues, found in the activation loop with acidic residues, using site-directed mutagenesis (S221D and T227E for CAMKK6, and S195E and S201E for CAMKK9; Lee, 2008). CAMKK6, CAMKK9, MPK3, MPK4, MPK6 and MPK11 were cloned by Dr. Jin Suk Lee into pGEX 4T-2 vector, to create recombinant proteins containing an N-terminal Glutathione S-transferase (GST) tag. Full cDNA of WT MYB75, as well as phosphonull mutants ($MYB75^{T126A}$, $MYB75^{T131A}$ and $MYB75^{T126/131A}$) were cloned by Dr. Zhenhua Yonge into pGEX 4T-1 to generate recombinant proteins with N-terminal GST tags. All expression vectors were transformed into chemically competent *E.coli* (BL21). Induction of recombinant protein expression was performed by adding 0.5mM isopropyl 1-thio-ß-galactopyranoside (IPTG), to liquid cultures in mid-log phase, followed by an additional incubation for 4h at 25°C. Recombinant proteins were purified using Glutathione Sepharose® 4B beads (GE Healthcare), according to manufacturer's protocol. The concentration of each purified recombinant protein was determined using Bio-Rad protein assay, with BSA as a standard.

2.6.2.2 *In vitro* kinase assay

This experiment was performed by Dr. Zhenhua Yonge.

Phosphorylated MAPKs were prepared as described in Ellis and Lee (2007), by pre-incubating purified GST-MPK3 with GST-CAMKK9, and each GST-MPK4, GST-MPK6 and GST-MPK11 with GST-CAMKK6, at a CAMKK:MPK ratio of 1:4, in kinase reaction buffer (25mM Tris-HCl pH7.5, 5mM ß-glycerolphosphate, 2mM dithiothreitol, 10mM $MgCl_2$, 200µM ATP), at 30°C

for 30 min. MYB75 *in vitro* phosphorylation was performed by combining 3mg of each GST-MYB75 phosphovariant (T126A, T131A and T126/131A) with 1mg of each activated GST-MPK, in 20ml of kinase reaction buffer. The reaction was initiated with 1µCi [Y-32P] ATP, and incubated at 30°C for 45 min, and terminated by adding 5µL of 4xSDS loading buffer, boiling the samples for 5min, and cooling them on ice. The samples were resolved on a 12% SDS-PAGE gel, transferred to a nylon membrane and visualized using autoradiography, and Coomassie brilliant blue R-250 staining.

2.6.3 Intracellular localization of different phosphovariants of MYB75 protein: cloning of MYB75:GFP constructs and Agrobacterium-mediated infiltration of Nicotiana benthamiana epidermis (performed by Dr. Liu).

Full cDNA of each $MYB75^{WT}$, $MYB75^{T131A}$ and $MYB75^{T131E}$ was amplified by PCR using the forward-5'CGGGGTACCATGGAGGGTTCGTCCAAAGG, and reverse-5' CGCTCTAGAATCAAATTTCACAGTCTCTC primers. Each PCR product was purified, digested with *KpnI* and *XbaI* restriction enzymes, and ligated, using T4 DNA ligase (Invitrogen), into the binary vector pCAM1300-35S-GFP (which was previously digested with KpnI and XbaI), to create MYB75:GFP fusion proteins. The constructs were introduced into competent *Agrobacteria tumefaciens* strain GV3101. For transient expression in *N. benthamiana*, Agrobacterial cultures, carrying each construct were grown overnight at 30°C. The following day, OD_{600} was determined and the bacterial cells were harvested by centrifugation. Each culture was resuspended in infiltration buffer (10mM MES pH5.6, 10mM $MgCl_2$, 0.15mM acetosyringone), to a final OD_{600}=1.0. Infiltration was performed by injecting the suspension into the abaxial side of mature leaves of three-week-old *N. benthamiana* plants (kept covered overnight to induce

stomatal opening), using a plastic syringe. The plants were incubated for two days after the infiltration. After two days the transformed leaves were sampled and the area infiltrated was cut out and mounted in water unto microscope slides. Images were acquired using a Zeiss Pascal scanning confocal microscope.

2.6.4 Protein degradation assay

2.6.4.1 Constructs and plant material

Plants used in this assay were *Arabidopsis* seedlings (Col-0 background) carrying *MYB75* gene (WT and T131E) fused in frame with a 3X Hemagglutinin tag at the N-terminus, and under the control of a dexamethasone-inducible promoter; *DEXpr:3xHA:MYB75 gene* (see section 3.6.1). Heterozygous T2 seedlings were selected on *½ Murashige* and *Skoog* (½MS) agar medium, containing 30µg/ml hygromycin and surviving seedlings were used for the protein degradation assay described below. Phosphovariant genotypes of all transgenic plants were confirmed by sequencing the transgene.

2.6.4.2 Time-course protein degradation assay

Arabidopsis seedlings were germinated and grown on petri plates, containing *½* MS agar medium with hygromycin, under long day conditions (16h light/8h dark), and light fluence of ~35µmol m^{-2} s^{-1}. Nine day old *Arabidopsis* seedlings carrying *DEXpr:3XHA:MYB75*^{WT} and *DEXpr:3XHA:MYB75*^{T131E} were transferred from selection plates to liquid ½MS in 24 well plates, with 1ml of medium in each well and approximately 20-40 seedlings per well. Plants were incubated overnight under the same light conditions to allow them to adjust to the liquid medium. The next day, the medium was removed and replaced with liquid ½ms containing 30µM dexamethasone (DEX; Sigma Aldrich), and 50µM MG132 proteasome inhibitor (Santa

Cruz Biotech), to induce *MYB75* gene expression and prevent protein degradation respectively. After addition of DEX and MG132 the seedlings were incubated under continuous light (~35µmol m^{-2} s^{-1}) overnight, to increase MYB75 protein accumulation. The next day the medium was removed, and the seedlings were washed at least three times with liquid ½MS, before adding 1ml of ½MS containing 1mM cycloheximide (CHX; Sigma Aldrich) to each well, to block protein translation. At each time point (1h,2h,4h and 8h) all the seedlings were harvested from a single well, dried by blotting on a kimwipe, weighed and immediately frozen in liquid nitrogen. MYB75 protein in each pool of seedlings was detected by western blot analysis, using an anti-HA primary antibody and relative protein levels were determined by evaluating band intensity using ImageJ.

2.6.4.3 SDS-PAGE and Western Blot analysis

Plant tissue expressing 3XHA-tagged MYB75 was frozen in liquid nitrogen, ground to a fine powder and 2XSDS loading buffer was directly added to the ground tissue. In assays where relative protein quantification was required, fresh weight of the plant tissue was determined, and 1µL of 2xSDS loading buffer was added for every 1mg of plant tissue, to facilitate equal loading of protein lysate. For each sample, 10µL of plant lysate was loaded per well and protein samples were resolved on SDS-PAGE (10% acrylamide). Wet protein transfer from SDS-PAGE gel to Immun-Blot® PVDF membrane (Biorad) was performed for 1h at 100V. Western blot detection of recombinant MYB75 protein was performed using a 1:1000 dilution of a primary anti-HA antibody (high affinity rat-monoclonal, clone 3F10, Roche), and a 1:5000 dilution of a secondary antibody conjugated with HRP (goat anti-rat IgG-HRP Santa Cruz Biotech Sc-2032). Chemiluminescent signal detection was performed using ECL western blot reagent (Pierce ™

ECL plus) and recorded on photosensitive film (Bioflex Blue Lite EC by Mandel Scientific). After western blot detection, each PVDF membrane was stained with IDGel™ PONCEAU dye (DGel Electrosystems Inc.) to determine relative amount of total protein in each well. All blots and PONCEAU-stained membranes were scanned for subsequent analysis using ImageJ.

2.6.4.4 ImageJ quantification of relative protein levels

ImageJ was used to determine relative protein levels, by quantifying band intensity in western blots images. In blots where high levels of protein resulted in signal bleed through between individual lanes, such that bands appeared fused, individual bands were moved apart in Microsoft Paint prior to conducting ImageJ analysis, ensuring that neither background nor individual band intensity was altered (see Appendix, Fig S2.1). Band intensity was determined for each western blot sample (MYB75 band), and corresponding lane from PONCEAU stained membrane. Relative MYB75 protein quantity detected in the western blot was determined by dividing the area representing western blot band intensity by the normalized area obtained from the PONCEAU stain of the corresponding well. Each semi-quantitative western blot analysis was performed at least twice, to ensure that the patterns of protein degradation are reproducible. Results displayed in Fig 2.5 are from a single representative experiment.

CHAPTER 3 The impact of MYB75 protein phosphorylation status on production of anthocyanins and flavonoids in *Arabidopsis* plants

3.1 Introduction

The transient nature of protein phosphorylation presents a large obstacle to understanding the impact of this post-translational modification on protein function *in vivo,* and the effect it has on processes controlled by the protein in question. With transcription factors such as MYB75 it is particularly challenging, as any alterations to protein function can have pleiotropic effects on the organism. To understand how phosphorylation might be impacting MYB75 function *in vivo* I chose to create stable transgenic *Arabidopsis* lines expressing different phosphovariant mutant forms of the MYB75 protein. I then examined the impact of expression of these phosphovariant proteins on the plant phenotype. MYB75 is known to play a role in cell wall development (Bhargava *et al,* 2013) and may be implicated in other developmental processes, either directly or through its influence on flavonol levels (Buer and Djordjevic 2009; *Peer et al*, 2001). However, phenotypic abnormalities such as changes in cell wall thickness or developmental modifications can be difficult to quantify and interpret, particularly in lines where *MYB75* expression is driven by a constitutive CAMV35S promoter, which results in ectopic production of the protein. Anthocyanin accumulation, on the other hand, can be visually monitored in plants, and total anthocyanin quantities can be measured using biochemical extraction and spectrophotometric determination methods. Furthermore, anthocyanin levels are very responsive to MYB75 activity. Accumulation of anthocyanin visibly

spikes in *Arabidopsis* plants that are over-expressing *MYB75*, such as the *PAP1-D* over-expression lines, first described by Borevitz *et al,* (2000).

The work described in this chapter explores the ability of different MYB75 phosphovariants to drive anthocyanin production in *Arabidopsis,* under regular growth conditions and under stress, such as continuous light and elevated sucrose, both conditions that are known to induce MYB75-dependent anthocyanin accumulation. The ultimate goal of these experiments was to gain insight into how phosphorylation might affect the ability of MYB75 to drive transcription of anthocyanin biosynthetic genes in *Arabidopsis.* This chapter also describes how MYB75 protein accumulation is affected by different conditions, building on our results from Chapter 2, where the phosphovariant $MYB75^{T131E}$ was shown to be more labile than $MYB75^{WT}$. Finally, I describe how the biochemical profiles of flavonol and anthocyanin compounds are affected in *Arabidopsis* plants over-expressing different phosphovariants of MYB75.

The first part of this chapter describes initial attempts to create transgenic *Arabidopsis* lines expressing different phosphovariant versions of MYB75. While these experiments ultimately did not yield transgenic lines that lent themselves to robust analyses, they did provide useful insights into the functional importance of introns in the *MYB75* gene and highlighted some differences between the Nossen and Col-0 *Arabidopsis* ecotypes, with respect to anthocyanin production. The remainder of the chapter describes work performed using transgenic *MYB75* over-expression lines, in which the gene version of each phosphovariant, with an N-terminal 3xHA- epitope tag, was expressed under the control of a strong, constitutive promoter (CAMV35S).

3.2 Expression of different *MYB75* phosphovariants from the *MYB75* endogenous promoter

My initial attempt to create transgenic MYB75 phosphovariant plants involved transforming *Arabidopsis myb75*$^{-}$ null mutants (Nossen background) with each *MYB75* phosphovariant cDNA, under the control of the *MYB75* endogenous promoter. This project was initially undertaken by Dr. Zhenhua Yonge, who created the constructs and transformed *Arabidopsis* plants, at which point I took over, and began selecting T1 plants by screening for enhanced anthocyanin production under high light conditions. The ability of each MYB75 phosphovariant to drive anthocyanin production was tested simultaneously with promoter functionality, by stressing the adult transgenic plants with continuous light, for at least 48hours before measuring anthocyanin content in mature rosette leaves. Complementation of anthocyanin deficiency typical of *myb75*$^{-}$ null mutant plants, by each phosphovariant, was evaluated by comparing anthocyanin levels in transgenic lines to levels in Nossen wild type plants, grown under the same conditions. Analysis of numerous T1 plants generated with each phosphovariant revealed that *MYB75*^{T126A} -expressing plants, grown under light stress conditions were able to accumulate average anthocyanin levels, comparable to those seen in Nossen wild type plants. In contrast, plants carrying *MYB75*^{T131A} and *MYB75*$^{T126/131A}$ phosphovariants showed only marginal levels of anthocyanin production, which did not differ significantly from those seen in the parental *myb75*$^{-}$ mutant phenotype (Fig 3.1A). In other words, these phosphovariant forms did not show complementation of the *myb75*$^{-}$ mutant anthocyanin accumulation phenotype.

The anthocyanin accumulation data presented in Fig 3.1 (A) were generated using pooled tissue samples, derived from several individual transgenic lines. When data from the individual lines were plotted separately, however (Fig 3.1B), it is obvious that the apparent genotype-specific differences seen in Fig 3.1 (A) data stemmed from pronounced differences seen in between individual lines. This was particularly clear for the *MYB75*^{T126A} lines, where lines 1,2,5 and 6 showed anthocyanin levels comparable to Nossen wild type plants, while lines 3 and 4 displayed anthocyanin levels closer to those of the untransformed *myb75*$^{-}$ mutant (Fig 3.1B). Despite these large differences between individual transgenic lines, the overall pattern suggested that blocking possible phosphorylation at threonine 126 did not interfere with the ability of the phosphomutant MYB75 to upregulate anthocyanin production under light stress, whereas blocking phosphorylation at threonine 131 renders MYB75 ineffective as a complementing agent. Upon examining the levels of *MYB75* transcripts in these lines, however, using semi-quantitative reverse transcription polymerase chain reaction, it became clear that *MYB75* expression levels correlated with anthocyanin production in each line. (Fig 3.1C). The activity of the endogenous *MYB75* promoter is highly sensitive to light, at least in part through positive regulation by HY5 (Shin *et al*, 2013), and accordingly, in our experiments *MYB75* expression was relatively high under continuous light, in both Col-0 and Nossen wild type plants, as well as in *MYB75*^{T126A} lines 1,2 and 5, as shown in Fig 3.1C (lines 6 RNA was degraded and was not included in the analysis). The failure of *MYB75*^{T131A} lines to yield *MYB75* expression levels comparable to wild type, made these lines unsuitable for further experiments. A similar problem was encountered with *MYB75*^{T126E} and *MYB75*^{T131E}, transgenic lines; transgenic *MYB75*

expression in these plants was extremely low, and no complementation of the *myb75*$^{-}$ anthocyanin deficiency phenotype was observed (data not shown).

Fig 3.1

A Anthocyanin production under continuous light, in 6-week-old *Arabidopsis* plants carrying *MYB75*pr:*MYB75*cDNA transgene
-*myb75*⁻ Nossen background-

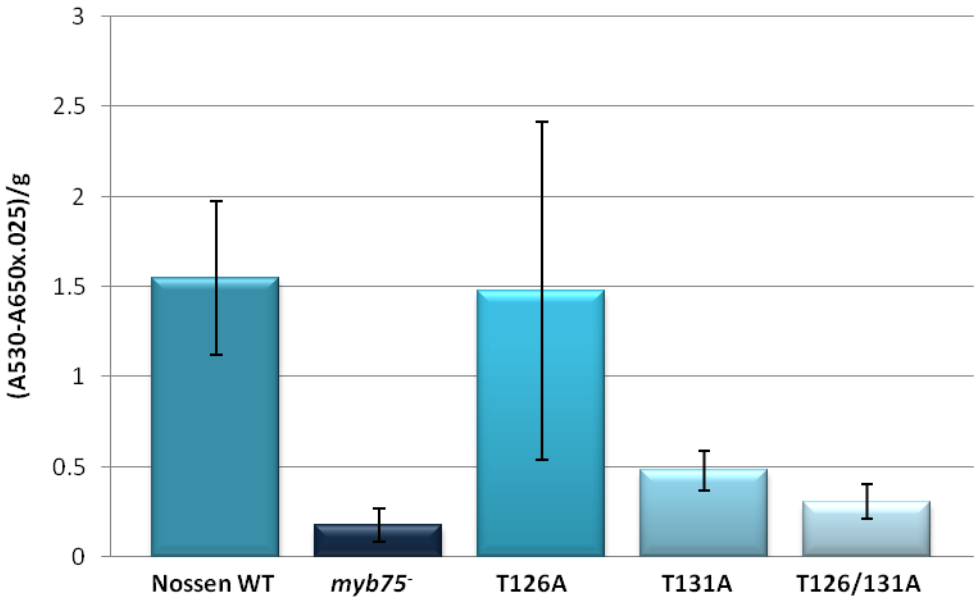

B Anthocyanin production in individual *Arabidopsis* lines carrying the *MYB75*pr:*MYB75*cDNA transgene, under continuous light
-*myb75*⁻ Nossen background-

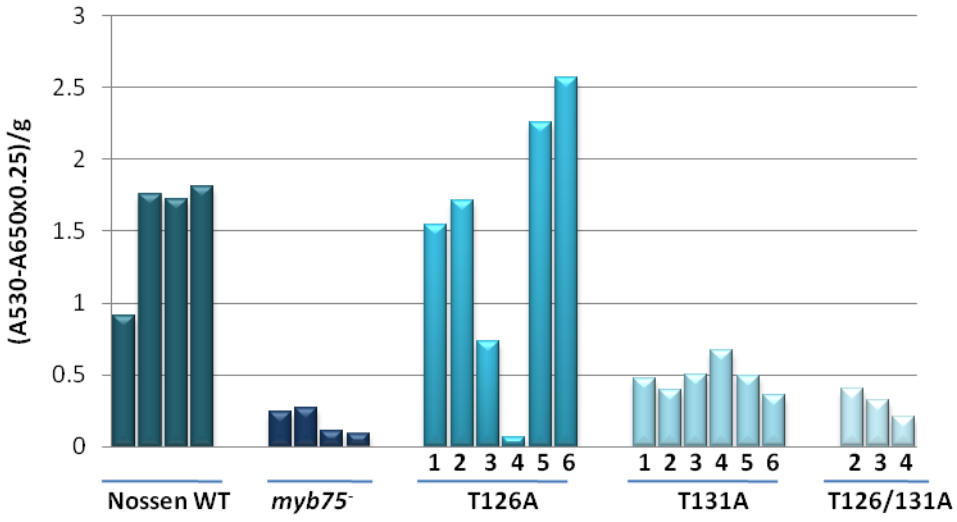

Fig 3.1 continued

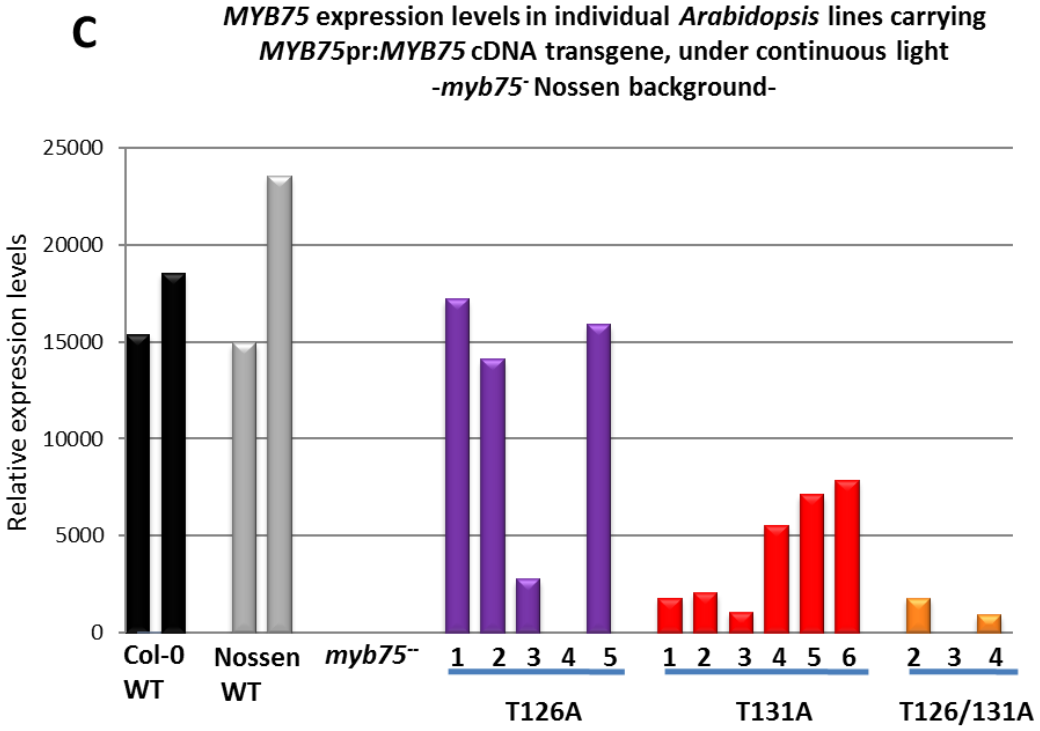

Fig 3.1 Complementation of anthocyanin biosynthesis in *Arabidopsis myb75*- null mutants, by different MYB75 phosphovariants, driven by the *MYB75* endogenous promoter. *MYB75* cDNA (including wild type and each phosphovariant single and double point-mutant), was introduced into a binary vector, along with ~2.7kb of sequence upstream of the MYB75 translational start site, as the endogenous *MYB75* promoter. Each *MYB75*pr:*MYB75 cDNA* construct was transformed into *myb75*- mutant plants (Nossen background), and several lines were isolated for each phosphovariant genotype. The ability of each phosphovariant to complement anthocyanin production in *myb75*- mutants was evaluated in ~6-week-old heterozygous T2 plants, exposed to continuous light, for over 48 hours. Total anthocyanin was extracted from mature rosette leaves, using 49% methanol, 1% acetic acid aqueous solution. Anthocyanin levels were evaluated spectrophotometrically and normalized to fresh weight using the formula (A530-A650X.25)/g. Expression of recombinant *MYB75* was determined using semi-quantitative reverse transcription polymerase chain reaction (RT-PCR) and quantified using ImageJ software. Total anthocyanin levels for each genotype are shown in (A) and represent average values for 6-12 plants (see materials and methods), error bars represent ±SD. Average anthocyanin levels suggest that anthocyanin production was recovered in MYB75^{T126A} lines, but not in MYB75^{T131A} or MYB75$^{T126/131A}$ mutants (A). Examination of anthocyanin levels in individual lines revealed that only lines 1,2,5 and 6 from MYB75^{T126A} genotype produced anthocyanin levels comparable to Nossen wild type (B). Gene expression analysis revealed that only lines which showed anthocyanin complementation were expressing recombinant MYB75 to levels comparable to wild type plants (C).

Assessing the impact of MYB75 phosphorylation on anthocyanin production required that all phosphovariants be expressed at comparable levels, in order to correlate anthocyanin quantity with presence of MYB75 protein. Furthermore, since MYB75 protein stability appeared to be affected by phosphorylation, as demonstrated in Chapter 2, detectable protein levels were essential to support any claim that a biochemical change might be due to MYB75 phosphorylation status. In an ongoing effort to establish *Arabidopsis* lines with stable expression of MYB75 protein, Dr. Xiao Min Liu attempted to detect different tagged versions of $MYB75^{T131A}$ and $MYB75^{T131E}$, when expressed in a *myb75*$^{-}$ null mutant background (Nossen ecotype). Unfortunately, lines expressing hemagglutinin epitope-tagged (HA-tagged) *MYB75* cDNA, driven by the endogenous *MYB75* promoter did not yield any detectable protein, for any of the phosphovariants (data not shown). Use of a strong constitutive (CAMV35S) promoter to drive FLAG-tagged *MYB75* cDNA lines (also created by Dr. Liu) yielded marginally better results; protein was detectable only after transformed seedlings were incubated overnight with proteasome inhibitor, MG132, under continuous light. Protein could not be detected in soil grown mature plants, and no changes in anthocyanin levels were observed, either visually or after extraction and spectrophotometric evaluation (data not shown).

I initially attributed the failure to recover a single line with easily detectable ectopic MYB75 protein expression, even when the cDNA expression was being driven by a strong constitutive promoter, to the ecotype background being used. Since Nossen wild type plants were known to produce slightly less anthocyanin than the Col-0 wild type (Teng *et al.,* 2005), I hypothesized that MYB75 protein levels might be under tighter regulation in the Nossen ecotype, either through enhanced MYB75 protein degradation or through artificial selection of

transgenic lines with lower *MYB75* transgene expression, driven by embryonic and/or seedling lethality of T1 plants that express higher levels of MYB75. However, although attempts to express tagged *MYB75* cDNA from a CAMV35S promoter in the Col-0 background yielded plants with strong anthocyanin production, it was still not possible to detect the recombinant MYB75 protein in tissue extracts (data not shown). Finally, I decided to use the full gene version of *MYB75* instead of the cDNA, since previous studies by Borevitz *et al.,* (2000) and Dare *et al.,* (2008), involved over-expression of the full length *MYB75* gene.

I first used site-directed mutagenesis to generate $MYB75^{T131A}$ and $MYB75^{T131E}$ versions of the *MYB75* gene. I then chose to use the constitutive CAMV35S promoter rather than the endogenous promoter, to drive the expression of the full gene variants. This was done in order to ensure high levels of *MYB75* expression, but also to avoid possible autoregulation effects alluded to in the literature (Dare *et al.,* 2008), where the authors suggested that MYB75 may affect its own expression, an idea that is substantiated by the presence of PCE cis-elements in the *MYB75* promoter. Such autoregulation has been demonstrated for TT8, (a transcriptional regulator of anthocyanin biosynthesis and a binding partner of MYB75). TT8 was shown to regulate its own expression in plants by binding to its own promoter (Baudry *et al.,* 2006). If such an autoregulation mechanism existed for *MYB75* and were in any way affected by the protein's phosphorylation status, levels of transgenic MYB75 could be differentially influenced in individual phosphovariant lines, thus leading to different expression levels of the protein. Since assessing the ability of each phosphovariant to drive anthocyanin production requires that the transgenic lines used in the analysis produce comparable levels of recombinant MYB75, it was important to eliminate any variables that could impact expression levels of individual

phosphovariants. I reasoned that using a constitutive promoter would eliminate any differences in recombinant protein expression that might result from autoregulation and allow me to obtain high levels of MYB75 protein expression, thereby facilitating correlation of recombinant protein levels with anthocyanin accumulation.

In addition to this consideration, I chose to use Col-0 wild type plants to transform the recombinant full length *MYB75* gene phosphovariant constructs, rather than use the Nossen background, since Col-0 plants over-expressing MYB75 (*PAP1-D*) are known to accumulate very high levels of anthocyanins (Borevitz *et al.,* 2001). The *PAP1-D* phenotype thus, provides a reference point for the anthocyanin levels we can expect to obtain from successful *MYB75* over-expression. Col-0 plants also displayed higher levels of anthocyanin accumulation in our own experiments than did plants of the Nossen ecotype. This is consistent with published data by Teng *et al*., (2005; Fig 2) where natural variation in anthocyanin accumulation, elicited by sucrose treatment was evaluated across 43 separate ecotypes, and Col-0 plants displayed higher levels of anthocyanin production than did the Nossen ecotype.

I generated multiple lines expressing the full gene version of wild type, phosphonull and phosphomimic *MYB75* (referred to as $MYB75^{WT}$, $MYB75^{T131A}$ and $MYB75^{T131E}$ respectively), under the control of the CAMV35S promoter. In each case the ectopic protein carried an N-terminal 3xHA- epitope tag to enable easy protein detection. These lines will be referred to here as *35pr:3xHA:MYB75 gene* lines, and the shorthand notation used throughout this thesis is *35Spr:MYB75* ($MYB75^{WT}$, $MYB75^{T131A}$ and $MYB75^{T131E}$, where specification of the phosphovariant was required).

Several lines were established for each phosphovariant by immunoscreening T1 plants to identify those which were producing detectable levels of MYB75 protein. Such plants also consistently displayed bright purple colouration in mature rosette leaves, resulting from accumulation of anthocyanins. Four lines were isolated for*35Spr:MYB75*^{WT}; L2, L11, L12 and L14 (L2 was rarely used due to its low germination rates). In addition, three lines were established for *MYB75*^{T131A}; L1, L22 and L23, and four for *MYB75*^{T131E}; L2, L4, L5 and L9. I chose to use heterozygous T2 plants throughout this thesis, in order to save time and avoid losing transgene expression through gene silencing over generations, which has been reported in *Arabidopsis* and transgenic crops where the 35S promoter was used (reviewed in Rajeevkumar *et al* 2015).

3.3 Impact of sucrose and light on MYB75 protein stability and anthocyanin production in *Arabidopsis* seedlings

35Spr:3xHA:MYB75 gene lines were isolated by immunoscreening a large number of T1 plants (at least 50 plants were screened per genotype) for MYB75 protein expression, using western blotting and a monoclonal antibody raised against the hemagglutinin polypeptide. Several lines of each phosphovariant, expressing detectable MYB75 protein, were isolated in this fashion, all the T1 plants which showed detectable protein levels also displayed purple colouration in mature rosette leaves, resulting from anthocyanin accumulation, reminiscent of *PAP1-D*. Curiously however, none of these lines showed any visible signs of anthocyanin production while growing on petri plates under long day conditions as seedlings (see Materials and Methods), that are comparable to *PAP1-D* seedlings, which displayed a distinct purple colour, visible with the naked eye, under the same conditions. This lack of anthocyanin accumulation in *35Spr:MYB75* seedlings in petri dishes could have been caused by a number of

environmental factors, suppressing anthocyanin biosynthesis, or promoting anthocyanin degradation, including lower light fluence in the chamber where the petri plates were incubated, than in the growth chambers where the mature plants were grown (see Materials and Methods).

Sucrose and light are both known to positively regulate *MYB75* expression and anthocyanin production. While sucrose has been shown to affect *MYB75* primarily at the transcriptional level (Teng *et al.,* 2005), light is also known to promote MYB75 protein stability by destabilizing COP/SPA ubiquitin ligase complexes, which target MYB75 protein for degradation in the dark (Maier *et al*, 2013). The goal of the first series of experiments I conducted (using transgenic lines over-expressing the full gene version of each MYB75 phosphovariant), was to examine how sucrose and light affected the levels of recombinant MYB75 protein in seedlings, and ultimately to determine if there are any differences between the phosphovariants of MYB75, in terms of protein stability or ability to drive anthocyanin production at early stages of the plant life cycle.

To test the impact of sucrose and light on *35Spr:3xHA:MYB75 gene* lines, heterozygous T2 seedlings were germinated on ½ MS medium with hygromycin and grown for ten days. Ten-day-old seedlings were transferred to petri plates containing solid ½MS medium supplemented with 6% sucrose and incubated under continuous light for 24 hours, using 20-30 seedlings for each phosphovariant, with proportional representation of each line. The untreated control plants were kept on the original plates without sucrose and incubated under short day photoperiod (16 hours dark, 8 hours light). Although *35Spr:MYB75* seedlings did not display accumulation of anthocyanin comparable to *PAP1-D* lines, closer examination of *35Spr:MYB75*

seedlings, using a dissecting scope (see Material and Methods), revealed that even under short day conditions, without sucrose, *35Spr:MYB75 gene* lines displayed subtle signs of anthocyanin production, not seen in the Col-0 wild type controls. Seedlings of over-expressor lines, including *35Spr:MYB75^{WT}, 35Spr:MYB75^{T131A}* and *35Spr:MYB75^{T131E}*, but not Col-0 WT, displayed limited but visible accumulation of anthocyanins near the apical meristem (Fig 3.2A). After treatment with 6% sucrose under continuous light, all plants, including Col-0 wild type controls, showed visible signs of increased anthocyanin accumulation, manifested as purple colouration in all plant organs, with some variation in colour intensity between individuals of each line (Fig 3.2A). Notably, some of the transgenic seedlings over-expressing *MYB75^{WT}, MYB75^{T131A}* and *MYB75^{T131E}* displayed darker purple colouration than the Col-0 wild type plants on sucrose; this increased anthocyanin accumulation was particularly apparent in emerging leaves. Spectrophotometric quantification of total anthocyanin content in each genotype corroborated these visual observations, confirming that in the short-day treatment without sucrose, all three phosphovariants produced more anthocyanin than wild type controls (Fig 3.2B). Furthermore, anthocyanin levels under these conditions were twice as high in the *MYB75^{T131A}* genotype then in either *MYB75^{WT}* or *MYB75^{T131E}*. This latter trend was also observed in sucrose-treated plants, where anthocyanin levels spiked in all the genotypes, but were higher in *MYB75^{T131A}* than in the other two phosphovariants (Fig 3.2B). Although all plants, including the wild type controls displayed an increase in anthocyanin levels after sucrose treatment, the *35Spr:MYB75* lines showed greater anthocyanin accumulation than did Col-0 wild type plants, suggesting that ectopic expression of the transgene contributes to an increase in anthocyanin quantity under these experimental conditions.

The variation in anthocyanin levels observed between different MYB75 phosphovariants in these experiments might indicate that different MYB75 phosphorylation states vary in their ability to drive anthocyanin production in *Arabidopsis* seedlings. Alternatively, differences in phosphovariant protein stability could affect the amount of recombinant MYB75 present in each phosphovariant genotype, which in turn could lead to genotype differences in total anthocyanin accumulation. To test the second hypothesis, I examined the relative levels of MYB75 protein for each genotype under each treatment condition. Western blot detection and quantification of recombinant HA-tagged MYB75 (Fig 3.2C) revealed that $MYB75^{T131E}$ protein levels are lower than the levels of the other phosphovariants, under short day conditions. $MYB75^{WT}$ protein levels were only marginally higher than the levels of $MYB75^{T131E}$, while the levels of $MYB75^{T131A}$ recombinant protein were the highest among all three genotypes.

In response to sucrose and light treatments, recombinant MYB75 protein levels increased in all phosphovariant plants. Protein levels of $MYB75^{T131E}$ showed the most dramatic increase between seedlings incubated under short day conditions, without sucrose, and continuous light with 6% sucrose. $MYB75^{T131E}$ protein levels were also the highest among all three phosphovariants, after incubation on 6% sucrose with continuous light. In $MYB75^{WT}$ and $MYB75^{T131A}$ plants protein levels after light and sucrose treatment were comparable ($MYB75^{WT}$ being slightly lower), however, the change in protein levels between treatments was more dramatic in $MYB75^{WT}$, than in $MYB75^{T131A}$ which showed only a modest increase between plants under short day conditions and continuous light with sucrose (Fig 3.2C).

Fig 3.2

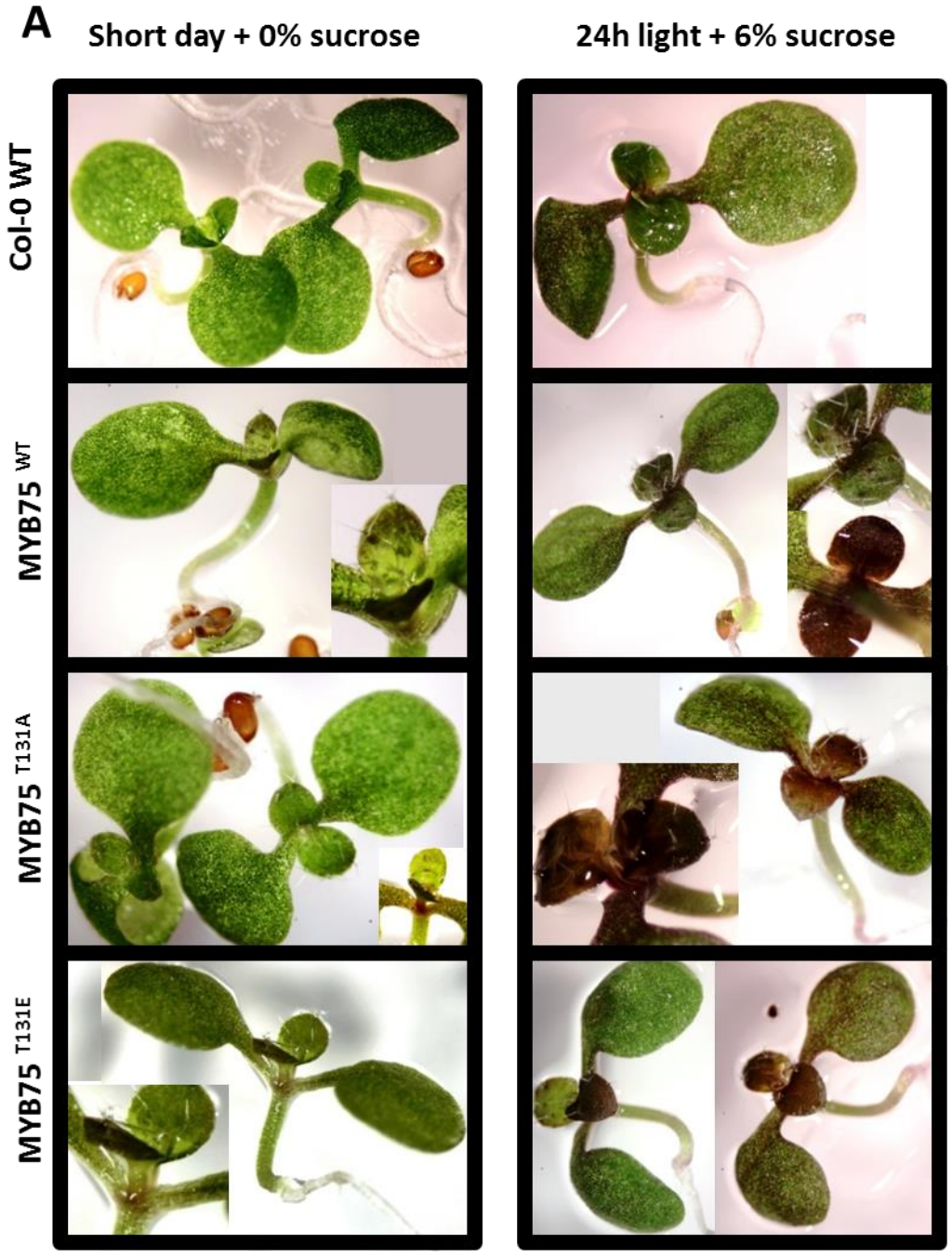
A
Short day + 0% sucrose
24h light + 6% sucrose
Col-0 WT
MYB75 WT
MYB75 T131A
MYB75 T131E

Fig 3.2 continued

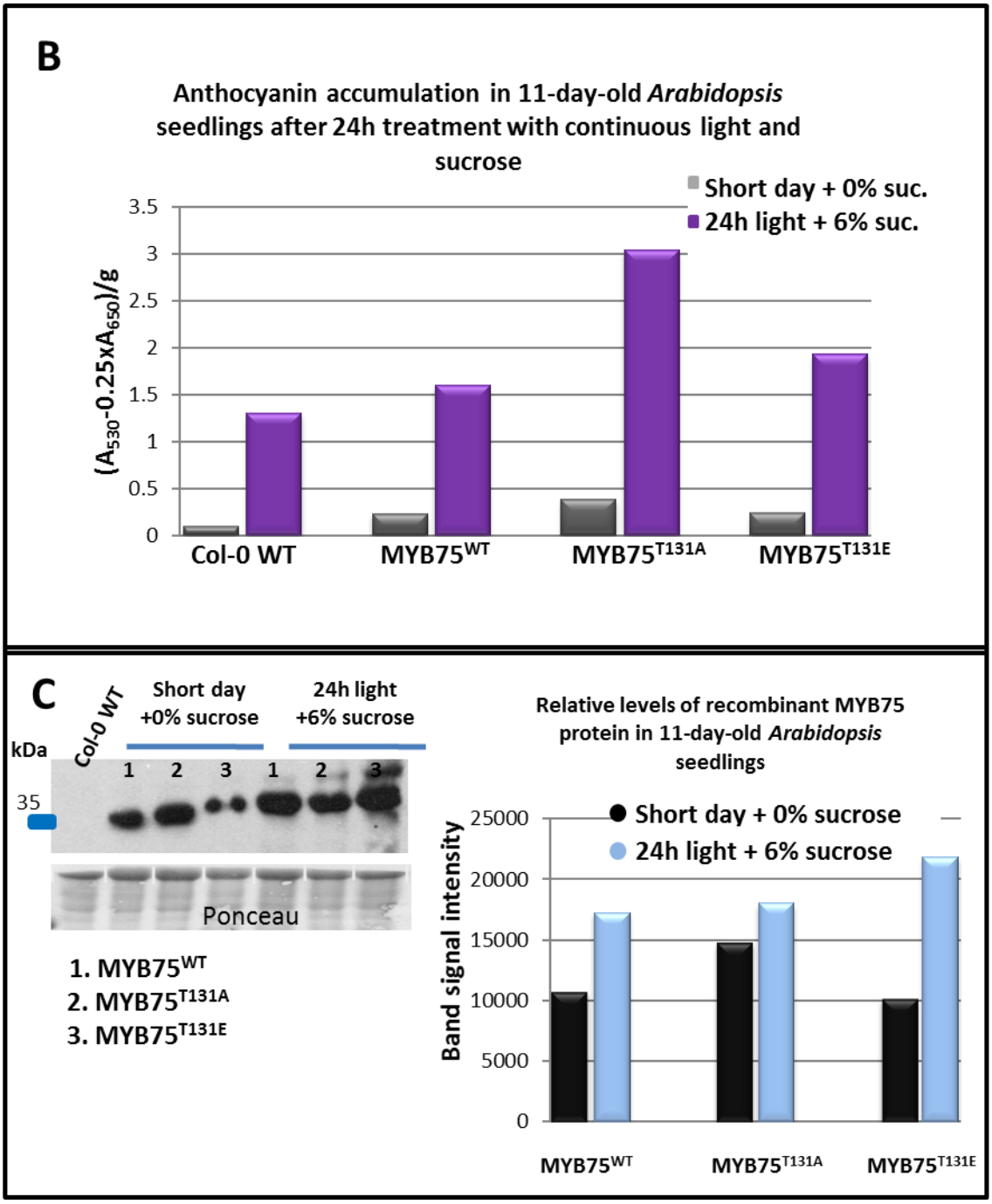

Fig 3.2 Light and sucrose-driven changes in anthocyanin production, and levels of recombinant MYB75 protein, in 11-day-old *Arabidopsis* seedlings expressing MYB75^{WT}, MYB75^{T131A} and MYB75^{T131E} under the control of a constitutive 35S promoter. Heterozygous T2 seedlings were germinated on ½MS medium containing 30µM hygromycin and grown under 16h light/8h dark conditions. At 10-days-old, seedlings from each genotype were transferred to ½MS plates containing 6% sucrose, and incubated under continuous light for 24h, while the seedlings on the original plate were covered with foil for 16h to simulate short day lighting conditions. Seedlings were photographed using a digital camera mounted on a dissecting microscope. Anthocyanin and protein quantification was performed using a pool of 20-30 seedlings for each treatment. Each pool of seedlings was used for total anthocyanin extraction and spectrophotometric quantification, using the formula $Q_{anthocyanin}$=[A530-(A650x0.25)]/mass(g). Western blot detection of recombinant MYB75 protein was used in conjunction with ImageJ software to quantify protein levels. Under short day conditions without sucrose, anthocyanin accumulation could be seen in the apical meristem region in all three phosphovariant genotypes, but not in Col-0 WT controls (A). After application of sucrose, under continuous light, all plants, including Col-0 WT controls accumulated abundant anthocyanin in all plant organs. Anthocyanin production in *35Spr:MYB75* lines, was higher than in Col-0 WT in all treatments (B). Increased levels of recombinant MYB75 protein was observed for all three phosphovariants after light and sucrose treatment and corresponded to the increased anthocyanin levels. MYB75^{T131E} showed the most dramatic change in recombinant protein levels, after treatment with light and sucrose, while MYB75^{T131A} protein levels showed the least amount of change between treatments, maintaining consistently higher levels of recombinant MYB75 under all conditions than the other phosphovariants of MYB75 (C).

To corroborate the results obtained in this experiment (Fig 3.2), and to further explore the individual effects of sucrose and light stress treatments on MYB75 protein levels, the experiment was repeated under slightly different conditions. First, the plants were older than before (14 days vs. 11 days), and thus had more developed emerging leaves and more overall biomass, which facilitated more accurate measurements of fresh weight, required to quantify total anthocyanin levels. Then different treatments were used; 48 hours of growth in continuous darkness without sucrose, 48 hours of growth in continuous light without sucrose, and 48 hours of growth in continuous light with 6% sucrose. As seen previously, levels of MYB75^{T131E} protein were lower than levels of either MYB75^{WT} and MYB75^{T131A}, after incubation in the dark, confirming that this phosphovariant is less stable than MYB75^{WT} and MYB75^{T131A}

under these conditions (Fig 3.3). As before, recombinant MYB75 protein levels increased dramatically in MYB75^{WT} and MYB75^{T131E} plants after incubation under continuous light but showed only a modest increase in MYB75^{T131A} lines. Surprisingly, application of light alone had a greater positive effect on protein levels in all genotypes than did the treatment with light and sucrose together (Fig 3.3B). Most strikingly, western blot analysis and signal quantification with ImageJ suggest that only MYB75^{T131E} protein levels increase after treatment with sucrose and light together, compared to dark-treated plants, while the other phosphovariants treated simultaneously with sucrose and light displayed protein levels comparable to those seen in seedlings incubated in the dark without sucrose. Unfortunately, the limited availability of T2 generation plant material made it impossible to repeat the experiment enough times to generate data sets amenable to statistical analysis. However, the results seen in figures 3.2C and 3.3 are consistent with the trends observed in the protein degradation experiments performed in Chapter 2, which suggest that MYB75^{T131E} is more labile than MYB75^{WT} under the conditions used (Fig 2.5). Most importantly, the data in Figures 3.2 and 3.3 consistently demonstrate that levels of MYB75^{T131A} are generally unaffected by these stress treatments. These observations fill the gap in the results from the previous protein degradation experiments, when only *DEXpr:MYB75^{WT}* and *DEXpr:MYB75^{T131E}* lines were available. Finally, these data suggest that phosphorylation of MYB75 may be impacting anthocyanin production by influencing the cellular levels of MYB75 protein, since increases in protein levels were paralleled by increases in total anthocyanin production in all three phosphovariants (Fig 3.2B).

To compare the ability of each MYB75 phosphovariant to drive anthocyanin production, anthocyanin quantification had to be performed in an experimental system that allowed

harvest of enough biomass, to enable statistical analysis to be performed. Thus, the focus of the project shifted to the use of mature *Arabidopsis* plants.

Fig 3.3

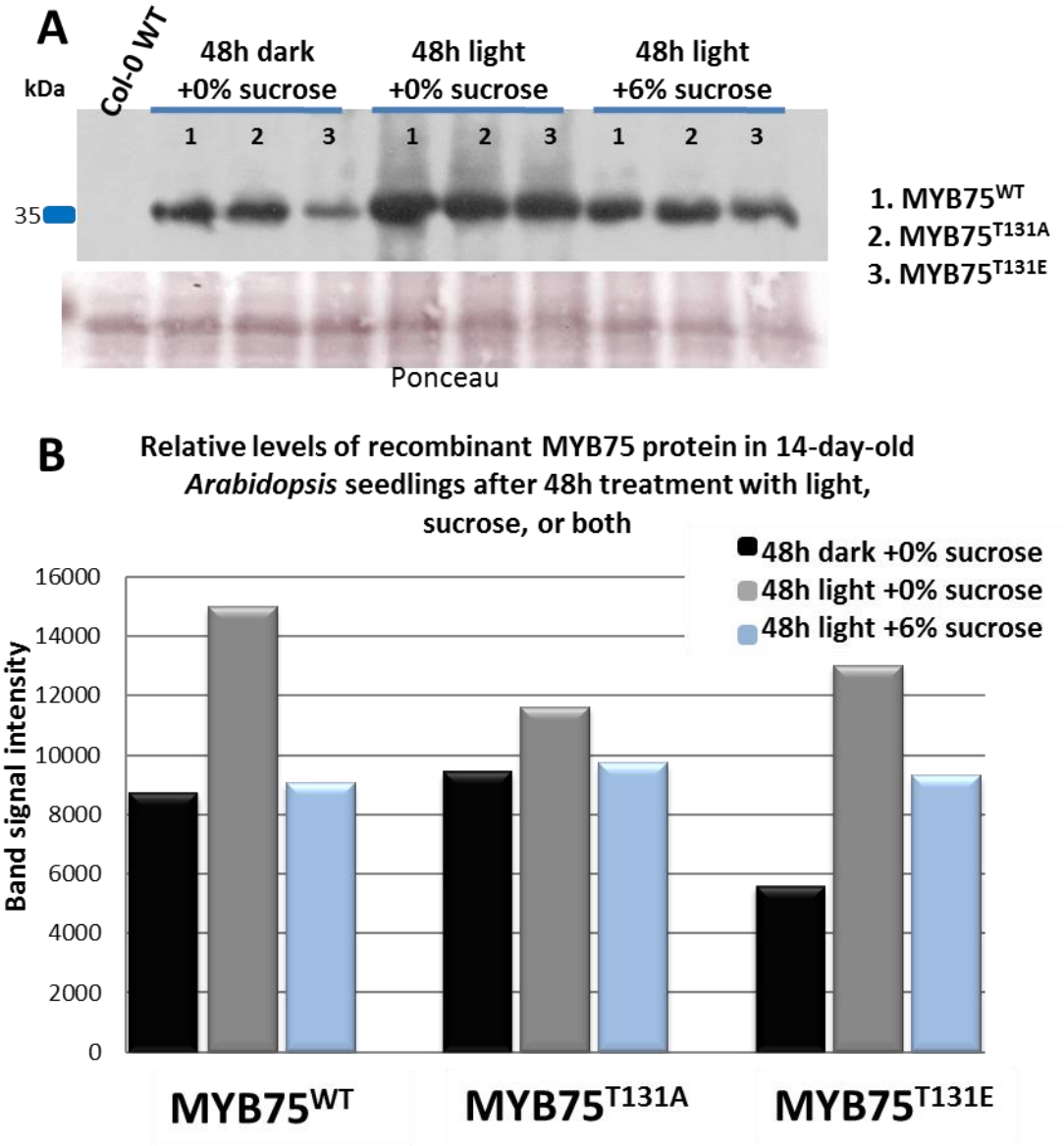

Fig 3.3 The impact of light and sucrose on stability of recombinant MYB75^{WT}, MYB75^{T131A}, and MYB75^{T131E} protein, in 14-day-old *Arabidopsis* seedlings. Heterozygous T2 seedlings carrying *35Spr:3xHA:MYB75 gene* constructs were germinated on ½ MS medium containing 30µM hygromycin. Twelve days after germination the seedlings were transferred to media without antibiotic, either with or without 6% sucrose. Approximately 30 seedlings were used for each treatment: the treatments included 48 hours in the dark without sucrose, 48 hours under continuous light without sucrose, and 48 hours under continuous light with 6% sucrose. After 48 hours the seedlings were harvested and recombinant MYB75 was detected in total plant tissue extracts by western blot analysis (A). Relative amount of recombinant MYB75 protein in each pool of seedlings was quantified using the western blots shown in 3.3A and ImageJ software (B).

3.4 Anthocyanin production in mature *Arabidopsis* plants over-expressing different MYB75 phosphovariants

3.4.1 Total anthocyanin quantification in mature *Arabidopsis* lines over-expressing MYB75

All *Arabidopsis* lines carrying *35Spr:3xHA:MYB75 gene* constructs had individual plants that displayed visible signs of anthocyanin accumulation, shortly after being transferred from petri dishes to soil, when grown under long day photoperiod; 16 hour light/ 8 hours dark. Vivid purple colouration could be observed across all lines, throughout different rosette stages (Fig 3.4A), throughout mature stages and senescence. Some differences were observed between individual lines of *35Spr:MYB75^{WT}*. Lines 2 (not shown) and 11 displayed anthocyanin accumulation that was most concentrated near the centre of the rosette and in mid veins of rosette leaves, while lines 12 and 14 showed more even distribution of anthocyanin throughout the epidermis. *MYB75^{T131A}* lines 1, 22 and 23, as well as *MYB75^{T131E}* lines 2,4,5 and 9 showed expression patterns similar to *MYB75^{WT}* lines 12 and 14, with anthocyanin accumulation visible throughout the epidermis of aerial organs (Fig 3.4A). In *MYB75^{WT}* lines 2 and 11, all plants showed uniformly high, visible levels of anthocyanin accumulation. On the other hand, in *MYB75^{WT} lines 12 and 14, MYB75^{T131A}* lines 1,22 and 23, and *MYB75^{T131E}* lines 2,4,5, and 9 purple colouration was observed in only a portion of the plants (Fig 3.4A). No consistent ratio of green to purple plants was observed within any of the lines, and some plants changed colour throughout development, suggesting either stochastic silencing of the transgene, or variations in developmentally controlled turnover of MYB75 protein between individual plants. Hygromycin-based selection of transgenic plants prior to transfer onto soil eliminated any possibility that the green plants are simply not carrying the transgene, and hygromycin-induced

mortality of approximately one third was observed in each line, consistent with the presence of a single insert in the transformants. Gene expression analysis by RT-PCR showed that both purple and green plants were expressing recombinant *MYB75,* whereas western blot detection of recombinant MYB75 showed that protein production was only detectable in purple plants (Fig 3.4B). Together these results indicate that post-translational silencing of MYB75 protein expression may be occurring in individual plants resulting in failure to accumulate high levels of anthocyanins in these individuals. Since the focus of these experiments was to examine the relationship between MYB75 phosphorylation status and anthocyanin production, only purple plants were used for biochemical and gene expression analyses in the remainder of this chapter.

Fig 3.4

A *35Spr:MYB75 gene Arabidopsis* plants at different rosette stages

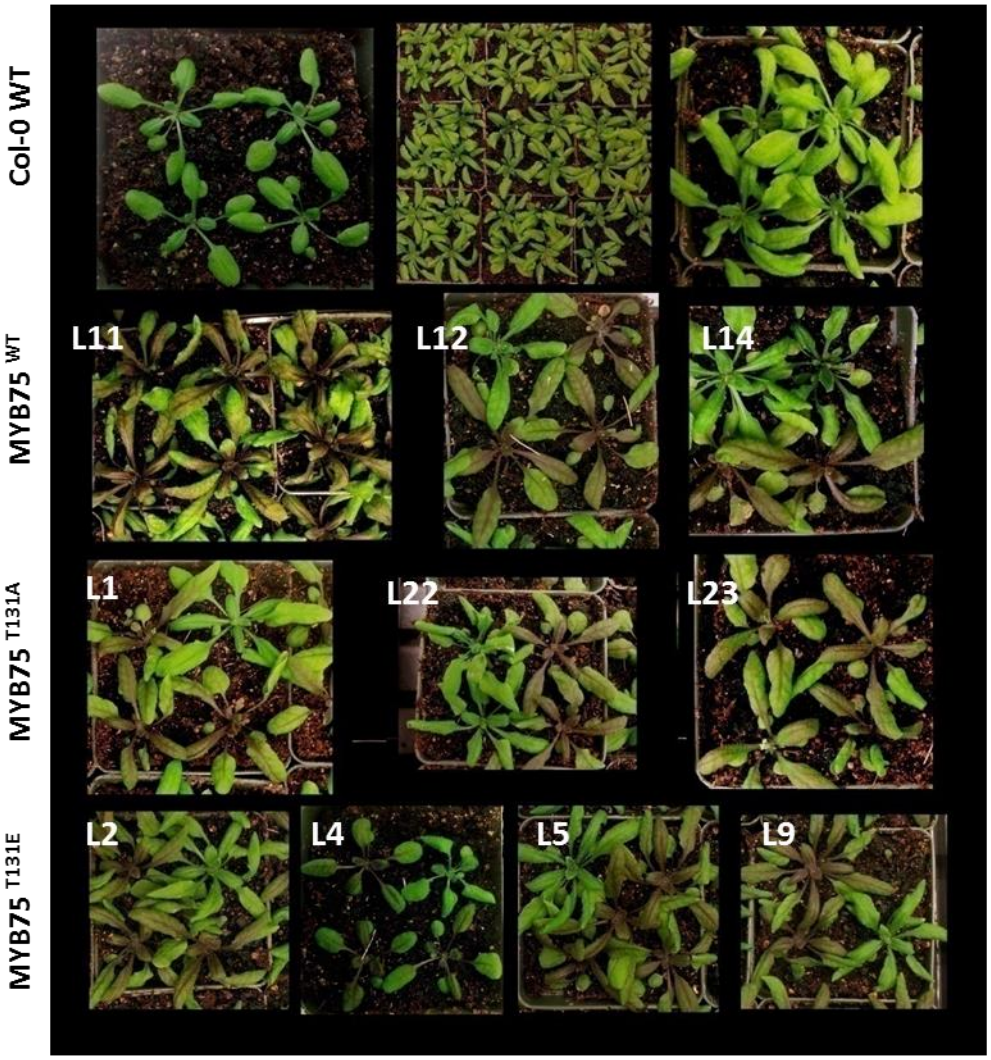

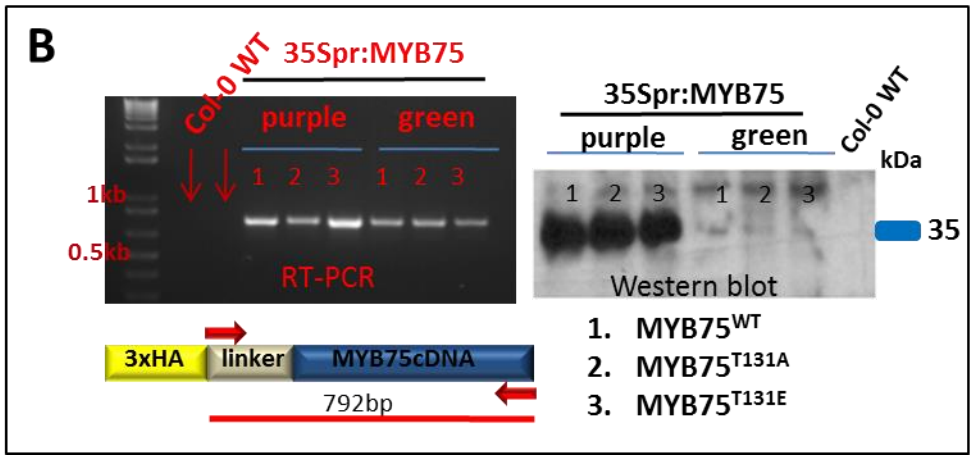

Fig 3.4. Visible anthocyanin accumulation in *35Spr:3xHA:MYB75 gene* plants at different rosette stages correlates with expression of recombinant MYB75 protein in all phosphovariants. Heterozygous T2 plants were transferred from hygromycin selection plates to soil around 10 days after germination and grown under regular photoperiod conditions: 16h light/8h dark. *MYB75^{WT}* line 11 showed consistent visible accumulation of anthocyanins in all individuals: in this line the concentration of purple pigment was most predominant near the centre of the rosette and in leaf vasculature. Lines 12 and 14 of the *MYB75^{WT}* phosphovariant, as well as all lines from *MYB75^{T131A}* (lines 1,22 and 23) and *MYB75^{T131E}* (lines 2,4,5 and 9) displayed bright purple colour in the epidermis of some plants, while others remained green, with no specific ratio of green to purple plants (A). Gene expression analysis performed using reverse transcription polymerase chain reaction (RT-PCR) revealed that green and purple plants expressed recombinant MYB75, while western blot analysis detected recombinant protein only in purple plants (B).

Observation of wild type *Arabidopsis* plants during their growth cycle revealed that Col-0 and Nossen ecotypes do not show visible signs of anthocyanin production until about six weeks of age, when grown under long day photoperiod and regular light conditions (see Materials and Methods). Shortly after six weeks, as the plants approach senescence, they display a spike in anthocyanin production, with visible purple colouration accumulating in mature rosette leaves, stems and other aerial organs. The high degree of variation between individual wild type plants in levels of total anthocyanins accumulated, after six weeks of age, makes quantitative biochemical analysis at this stage problematic. Furthermore, senescing plants express higher levels of endogenous MYB75; as depicted in eFP Browser, where MYB75 transcript abundance is shown to be significantly higher in senescing rosette leaves than any other tissues or developmental stage (Schmid *et al.,* 2005).

Since *35Spr:3xHA:MYB75* gene lines possess both the transgene and the endogenous *MYB75* gene, this extra copy can potentially lead to background MYB75 activity which would interfere with any interpretation of biochemical data in these lines. Thus, for analysis of anthocyanin production in mature *Arabidopsis*, plant tissue was harvested at approximately five

weeks of age, a stage when endogenous *MYB75* expression levels are relatively low compared to recombinant *MYB75* expression, while expression of recombinant MYB75 protein was abundant and comparable between different phosphovariant lines (Fig.3.4B). This difference in *MYB75* expression was clearly demonstrated when visually comparing 5-week-old *35Spr:MYB75* plants with Col-0 wild type plants; the*35Spr:MYB75* plants were bright purple, while the Col-0 wild type controls were uniformly green.

Total anthocyanin quantification in mature *35Spr:MYB75* lines revealed a significant increase in anthocyanin levels across all three phosphovariants compared to Col-0 WT controls. However, there was no significant difference between the various phosphovariants in their ability to drive total anthocyanin accumulation (Fig 3.5A). The anthocyanin quantification data was corroborated by gene expression analysis. Quantitative RT-PCR (qPCR) revealed that $MYB75^{WT}$, $MYB75^{T131A}$ and $MYB75^{T131E}$ lines displayed increased expression of flavonoid and anthocyanin biosynthesis genes compared to Col-0 WT controls (Fig 3.5B). The genes analysed in this figure have previously been shown to be direct targets of MYB75 (Dare *et al.,* 2008). These target genes include chalcone synthase (*CHS*), dihydroflavonol reductase (*DFR*), anthocyanin synthase (*ANS*), UDP-glucose flavonoid glucosyltransferase (*UGT75C1*) and glutathione S-transferase (*GST*). The variability observed in gene expression levels was consistent with the biochemical variation found between those individuals, in terms of total levels of anthocyanin. Despite this variation, the overall pattern of these results corroborated published data showing upregulation of MYB75 target genes in *35Spr:MYB75 Arabidopsis* lines, and demonstrated, that under these experimental conditions, MYB75 phosphorylation status

does not have a significant impact on expression of core flavonoid biosynthetic genes or on anthocyanin levels, in the Col-0 wild type background.

I then considered the possibility that anthocyanin production in each transgenic line might be the result of not only the activity of the recombinant MYB75 protein, but the activity of the endogenous *MYB75* gene. However, neither qPCR, nor semi-quantitative RT-PCR analyses yielded a detectable signal when performed with primers specifically designed to detect only the endogenous *MYB75* transcripts (data not shown), indicating that, at least at this stage, transcription of endogenous *MYB75* is negligible compared to the levels of transgene transcripts. Therefore, I concluded that the increased expression of anthocyanin and flavonoid biosynthesis genes, observed in the *35Spr:MYB75* lines, was being driven primarily by the presence of elevated levels of recombinant MYB75, and that this process was not impacted by phosphovariant status at threonine 131.

Fig 3.5

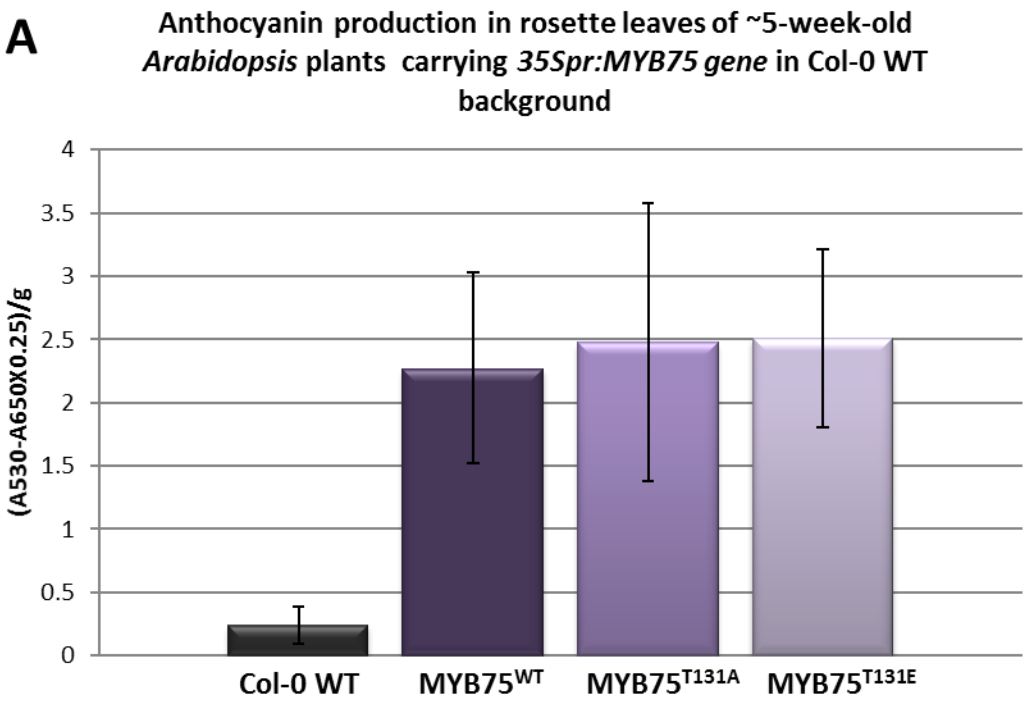
A
Anthocyanin production in rosette leaves of ~5-week-old *Arabidopsis* plants carrying *35Spr:MYB75 gene* in Col-0 WT background
(A530-A650X0.25)/g
4
3.5
3
2.5
2
1.5
1
0.5
0
Col-0 WT
MYB75WT
MYB75T131A
MYB75T131E

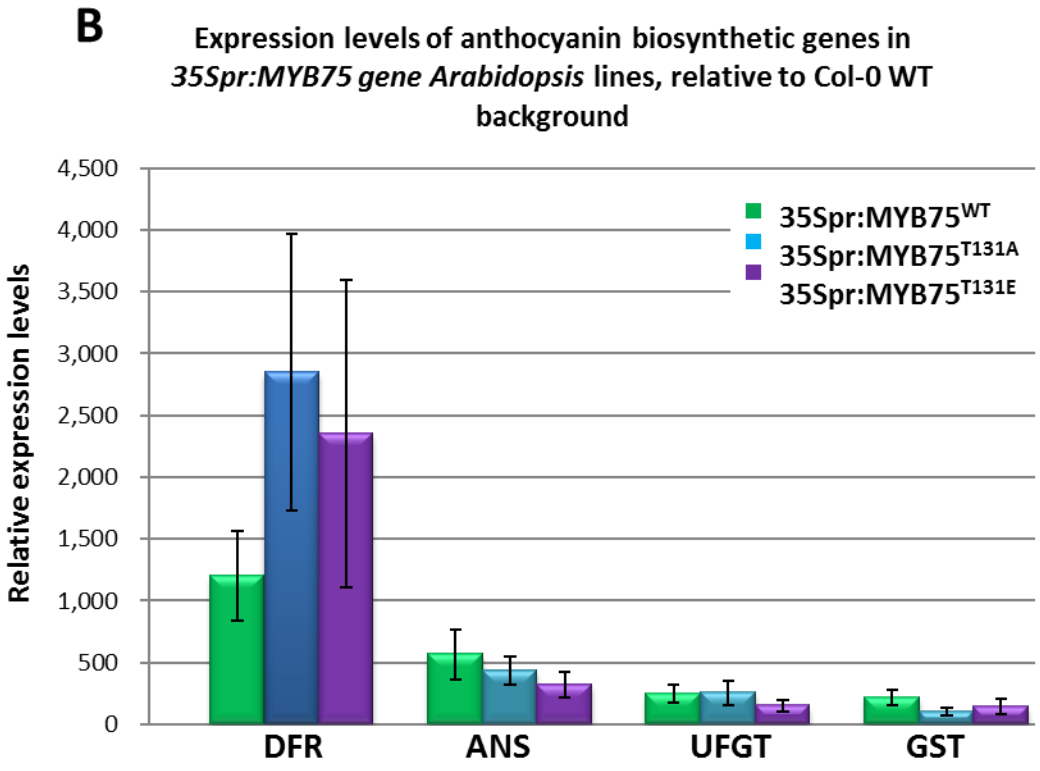
B
Expression levels of anthocyanin biosynthetic genes in *35Spr:MYB75 gene Arabidopsis* lines, relative to Col-0 WT background
Relative expression levels
4,500
4,000
3,500
3,000
2,500
2,000
1,500
1,000
500
0
35Spr:MYB75WT
35Spr:MYB75T131A
35Spr:MYB75T131E
DFR
ANS
UFGT
GST

Fig 3.5 continued

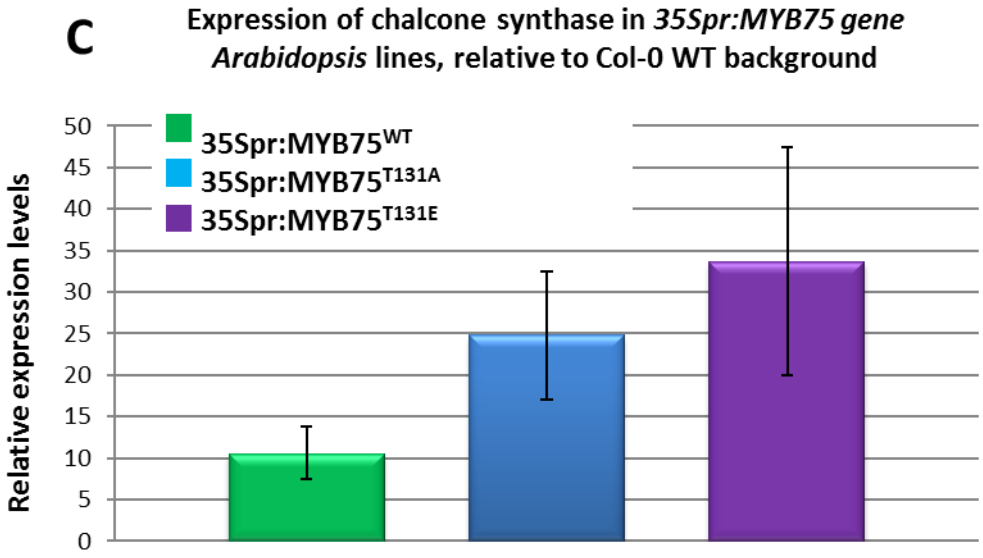

Fig 3.5 Quantification of total anthocyanin levels and relative expression of anthocyanin biosynthetic genes in rosette leaves of mature, 5-week-old *Arabidopsis* plants expressing different phosphovariant forms of MYB75 from a constitutive 35S promoter (CAMV35S).
(A) Rosette leaves were harvested from ~5 -week-old *Arabidopsis* plants, grown under regular photoperiod conditions, 16h light/8h dark. Total anthocyanin was extracted from mature rosette leaves and measured spectrophotometrically. Approximately 23-48 samples were used for each genotype (see Materials and Methods), with each sample containing tissue from 1-2 plants. Error bars representing ± SD (A). Quantitative real-time PCR was performed on total RNA, extracted from rosette leaves of ~5-week-old plants. Relative expression levels were determined as described in Pfaffl (2001), using actin1 and actin8 as reference genes. Each average represents six biological replicates and two technical replicates, error bars represent ±SE (B,C).

3.4.2 Flavonoid profiles of mature *Arabidopsis* plants over-expressing MYB75, as determined by high performance liquid chromatography

The total anthocyanin levels did not differ significantly between plants over-expressing different phosphovariants of MYB75, in mature rosette leaves, where levels of recombinant

protein were comparable between different phosphovariants (Fig 3.4 and 3.5). However, the assay used in the previous section only provides a crude estimate of total anthocyanin levels and does not reveal any details about the biochemical species of flavonoids present in the extract. Therefore, high performance liquid chromatography (HPLC) was used to determine whether there were any changes in the flavonoid profiles, i.e. in the relative abundance of specific molecular species in the extracts obtained from different phosphovariant genotypes. This experiment included analysis of flavonol compounds as well as anthocyanins. MYB75 has been shown to affect the initial steps of flavonoid metabolism through regulation of early flavonoid biosynthesis enzymes (Dare *et al.,* 2008, Borevitz *et al.,* 2000), and these biosynthetic intermediates are thought to be directed towards other flavonoid end-products, including the anthocyanin branch and the flavonol branch, through metabolic channelling (Tohge *et al.,* 2005; Stracke *et al.,* 2007).

Total flavonoids were extracted from mature rosette leaves of 5-week-old *Arabidopsis* plants using 50% aqueous methanol and prepared for HPLC analysis and quantification. To ensure that total extract concentrations were comparable between samples, the amount of methanol added to the plant tissue was proportional to the fresh weight of plant tissue used in each sample (see Materials and Methods). The chromatography and peak quantification was performed by Dr. Simone Castillarin and Dr. Lina Madilao. Although Col-0 wild type plants were also analysed as a baseline reference, the impact of each T-131 phosphovariant mutation (T131A and T131E) on biochemical profiles was assessed by comparing *35Spr:MYB75*^{T131A} and *35Spr:MYB75*^{T131E} lines to the WT over-expressor, *35Spr:MYB75*^{WT}.

As previously reported in the literature, total anthocyanin levels in all *MYB75* over-expressing lines were about 50 times greater than in Col-0 WT (Fig 3.6 A), while flavonol levels only showed a marginal increase in *35Spr:MYB75* lines compared to Col-0 WT controls (Fig 3.6 B).

Qualitatively, the anthocyanin profiles were similar for all three MYB75 over-expressing genotypes. The molecular species present included A5, A6, A8, A9, A10, A11 and A13, with A11 being the most abundant anthocyanin, as previously reported in the literature (Tohge *et al.,* 2005). However, several of the resolved peaks showed statistically significant differences in the abundance, as assessed by peak area. The T131A and T131E mutations resulted in a decrease in the abundance of A5, A8 and A13, with A5 and A8, by about half in both phosphovariants compared to the WT over-expressor, while levels of A13 in the mutant lines are only at 1/5 the amount found in *35Spr:MYB75*^{WT}(Fig 3.6 A).

In order to interpret these results, it is important to first discuss how different anthocyanin molecular species are generated. The aglycone core of flavonoid molecules (e.g. cyanidin, for anthocyanins, and quercetin and kaempferol for flavonols) are products of phenylpropanoid metabolism. However, most of the molecular diversity among these compounds is generated through modifications of their aglycone skeletons by methylation and glycosylation as well as acylation reactions involving addition of organic acids (sinapoyl, malonyl and *p*-coumaroyl moieties) to the flavonoid molecule at various positions. This process of flavonoid decoration is mediated by a suite of enzymes of which only a small number have been biochemically characterized.

Anthocyanin modification occurs in sequential stages and, in *Arabidopsis thaliana* ultimately leads to the generation of highly decorated anthocyanin (A11) that contains a malonyl, sinapoyl and glucoasylated *p*-coumaroyl groups (Fig 3.6). The different enzymes required for anthocyanin decoration in *Arabidopsis*, and their biochemical functions are depicted in Fig 3.7. In summary, the core cyanidin molecule is glycosylated at the C3 and C5 positions of the flavonoid C and A rings respectively, in reactions catalyzed by UGT75C1 (anthocyanin 5-O-glucosyltrasferase), and UGT79B1, (flavonoid 3-O-glucosyltransferase) (Tohge *et al.,* 2005). The glucosyl group attached to C3 position is then decorated with a xylosyl group and *p*-coumaroyl groups, while the glucosyl group at C5 position can be malonylated (reviewed in Sasaki *et al.,* 2014). Glycosylation of the 3 position, as well as the subsequent decorating of the glycosyl moiety are thought to precede glycosylation at C5 (reviewed in Sasaki *et al.,* 2014).

UGT75C1 has been identified as a direct target of MYB75 (Dare *et al.,* 2008), but according to our results its expression was not affected by the T131A and T131E mutations (Fig 3.5). Other genes which are known to show increased expression in *PAP1-D* (MYB75 over-expressor) plants include *UGT78D2, At3AT1* and *At3AT2* (Tohge *et al.,* 2005; Luo *et al.,* 2007), however, it is not known whether these or any other anthocyanin modifying genes are direct transcriptional targets of MYB75. In some cases, gene deletion/silencing experiments can generate plants in which interpretation of the anthocyanin profiles is relatively straightforward, particularly when the mutation results in failure to produce an anthocyanin species containing a specific modifying group. For instance, an insertional mutant with a disrupted *At5MAT* gene, was found to lack malonylated anthocyanins, A5, A8 and A9 (Luo *et al.,* 2007). On the other hand, some anthocyanin modifications are important for overall stability of the pigment

molecule and mutations in these genes can result in a reduction in the total anthocyanin content. For example, deletion of *UGT78D2* resulted in a 21% reduction of total anthocyanins, indicating that glycosylation of the C3 position of the anthocyanin C ring is important for overall stability and/or sequestration of the molecule (Tohge *et al.,* 2005).

The common structural feature shared by anthocyanins A5, A8 and A13 (all of which are reduced In $MYB75^{T131A}$ and $MYB75^{T131E}$ mutants) is the *p*-coumaroyl group at the R2 position. This could mean that expression of *At3AT1* and *At3AT2*, whose gene products are required for anthocyanin *p*-coumaroylation, is reduced in $MYB75^{T131A}$ and $MYB75^{T131E}$ compared to $MYB75^{WT}$. However, neither $MYB75^{T131A}$ nor $MYB75^{T131E}$ are entirely deficient in the expression of these enzymes, since both mutants accumulate A11 (which has a *p*-coumaroyl group) to levels comparable to $MYB75^{WT}$ plants. Furthermore, all three phosphovariants of *MYB75* have significantly more anthocyanins, including more of each molecular species, than does the Col-0 WT control, indicating that all the anthocyanin-modifying enzymes required to produce these compounds are upregulated in *MYB75*-over-expressing plants, regardless of the phosphovariant form of the protein.

Flavonol profiles in the rosette leaves of *PAP1-D* plants, as reported in the literature, display a 30% reduction in kaempferol glycosides, and a ten-fold increase in quercetin derivatives compared to WT controls (Tohge *et al.,* 2005). This shift in flavonol abundance was not observed in our experiment. Instead overall flavonol levels were slightly elevated in all *35Spr:MYB75* lines compared to the Col-0 WT controls, and the types of molecular species found across all genotypes were qualitatively comparable. When compared to $35Spr:MYB75^{WT}$, the phosphomutant over-expressor, $35Spr:MYB75^{T131A}$ displayed a decrease in F8, (quercetin-

dirhamnoside), as well as an unknown flavonol compound corresponding to peak 6. Conversely, *35Spr:MYB75*^{T131E} plants displayed an increase in several types of flavonols, including three kaempferol glycosides, F2, F3 and F20, and a quercetin glycoside, F5. Fig 3.8 lists some of the flavonol modifying enzymes characterized to date, which are responsible for the addition of rhamnosyl and glycosyl groups to the flavonoid A and C rings, at the indicated positions. In contrast to the pattern seen in *PAP1-D* plants, it appears that ectopic expression of MYB75 may be impacting the biosynthesis of the flavonol aglycone core. Among the phosphovariant genotypes, the phosphomimic form of MYB75^{T131E} appears to have a stronger positive influence on flavonol accumulation.

Fig 3.6 A

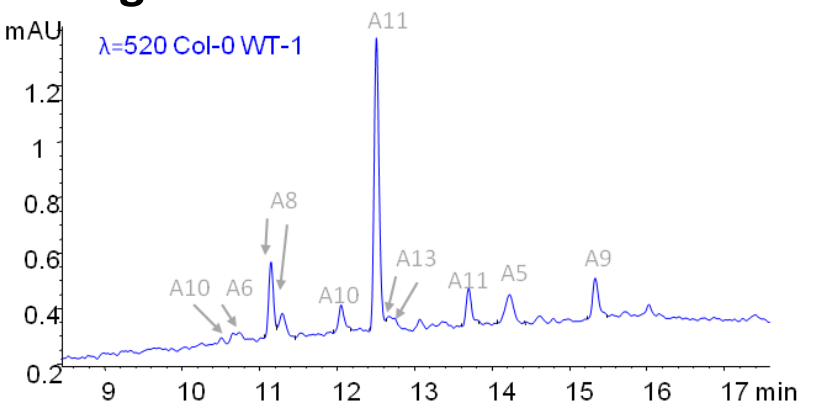

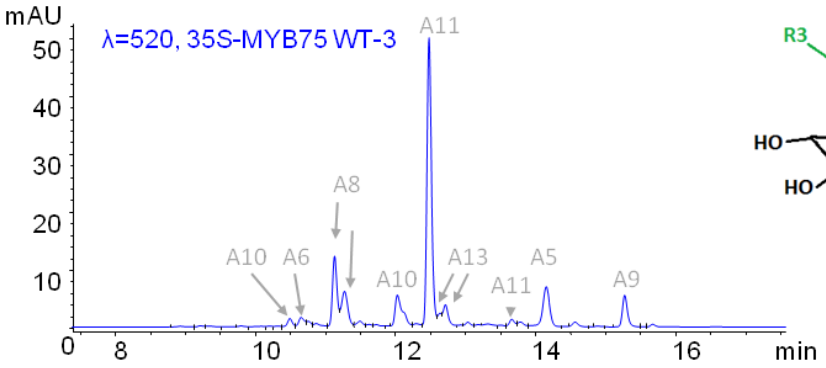

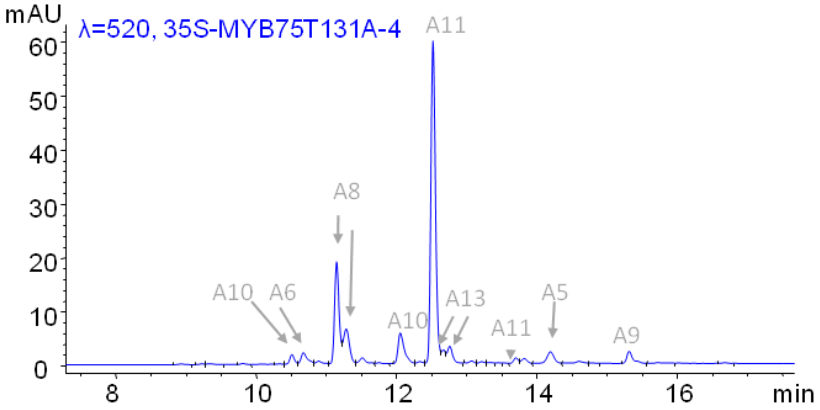

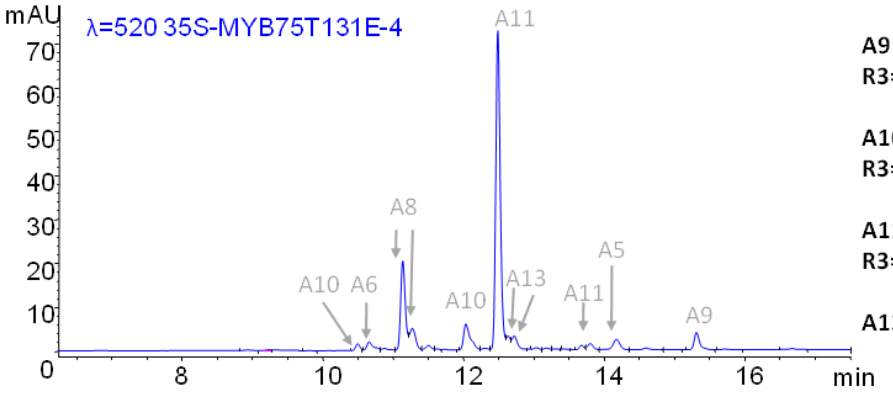

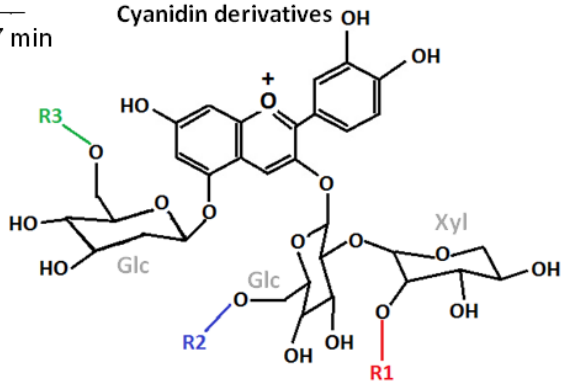

A1 : R1=H, R2=H, R3=H

A2: R1=H, R2=H, R3=malonyl

A3: R1=H, R2=*p*-coumaroyl, R3=H

A4: R1=sinapoyl, R2=H, R3=H

A5: R1=H, R2=*p*-coumaroyl, R3=malonyl

A6: R1=H, R2=*p*-coumaroyl-Glc, R3=H

A7: R1=sinapoyl, R2=*p*-coumaroyl, R3=H

A8: R1=H, R2=*p*-coumaroyl-Glc, R3=malonyl

A9: R1=sinapoyl, R2=*p*-coumaroyl, R3=malonyl

A10: R1=sinapoyl, R2=*p*-coumaroyl-Glc, R3=H

A11: R1=sinapoyl, R2=*p*-coumaroyl-Glc, R3=malonyl

A13: R1=H, R2= *p*-coumaroyl

Fig 3.6 A continued

R-time (min)	Peak ID	PEAK AREAS				Significant changes
		Col-0 WT	35Spr:MYB75^{WT}	35Spr:MYB75^{T131A}	35Spr:MYB75^{T131E}	
10.4	A10		7.78 ± 1.42	7.32 ± 2.42	5.12 ± 1.76	
10.6	A6		9.78 ± 1.60	11.50 ± 4.72	9.10 ± 3.08	
11.1	A8	0.584	67.00 ± 13.9	74.98 ± 27.12	73.15 ± 16.26	
11.2	A8		45.62 ± 13.04	32.35 ± 12.53	22.70 ± 6.47	▼ T131A,T131E
12.01	A10		43.48 ± 9.13	30.62± 13.40	32.02 ± 8.17	
12.4	A11	1.555	257.18 ± 59.29	225.3 ± 95.08	251.8 ± 77.21	
12.6	A13		8.95 ± 1.78	8.50± 3.64	10.92 ± 4.73	
12.7	A13		24.70 ± 6.19	16.15 ± 6.00	12.72 ±5.38	▼ T131A,T131E
13.6	A11		6.88 ± 2.04	4.98 ± 2.71	6.10 ± 2.72	
14.1	A5	0.4025	51.40 ± 26.35	12.8 ± 4.09	14.52 ± 2.96	▼ T131A,T131E
15.3	A9		25.35 ± 9.23	10.68 ± 5.41	13.98 ± 9.85	

Fig 3.6 B

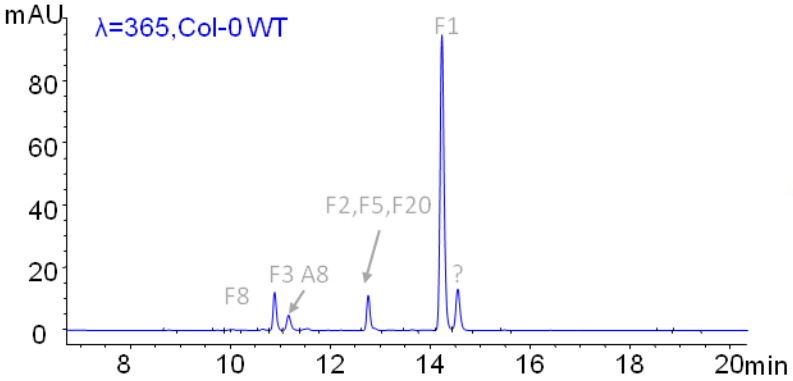

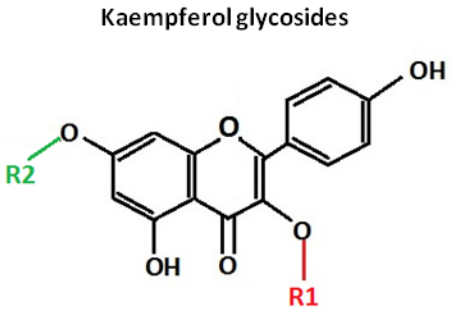

F1: R1=Rha, R2=Rha
F2: R1=Glc, R2=Rha
F3: R1=Rha-Glc, R2=Rha
F20: R1=Rha, R2=Glc

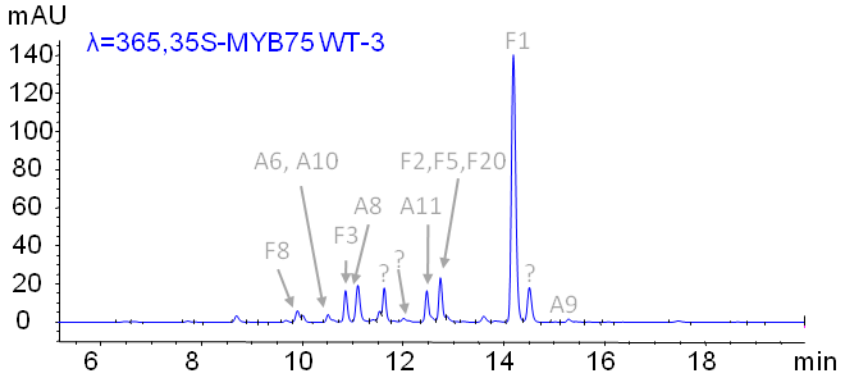

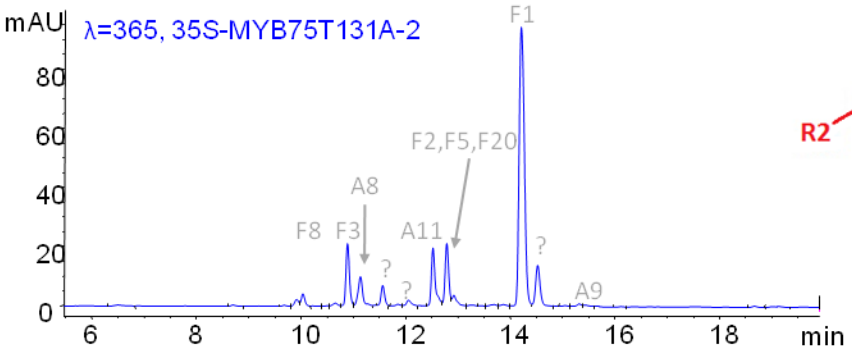

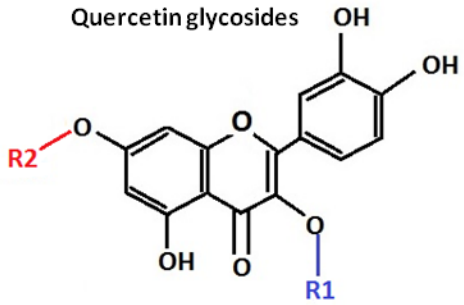

F5: R1=Glc, R2-Rha
F8: R1=Rha-Glc, R2=Rha

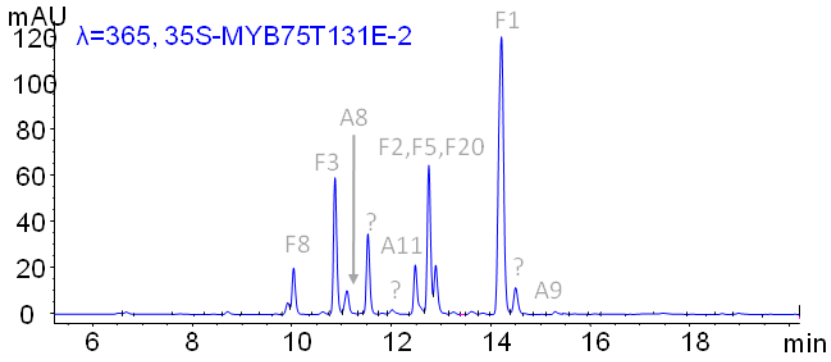

Fig 3.6 B continued

R-time (min)	Peak ID	PEAK AREAS				Significant changes
		Col-0 WT	35Spr:MYB75^{WT}	35Spr:MYB75^{T131A}	35Spr:MYB75^{T131E}	
9.9	F8	2.10 ± 1.69	29.78 ±9.13	10.98 ± 5.64	22.40 ± 2.46	↓T131A
10.6	A6,A10	2.25 ± 0.56	25.45 ± 4.17	6.35 ± 2.34	7.92 ± 1.18	
10.86	F3	62.22 ± 26.57	93.72 ± 11.30	91.85 ± 39.09	216.40 ± 43.62	↑T131E
11.1	A8	34.58 ± 11.68	113.32 ± 10.76	65.85 ± 24.82	63.45 ± 2.23	
11.6	?		24.58 ± 4.62			
11.82	?	4.68 ± 2.40	97.65 ± 8.55	34.82 ± 12.56	98.95 ± 44.98	↓T131A
12.49	A11	2.30	102.60 ± 23.38	88.50 ± 36.37	83.80 ± 22.81	
12.75	F2,F5, F2	58.45 ± 23.74	109.00 ± 5.79	106.28 ± 52.88	236.45 ± 50.03	↑T131E
14.18	F1	517.75± 125.1	858.55 ± 44.85	617.32 ± 172.49	816.38 ± 22.94	
14.5	?	77.02 ± 13.74	115.65 ± 6.05	79.68 ± 15.14	81.15 ± 5.84	
15.32	A9	1.18 ± 0.31	10.62 ± 3.80	4.62 ± 2.15	8.75 ± 5.05	

Fig 3.6. Biochemical profiling and quantification of flavonoid compounds in adult *35Spr:MYB75* plants using high performance liquid chromatography (HPLC). Heterozygous T2 plants were germinated on ½MS medium with hygromycin. Ten days after germination plants were transferred to soil and grown under 16h light, 8h dark light cycle. Mature rosette leaf tissue was harvested from 5-week-old plants and flavonoids were extracted in 50% methanol. Four samples were collected for each genotype, each sample was collected from at least two individual plants, from a single line. The lines used in this analysis were as follows: *35Spr:MYB75^{WT}* L11, L12, L14, *35Spr:MYB75^{T131A}* L1, L22, L23 and *35Spr:MYB75^{T131E}*, L2, L4, L5, L9. HPLC was performed as described in materials and methods. Major peaks were identified, and quantification of each compound was performed by integrating the area under each peak and taking the average among the four samples for each genotype. Statistical analysis was performed using ANOVA and post-hoc Tukey, to identify quantitative differences in the biochemical profiles between genotypes. Significant changes are highlighted in purple (A) and yellow (B) in the tables above. Phosphomutant and phosphomimic over-expressor lines (*35Spr:MYB75^{T131A}* and *35Spr:MYB75^{T131E}*, respectively) were compared to the WT over-expressor (*35Spr:MYB75^{WT}*). Flavonol quantification shows that compared to *35Spr:MYB75^{WT}* lines, T131A mutation results in decreased amounts of F8 (quercetin 3-7-dirhamnoside) and an unidentified compound (peak 6), whereas T131E mutation results in an increased amount of F3 (kaemferol 3-7-dirhamnoside) as well as compounds represented by peak 8, which include F2 (kaempferol 3-O-rhamnoside 7-O-glycoside), F5 (quercetin 3-7-dirhamnoside), and F20 (kaempferol 3-O-glucoside 7-O-rhamnoside (B).

Fig 3.7

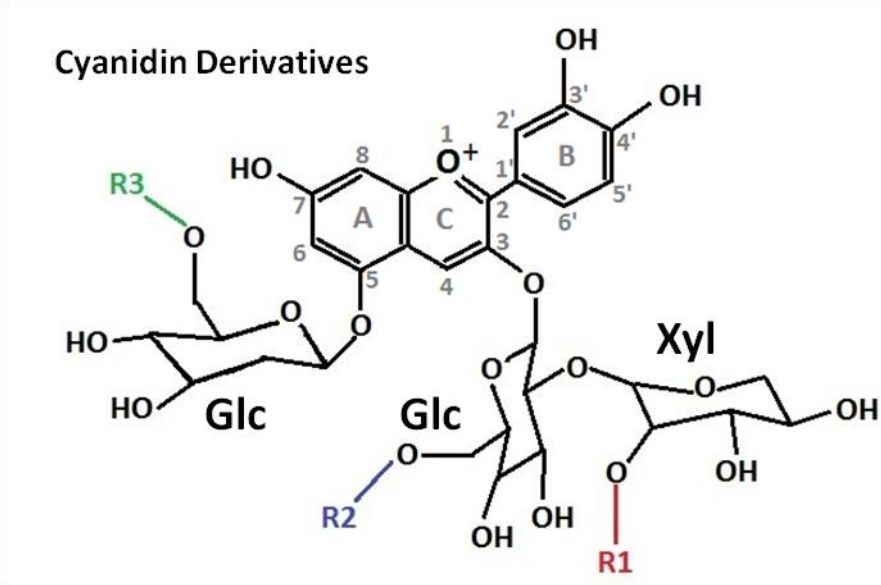

Fig 3.7 Anthocyanin modifying enzymes in *Arabidopsis.*

Gene name/AGI	Function	Reference
UGT78D2 (At5g17050)	**Flavonoid-3-O-glycosyltransferase,** Glycosylation of anthocyanidins and flavonols at C3	Tohge *et al.,* 2005.
UGT79B1 (At5g54060)	**Anthocyanin 3-O-glucoside: 2"-O-xylosyl-transferase,** Xylosylation of anthocyanin at glucosyl group attached to C3.	Yonekura-Sakakibara *et al.,* 2012.
UGT84A2 (At3g21560)	**Sinapic acid:UDP-glucose glucosyltransferase,** Synthesis of 1-O-sinapoylglucose for anthocyanin modification.	Yonekura-Sakakibara *et al.,* 2012.
UGT75C1 (At4g14090)	**Anthocyanidin 5-O-glucosyltransferase,** Glycosylation of anthocyanin "A" ring at position 5	Tohge *et al.,* 2005.
At3AT1 (At1g03940)	**Anthocyanidin 3-O-glucoside coumaroyl CoA transferase,** *p*-coumaroylation of anthocyanins at R2	Luo *et al.,* 2007.
At3AT2 (At1g03495)	**Anthocyanidin 3-O-glucoside coumaroyl CoA transferase,** *p*-coumaroylation of anthocyanins at R2	Luo *et al.,* 2007.
SAT (At2g3000)	**Sinapoyl-Glc:anthocyanin acyltransferase**, Sinapoylation of xylosyl group, at R1	Fraser *et al.,* 2007.
AT5MAT (At3g29590)	**Anthocyanin 5-glucoside malonyltransferase**, Malonylation of anthocyanin at R3	D'auria *et al,* 2007*;* Luo *et al*., 2007.
AtBLU10 (At4g27830)	**Anthocyanin 3-O-6-O-coumaroylglucoside: glucosyltransferase,** Glycosylation of *p*-coumaroyl group attached to R2.	Miyahara *et al.,* 2013.

Fig 3.8

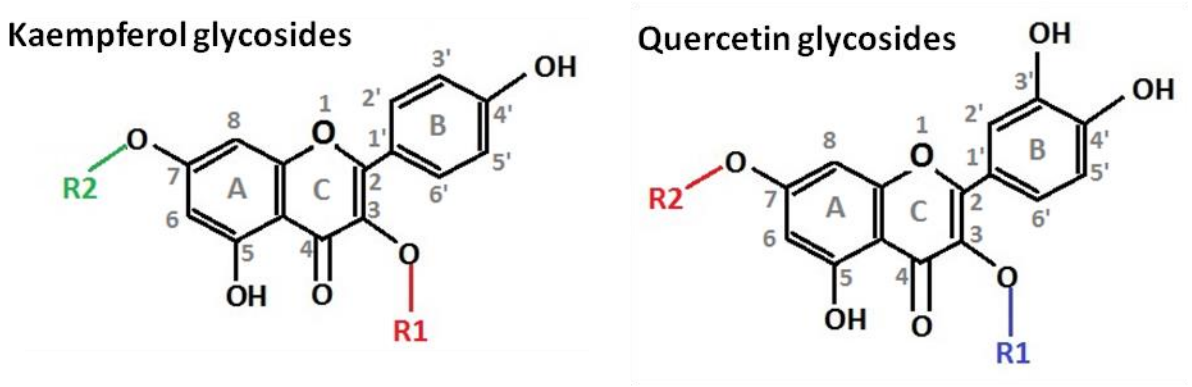

Fig 3.8. Flavonol modifying enzymes in *Arabidopsis*.

Gene name/AGI	Function	Reference
UGT78D1 (At1g30530)	**Flavonol-3-O-rhamnosyltransferase**, Addition of rhamnosyl group at R1	Jones *et al.,* 2003.
UGT78D2 (At5g17050)	**Flavonoid-3-O-glucosyltransferase,** Addition of glucosyl group at R1	Tohge *et al.,* 2005.
UGT78D3 (At1g30530)	**Flavonol-3-O-arabinosyltransferase**, Addition of arabinosyl group at R1	Yonekura-Sakakibara *et al.,* 2008.
UGT73C6 (At2g36790)	**Flavonol-7-O-glucosyltransferase**, Addition of glucosyl group at R2	Jones *et al.,* 2003.
UGT89C1 (At1g06000)	**Flavonol-7-O-rhamnosyltransferase**, Addition of rhamnosyl group at R2	Yonekura-Sakakibara *et al.,* 2007.
UGT71B5	**Quercetin 3-O-glucosyltransferase**, Addition of glucosyl group at R1	Lim *et al.,* 2004.
OMT1 (At5g54160)	**Flavonol-3-O-methyltransferase**, Addition of a methyl group to R1	Muzac *et al.,* 2000.
F3'H (TT7) (AT5G07990)	**Flavonoid 3'-hydroxylase,** Addition of hydroxyl group to carbon 3 of B ring	Schoenbohm *et al.,* 2005.
F3H (TT6) (AT3G51240)	**Flavonone 3'-hydroxylase,** Addition of hydroxyl group to carbon 3 of C ring	Pelletier and Shirley, 1996.

3.5 Discussion

The aim of the experiments described in this chapter was to investigate how the phosphorylation status of MYB75 might affect flavonoid metabolism *in vivo*, by examining the biochemical phenotypes of plants carrying different phosphovariant versions of *MYB75*. My initial attempts to express *MYB75* from its endogenous promoter, in the *myb75*$^{-}$ background did not yield consistent expression levels of the *MYB75* phosphovariants in these transgenic lines, making complementation analysis impossible. The possibility that transcriptional autoregulation of MYB75 might be a feature of the MYB75 regulatory network, and the potential impact of phosphorylation status on such a putative process, may provide a possible explanation for differences in expression levels of the various phosphovariants, when driven by the endogenous *MYB75* promoter. However, another possibility (and perhaps a more likely explanation) for my failure to isolate transgenic lines expressing adequate levels of *MYB75*, could be involvement of this gene in early developmental processes. According to expression data in eFP Browser, mature *Arabidopsis* plants display the highest levels of *MYB75* expression in senescing leaves (Winter *et al.,* 2007; Schmit *et al.,* 2005). However, a closer look at the developmental expression of *MYB75* reveals very specific expression pattern in the embryo, beginning with the heart stage, where *MYB75* expression levels are slightly elevated in cotyledons, compared to other organs. The torpedo stage displays an even more intricate distribution of *MYB75*, with the highest expression levels observed in the root apical meristem (Fig 3.9).

Fig 3.9

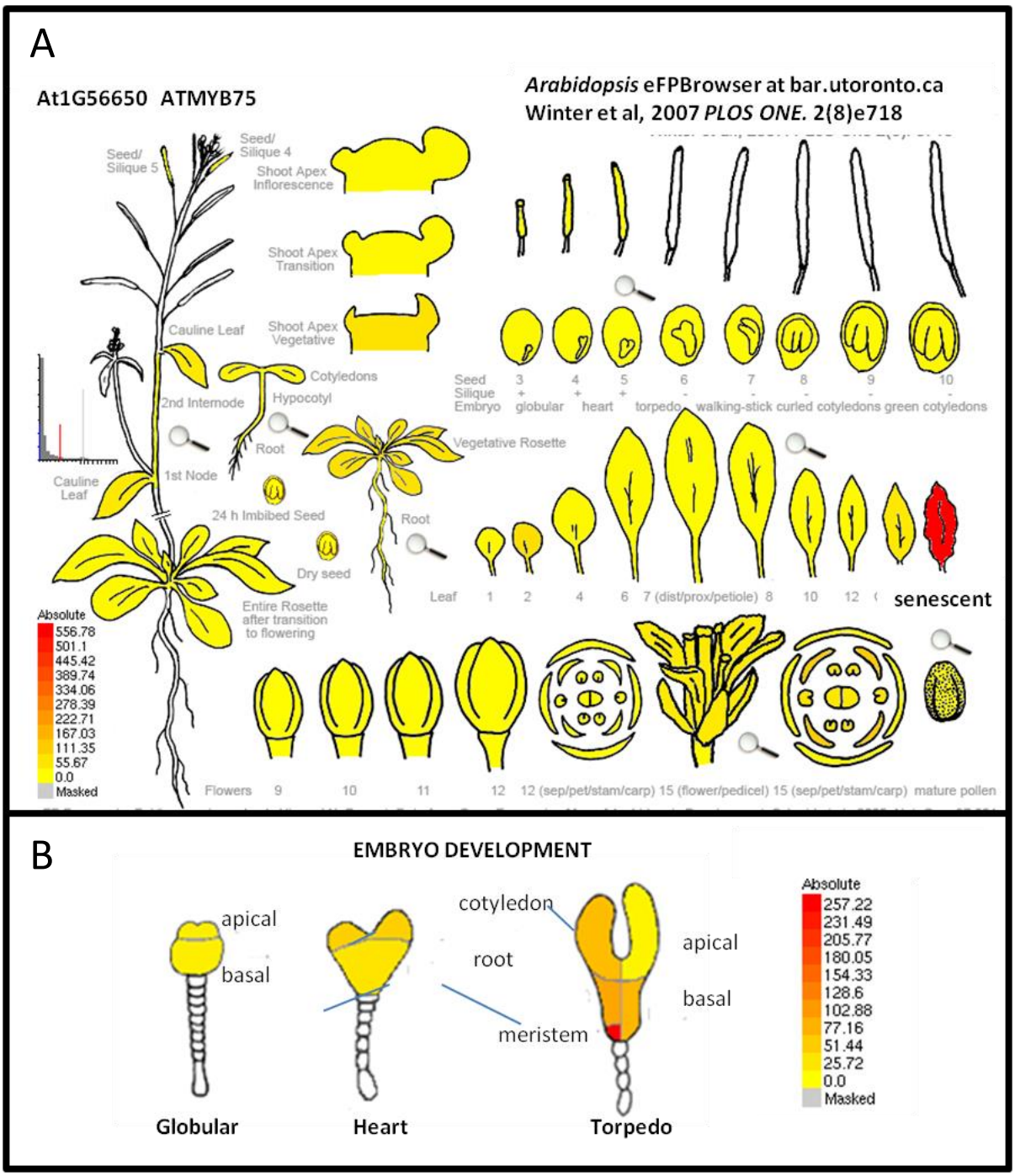

Fig 3.9 Relative levels of *MYB75* expression in *Arabidopsis,* throughout developmental stages (A) and during embryo development (B). *Arabidopsis* eFPBrowser at bar.utoronto.ca. (Winter *et al*., 2007; Schmit *et al.,* 2005).

The precise patterning of *MYB75* expression in these organs indicates a possible involvement of *MYB75* in development at early embryonic growth stages. Perturbation in *MYB75* expression levels (and possibly phosphorylation status) in these developing tissues could potentially be lethal to the embryo. Failure to isolate any lines at all from transformation experiments with certain phosphovariants under the control of the endogenous *MYB75* promoter might also indicate that these particular phosphovariants are embryo-lethal. The idea of embryo lethality arising from MYB75 mis-expression is supported by the observation that successful over-expression of the *MYB75* gene (*35Spr:3xHA:MYB75 gene* lines) consistently yielded only a few lines, despite screening over 50 individual T1 plants for each genotype. In addition to low recovery of transgenic progeny, the surviving lines did not display the canonical *PAP1-D* phenotype at early seedling stages, and only began to display prominent purple colour at mature stages, or when seedlings were transferred medium containing sucrose. In conclusion, although complementation experiments did not yield informative results with respect to anthocyanin accumulation patterns, they did highlight the possible importance of this gene in other developmental processes. I therefore wanted to address the question of whether MYB75 could be influencing development indirectly, through regulation of phenylpropanoid/flavonoid biosynthesis genes, or whether, like its bHLH and WDR partners, MYB75 participates directly in regulation of genes participating in development.

Repeated attempts to express different MYB75 phosphovariants using a 35S promoter to drive the cDNA version of *MYB75* failed to yield detectable proteins levels, in *myb75*$^{-}$ mutant (Nossen), and Col-0 backgrounds. Although the lack of detectable MYB75 protein in these lines was very surprising at first, a recent publication shed light on a possible reason for this pattern.

It appears that the first intron of *MYB75* is vital for transcriptional upregulation in response to sucrose (Broekling *et al.,* 2016). Most importantly, those authors showed that *PAP1Dwg:GUS,* (a reporter construct consisting of the *MYB75* promoter, together with the full length gene, including all introns and exons), displayed not only responsiveness to elevated sucrose but a much wider distribution of reporter expression across different tissues and organs, than did the *PAP1Dpro:GUS* reporter (Broekling *et al.,* 2016). The visual reporter expression pattern was confirmed by RT-PCR analysis and coincided with *AtGenEXPRESS* gene expression data (Broekling *et al.,* 2016; Schmid *et al.,* 2005). In the study by Broekling *et al.,* (2016) *PAP1Dwg:GUS* lines grown on 2% sucrose displayed GUS activity in the hypocotyl, root, and emerging leaves of 14-day-old seedlings, with high concentration of GUS activity along petioles and mid vein; in contrast, no GUS activity was observed in *PAP1Dpro:GUS* lines at this stage of development. The ability of introns to boost gene expression in a manner comparable to *cis*-elements found in promoter sequences has been widely reported in plants and animals (Laxa, 2016). Additionally, introns have been shown to be important for mRNA stability in *Arabidopsis* and other species (Narsai *et al.,* 2007; Wang *et al.,* 2007). Thus, my use of the full-length *MYB75* gene instead of the cDNA was probably vital in ensuring sufficient *MYB75* expression, and yielding detectable levels of MYB75 protein, in *35Spr:3xHA:MYB75 gene* lines.

Despite being under the control of a strong constitutive 35S promoter, visible anthocyanin accumulation in *Arabidpopsis* plants carrying *35Spr:3xHA:MYB75 gene* constructs was only observed once they were transferred to soil. The most likely explanation for this delayed response is the difference in light fluence between the growth space where plants were selected on petri dishes containing hygromycin and the growth chamber where the plants

were soil-grown (see Materials and Methods). Anthocyanin accumulation in petri plates may also have been suppressed by accumulation of ethylene, due to poor gas diffusion in the closed petri dishes in which the seedlings were germinated (Jeong *et al.,* 2010). This type of environmental control of anthocyanin production in *35Spr:PAP1D* plants has been reported in the past (Rowan *et al.,* 2009). When *35Spr:PAP1D Arabidopsis* plants were grown under high light and low temperature conditions they accumulated abundant anthocyanins and the leaves displayed purple colouration. This increase in anthocyanin levels coincided with an increase in expression of flavonoid biosynthetic genes, including (*PAL1, CHS, CHI, F3H, F3'H* and *DFR)* as well as regulatory genes, including *TT8*, *GL3* and *EGL3*. However, when these *MYB75* over-expressing plants were transferred to low light and high temperature conditions expression levels of these genes, along with anthocyanin production decreased dramatically (Rowan *et al.,* 2009). Some of this environmental control of anthocyanin production appears to act through transcriptional regulation of MYB75-interacting partners, including TT8, EGL3 and GL3. However, posttranslational regulation of MYB75, including turnover/stability of the MYB75 protein, cannot be excluded from playing a part in this process as well.

When transgenic seedlings were grown on petri plates under continuous, low fluence light and 6% sucrose, they showed signs of anthocyanin accumulation, typical of the *PAP1-D* phenotype. Pigment accumulation in seedlings carrying *35Spr:MYB75 gene* constructs was visibly stronger than in Col-0 WT plants (Fig 3.2). In addition, the levels of total anthocyanin accumulation correlated with MYB75 protein levels for all the phosphovariants (Fig 3.2 B, C and Fig 3.3). MYB75 protein levels decreased in the dark, as anticipated, but the MYB75^{T131A} phosphovariant showed the smallest decrease, indicating that it may be less susceptible to

degradation than MYB75^{WT} and MYB75^{T131E}. The observation that phosphorylation at T-131 renders MYB75 less stable in the dark, appears to contradict the conclusions presented by Li *et al* (2016), who reported that phosphorylation at both T126E and T131E was necessary to stabilize MYB75 protein. One way to reconcile my data with their published results is to entertain the possibility that phosphorylation at threonine 131 alone has the opposite effect on protein stability than phosphorylation at both sites. Multisite phosphorylation has been well documented in mammals and has been shown to be an important mechanism of transcription factor-regulation through integration of multiple input signals (reviewed in Holmberg *et al.,* 2002). Phosphorylation at different sites of a given protein can affect different aspects of protein function or have opposing effect on the same function. For instance, phosphorylation of the p53 tumour suppressor factor at Ser315 by the kinase Cdk2 increases the ability of p53 to bind DNA (Vousden, 2002; Apella and Anderson, 2001), while phosphorylation at Ser15, Thr18, Ser20 and Ser37 by several different kinases, disrupts the interaction between p53 and Mdm2, (an E3 ubiquitin ligase), prevents p53 from being targeted for degradation, and facilitates its nuclear translocation. Stability of p53 is also regulated through phosphorylation by several different kinases: phosphorylation at Ser33, Thr81 and Ser392 stabilizes p53, while phosphorylation at Thr55, Ser371 and Ser376 triggers degradation (Bech-Otschir et *al.,* 2001; Saito *et al.,* 2002). Other examples include the HSF1 transcription factor, whose transcriptional activity can be both positively and negatively regulated through phosphorylation of different sites (Holmberg *et al.,* 2001; Chu *et al.,* 1998). In *Arabidopsis,* HsfA2 (heat stress factor A2), is a transcription factor that plays a role in response to heat stress and is phosphorylated by MPK6 at Thr249. This phosphorylation event induces translocation of HsfA2 to the nucleus (Evrard *et*

al., 2013). In the same publication the authors showed that total inhibition of phosphorylation reduced the cellular abundance of Hsf2 protein, but that MPK6 was not important for Hsf2 stability, implying that phosphorylation at other sites was responsible for stabilizing the protein (Evrard *et al.,* 2013). Examples of plant multisite phosphorylation are less well-documented than those from mammalian systems. However, there is enough evidence to suggest that this phenomenon is broadly conserved between species, and is particularly prevalent in transcription factors which, like MYB75, require the integration of multiple stimuli to fulfil their function. Therefore, it is possible that phosphorylation of MYB75 at Thr131 versus phosphorylation at both threonine 126 and 131 may have opposing effects on protein stability.

The exact degradation pathway that is affected by phosphorylation status is not entirely clear. Although Li *et al.,* (2016) showed that COP1 and MPK4 had opposing effects on anthocyanin accumulation, the *cop1/mpk4* double mutant accumulated very little anthocyanin, indicating that the stabilizing effect of MYB75 phosphorylation by MPK4 is not dependent on MYB75 binding the COP/SPA complex (Li *et al.,* 2016, Fig8D). This is congruent with my data presented in Chapter 2, where MYB75 binding to SPA proteins was not affected in any of the phosphovariants (Fig 2.4). Furthermore, Li *et al.,* (2016) demonstrated that all MYB75 phosphovariants still respond to changes in light intensity (Li *et al.,* 2016, Fig8A), which I also observed in my results (Fig 3.2 and 3.3), reinforcing the idea that there is likely an additional mechanism of MYB75 turnover; one that is affected by phosphorylation, but not necessarily tied to turnover mediated by COP/SPA complexes.

Five-week-old *Arabidopsis* plants over-expressing *MYB75^{WT}, MYB75^{T131A}* and *MYB75^{T131E}* showed visible signs of anthocyanin accumulation and produced abundant MYB75 protein (Fig 3.4). However, no significant differences were observed in the total anthocyanin production (Fig 3.5A) or expression of anthocyanin biosynthetic genes between different phosphovariants (Fig 3.5 B, C). On the other hand, HPLC analysis of anthocyanin and flavonol biochemical profiles, revealed quantitative differences in some biochemical species between *MYB75^{WT}*, and the phosphovariant over-expressors*, MYB75^{T131A}* and *MYB75^{T131E}*.

Analysis of anthocyanin profiles by HPLC revealed a reduction in the levels of the A5, A8 and A13 components in both, *MYB75^{T131A} and MYB75^{T131E}* compared to the *MYB75^{WT}* over-expressor (Fig 3.6A). The common feature among these compounds is a *p*-coumaroyl group (which is glycosylated in A8) at the R2 position. This would suggest that the expression of enzymes required for the catalysis of anthocyanin *p*-coumaroylation, (At3AT1 and At2AT2; Luo *et al.,* 2007) is reduced in the phosphomutant plants compared to MYB75^{WT}. The challenge with this interpretation is that other biochemical species containing a *p*-coumaroyl group, which include A3, A6, A7, A9, A10 and A11, in the anthocyanin HPLC profiles, appear to be unaffected and accumulate to comparable levels among the three over-expressor genotypes (Fig 3.6A). This suggests a more complex relationship between MYB75 phosphorylation status and the abundance of these metabolic products, than simply a change in the ability of MYB75 to regulate transcription of specific biosynthetic enzymes. Finally, the reduction of A5, A8 and A13 in both *MYB75^{T131A}* and *MYB75^{T131E}* genotypes might indicate that the activity of both phosphorylated and unphosphorylated MYB75 is required for most efficient production of these compounds.

MYB75 has been shown to regulate some of the anthocyanin modifying enzymes. UGT75C1, which catalyzes glycosylation of the anthocyanin A ring at the C5 position, was shown earlier to be a direct target of MYB75 (Dare *et al.,* 2008). In addition, UGT78D2 (flavonoid-3-O-glycosyltransferase), as well as the enzymes required for *p*-coumaroylation, At3AT1 and At2AT2, are up-regulated in *PAP1-D* plants (Tohge *et al.,* 2005, Luo *et al.,* 2007). Finally, analysis of publicly available microarray data showed that *UGT79B1* and *UGT82A2* were co-expressed with anthocyanin biosynthetic genes, including *MYB75* (Yonekura-Sakakibara *et al.,* 2012). Asides from *UGT75C1* (Dare *et al.,* 2008), it is not known if MYB75 can regulate the expression of anthocyanin modifying genes directly and whether phosphorylation status might have an impact on this process.

Anthocyanin and flavonol profiles in plants change in response to environmental stimuli and stress. For instance, in wild type *Arabidopsis* seedlings grown under high light conditions on ½MS medium with 3% sucrose, showed higher proportion of anthocyanin A9 compared to control conditions, where A11 was the predominant molecular species (Kovinich *et al.,* 2014). In the same study, the control plants displayed accumulation of only A8, A9 and A11, while in seedlings treated with sucrose and high light A3, A5, A7, A8, A9 and A11 were detected. The authors concluded that some anthocyanin species, such as A3, A5 and A7 accumulate exclusively in response to stress, while others, such as A11 are present constitutively. Furthermore, the authors demonstrated that expression levels of many anthocyanin modifying enzymes responded to stress, and that changes in the level of expression of a particular enzyme corresponded to changes in the abundance of a biochemical species whose formation requires its catalytic activity.

It is difficult to compare my results to the data published by Kovinich *et al.,* (2014), as the age and genotypes of the plants used in my work are different from theirs. However, those authors demonstrated an important fundamental point: plants have a way of regulating which anthocyanin species accumulate in response to a particular stress signal, and that this process is at least in part controlled at the transcriptional level. In addition to stress-induced changes, anthocyanin profiles differ in different tissues and organs; in this case, as in stress response, differential expression of anthocyanin modifying enzymes appears to be a major mechanism driving changes in biochemical profiles (reviewed in Saito *et al.,* 2013).

It is important in interpreting my data to consider that regulation of anthocyanin biosynthesis and decoration is likely a coordinated effort involving different transcriptional regulators, responsive to specific environmental and developmental cues. From this perspective, it is therefore possible that spatial and temporal distribution of MYB75 protein plays a part in that process. According to my results, MYB75^{T131E} is more labile than MYB75^{T131A}, particularly in the dark. It is also apparent that treatment with sucrose and/or continuous light has a stabilizing effect on MYB75, with the greatest change in protein abundance observed in MYB75^{T131E}. These data indicate that phosphorylation of MYB75 at threonine 131 makes the protein more susceptible to turnover under specific conditions, which in turn can lead to differential spatial and temporal distribution of phosphorylated and unphosphorylated forms of MYB75, depending on the cellular environment. Therefore, it is possible that the differences in the biochemical profiles observed between phosphovariants are a result of differences in distribution of MYB75 protein, between different tissues and cell types within the mature leaves that were being sampled.

MYB75 is known to affect flavonol production. Leaves of *PAP1-D*-over-expressing *Arabidopsis* plants have reduced amounts kaempferol dirhamnoside (F1), which is the major flavonol in that tissue, where it comprises ~50% of the flavonol content in wild type plants (Tohge *et al.,* 2005). On the other hand, the same study reported an increase in quercetin glycosides (F4-F6) in *PAP1-D* over-expressing plants, with levels ten times higher than in wild type controls (Tohge *et al.,* 2005). My experiments tell a somewhat different story; first, all the flavonol species increase in quantity in *MYB75* over-expressing lines compared to Col-0 WT (Fig 3.6B). Second, the 35Spr:$MYB75^{T131A}$ genotype shows a decrease in F8, (a quercetin derivative) compared to $35Spr:MYB75^{WT}$ lines. Finally, $MYB75^{T131E}$ lines have the highest flavonol levels, with a significant increase in kaempferol glycosides (F2 and F3) as well as quercetin glycosides (F5 and F20), relative to the $MYB75^{WT}$ over-expressor.

MYB75 is a direct transcriptional activator of genes encoding the flavonoid biosynthetic enzymes *CHS* and *F3H* (Dare *et al.,* 2008), as well as *UGT75C1* glycosyltransferase (Tohge *et al.,* 2005), all of which are important for flavonol accumulation. However, there is no report of MYB75 affecting the expression of flavonol synthase (*FLS*), whose activity is required for the biosynthesis of kaempferol and quercetin aglycones, nor is there any record of MYB75 regulating any of the flavonol modifying enzymes listed in Fig 3.8. Like anthocyanins, different flavonol molecular species accumulate in different tissues and in response to different stimuli (Tohge *et al.,* 2005). Therefore, differential degradation of each MYB75 phosphovariant may be the driving mechanism for differences in biochemical profiles. We cannot however exclude the possibility that MYB75 plays a role in driving the expression of particular flavonol modifying

enzymes, and that MYB75^{T131E} is a more potent activator of this process than the other phosphovariants.

Another possible explanation for increased flavonol levels in *35Spr:MYB75^{T131E}* plants compared to the other over-expressor genotypes, is that MYB75 phosphorylation status has an indirect impact on flavonol biosynthesis, through its interaction with TCP3. As previously described, TCP3 binds to MYB75 and facilitates the formation of the MYB-bHLH-WDR complex, which is responsible for enhancing transcription of anthocyanin biosynthetic genes. However, TCP3 is also reported to interact with MYB12 and MYB111, thereby increasing transcription of flavonol biosynthetic genes (Li and Zachgo, 2013). TCP3 thus plays a role in metabolic channelling, and can influence both anthocyanin and flavonol biosynthesis, depending on the interacting partners. MYB75 itself can negatively influence flavonol levels, through metabolic channelling of flavonoid precursors into the anthocyanin branch. However, the interplay between TCP3 and different MYBs provides an additional explanation as to why some studies, such as Tohge *et al.,* (2005) reported decreased levels of certain flavonols in *PAP1D* over-expressing plants. Over-expression of MYB75 protein may result in sequestration of TCP3, making it unavailable for interaction with MYB12 and MYB111, and thereby negatively influence transcription of the flavonol biosynthetic genes. This idea falls in line with the Y2H data presented in Chapter 2, where MYB75^{T131E} displayed a weaker interaction with TCP3 than did any other phosphovariant in yeast (Fig 2.4). If this is also true *in planta* a reduction in MYB75-TCP3 interaction strength could mean that in *35Spr:MYB75^{T131E}* plants, more TCP3 would be available to interact with MYBs associated with flavonol biosynthesis. Conversely, MYB75^{T131A} might sequester TCP3, preventing it from binding to MYB12 and MYB111, resulting

in the reduced flavonol content observed in Fig 3.6B. Assuming our phosphovariants accurately represent protein phosphorylation status, then flavonol profiles in *35Spr:MYB75*^{WT} would vary depending on the proportion of MYB75 that is phosphorylated, which is ultimately dictated by environmental and developmental cues. While this variable sequestration hypothesis would potentially explain the differences in total flavonol levels observed in plants over-expressing MYB75, it does not explain why some biochemical species of flavonols increase while others decrease in specific MYB75 phosphovariant lines.

MYB11, MYB12 and MYB111 are known to regulate flavonols biosynthesis and have been shown to impact core flavonol biosynthetic genes, including chalcone isomerase, flavonol 3-hydroxylase and flavonol synthase (Stracke *et al.,* 2007). These MYBs also appear to influence expression of flavonol modifying enzymes. Interestingly, each gene has a different expression pattern and a distinct influence on flavonol profiles, indicating that spatial and temporal distribution of flavonoid-regulating transcription factors does influence the biochemical profiles, and that a particular tissue and cell type is wired to produce a unique set of molecular species of flavonoids at a given growth stage. Although the regulation of flavonoid biosynthetic genes by MYB transcription factors has been well characterized, little is known about the way flavonoid modifying enzymes are regulated, and what transcriptional regulators are involved. It is clear that most genes participating in phenylpropanoid metabolism are controlled by several transcription factors, reinforcing the idea that the biochemical profile is a result of cooperative action of multiple transcriptional regulators found in a particular cellular milieu. This picture is further complicated by the different stability of each biochemical species (Rowan *et al.,* 2009); thus, biochemical profiles are not only controlled through the biochemical activity of gene

products required to catalyze synthesis of specific compounds, but also by the activity of enzymes responsible for their turnover.

In addition to responding to stress, spatial and temporal regulation of flavonoid metabolism is developmentally controlled, implicating these compounds in development. Flavonols have been shown to influence auxin transport and therefore can potentially have a profound impact on a variety of developmental processes. Although MYB75 has been shown to influence flavonol content in *Arabidopsis*, none of the studies on MYB75 have explored developmental changes in plants either lacking or over-expressing the protein. My data suggests that MYB75 phosphorylation status has an impact on the biochemical profiles of anthocyanins and flavonols, and that *35Spr:MYB75*^{T131E} plants in particular, accumulate more quercetin and kaempferol glycosides than do plants over-expressing *35Spr:MYB75*^{WT} or *35Spr:MYB75*^{T131A}. *MYB75* expression patterns reported in the eFPBrowser database also suggest that this protein has a highly specific and vital role to play during embryogenesis. Therefore, my results as well as previously published data prompted me to examine *MYB75*-over-expressing plants at different life stages to determine if there are any developmental differences between different phosphovariant over-expressor lines.

3.6 Materials and Methods

3.6.1 Creation of transgenic *Arabidopsis* plant lines expressing different phosphovariant forms of MYB75 protein

3.6.1.1 Creation of MYB75 phosphovariants by point mutation, using site-directed mutagenesis

To generate the full gene version of each phosphovariant, site-directed mutagenesis was used to replace the threonine residue (either T126 or T131) with an alanine or a glutamic acid. *MYB75* gene locus was PCR-amplified using Phusion® polymerase, and the primers F-5' GCCGGATCCATGGAGGGTTCGTCC AAAGGGC and R-5' GCCCTGCAGCTAATCAAATTTCACAG TCTCTCC. Purified PCR products were digested with *BamHI* and *PstI* restriction endonucleases and ligated into linearized pUC19 vector using T4 DNA ligase. The resulting construct was used as a template for the creation of *MYB75*-gene phosphovariants by employing the Q5 ® site-directed mutagenesis kit (New England Biolabs), in conjunction with primers shown in table 3.1 Mutagenized versions of *MYB75* were sequenced to verify that each threonine residue was appropriately replaced with either alanine or glutamic acid, and to ensure that there are no errors in the gene sequence.

Table 3.1

Table 3.1 Primers for site-directed mutagenesis, used to generate each phosphovariant version of the full length *MYB75* gene.

cDNA	Primer sequences and modification	Thr (WT codon)	Ala	Glu
WT MYB75	ATTACGCCCATTCCTACAACACCGG	T126-> ACG T131-> ACA	-------	-------
T126A	F- GACATTGCGCCCATTCCTACAACACC R- TCTCTTTTTCATCTTTATCTTACAACACGGTTCATG	ACG	GCG	---
T131A	F- TACAGCACCGGCACTAAAAAACAATGTTTATAAGCC R- GGAATGGGCGTAATGTCTCTCTTTTTCATC	ACA	GCA	---
T126/131A	F- TACAGCACCGGCACTAAAAAACAATGTTTATAAGCC R- GGAATGGGCGCAATGTCTCTCTTTTTCATC	ACG ACA	GCG GCA	---
T126E	F- GACATTGAGCCCATTCCTACAACACC R- TCTCTTTTTCATCTTTATCTTACAACACGGTTCATG	ACG	---	GAG
T131E	F- TACAGAACCGGCACTAAAAAACAATGTTTATAAGCC R- GGAATGGGCGTAATGTCTCTCTTTTTCATC	ACA	---	GAA
T126/131E	F- TACAGAACCGGCACTAAAAAACAATGTTTATAAGCC R- GGAATGGGCTCAATGTCTCTCTTTTTCATC	ACG ACA	---	GAG GAA

3.6.1.2 Cloning constructs for plant transformation

Constructs carrying cDNA of *MYB75* phosphovariants were provided by Dr. Zhenhua Yonge: these included *MYB75*^{T126A}, *MYB75*^{T131A}, *MYB75*$^{T126/131A}$, *MYB75*^{T126E}, *MYB75*^{T131E} and *MYB75*$^{T126/131E}$, which Dr. Yonge generated by site-directed mutagenesis. All of the above phosphovariants were cloned by Dr. Yonge into the gateway entry vector pENTR2B, behind an endogenous *MYB75* promoter, encompassing 2742bp of genomic sequence upstream of the *MYB75* translational start site (Fig 3.10). The *MYB75pr:MYB75 cDNA* constructs were transferred into the binary gateway vector pEARLY-GATE301, by recombination based cloning, using LR Clonase II (Thermo Fisher Scientific). The resulting constructs were subsequently used to transform *myb75*$^{-}$ (Nossen) mutant plants.

Fig 3.10

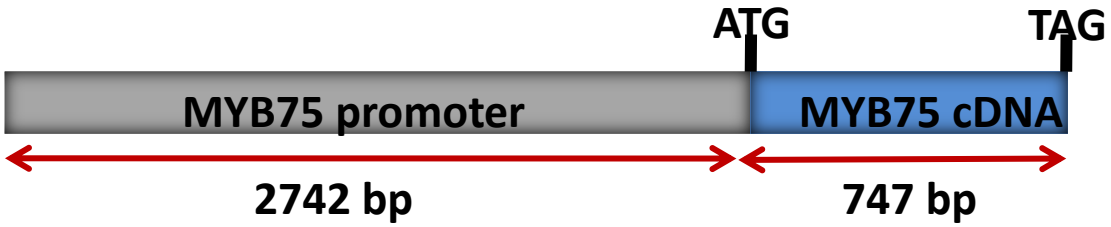

Fig 3.*10 MYB75 promoter- MYB75 cDNA* cassette, used to transform *Arabidopsis* plants *(myb75*$^{-}$ Nossen).

GATEWAY® recombination-based cloning was employed to generate constructs that were transformed into *Arabidopsis* plants to over-express full gene versions of *MYB75*, with an N-terminal 3X Hemagglutinin-epitope tag, under the control of a constitutive CAMV35S promoter. Each phosphovariant was amplified from mutagenized *MYB75* gene templates described in 3.6.1.1, by PCR, using Phusion® polymerase and GATEWAY® compatible primers: F-5' GGGGACAAGTTTG TACAAAAAAGCAGGC TTCATGGAGGGT TCGTCCAAAGGGC and R-5'GGGGACCACTTTGTACAAGAAAGCTGGGTCCTAATCA AATTTCACAGTCTCTCC . Purified PCR products were inserted into the entry vector pDONRzeo (invitrogen), by recombination-based cloning, using the BP Clonase II enzyme (Thermo Fischer Scientific), and transformed into TOP10 competent *E.coli* cells (Thermo Fischer Scientific). Successful clones were isolated and sequenced for subsequent recombination, using LR Clonase II enzyme (Thermo Fischer Scientific), into the GATEWAY® compatible binary vector, pGWB15, which contains a 35S promoter an N-terminal 3xHA- epitope tag sequences. The constructs *35Spr:3XHA:MYB75*^{WT},

35Spr:3XHA:MYB75^{T131A}, and *35Spr:3XHA:MYB75*^{T131E} were transformed into *Arabidopsis* Col-0 WT plants.

Dexamethasone-inducible lines were generated by PCR amplifying *3xHA:MYB75 gene* fusion cassette using the *35Spr:3xHA:MYB75 gene* constructs, described above, as templates. Each *3xHA:MYB75* cassette (*MYB75*^{WT}, *MYB75*^{T131A} and *MYB75*^{T131E}) was amplified by PCR using Phusion® polymerase, and the primers F-5' CCGCTCGAGATGGGG TTAATTAAC ATCTTTTACCC and R-5' GGCCTCGAGCTAATCAAATTTCAC AGTCTCTCCATCG. Purified PCR products were digested with XhoI restriction endonuclease and ligated into the binary vector pTA7002, which was linearized with XhoI. The generated constructs *DEXpr:3XHA:MYB75*^{WT}, *DEXpr:3XHA:MYB75*^{T131A}, and *DEXpr:3XHA:MYB75*^{T131E} were sequenced to confirm appropriate cassette orientation downstream of the DEX promoter, and were subsequently transformed into *Arabidopsis* Col-0 WT plants.

3.6.1.3 Plant growth conditions and transformation

Arabidopsis seeds were surface-sterilized using chlorine gas and plated on petri dishes containing ½ Murishige and Skoog (½MS) medium, with 0.8% plant agar. All seeds were vernalized at 4°C in the dark for 3-4, days before being put into the light. Seeds were germinated under a light fluence of ~30 µmol $m^{-2}s^{-1}$ and 16h light/8h dark photoperiod, at 21°C and grown under these conditions until they were transferred to soil. Between 7-12 days after germination seedlings were planted in soil and transferred to a growth chamber with a light fluence of ~100-120 µmol $m^{-2}s^{-1}$, photoperiod of 16h light/8h dark, and temperature of 21°C.

Plant transformation was performed using *Agrobacterium tumefaciens* GV3101 strain. Each construct destined for transformation into plants was first transformed into chemically

competent *Agrobacteria.* Successfully transformed *Agrobacteria* were selected on LB media with 50µg/ml gentamycin and a second antibiotic specific for each construct (Table 3.2). To perform plant transformation by floral dipping, 100ml of *Agrobacterium* culture was grown for each construct, in liquid LB medium with antibiotics, at 28°C, in the dark, until OD_{600} ~ 0.8. Cultures were harvested by centrifugation at 5500 x g, for 20 min at room temperature and resuspended in transformation solution (30ml distilled water, 1.5g sucrose, 9µL Silwet-77). Flowers of ~5-week-old *Arabidopsis* plants grown under 16h light/8h dark photoperiod were submerged in the transformation suspension for 1-2 min, with gentle agitation. Dipped plants were laid down in trays, covered, and left in the dark overnight. The following day the plants were returned into the growth chamber. Each plant was dipped twice, with each dip being one week apart, to increase the number of transformants. Seeds (T0) from transformed plants were harvested and plated on ½MS plates with appropriate selection, to isolate successfully transformed T1 plants (Table 3.2). Dr. Zhenhua Yonge transformed *myb75*$^{-}$ Nossen mutants with *MYB75pr:MYB75 cDNA* constructs (all phosphovariants). I performed the transformations of *35Spr:3xHA:MYB75 gene* and *DEXpr:3xHA:MYB75 gene* lines.

Lines over-expressing MYB75 (*35Spr:3xHA:MYB75 gene*) were isolated by visually screening adult T1 plants for anthocyanin accumulation, which was manifested as purple colouration in the rosette leaves. The visual screen was followed by western blot detection of recombinant MYB75 protein, using an anti HA-tag antibody. *DEXpr:3xHA:MYB75 gene* lines were isolated by spraying adult T1 plants with 30µM DEX, and looking for anthocyanin accumulation visually, and immunoscreening for recombinant protein production. All lines which displayed dark purple colour also showed high levels of recombinant MYB75 protein

expression. Several plant lines were established for each genotype*: 35Spr:MYB75^{WT}*; L11, L12, L14, 35Spr:*MYB75^{T131A}*; L1, L22, L23*, 35Spr: MYB75^{T131E}*; L2, L4, L5 and L9, *DEXpr:3xHA:MYB75^{WT}*; L1, L3, L4, L5 and *DEXpr:3xHA:MYB75^{T131E}*; L6, L7 and L9. These lines were used in subsequent experiments, using equal proportions of each line to represent a specific genotype.

Table 3.2

Table 3.2 List of constructs used for stable transformation of *Arabidopsis* plants to create lines expressing various MYB75 phosphovariants under endogenous (*MYB75pr)*, constitutive (*35Spr*) and inducible (*DEXpr)* promoters.

CONSTRUCT	VECTOR	Selection bacteria	Selection Plants	Plant background
MYB75pr:MYB75^{WT} (cDNA)	pEarleyGate301	Kan *	Basta **	*myb75*$^{-}$ Nossen
MYB75pr:MYB75^{T126A} (cDNA)	pEarleyGate301	Kan	Basta	*myb75*$^{-}$ Nossen
MYB75pr:MYB75^{T131A} (cDNA)	pEarleyGate301	Kan	Basta	*myb75*$^{-}$ Nossen
MYB75pr:MYB75^{T126E} (cDNA)	pEarleyGate301	Kan	Basta	*myb75*$^{-}$ Nossen
MYB75pr:MYB75^{T131E} (cDNA)	pEarleyGate301	Kan	Basta	*myb75*$^{-}$ Nossen
MYB75pr:MYB75$^{T126/131A}$ (cDNA)	pEarleyGate301	Kan	Basta	*myb75*$^{-}$ Nossen
MYB75prMYB75$^{T126/131E}$ (cDNA)	pEarleyGate301	Kan	Basta	*myb75*$^{-}$ Nossen
35Spr:3xHA:MYB75^{WT} (gene)	pGWB15	Kan	Hyg ***	Col-0 WT
35Spr:3xHA:MYB75^{T131A} (gene)	pGWB15	Kan	Hyg	Col-0 WT
35Spr:3xHA:MYB75^{T131E} (gene)	pGWB15	Kan	Hyg	Col-0 WT
DEXpr:3xHA:MYB75^{WT} (gene)	pTA7002	Kan	Hyg	Col-0 WT
DEXpr:3xHA:MYB75^{T131A} (gene)	pTA7002	Kan	Hyg	Col-0 WT
DEXpr:3xHA:MYB75^{T131E} (gene)	pTA7002	Kan	Hyg	Col-0 WT

*Kan= Kanamycin 50µg/ml **Basta= Glufosinate/Basta 10µg/ml ***Hyg= Hygromycin 30µg/ml

3.6.2 Sucrose treatment of *Arabidopsis* seedlings

Heterozygous T2 seedlings carrying *35Spr:3xHA:MYB75 gene* (*MYB75^{WT}, MYB75^{T131A}* and *MYB75^{T131E}*) were grown on petri dishes containing ½MS medium supplemented with hygromycin, under growth conditions described in section 3.6.1.3. At ten days post germination

the seedlings were transferred to ½MS medium containing 6% sucrose and incubated for 24 hours under continuous light, at a fluence of ~35 µmol $m^{-2}s^{-1}$. Control plants were left in dark on ½MS without sucrose. The seedlings were photographed using a Cannon (EOS rebel T5) digital camera mounted on a Zeiss Stemi 2000-C dissecting scope. Anthocyanin quantification was performed as described in section 3.6.3 using a pool of 20-40 seedlings for each phosphovariant. Western blot analysis was performed as described in section 2.6.4.3 using a pool of 20-40 seedlings for each phosphovariant.

3.6.3 Total anthocyanin quantification

MYB75pr:MYB75 cDNA plants (*myb75*$^{-}$ Nossen background) were sampled after 48h of continuous light, at a fluence ~100-120 µmol $m^{-2}s^{-1}$, to observe promoter responsiveness to light and to determine if any of the MYB75 phosphovariants can complement the *myb75*$^{-}$ mutant phenotype in terms of anthocyanin accumulation. Plant lines carrying *35Spr:3xHA:MYB75* gene constructs (*MYB75*^{WT}, *MYB75*^{T131A} and *MYB75*^{T131E}), were grown and sampled under 16h light/8h dark conditions (fluence ~100-120 µmol $m^{-2}s^{-1}$). Anthocyanin quantification was performed as described by Mehrtens *et al.,* (2005). Mature rosette leaves from ~5week old plants were collected into microcentrifuge tubes (1-2mg) and fresh weight was recorded for each sample. The tissue was frozen in liquid nitrogen, ground to a powder and resuspended in 1ml of extraction solution (49.5% methanol, 49.5% distilled water, 1% acetic acid). The samples were incubated at 45°C for 4h, centrifuged at 15000 rpm and the cleared supernatant was transferred to a cuvette. Absorbance was measured at A_{530} and A_{650} and total anthocyanin quantity was determined using the equation $Q_{anthocyanin}$=[A530-(A650x0.25)]/mass(g).

3.6.4 Recombinant MYB75 protein extraction, immunodetection and relative quantification of protein levels using ImageJ

Detection of recombinant MYB75 protein was performed as described in Chapter 2, sections 2.6.4.2, 2.6.4.3, and 2.6.4.4.

3.6.5 RNA extraction, reverse-transcription PCR and qPCR

RNA extraction from mature rosette leaves of ~5-week-old *Arabidopsis* plants was performed using TRIzol® reagent (Thermo Fischer Scientific), according to manufacturer's protocol. RNA quality was evaluated by running 5µL of RNA on 2% agarose gel, and the RNA concentration was determined spectrophotometrically using NanoDrop® (Thermo Fischer Scientific). Reverse transcription was performed using SuperscriptII (Invitrogen) to obtain total cDNA.

Semi-quantitative RT-PCR was performed using MangoMix™ (Bioline), and by running the PCR reaction for 25 cycles. The resulting products were analysed by gel electrophoresis and relative amount of cDNA for each gene was quantified by evaluating band intensity using ImageJ. Real time PCR (or qPCR) was performed using SsoAdvanced™ Universal SYBR® Green Supermix (BIO-RAD), on a CFX connect real time system (BIORAD). Primers used for these experiments are shown in table 3.3. To differentiate between endogenous and recombinant *MYB75* expression, two different primer sets were designed. One set of primers was designed to amplify the end of the *MYB75* gene to the UTR (not present in the recombinant transcript), in order to detect endogenous *MYB75*, while recombinant *MYB75* expression was detected using a forward primer that binds the linker sequence between the HA-epitope tag and a reverse primer that binds to the end of the *MYB75* coding region.

Quantification of relative gene expression, by real-time PCR was performed as follows. Primer efficiency was determined for each primer set prior to running the final qPCR. Raw Ct data was processed using the Pfaffl mathematical model (Pfaffl 2001), where the expression ratio= $[E_{target}^{\Delta Ct(control-sample)}] \div [E_{reference}^{\Delta Ct(control-sample)}]$. This formula was used to account for differences in amplification rates caused by primer efficiencies higher than 100% (100% efficiency E=2.0). The housekeeping genes used as reference samples were actin1 and actin 8, and the control genotype used was Col-0 WT.

Table 3.3

Table 3.3 Primer sequences used for semi-quantitative RT-PCR and qPCR.

GENE and AGI code	FORWARD	REVERSE	Product size (bp)	Primer Efficiency
Act1 At3G18780	CCACCTGAAAGGAAGTACAGTG	GTGAACGATTCCTGGACCTG	119	2.57
Act8 At1G49240	TCTAAGGAGGAGCAGGTTTGA	TTATCCGAGTTTGAAGAGGCT	131	2.15
MYB75 At1G56650 (endogenous)	T CCT AGA GGA AAG CCA AGA GG	ACACAAACGCAAACAAATGTTCG	159	2.27
MYB75 At1G56650	T CCT AGA GGA AAG CCA AGA GG	CTAATCAAATTTCACAGTCTCTCCATCG	132	
HA:MYB75	CAGTGCAGCGCTGTTATCACAAG	CTAATCAAATTTCACAGTCTCTCCATCG	792	
DFR At5G42800	CGTTCGAGATCCCGGTAATTTG	ATGGCATCATCGTAGCTTCCTT	120	2.5
ANS At4G22880	CGAGTCAGACGATGAAAAGATCCGTGAG	CGGCTTTCTTGACACGCTCCATTAGATCA	131	2.58
UGT75C1 At4G14090	CTCAAACGATGTGGTTCAAACGCCCT	CGGTGATAGGCTCTGTTTCGGTGG	82	2.58
GST At5G17220	GGCTGACGTGGAGACCTA	CCAAGACCACTCCTAGCTTCAC	137	2.54
CHS At5G13930	ACACATGTGTGCTTACATGGC	TTAGGGACTTCGACCACCAC	69	2.82

3.6.6 Biochemical profiling of flavonoids and anthocyanins in *35Spr:3xHA:MYB75 gene* plants by high performance liquid chromatography

Mature rosette leaves of ~5-week-old *Arabidopsis* plants carrying *35Spr:3xHA:MYB75* (*MYB75^{WT}, MYB75^{T131A}, MYB75^{T131E}*), grown on soil under 16h light/ 8h dark light cycle under a light fluence of ~100-120 µmol $m^{-2}s^{-1}$ were harvested, weighed and ground on liquid nitrogen. For each phosphovariant genotype a total of four samples were used, each sample containing tissue from 2-3 plants. All lines belonging to a particular phosphovariant genotype were equally represented in the samples tested. Total phenolic extraction was performed in 50% methanol

solution, using an extraction volume proportional to the fresh weight of the tissue in each sample, to ensure exctracts were equally concentrated. Samples were analysed by liquid chromatography (LC) and LC-mass spectrophotometry (MS) by Dr. Lina Midilao, while quantitative analysis of the resolved peaks was performed by Dr. Simone Castellarin. Anthocyanins were measured on an Agilent 1100 LC/MSD Trap XCT Plus mass spectrometer. Separation of anthocyanin compounds was achieved on an Agilent Zorbax SB-C18 column (150mm × 4.6mm ID, 1.8µm, 3.5um pore size) held at 57°C. The mobile phases were: water-formic acid (2%), solvent A, and acetonitrile-formic acid (2%), solvent B. Flow rate was 0.8ml/min. The solvent gradient program was 0.5min, 6% B; 4 min, 10 % B; 13min, 25 % B; 20 min, 35% B; 25min, 60% B; 30min, 95% B; and 32min, 6% B. A Diode array detector was used to detect absorbance at 365 nm for flavonols and 520 nm for anthocyanins. The flavonols and anthocyanins mass spectra were analysed after electrospray ionization (ESI) in alternating positive and negative ionization mode with a scan range between 50 and 850 m/z. Annotation of compounds was based on the comparison of absorption spectra, MS fragmentation patterns, and relative elution time with the ones of *Arabidopsis thaliana* flavonols and anthocyanins reported in previous studies, as a reference (Yonekura-Sakakibara *et al.,* 2008; Yonekura-Sakakibara *et al.,* 2012; Shi and Xie 2014). Quantity of each flavonol and anthocyanin molecular species was reported a speak areas. Statistical analysis was performed to determine differences in the quantity of each compound: statistics (ANOVA and Tukey test for separating the averages) for each peak as well as for the total area.

CHAPTER 4 Developmental changes in *Arabidopsis* plants over-expressing MYB75^{T131A} and MYB75^{T131E} phosphovariants

4.1 Introduction

By definition, plant secondary metabolites such as flavonoids are dispensable for immediate survival and reproduction. Over the years of plant research, in controlled laboratory settings we have come to accept this view, and in some ways overlooked the profound impact that these compounds can have on development. In deciduous trees, autumnal leaf senescence reveals the accumulation of foliar anthocyanins, manifested as bright red and orange colours. It is widely believed that anthocyanins play a photoprotective role, shielding the photosynthetic machinery from damaging light, at a stage when other protective mechanisms, as well as cellular repair machinery are shutting down. Shielding the photosystems from excess light prevents photoinhibition and enables ongoing energy production, during nutrient resorption from senescing leaves. This process ensures that nutrient stores in perennial tissues are sufficient for overwintering and for supporting new growth during the subsequent spring (Field *et al.,* 2001; Hoch *et al.,* 2001; Hoch *et al.,* 2003). Autumnal anthocyanin accumulation is induced by cold temperatures but appears also to be closely tied to the onset of chlorophyll degradation (Ishikura,1973; Hoch *et al.,* 2001), indicating that plastid-derived signals may play a role in regulating anthocyanin production. In *Arabidopsis* leaf senescence also involves nutrient remobilization, resorption, and redistribution to reproductive organs. However, unlike studies of deciduous trees in the field, chronic stress experiments with *Arabidopsis* performed in a laboratory setting, did not show any correlation between anthocyanin levels and chlorophyll turnover (Misyura *et al.,* 2012). Furthermore, analysis of *transparent testa* mutants indicated

that the inability to produce anthocyanins did not impact the plant's ability to remobilize nutrients under chronic moderate stress conditions (Misyura *et al.,* 2013). Nevertheless, anthocyanins play a vital role in development, as they control how much visible light reaches the photosynthetic machinery, which can ultimately affect light harvesting, photosynthesis and photomorphogenesis (reviewed in Steyn *et al.,* 2002).

Flavonols also have an established role in development, due to their ability to modulate auxin flow (Brown *et al*, 2001). In his pioneering study, Brown *et al*., (2001) demonstrated that *Arabidopsis* seedlings grown on a medium containing the flavonoid precursor, naringenin, exhibited phenotypes similar to seedlings grown on NPA (N-1-naphtylphtalamic acid; a potent auxin inhibitor), including decreased root growth and gravitropism. Brown *et al.,* (2001) demonstrated that the flavonoid deficient *tt4* mutants displayed elevated auxin flow in seedlings, and in stems of mature plants. In wild type *Arabidopsis* plants auxin flow was highest in stem segments close to the apex and slightly lower in basal sections. Conversely, *tt4* mutants lacking the key flavonoid biosynthetic enzyme chalcone synthase (CHS), displayed an increase of over 300% in auxin flow near the stem base and significantly higher overall rate of basipetal auxin flow, from the shoot to the root (Brown *et al.,* 2001).

The *transparent testa (tt)* mutations in Arabidopsis have provided crucial insights into the relationship between flavonoid metabolism and plant development. Fig 4.1 displays a simplified flavonoid biosynthetic pathway with abbreviated gene names and the corresponding *transparent testa* mutations. Analysis of different *transparent testa* mutants, in the Landsberg (Ler) *Arabidopsis* ecotype, which are deficient in different flavonoid biosynthetic enzymes and regulatory proteins, has revealed a range of phenotypic changes in root and shoot architecture.

These mutants displayed a change in the number, position and initiation site of root hairs, and lateral roots. In aerial tissues they displayed changes in inflorescence height and number, as well as changes in silique density (Buer and Djorjevic, 2009). Further examination of *transparent testa* mutants revealed that *tt4* (*CHS*), *tt5* (*CHI*) and *tt7* (*F3'H*) had numerous lateral root initiation points, located close to each other, resulting in aberrant root architecture, while mutations in the regulatory genes, *tt8* and *ttg2* led to a shallower root system (Buer *et al.,* 2013; Fig 3, Table4). Analysis of aerial organ development revealed that the mutants *tt1, tt2* (MYB transcription factor) and *tt4* had slower leaf expansion, while *tt8* plants showed faster leaf expansion. Bolting time and inflorescence elongation rates were faster in *tt8, ttg1* and *ttg2* and slower in *tt4, tt6* and *tt7* (Buer *et al.,* 2013; Table6).

In WT *Arabidopsis* plants different molecular species of flavonols displayed specific distribution patterns. Quantification of flavonols in different tissues of *Arabidopsis* seedlings revealed that quercetin and kaempferol accumulated in the upper root, root-hypocotyl transition zone and, to a smaller extent in the upper hypocotyl. Staining with diphenylboric acid 2-aminoethyl ester (DPBA), enables *in vivo* visualization of flavonol distribution using fluorescence microscopy: quercetin derivatives produce golden yellow fluorescence, while kaempferol and naringenin (and their corresponding glycosides) fluoresce yellow-green. This method, in conjunction with biochemical analyses of different plant organs, has been instrumental in determining the distribution of flavonols in *Arabidopsis.* In young seedlings, kaempferol was the primary flavonol in the lower root, while small amounts of quercetin were found in the lower hypocotyl (Peer *et al.,* 2001). Developing cotyledons contained mainly glycosylated flavonols, while aglycones were the predominant flavonols in hypocotyls, upper

root and root-hypocotyl transition zone, for a brief period of time, between 3 and 7 days post-germination (Peer *et al.,* 2001). In developing seedlings quercetin is widely distributed throughout the root, with brightest gold-yellow fluorescence observed in cotyledonary nodes of DPBA-treated seedling. Generally, flavonols were found to be most concentrated in transition zones and actively growing tissues, such as the root-hypocotyl junction, cotyledonary nodes and root elongation zone (Peer *et al.,* 2001; Buer *et al.,* 2013). In some cases these compounds display a cell specific localization pattern; yellow-green fluorescence, indicative of kaempferol accumulation was observed in a ring of cells near the root cortex, with a cone of gold-yellow quercetin-containing cells located below (Peer *et al.,* 2001; Fig 2). In mature plants flavonoids accumulated only in actively growing tissues, including immature siliques, flowers and upper inflorescence stems, where primary growth was ongoing (Peer *et al.,* 2001; Fig 3). Quercetin predominated in floral organs and upper inflorescence stems, with higher concentration of aglycones found in growing tissues, close to the apex, and decreased closer to the base. Anthocyanin accumulation on the other hand, showed the opposite pattern, with higher levels of anthocyanins near the base, and less anthocyanins near the apex (Peer *et al.,* 2001; Fig 4).

Mutations in flavonoid biosynthetic and regulatory genes led to alterations in flavonoid accumulation patterns, and in many cases changes in auxin flow in specific parts of the plant. For instance, the *tt3* mutant, containing a lesion in the *DFR* gene, accumulated more flavonols in the root tips, and concurrently showed a decrease in root-ward auxin flow. Similarly, *tt7*-plants with a mutation in *F3'H*, had lower levels of quercetin and, were devoid of kaempferol aglycone, in the root-shoot junction; this mutant also showed decreased basipetal (rootward) and acropetal (shootward) auxin transport. Conversely, the mutants *tt5* and *tt6* displayed

increased basipetal auxin transport; the root tips of the mutants*, tt5, tt6,* and *tt7* were deficient in quercetin-3-glycoside, although *tt5* accumulated this compound in the root-shoot junction (Buer *et al.,* 2013). These experiments illustrate a complex relationship between auxin flow and accumulation of different flavonol biochemical species at specific locations in the plant. In most cases, mutations that result in reduced total flavonol levels lead to overall increased auxin flow (such as in *tt4* mutants). In other cases however, auxin flow was reduced as a result of failure to accumulate specific flavonol compounds (for instance in the *tt7* mutant) (Buer *et al.,* 2013). The most plausible explanation for this observation is that auxin flow requires canalization, that is to say, site specific auxin accumulation, which normally drives development and organogenesis and requires auxin flow be restricted to specific cell channels or routes. It appears that accumulation of flavonols in organ junctions and areas of active growth, could be playing a role in controlling auxin flow and direction, and thereby influence development. What remains unclear is how each molecular species of flavonol acts to influence auxin flow and how the distribution of these specific flavonols can influence development through regulation of auxin distribution. Fig 4.1 displays a simplified flavonoid biosynthetic pathway with abbreviated gene names and corresponding *transparent testa* mutations.

Increasing evidence suggest that specific molecular species of flavonols play unique roles in controlling auxin flow. Initially it was thought that only aglycones have a biological role to play in auxin distribution, while the glycosides had no effect on auxin flow (reviewed in Peer *et al.,* 2001). However, subsequent experiments demonstrated that the apparent lack of biological function for the glycosides *in vitro* was caused by failure of plants to take up exogenously applied flavonol glycosides (Buer *et al.,* 2013), and recent work revealed that

kaempferol 3-O-rhamnoside-7-O-rhamnoside can inhibit polar auxin transport (Yin *et al.,* 2014). These authors found that a mutation in *UGT78D2* (flavonol-3-O-glycosyltransferase) led to increased accumulation of kaempferol 3-O-rhamnoside-7-O-rhamnoside. The *ugt78d2* null mutant plants displayed reduced basipetal auxin flow in stems as well as reduced apical dominance and increased branching. Additionally, *ugt78d2* mutants displayed a dwarf phenotype, resembling the *abcb1*/*abcb19* double mutant known to be defective in auxin transport channels. Analysis of several mutants defective in different steps of flavonol modification demonstrated that it was specifically the accumulation of kaempferol 3-O-rhamnoside-7-O-rhamnoside (K1) that was responsible for the observed phenotypes (Yin *et al.,* 2014). Recent analysis of another *Arabidopsis* mutant*,* with a lesion in *UGT89C1* (flavonol-7-O-rhamnosyltransferase) revealed that plants deficient in 7-rhamnosylated flavonols have severe phenotypic defects, including deformed trichomes, upward bending cotyledons, and abnormally shaped epidermal cells (Kuhn *et al.,* 2016). Unlike *tt* mutants, mutation in *ugt89c1* did not result in alteration to auxin flow. Instead, null mutants accumulated higher levels of the auxin precursor, indole-3-acetonitrile (IAN), as well as various degradation products, indicating that 7-rhamnosylated flavonols affect auxin metabolism rather than transport. These developmental phenotypes, as well as the accumulation of auxin derivatives, are suppressed in mutant backgrounds where the flavonol backbone is not produced, such as *fls* and *tt4,* reinforcing the idea that specifically decorated flavonols play unique roles in plant development (Yin *et al.,*2014; Kuhn *et al.,* 2016). Interestingly, localization studies using fluorescent protein fusions, showed that UGT89C1 gene products localized near sites of vascular development in the root (Kuhn *et al.,* 2016; Fig 5).

Fig 4.1

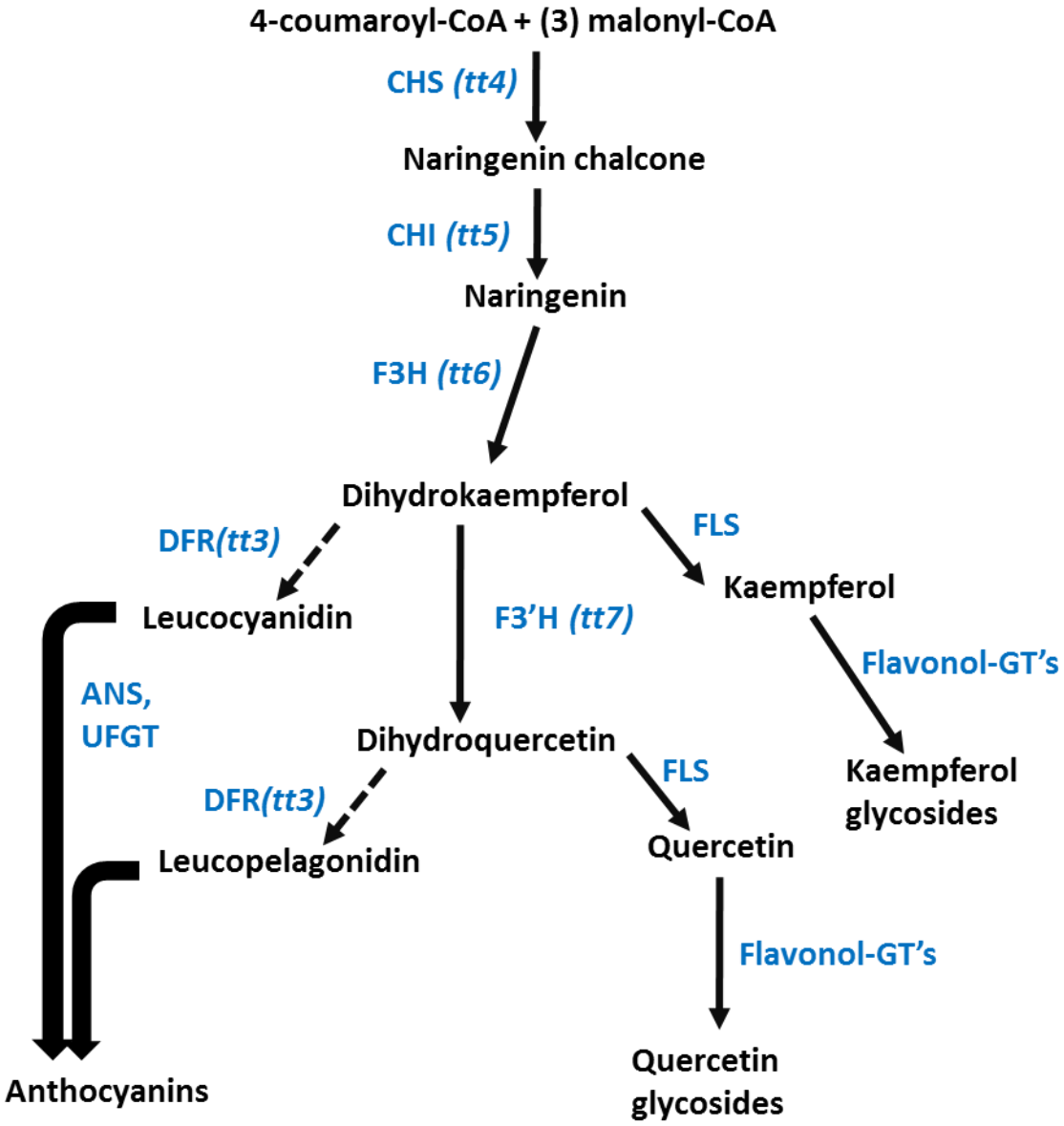

Fig 4.1 Simplified flavonoid biosynthetic pathway in *Arabidopsis,* depicting key flavonoid biosynthetic enzymes and corresponding *tt* mutants; adapted from Buer *et al.,* 2013.

Flavonols have been shown to affect auxin fluxes in several ways. For instance, exogenous application of quercetin to *Arabidopsis* roots triggered relocation of the PIN1 auxin efflux channels, redirecting auxin flow during the gravitropic response (Santelia et *al.,* 2007).

Another study demonstrated that the expression patterns of different PIN efflux channel proteins (PIN1, PIN2, PIN3 and PIN4) changed in *tt3* and *tt4* mutants. The authors also showed, using immunolocalization, that PIN efflux channels, normally restricted to the vascular cells, were mislocalized in *tt* mutants, and could be found in the cortex and epidermis, adjacent to the vasculature (Peer *et al.,* 2004). Interestingly, treatment of *tt4 Arabidopsis* plants with am auxin influx inhibitor restored normal PIN localization, indicating that changes in gene expression and localization patterns of PIN channels in *tt* mutants was caused by deregulation of auxin transport, in the absence of flavonols (Peer *et al.,* 2004).

More recently, another group of auxin efflux channels ABCB1/PGP1 and ABCB19/PGP19, were shown to be a target of flavonol-mediated inhibition of auxin transport. In this case, flavonols were shown to negatively regulate auxin transport by disrupting the interaction between the ABCB/PGP channel and TWD1 (*twisted dwarf 1*) protein, which form a complex necessary to mediate auxin transport (Bailly *et al.,* 2008). The exact mechanism by which flavonols modulate PIN channel function has not been established, however, there is evidence to suggest that flavonols influence cell signalling, particularly kinase/phosphatase activity of proteins that regulate PIN channel trafficking and localization to specific membranes (reviewed in Peer and Murphy, 2007). Possible targets include the serine/threonine kinase PINOID (At2g34650) (Christensen *et al.,* 2000; Benjamins *et al.,* 2001; Friml *et al.,* 2004) as well as WAG kinases (At1g53700, At3g14370) (Santner and Watson, 2006). Although we are only beginning to elucidate how flavonols influence auxin signalling, it is clear that these phenolics have a profound effect on auxin flow. It is worthwhile at this point in our discussion to describe how

auxin is believed to influence development through localized accumulation and regulation of gene expression, in a cell autonomous fashion.

Auxin can drive global changes in gene expression required for development and differentiation, by driving expression of genes required for hormone biosynthesis and signalling, as well as transcription factors, including global regulators. Auxin affects gene expression primarily by driving the degradation of Aux/IAA repressors, which bind to Auxin Response Factors (ARFs), suppressing their ability to drive expression of auxin-responsive genes (reviewed in Chapman and Estelle, 2009).The products of auxin-responsive genes act as the initiators of signalling and gene expression cascades, that can impact a wide range of physiological and developmental processes, with auxin distribution acting as a spatial and temporal cue for developmental programming of specific cell populations (reviewed in Chapman and Estelle, 2009; Fabregas *et al.,* 2015).

Auxin synthesis, transport and perception are vital at all stages of development, starting from embryogenesis, where spatial and temporal distribution of auxin concentration maxima determine cell fate and subsequent positional organogenesis. Mutations in genes required for auxin biosynthesis, transport or perception lead to severe defects in early development (reviewed in Möller and Weijers, 2009). A prominent example of how auxin impacts embryogenesis includes the MONOPTEROS (MP) mutant, defective in a transcription factor required to elicit auxin response. *Arabidopsis mp* mutants fail to develop hypocotyls and roots, resulting from the inability to establish a normal apical-basal tissue pattern during embryogenesis (Berleth and Jürgens, 1993). Auxin biosynthesis can also have a profound impact on early development; the *Arabidopsis* quadruple mutant (*yuc1/yuc4/yuc10/yuc11)*

defective in embryo-specific flavin monooxygenases (required for auxin biosynthesis), fail to develop a hypocotyl and a root meristem (Cheng *et al.,* 2007). Auxin transport mutants, defective in one or more PIN efflux channels show a variety of developmental abnormalities, stemming from aberrant cell division during various stages of embryogenesis (reviewed in Möller and Weijers, 2009).

During post-embryonic development, positioning of organs and tissues within the plant body are highly dependent on specific spatial and temporal distributions of local auxin concentration maxima (Heisler *et al.,* 2005; reviewed in Fukuda *et al.,* 2004), and the creation of these maxima depends largely on localization of specific auxin efflux and influx channels (Gälweiler *et al.,* 1998; Heisler *et al.,* 2005; reviewed in Fabregas *et al.,* 2015). For instance, localization of PIN1 efflux channels can direct auxin flow to sites of organ initiation (Heisler *et al.,* 2005). Furthermore, auxin accumulation was shown to drive PIN1 expression, indicating that there is a positive autoregulatory mechanism that helps to establish the accumulation of auxin maxima at specific positions in the plant (Heisler *et al.,* 2005). In summary, auxin flow initiates a sequence of events, driven by changes in gene expression, that ultimately lead to tissue differentiation and organogenesis.

Most of the plant body architecture is derived from differentiation of meristematic cells located in the shoot apical meristem (SAM) and root apical meristem (RAM): these meristems give rise to aerial parts of the plant and root system, respectively. Two additional meristematic tissues, the procambium and cambium give rise to the plant vascular tissues during primary and secondary growth, respectively. The procambium develops in emerging organs and forms continuous cell files, which eventually develop into mature vasculature. Establishment and

maintenance of the procambium is dependent on polar auxin flow, driven primarily by the localization of PIN channels to the basal side of cells (reviewed in Fukuda, 2004; Krecek *et al.,* 2009). Development of the procambium as continuous, connected cell files, which ultimately ensures continuity of plant vasculature, is driven by auxin canalization in narrow cell files, and drainage of auxin from neighboring tissues. This process is at least, in part, driven by positive a feedback loop, whereby auxin upregulates expression of PIN channels. Thus, auxin efflux from one cell to the next increases auxin flow through that cell, leading to auxin canalization through continuous cell files (Sachs, 1981;2000; reviewed in Fukuda *et al.,* 2004).

Besides establishment and positioning of the procambium, auxin plays a central role in the differentiation and development of the plant vasculature, essential for transport of water and nutrients throughout the plant. The plant vascular system is composed of xylem, which transports water and minerals, and phloem, which transports photoassimilates. Each of these tissues contains distinct cell types: the phloem is composed of sieve elements and companion cells as well as phloem parenchyma cells, while the xylem made up of tracheary elements and xylem fibres and xylem parenchyma cells. During primary growth all of these cell types originate from the procambium, and therefore their development depends on auxin transport and auxin response. *Arabidopsis* AtPIN1 channel localizes in vascular bundles, in procambium and xylem parenchyma cells, and is the primary PIN channel required for vascular development in aerial tissues (Gälweiler *et al*, 1998). The role of auxin in vascular development is best depicted in studies of xylary vessel differentiation. Auxin drives xylem differentiation through activation of global regulators such as MONOPTEROS (ARF5), which in turn drives the expression of HD-ZIP family transcription factors (such as AtHB8) that lead to global changes in gene expression,

driving vessel differentiation (Matson *et al.,* 2003). For instance, auxin, along with cytokinin positively regulate the expression of the transcription factors VND6 and VND7 which are global regulators of xylem differentiation (Kubo *et al.,* 2005). These transcriptional regulators trigger a cascade of changes in gene expression that eventually orchestrate key events in vessel differentiation, such as secondary cell wall deposition and programmed cell death (reviewed in Shuetz *et al*, 2013). Vascular differentiation is a complex process that involves vast regulatory cascades and signalling networks that are beyond the scope of this thesis. The key takeaway for this discussion is that auxin transport and canalization are vital driving mechanisms for vascular development, including vascular continuity, as well as vessel anatomy and positioning.

As a known regulator of flavonoid biosynthesis, MYB75 clearly has an influence on development, at least at the level of metabolite accumulation. However, recent work from the Ellis and Douglas labs has demonstrated that MYB75 is also a regulator of cell wall development (Bhargava *et al.,* 2013), a process closely tied to vascular differentiation and therefore influenced by auxin. The significance of the findings by Bhargava *et al.,* (2013) is that MYB75 probably has additional transcriptional targets, beyond flavonoid biosynthetic genes, and that those targets could be playing a much broader role in plant development. Finally, MYB75 has been identified as a target for phosphorylation by MAP kinases (Li *et al;* 2016), which play a role in mediating plant stress responses as well as in development. Together, these observations raised the question whether mis-expression of MYB75 or its phosphorylated isoforms might have developmental consequences beyond potential changes in anthocyanin accumulation.

In this chapter, I describe distinct developmental phenotypes that appeared in plants over-expressing different phosphovariants of MYB75 and analyse differential gene expression

patterns in *35Spr:MYB75 gene* over-expressing lines. It is important to note that the data described in this chapter is not a true depiction of the role of MYB75 in development, as the CAMV35S promoter used to over-express different MYB75 phosphovariants leads to ubiquitous protein expression in tissues and developmental contexts where MYB75 would not typically be found. Additionally, the previously observed differential degradation of MYB75^{T131E} phosphovariant, implies that phosphovariants may have different distribution throughout the plant, which further complicates interpretation of my results. Nevertheless, *35Spr:MYB75* over-expressor lines are a powerful tool to identify additional processes that can potentially be influenced by MYB75 phosphorylation status, and to identify new target genes for this transcription factor.

4.2 Impaired germination rates in *MYB75pr:MYB75 cDNA* plants, expressing *MYB75^{T131A}* and *MYB75^{T131E}* phosphovariants

In Chapter 3 I described early attempts to express *MYB75* cDNA by the endogenous *MYB75* promoter, in a *myb75^{-}* background. After screening a large number of T1 plants for anthocyanin production and recombinant *MYB75* expression, it was determined that some phosphovariants were failing to complement the *myb75^{-}* mutation because of very low transgene expression. One possible explanation for this is that the expression of one or another phosphovariant is detrimental to early developmental stages, such as embryogenesis or germination, resulting in artificial selection of plants that express very low levels of *MYB75*. Because of low transgene expression these lines were abandoned after the initial screen, and *MYB75pr:MYB75^{WT}cDNA* control lines were never established. Nevertheless, I wanted to determine if *MYB75pr:MYB75^{T131A}* and *MYB75pr:MYB75^{T131E}* plants showed impaired

germination, in order to test my hypothesis that MYB75 expression and phosphorylation status can have an impact on early development. For this purpose I used seeds from homozygous parent plants, from independent lines including six *MYB75pr:MYB75*^{T131A} and four *MYB75pr:MYB75*^{T131E} lines. The seeds were plated on ½ MS medium and germination was scored 10 days after placing them in the light. Both Nossen WT and *myb75*$^{-}$ mutant showed germination rates close to 100%. In contrast, lines carrying *MYB75*^{T131A} and *MYB75*^{T131E} transgene displayed severely impaired germination (26.8% and 62%, respectively) (Fig 4.2). It is challenging to assess this phenotype in the absence of *MYB75pr:MYB75*^{WT} transgenic control, nevertheless when the two phosphovariants are compared to each other, it is apparent that germination is significantly lower in *MYB75*^{T131A} expressing plants than in *MYB75*^{T131E} , indicating that unphosphorylated MYB75 has a greater negative effect on germination than the phosphorylated version. An alternative explanation is that there is simply less recombinant protein in *MYB75*^{T131E} lines, as this phosphovariant protein was shown to be more labile under certain conditions (see Chapters 2 and 3). Although this data is preliminary, the low germination rates support the idea that my failure to isolate transgenic lines expressing high levels of *MYB75pr:MYB75*^{T131A} and *MYB75pr:MYB75*^{T131E} was caused by artificial selection for plants that express lower levels of MYB75. This idea, that ectopic expression of MYB75 is deleterious at early stages of development may also explain why I was subsequently only able to isolate a very small number of *35Spr:MYB75 gene* lines, despite screening large numbers of T1 transformants.

Fig 4.2

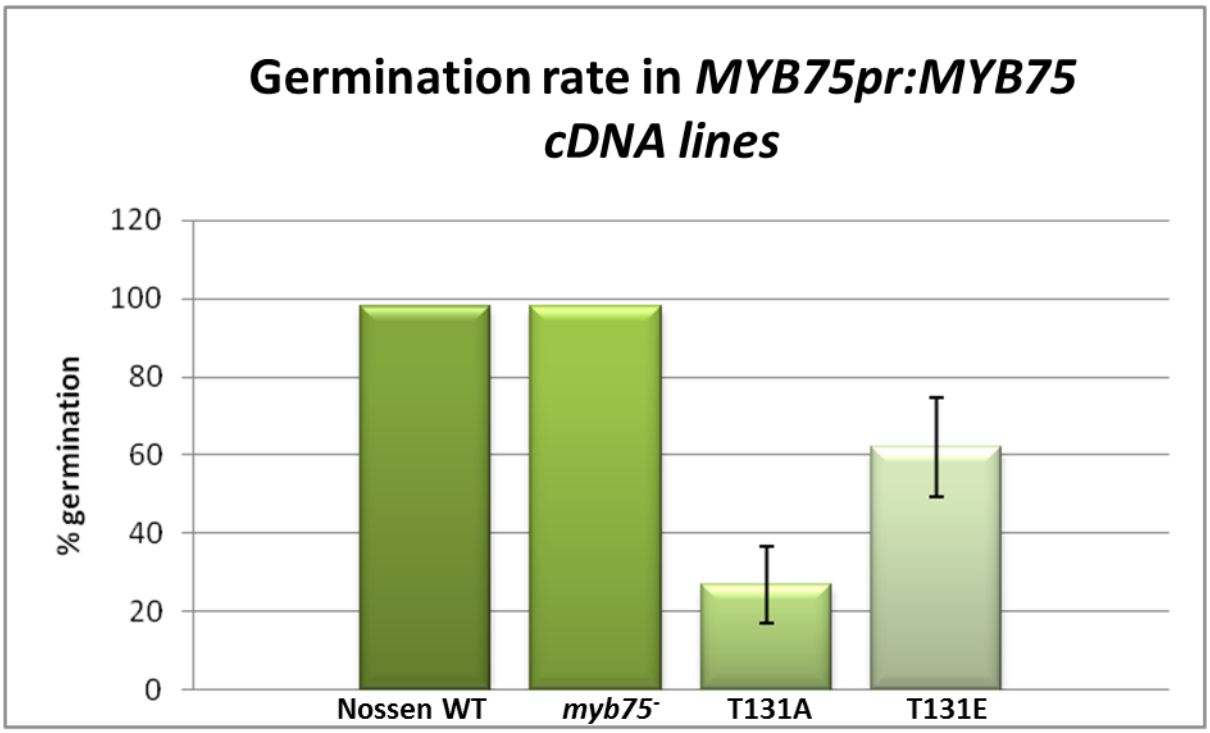

Fig 4.2. Germination rates in *MYB75pr:MYB75 cDNA* lines in the *myb75*$^{-}$ Nossen background. Seeds from homozygous T3 plants were plated on ½ MS medium along with *myb75*$^{-}$ and Nossen controls. After vernalization the petri dishes containing transgenic seeds and controls were transferred into the light, and germinated under 8h dark, 16 h light photoperiod. Germination rate was scored ten days after transferring the plates into light. Percentage germination was determined for each line by counting the total number of seeds and the total number of germinated plants. Percentages of germinated plants were averaged for each genotype. Bars represent standard deviation in the germination percentage. Germination rates were 26.8% (SD=9.99) for *MYB75pr:MYB75*^{T131A} plants and 62% (SD=12.62) for *MYB75pr:MYB75*^{T131A} . These data indicate that *MYB75*^{T131A} plants have a significantly lower germination rate than *MYB75*^{T131E}. T test P <0.05.

4.3 Flowering time and senescence are delayed in *Arabidopsis* plants over-expressing *MYB75*^{T131E}

As described in Chapter 3, plants over-expressing *MYB75* gene (*35Spr:MYB75 gene*) did not show anthocyanin accumulation at the seedling stages, unless stressed with continuous light or elevated sucrose concentration in the media. On the other hand, mature plants showed

abundant MYB75 protein expression, accompanied by high levels of anthocyanin production. To determine how *MYB75* over-expression and protein phosphorylation status affect development, I monitored the time of bolting and flowering, as well as onset of senescence in *35Spr:MYB75^{WT}, 35Spr:MYB75^{T131A}*, and *35Spr:MYB75^{T131E}* lines. These experiments were initiated because I noticed that different transgenic lines seemed to flower at different times. However, in order to investigate these flowering-related phenotypes systematically, I needed to synchronize the growth of different MYB75 over-expressor lines along with Col-0 WT controls.

Approximately ten days after germination, lines over-expressing different MYB75 phosphovariants (*35Spr:MYB75^{WT}, 35Spr:MYB75^{T131A}*, and *35Spr:MYB75^{T131E}*) along with Col-0 WT controls were transferred to soil and grown side by side in the same chamber under regular photoperiod, 16h light/ 8h dark, and light fluence ~100-120 µmol $m^{-2}s^{-1}$. Instead of recording the precise time of bolting for each genotype, I focused on comparing them to each other. Wild type Col-0 plants began to bolt and flower after 4-5 weeks of growth. Transgenic *35Spr:MYB75^{WT}* plants showed differences in flowering time between different lines; Line11 displayed flowering time comparable to Col-0 WT plants, while Lines 12 and 14 produced an inflorescence stem and flowers before Col-0 WT of the same age (Fig 4.3 A). This apparent acceleration in development persisted after bolting, as MYB75^{WT} lines 12 and 14 displayed abundant formation of lateral branches and flowers, at a stage when Col-0 WT and *MYB75^{WT}* line 11 plants had only developed the main inflorescence (Fig 4.3A). Similar developmental acceleration was observed in *MYB75^{T131A}* lines 1, 22 and 13. Early bolting, flowering and development of numerous lateral branches was consistently observed in all *MYB75^{T131A}* plants, with only minor differences in developmental speed between lines (Fig 4.1A). Conversely, all

MYB75^{T131E} plants displayed a delay in bolting and flowering compared to Col-0 WT *Arabidopsis* (Fig 4.3A). The developmental delay observed in *MYB75*^{T131E} lines was most evident in later stages of development. At 7 weeks of age Col-0 WT as well *35Spr:MYB75*^{WT} and *35Spr:MYB75*^{T131A} lines ceased to flower, had formed mature siliques, and showed signs of senescence manifested as yellowing of the rosette leaves, and desiccating siliques, while all *35Spr:MYB75*^{T131E} lines displayed abundant flowers formation at 7 weeks, with only a few young siliques forming at this stage, and healthy green tissue throughout the plant (with no signs of senescence; Fig 4.3C). Despite the variability between individual lines in *MYB75*^{WT} plants, a clear trend emerged between the phosphovariant plant lines: development is accelerated in plants over-expressing *MYB75*^{T131A} and retarded in those over-expressing *MYB75*^{T131E} (Fig 4.3B).

Interestingly, even in lines where anthocyanin production varied in a seemingly stochastic manner, yielding both green and purple plants within the same population, plants of both colour classes displayed the flowering-related developmental phenotypes described above. In the previous chapter, Fig 3.4 demonstrated the stochastic nature of recombinant MYB75 protein accumulation in *35Spr:MYB75* lines, resulting in some plants being purple while others were green (except *MYB75*^{WT} line11 where all plants were purple). While all plants expressed the transgenic *MYB75,* only purple plants produced MYB75 protein levels that could be detected by immunoscreening. Those lines with detectable levels of MYB75 protein were also purple from abundant anthocyanin accumulation. Nevertheless, green plants still expressed *MYB75* transcripts, according to my RT-PCR results (Fig 3.4 B). The observation of similar developmental differences (with respect to bolting, flowering time and senescence) in both purple and green *35Spr:MYB75 gene* lines suggest that recombinant MYB75 is likely being

expressed in some tissues of green plants, and that this ectopic expression is sufficient to trigger the developmental change observed, even though it does not lead to anthocyanin accumulation typical of *PAP1-D* over-expression. This leads to the conclusion that perhaps it is phosphorylation status in combination with ectopic expression of MYB75, driven by the constitutive 35S promoter, rather than MYB75 abundance *per se*, that results in these phenotypes.

Fig 4.3

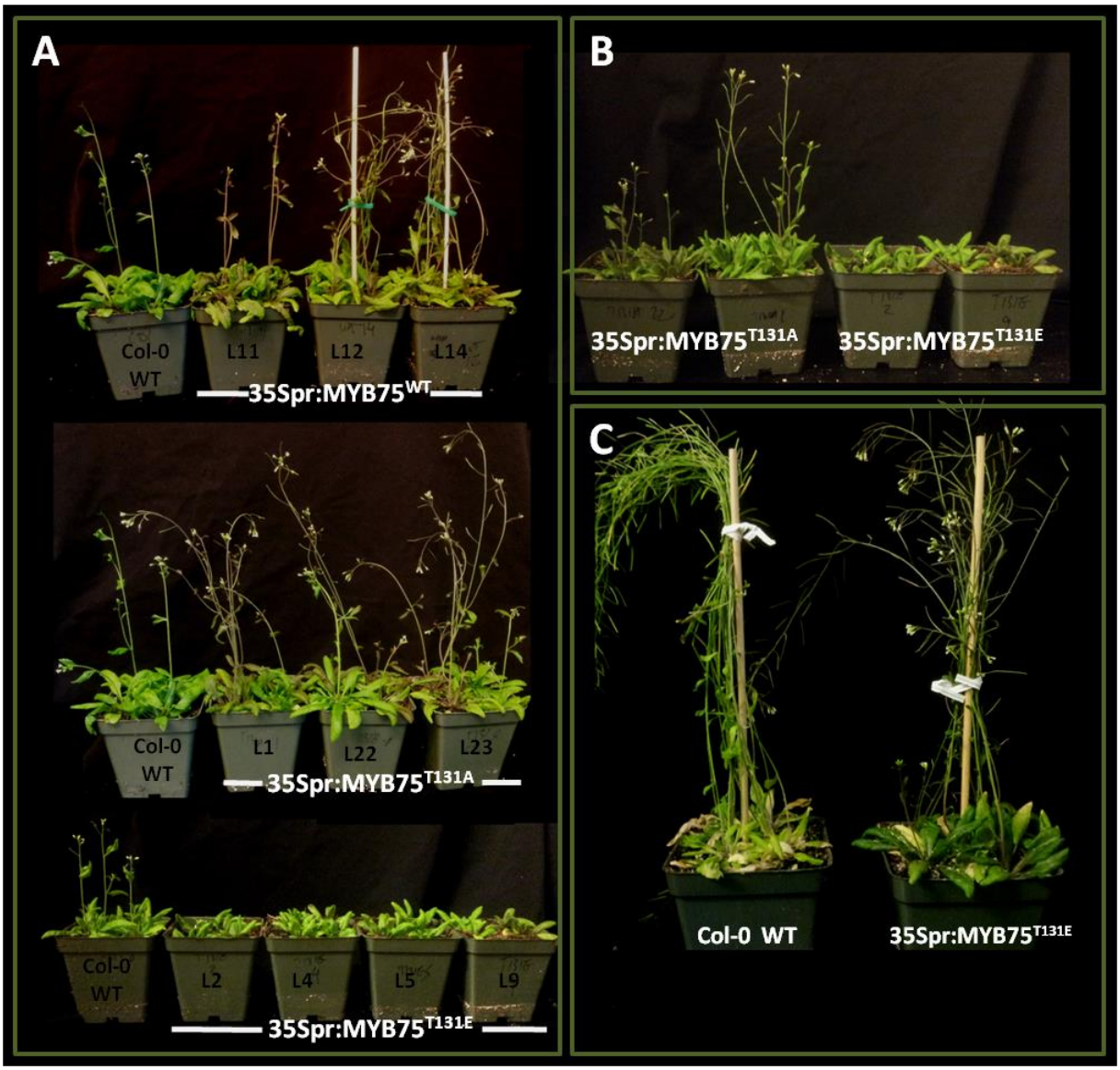

Fig 4.3 Developmental differences in bolting and flowering time of plants over-expressing different phosphovariants of *MYB75*. Heterozygous T2 plants were plated on ½MS medium with hygromycin, vernalized at 4°C in the dark for 3-4, days before being put into light, with a fluence of ~30 µmol $m^{-2}s^{-1}$ and 16h light/8h dark photoperiod, at 21°C. Between 7-12 days after germination seedlings were planted in soil and transferred to a growth chamber with a light fluence of ~100-120 µmol $m^{-2}s^{-1}$, photoperiod of 16h light/8h dark, and temperature at 21°C. Development, including bolting, flowering time and onset of senescence was monitored and recorded for all lines. Among *35Spr:MYB75^{WT}* lines, line 11 bolted and flowered at a rate comparable to Col-0 WT, while lines 12 and 14 displayed early bolting and flowering compared to Col-0 controls (A). All *35Spr:MYB75^{T131A}* lines bolted and flowered early compared to Col-0 WT (A). Conversely, *35Spr:MYB75^{T131E}* plants showed delayed bolting and flowering compared

Fig 4.3 (continued)
to Col-0 WT (A). Overall, the T131A mutation led to earlier bolting and flowering, while T131E mutation appears to slow down the transition from vegetative to reproductive growth (B). Furthermore, *35Spr:MYB75^{T131E}* lines displayed delayed maturation and senescence compared to Col-0 plants (D).

4.4 Ectopic vessel development in stems of mature *Arabidopsis* plants over-expressing different MYB75 phosphovariants

In Chapter 3, biochemical analysis by HPLC revealed that *MYB75^{T131E}* plants accumulated higher levels of specific flavonol species. As described in the introduction of this chapter these compounds are known to influence auxin flow, which affects almost every aspect of development. Auxin flow is closely tied to vascular differentiation, and perturbations in auxin transport often leads to abnormal vasculature. Furthermore, *MYB75* has been implicated in secondary cell wall formation (Bhargava *et al*., 2010), a process tightly linked to vascular development. I therefore decided to examine cross-sections of mature *Arabidopsis* plants over-expressing different phosphovariants of MYB75, to determine what effect (if any) the over-expression of each MYB75 phosphovariant had on the plant stem vasculature. Other than the cell wall phenotypes described by Barghava *et al*., in 2010, no other changes associated with vascular development have been reported in *myb75^{-}* or *PAP1-D* plants, however. In order to determine if *MYB75* over-expression or protein phosphorylation status has any impact on vascular development, I performed a stem sectioning experiment on mature *35Spr:MYB75 gene* plants and examined the distribution of vascular and supporting tissues in the cross-sections, using phloroglucinol-HCl and toluidine blue histochemical stains.

In wild type *Arabidopsis* stems the plant vasculature is organized into distinct vascular bundles, distributed along the stem circumference. The xylem tissues are found on the inner

side of the vascular bundles, close to the centre of the stem, while the phloem tissues are found on the outer side of each vascular bundle. A small population of meristematic procambial cells, which gives rise to xylem and phloem, is located between these two tissues in each vascular bundle. In mature stems these bundles display a distinct organization and can be easily recognized in a stem cross-section (Fig 4.4). Mature stems can also develop another meristematic tissue, called the cambium, which drives secondary growth. In woody species the cambium is prominent and can generate abundant secondary vasculature, leading to the formation of wood. In *Arabidopsis* cambium activity is limited to later stages of development and can contribute to small amount of secondary growth reminiscent of woody species (reviewed in Nieminen *et al*, 2004; Ragni and Greb, 2017). Interfascicular fibres are strong, lignified cells found organized in arcs between vascular bundles, which provide support for the stem (Fig 4.4).

Fig 4.4

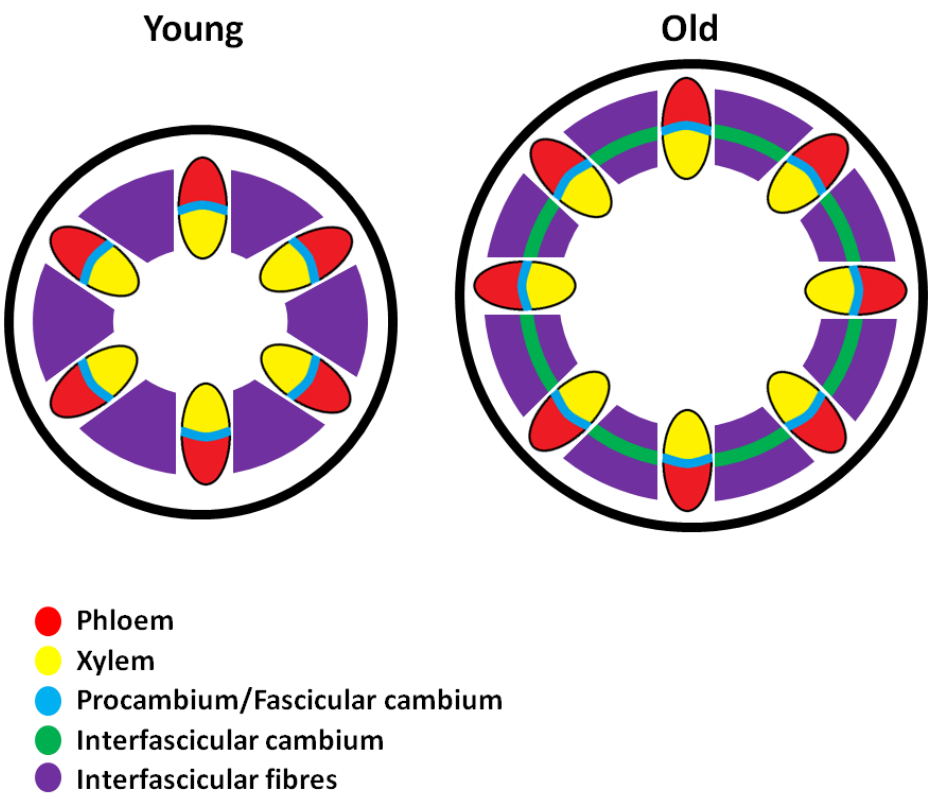

Fig 4.4 Diagramatic representation of *Arabidopsis* stem cross-sections, at young and mature stages, adapted from Rangi and Greb, 2017. The *Arabidopsis* inflorescence stem displays a distinct pattern of tissue organization. The vasculature is organized into bundles, comprised of xylem and phloem tissues, divided by a layer of meristematic cells, known as the procambium. During primary growth, procambial cells give rise to xylem and phloem, through periclinal cell division and subsequent differentiation. Xylem and phloem are comprised of vessels and sieve tube elements respectively, as well as fascicular fibres and parenchyma cells. Some parenchyma cells found between vascular bundles differentiate into interfascicular fibres, which develop heavily lignified cell walls, providing support to the plant stem. These interfascicular cells form arcs between the vascular bundles. Upon cessation of primary growth, another meristematic tissue, the cambium, emerges. Fascicular cambium is derived from the procambium, while interfascicular cambium arises from parenchyma cells found between vascular bundles. The cambium drives secondary growth, through anticlinal cell division, providing the plant with girth and rigidity. Reviewed in Rangi and Greb, 2017; Miyashima *et al.,* 2013.

My first round of stem sectioning was performed on plants that were just over 8 weeks old; at this stage, the developmentally delayed *35Spr:MYB75*^{T131E} lines had formed mature siliques and were beginning to show signs of senescence, while Col-0 WT, *35Spr:MYB75*^{WT} and

35Spr:MYB75^{T131A} plants had reached full senescence and were beginning to desiccate. All plants were watered in the usual cycle, to ensure that the stems did not dry out, which could lead to vascular collapse. The lower portions of the stems, approximately 5cm from the base of the main inflorescence stem, were hand-sectioned, and the stem sections were stained with phloroglucinol-HCl (see Materials and Methods). For economy of effort, only purple plants were used, ensuring that only specimens with higher levels of recombinant MYB75 protein expression were analysed. Phloroglucinol-HCl is a lignin specific stain, that reacts with cinnamaldehyde end groups in lignin, producing a red or fuchsia colour in interfascicular fibres, and a darker red/maroon colour in the xylem of vascular bundles (Mitra and Loqué, 2014).

As expected, wild type *Arabidopsis* stems showed a normal tissue organization, with vessels elements appearing as clusters of cells with dark reddish-brown-staining cell walls, restricted to vascular bundles (Fig 4.5A). On the other hand, transgenic plants showed what appear to be vessel-like cells in the interfascicular region, with dark reddish-brown staining walls, and a larger cell diameter compared to the surrounding fibres (Fig 4.5 B-D). In *35Spr:MYB75*^{WT} plants, the phenotype was relatively mild, with only a few isolated dark cell files in the interfascicular region, made up of cells with a slightly larger diameter than the surrounding fibres (Fig 4.5 B). In *35Spr:MYB75*^{T131A} plants, these darker staining cells were more prominent, with a diameter comparable to vessel elements found in the vascular bundles; however, only a few such cells, or very small cell clusters could be seen in the interfascicular region (Fig 4.5 C). In contrast, in plants over-expressing the phosphomimic MYB75^{T131E}, abundant development of vessel elements could be observed in the interfascicular region, with large cell clusters, resembling vessels, stretching between the vascular bundles. In some cases,

these clusters spanned the entire length of the interfascicular arc (Fig 4.5D). These phenotypes showed a great deal of variability for each phosphovariant; some of the transgenic stems examined did not show any abnormal tissue distribution at all. However at least 50% of the stems sectioned in plants each genotype (*MYB75*^{WT}, *MYB75*^{T131A} and *MYB75*^{T131E}) showed at least some ectopic vessel production, with a few isolated vessel-like cells in the interfascicular region. About 25-30% of the stems examined for each transgenic line showed the most extreme phenotypes (Fig 4.5), with prominent vessel cell-files in the interfascicular region of *MYB75*^{WT} and *MYB75*^{T131A}, and extensive vessel clusters, spanning the entire interfascicular arc in *MYB75*^{T131E} stems.

Fig 4.5

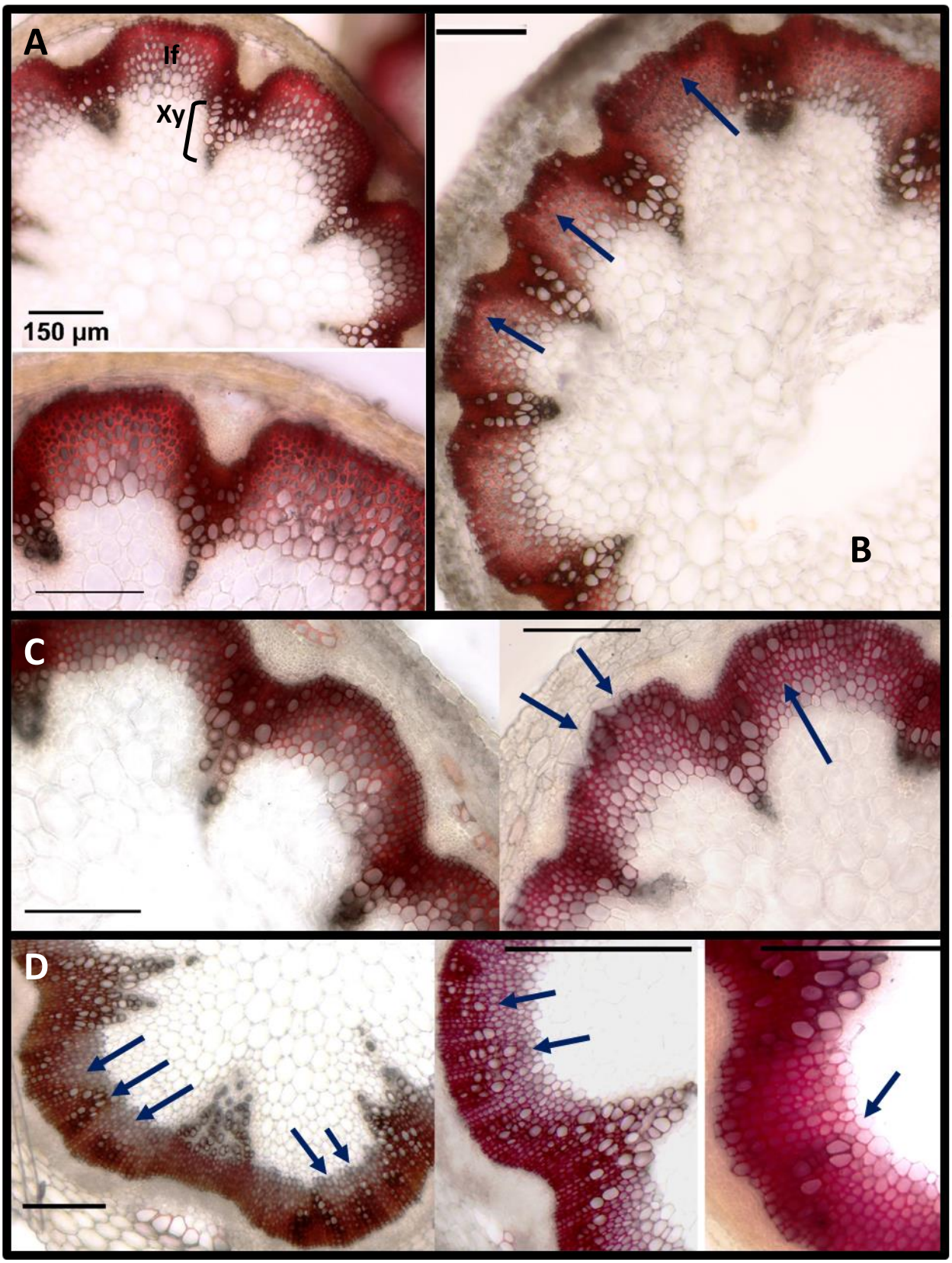

Fig 4.5 Ectopic vessels development in stems of 8-week-old *Arabidopsis* plants *over-expressing* different phosphovariants of MYB75. Heterozygous T2 plants carrying *35Spr:MYB75 gene* constructs were plated on ½ MS medium with hygromycin, Col-0 WT plants were plated on ½ MS without antibiotic. The seeds were vernalized at 4°C in the dark for 3-4, days before being put into light, with a fluence of ~30 µmol $m^{-2}s^{-1}$ and 16h light/8h dark photoperiod, at 21°C. Between 7 and 12 days after germination, seedlings were planted in soil and transferred to a growth chamber with a light fluence of ~100-120 µmol $m^{-2}s^{-1}$, photoperiod of 16h light/8h dark, and temperature at 21°C. After 8 weeks stems from Col-0 WT plants, as well as those from purple transgenic plants were harvested, and the bottom 5cm of each stem was hand sectioned and stained in phloroglucinol solution (2% w/v phloroglucinol in 95% ethanol), by submerging the sections in the solution and adding concentrated HCl dropwise. After 5min incubation the sections were washed three times in distilled water, mounted in water on slides and imaged using a Leica Mecatron precision DMR compound microscope. Stem sections from Col-0 WT plants (A) display normal distribution of vessels, within vascular bundles, where xylem vessels (Xy) can be seen as large perforated cells with dark reddish-brown staining walls. The interfascicular fibres (If) appear as bright red/fuchsia cells, organized in arcs between the vascular bundles. In *MYB75* over-expressing lines, ectopic vessels appear in the interfascicular region. *35Spr:MYB75^{WT}* (B) and *35Spr:MYB75^{T131A}* (C) lines show only a few vessel-like elements between the bundles, while *35Spr:MYB75^{T131E}* (D) lines display prominent files of vessels developing in the interfascicular region. Scale bars represent 150µm.

These results indicate that over-expression of *MYB75* leads to ectopic differentiation of cells in the interfascicular region that appear to be vessels, and that the MYB75^{T131E} phosphovariant is more effective at driving this process. At this point in development *Arabidopsis* plants can undergo secondary growth in their lower stems (Altamura *et al.,* 2001; reviewed in Ragni and Greb, 2017). Signs of this secondary growth were observed in all genotypes, including Col-0 WT, with the appearance of cells around the periphery of the stem, with dark staining cell walls, reminiscent of vessel elements (Fig 4.5). It was important at this point to distinguish this normal secondary growth, present in all genotypes, from what I believed to be ectopic vessel formation in *MYB75* over-expressing lines. Therefore, for my next round of sectioning I chose somewhat younger plants, in hopes of detecting phenotypic changes in their mature stem sections before, normal secondary growth would have begun. In

addition to phloroglucinol-HCl staining, I used toluidine blue stain, which offers a better colour contrast between vessels and fibres. In toluidine blue-stained sections, interfascicular fibre walls appear bright turquoise, whereas the xylem vessels are greenish grey. Finally, in order to show that the wall phenotypes observed in *35Spr:MYB75* plants correlated with transgene expression, it was important to determine whether recombinant MYB75 protein was actually being expressed in the stems. For this purpose, I performed a western blot and conducted RT-PCR analysis on tissue extracts from the lower 5cm of the mature *Arabidopsis* stems.

The histochemical analysis shown in Fig 4.6 (A) indicates that at this stage in development Col-0 WT plants do not appear to show significant signs of secondary growth. Furthermore, ectopic vessel differentiation was not observed in *35Spr:MYB75*^{WT} plants (Fig 4.6 B), and only a mild phenotype was seen in *35Spr:MYB75*^{T131A} plants (Fig 4.6 C). On the other hand, *35Spr:MYB75*^{T131E} plants showed prominent ectopic vessels developing as small bundles or cell files in the interfascicular arcs (Fig 4.6 D). In toluidine blue-stained cross-sections, the vascular bundles appear greenish grey, in contrast to the bright blue-green interfascicular fibres. Cell clusters with greenish grey walls can be seen in the interfascicular arcs of *35Spr:MYB75*^{T131E} stems, but not in the *35Spr:MYB75*^{WT} plants (Fig 4.6 E). As in the phloroglucinol-stained sections, these unusual cells have a larger diameter than the surrounding interfascicular fibre cells and are similar in appearance to vessels found in the vascular bundles. I therefore concluded that these are, in fact, ectopic vessel elements that develop in the interfascicular region of *MYB75* over-expressing transgenic plants, most prominently in *35Spr:MYB75*^{T131E} lines. Due to the limited availability of heterozygous T2 plants, only about a dozen plants were used for each genotype in each round of sectioning.

Nevertheless, within this sample pool *35Spr:MYB75*^{T131E} plants consistently showed more prominent ectopic vessel development than the other genotypes. Finally, western blot analysis and RT-PCR confirmed that the transgene was being expressed and that the corresponding recombinant protein was being produced in the stems of *35Spr:MYB75* plants. Interestingly, *MYB75*^{T131A} lines showed a much stronger signal in western blots, while MYB75^{WT} and MYB75^{T131E} protein versions were barely detectable. If this pattern is correct, it suggests that different MYB75 phosphovariants may accumulate to different levels in stems tissues, which could be an important consideration when interpreting how MYB75 over-expression and phosphorylation influence vascular development.

Fig 4.6

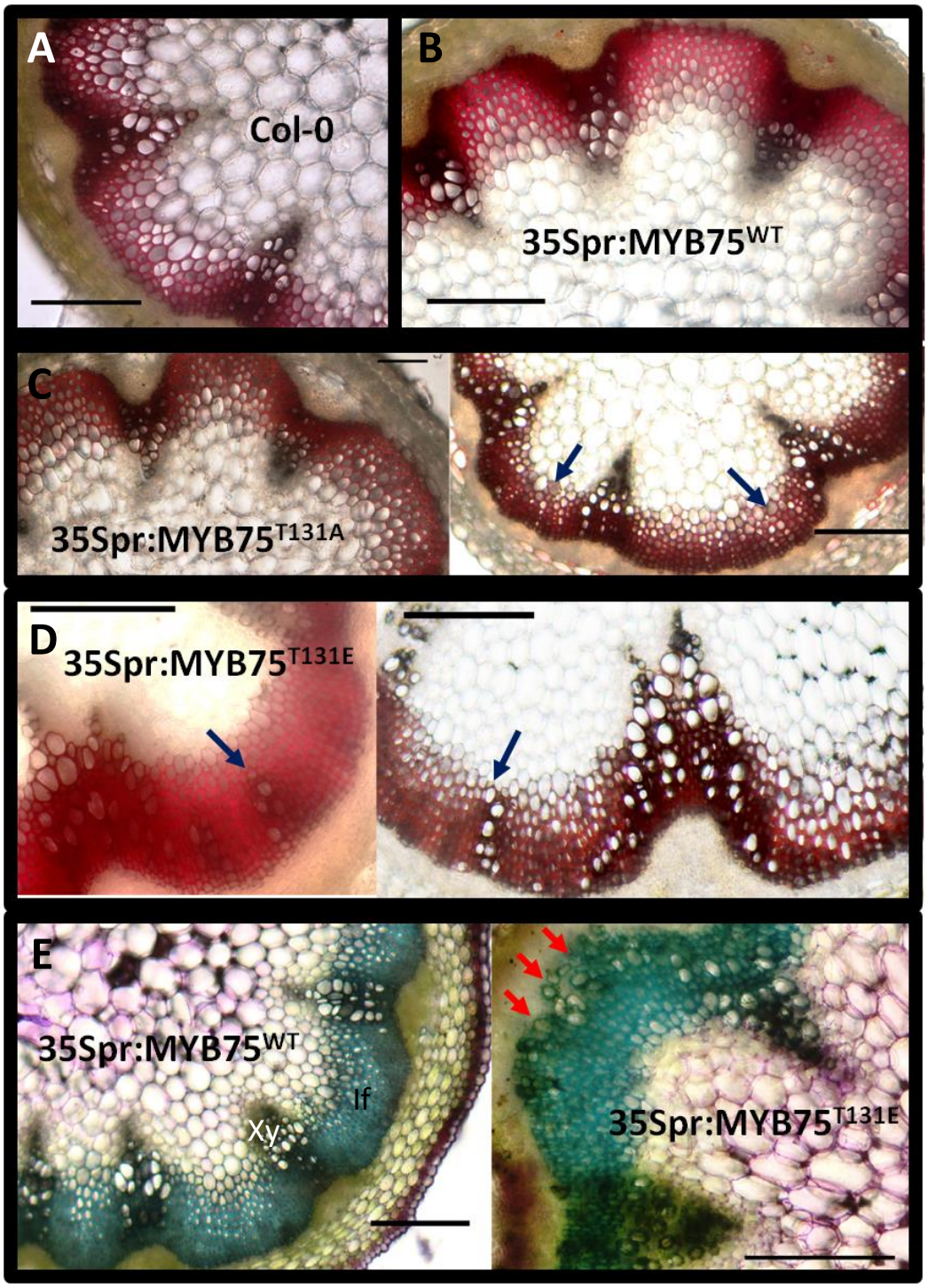
A
Col-0
B
35Spr:MYB75WT
C
35Spr:MYB75T131A
D
35Spr:MYB75T131E
E
35Spr:MYB75WT
If
Xy
35Spr:MYB75T131E

Fig 4.6 continued

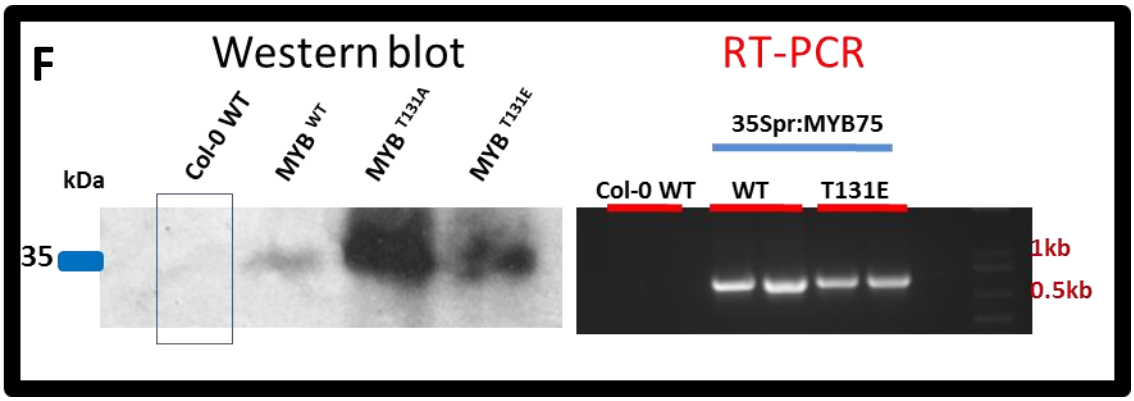

Fig 4.6 Ectopic vessel development in stems of 7-week-old *Arabidopsis* plants over-expressing different phosphovariants of MYB75. Heterozygous T2 plants carrying *35Spr:MYB75 gene* constructs were plated on ½MS medium with hygromycin, while Col-0 WT plants were plated on ½ MS without antibiotic. The seeds were vernalized at 4°C in the dark for 3, days before being put into light, with a fluence of ~30 µmol $m^{-2}s^{-1}$ and 16h light/8h dark photoperiod, at 21°C. Between 7 and12 days after germination seedlings were planted in soil and transferred to a growth chamber with a light fluence of ~100-120 µmol $m^{-2}s^{-1}$, photoperiod of 16h light/8h dark, and temperature at 21°C. After eight weeks stems from Col-0 WT plants, as well as from purple transgenic plants were harvested, and the bottom 5cm of each stem was hand sectioned and stained in phloroglucinol-HCl (A-D), or toluidine blue (E). Stem sections from Col-0 WT plants (A) display normal distribution of vessels, within vascular bundles, where xylem vessels can be seen as large perforated cells. In phloroglucinol-HCl stained sections, vessel walls appear dark reddish-brown, while interfascicular fibres are bright red/fuchsia arcs between the vascular bundles. Lines over-expressing 35Spr:$MYB75^{WT}$, displayed normal stem tissue organization (B, E left panel). In *35Spr:*$MYB75^{T131A}$ plants isolated cells or short cell files, reminiscent of vessels could be seen in the interfascicular region (C). In *35Spr:*$MYB75^{T131E}$ plants large clusters of vessels could be seen in the interfascicular region (D and E, right panel). In toluidine blue-stained sections interfascicular fibres are bright blue green, while xylem vessels are stained a greenish grey. The large lignified cells which form prominent clusters in the interfascicular region of *35Spr:*$MYB75^{T131E}$ plants, stain greenish grey, the same as vessel elements found in vascular bundles. Scale bars represent 150µm. Expression of *MYB75* in stems of *35Spr:MYB75* plants, was confirmed using RT-PCR and recombinant protein was detected using western blot and immunostaining with anti HA-tag antibody (F). Five stems of each genotype were pooled for each western blot and RT-PCR sample.

4.5 Global gene expression analysis in *Arabidopsis* plants over-expressing different phosphovariants of MYB75

Biochemical and gene expression analysis performed in Chapter 3 did not yield striking differences between *Arabidopsis* lines over-expressing different MYB75 phosphovariants, in terms of their ability to regulate core flavonoid biosynthetic genes. It thus appears that phosphorylation does not have a dramatic effect on transcription of genes encoding enzymes in the phenylpropanoid pathway that had previously been identified in the literature as targets of MYB75. However, detailed biochemical profiling of *35Spr:MYB75 gene* plants by HPLC revealed quantitative differences between T131A and T131E phosphovariants in accumulation of flavonol and anthocyanin molecular species. Throughout Chapter 4 I have described several developmental changes observed in the *35Spr:MYB75* lines. Biochemical profiling and developmental phenotypes described in Chapters 3 and 4, strongly suggested that MYB75 has a broader role to play in development than regulation of flavonoid metabolism. Furthermore, the distinct phenotypic differences between *35Spr:MYB75*^{T131A} and *35Spr:MYB75*^{T131E} genotypes led me to believe that these two forms of MYB75 are able to regulate different subsets of genes.

In order to explore this idea further, I conducted global gene expression analysis, using next generation sequencing of total RNA extracted from mature rosette leaves of plants over-expressing either *MYB75*^{T131A} or the *MYB75*^{T131E} phosphovariant, using Col-0 WT as the control. Rosette leaves from purple 5-week-old *Arabidopsis* plants were chosen as the source of RNA for two reasons: first I wished, to look for any correlation between the biochemical profiles obtained in Chapter 3 (Fig 3.6) and gene expression changes, which required using the same type of tissue as in the HPLC analysis; and second, mature rosette leaves of purple

35Spr:MYB75 plants consistently displayed high expression levels of recombinant MYB75 protein, and the amount of total protein produced in this tissue was comparable between different phosphovariants. I did not include *35Spr:MYB75*^{WT} plants in my analysis, primarily because without knowing the extent of MYB75 phosphorylation *in vivo*, results from *MYB75*^{WT} over-expressing lines would be uninterpretable. Instead, I compared MYB75^{T131A} and MYB75^{T131E}, separately to Col-0 WT, using published expression data on *35Spr:MYB75* and *PAP1-D* as an independent reference when discussing my results. The goal of this analysis was to obtain an overview of how MYB75 phosphorylation state affected gene expression. Venn analysis was conducted on the entire dataset (by Dr. Darren Wong), to determine which genes displayed changes in their expression levels, in either one or both phosphovariants. Only genes that were up-or down-regulated at least twofold in each phosphovariant (compared to Col-0 WT) were described in the final analysis (Fig 4.7 and Fig 4.8). When classifying genes, instead of using GO annotation I chose to create my own categories that were more pertinent to this study. Genes were classified according to their best characterized function which was determined (when possible) from relevant publications found in TAIR. Some genes were broadly classified in metabolism and homeostasis, as they appeared in various publications in broad biological contexts. These include genes required for biosynthesis of amino acids, carbohydrate metabolism and various membrane transport proteins. Some genes classified in this category were enzymes whose catalytic function has been predicted, but whose involvement in a precise biological process is not well defined, as they are implicated in a wide range of cellular processes. Genes in this category, as well as those classified as “unknown”, may need to be reclassified in the future, when their exact function is refined. For the purposes

of this study, I will focus on changes in the expression of genes that pertain to flavonoid biosynthesis and modification, auxin signalling, as well as genes that might explain developmental changes observed in different *MYB75*-overexpessing lines.

The total number of upregulated genes in lines over-expressing either phosphovariant of MYB75 is significantly larger than the number of downregulated genes, with a total of 219 genes upregulated at least twofold in either one or both phosphovariants, while only 93 genes were downregulated at least twofold (Fig 4.7A, Fig 4.8A), suggesting that MYB75 has a more prominent role as a positive regulator of gene expression and a relatively minor role as a repressor. Interestingly, no genes were up or down-regulated more than ten-fold in any of the phosphovariants. The number of genes upregulated was significantly larger in *35Spr:MYB75*^{T131E} plants than in *35Spr:MYB75*^{T131A}, with a total of 118 genes upregulated uniquely in *35Spr:MYB75*^{T131E} while only 17 genes were upregulated uniquely in *35Spr:MYB75*^{T131A} (Fig 4.7A). Similarly, among the genes downregulated in *MYB75*-over-expressing lines, 34 are unique to *35Spr:MYB75*^{T131E} while only 15 were unique to *35Spr:MYB75*^{T131A}. These results indicate that MYB75^{T131E} is more potent as both a positive and negative regulator of gene expression and that perhaps phosphorylation of MYB75 may enhance its ability to regulate expression of target genes. It is important to note that this discussion of gene expression changes does not attempt to provide a comprehensive explanation for the biochemical and developmental changes observed in the phosphovariant plants. The intent is to highlight general patterns and offer possible leads that are worth exploring in the future.

Fig 4.7

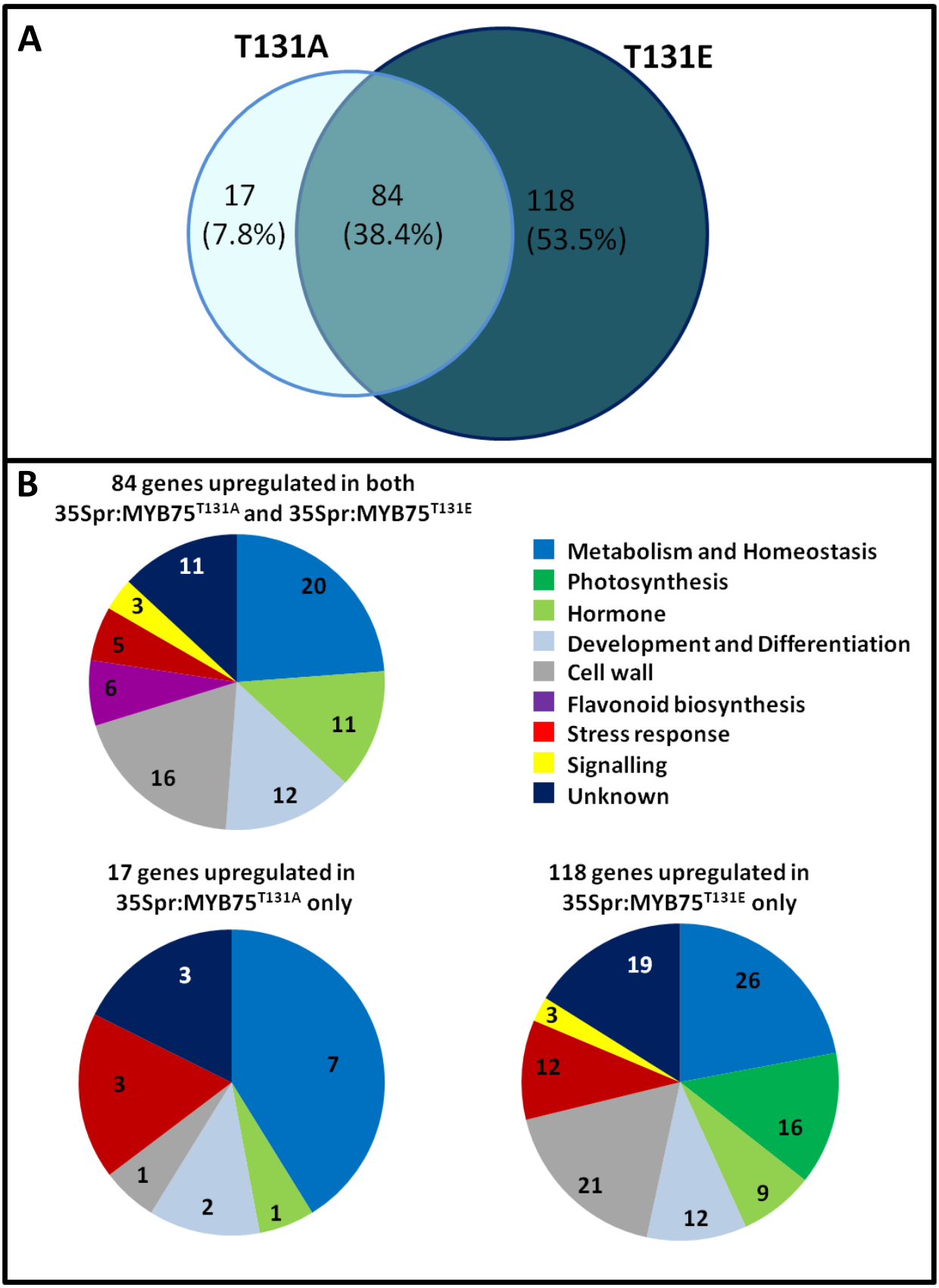
A
T131A
T131E
17
(7.8%)
84
(38.4%)
118
(53.5%)
B
84 genes upregulated in both
35Spr:MYB75T131A and 35Spr:MYB75T131E
20
11
12
16
6
5
3
11
Metabolism and Homeostasis
Photosynthesis
Hormone
Development and Differentiation
Cell wall
Flavonoid biosynthesis
Stress response
Signalling
Unknown
17 genes upregulated in
35Spr:MYB75T131A only
7
1
2
1
3
3
118 genes upregulated in
35Spr:MYB75T131E only
26
16
9
12
21
12
3
19

Fig 4.7 Genes upregulated in mature rosette leaves of *Arabidopsis* plants over-expressing MYB75^{T131A} and MYB75^{T131E}, compared to Col-0 WT plants.

Heterozygous T2 plants carrying *35Spr:MYB75^{T131A}gene* and *35Spr:MYB75^{T131E}gene* constructs were selected on ½ MS plates with hygromycin and grown alongside Col-0 WT plants under a light fluence of ~30 µmol $m^{-2}s^{-1}$ and 16h light/8h dark photoperiod, for ten days before being transferred to soil, in a growth chamber with a light fluence of ~100-120 µmol $m^{-2}s^{-1}$, photoperiod of 16h light/8h dark and a temperature of 21°C. Mature rosette leaves of 5-week-old *Arabidopsis* plants were harvested and total RNA was extracted using TRIZOL reagent. RNA from three lines was pooled for the *35Spr:MYB75^{T131A}* genotype (L1, L22 and L23) and four lines for the *35Spr:MYB75^{T131E}* genotype (L2, L4, L5, L9). Total RNA concentration in each sample was determined using NanoDrop® (ThermoFischer), and RNA quality (intactness) was evaluated by running 5µl of each sample on a 2% agarose gel. Final samples were obtained for each genotype by pooling equal amounts of total RNA from each line belonging to that genotype. The control samples for Col-0 WT was generated by pooling four samples each representing two different Col-0 WT plants. RNA sequencing was performed on each final sample using the *Illumina NextSeq500*, at 15-30 million reads. The data was trimmed and analysed by Dr. Darren Wong (Castellarin lab, UBC Wine Research Centre) as follows: trimmed reads were aligned to the *Arabidopsis thaliana* reference genome (TAIR 10 genome release), using the HISat2 alignment tool. Dr. Wong identified differentially expressed genes whose expression changed in *35Spr:MYB75^{T131A}* and *35Spr:MYB75^{T131E}* plants compared to Col-0 WT controls, as determined by the GFold program (Feng *et al.,* 2012), and performed VENN analysis on the entire dataset. The Venn diagram (A) was generated using the "venny" online tool (http://bioinfogp.cnb.csic.es/tools/venny/). The pie charts (B) were generated using only genes whose expression was upregulated at least twofold. Each gene was categorized based primarily on its function as described in the literature, while GO annotation in conjunction with information on related genes was used to classify genes whose function was poorly defined in published data. Gene expression data from which this figure was derived is available in supplmenetary materials in Table S4.1.

Fig 4.8

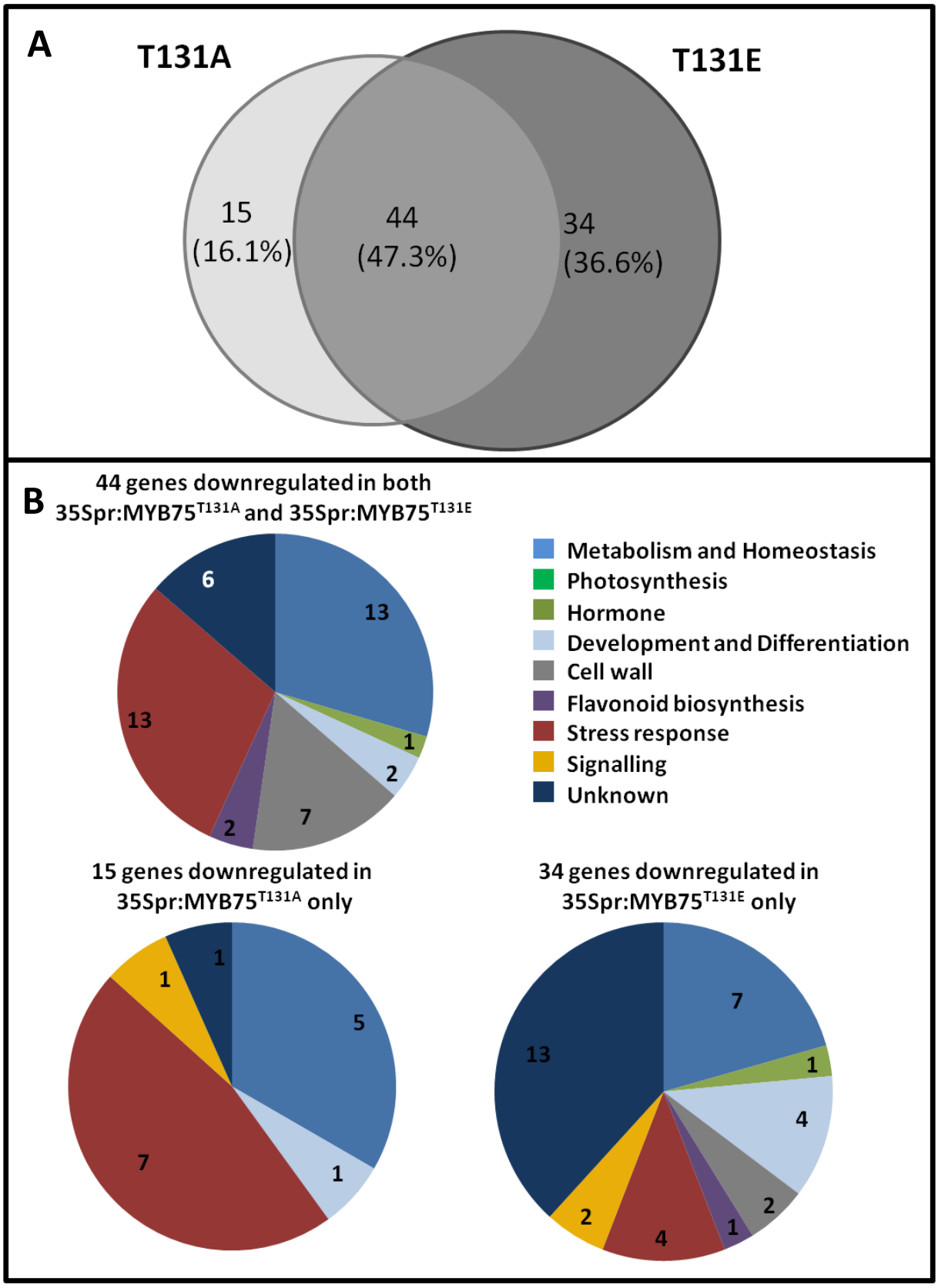
A
T131A
T131E
15
(16.1%)
44
(47.3%)
34
(36.6%)
B
44 genes downregulated in both
35Spr:MYB75T131A and 35Spr:MYB75T131E
6
13
13
1
2
2
7
Metabolism and Homeostasis
Photosynthesis
Hormone
Development and Differentiation
Cell wall
Flavonoid biosynthesis
Stress response
Signalling
Unknown
15 genes downregulated in
35Spr:MYB75T131A only
1
1
5
7
1
34 genes downregulated in
35Spr:MYB75T131E only
7
13
1
4
2
2
1
4

Fig 4.8 Genes downregulated in mature rosette leaves of *Arabidopsis* plants over-expressing MYB75^{T131A} and MYB75^{T131E}, compared to Col-0 WT plants.

Heterozygous T2 plants carrying *35Spr:MYB75^{T131A}gene* and *35Spr:MYB75^{T131E}gene* constructs were selected on ½ MS plates with hygromycin and grown alongside Col-0 WT plants under a light fluence of ~30 µmol $m^{-2}s^{-1}$ and 16h light/8h dark photoperiod, for ten days before being transferred to soil, in a growth chamber with a light fluence of ~100-120 µmol $m^{-2}s^{-1}$, photoperiod of 16h light/8h dark and a temperature of 21°C. Mature rosette leaves of 5-week-old *Arabidopsis* plants were harvested and total RNA was extracted using TRIZOL reagent. Three lines were used for *35Spr:MYB75^{T131A}* genotype (L1, L22 and L23) and four lines for the lines *35Spr:MYB75^{T131E}* genotype (L2, L4, L5, L9). Total RNA concentration in each sample was determined using NanoDrop® (ThermoFischer), and RNA quality (intactness) was evaluated by running 5µl of each sample on a 2% agarose gel. Final samples were obtained for each genotype by pooling equal amounts of total RNA from each line belonging to that genotype. Final samples for Col-0 WT were generated by pooling four samples, each representing two different Col-0 WT plants. RNA sequencing was performed on each final sample using the *Illumina NextSeq500*, at 15-30 million reads. The data was trimmed and analysed by Dr. Darren Wong (Castellarin lab, UBC wine research centre) as follows: trimmed reads were aligned to the *Arabidopsis thaliana* reference genome (TAIR 10 genome release), using HISat2 alignment tool. Dr. Wong identified differentially expressed genes whose expression changed in *35Spr:MYB75^{T131A}* and *35Spr:MYB75^{T131E}* plants compared to Col-0 WT controls, as determined by GFold (Feng *et al.,* 2012). VENN analysis was performed on the entire dataset. The Venn diagram (A) was generated using "venny" online tool http://bioinfogp.cnb.csic.es/tools/venny/. The Pie charts (B) were generated using only genes which were downregulated at least twofold. Each gene was categorized based primarily on its function as described in the literature, while GO annotation in conjunction with information on related genes were used to classify genes whose function was poorly defined in published data. Gene expression data from which this figure was derived is available in supplmenetary materials in Table S4.1.

4.5.1 Flavonoid

Gene expression analysis corroborated my conclusions from Chapter 3 with respect to expression levels of core flavonoid biosynthesis genes. Both *35Spr:MYB75^{T131A}* and *35Spr:MYB75^{T131E}* lines showed an increase in expression of anthocyanin biosynthesis genes (Fig 4.7B), as was reported in previous studies performed on *PAP1-D* and *35Spr:MYB75* plants (Borevitz *et al.,* 2001, Gonzalez *et al.,* 2008). As a result, the FLAVONOID category is found only in the pie chart representing genes that are upregulated by both phosphovariants (Fig 4.7B). These genes include leucoanthocyanidin dioxygenase (*LDOX*, At4g22880), and dihydroflavonol

reductase (*DFR*, At5G42800), as well as several anthocyanin modifying enzymes, including anthocyanidin 5-O-glycosyltransferase (*UGT75C1*, At4g14090), anthocyanin 3-O-glucoside: 2"-O-xylosyl-transferase (*UGT79B1*, AT5G54060), malonyl-CoA:anthocyanidin 5-O-glucoside-6"-O-malonyltransferase (*AT5MAT*,AT3g29590) and glutathione S-transferase (*GST,* At5G17220). Many of the genes that I had anticipated finding in the lists of up- and down- regulated transcripts did not meet the cutoff of two-fold change, or were not present in the 'differentially regulated' list. Two such genes that are worth mentioning are chalcone synthase (*CHS*) and phenylalanine ammonia-lyase (*PAL1*). *PAL1* was upregulated 2.2 fold in *35Spr:MYB75^{T131E}* plants but only 1.6 fold in *35Spr:MYB75^{T131A}* plants, and therefore was not included in Fig 4.7, since it did not meet the cutoff criteria, and could not be considered as uniquely upregulated in 35Spr:*MYB75^{T131E}* lines. Chalcone synthase (CHS) on the other hand was upregulated 1.5 fold only in *35Spr:MYB75^{T131E}* but was absent from the list of downregulated or upregulated genes in *35Spr:MYB75^{T131A}* lines. Although these fold changes are very low, if this data could be corroborated it would mean that MYB75^{T131E} is more efficient at up-regulating two major entry points into phenylpropanoid (*PAL1*) and flavonoid (*CHS*) pathways. This could explain, at least partially, some of the results of our biochemical analysis, which suggested that *MYB75^{T131E}*-over-expressing plants produce more flavonols than either *MYB75^{WT}* or *MYB75^{T131A}* -over-expressing lines. Interestingly, two regulatory genes, *MYB113* and *MYB90*, which are both homologues of *MYB75*, and reported to be positive regulators of anthocyanin biosynthesis were downregulated in both *35Spr:MYB75^{T131A}* and *35Spr:MYB75^{T131E}* plants, suggesting the existence of a negative feedback loop, whereby MYB transcription factors can shut down expression of their close homologues to control the accumulation of anthocyanins.

A gene encoding a known flavonol-modifying enzyme, quercetin 3-O-glycosyltransferase, (*UGT71B5*, At4G15280) was downregulated in *35Spr:MYB75*^{T131E} plants. This is somewhat surprising, as these lines displayed increased levels of several flavonols, including F5, (Quercetin-3-O-glucoside, 7-O-rhamnoside) which is glycosylated at the C3 position (Fig 3.6B). It is possible that there are other glycosyltransferases that can add a glycosyl group to the C3 position of quercetin, or that there is a sufficient supply of this enzyme to glycosylate the flavonol backbone, even under conditions where the *UGT71B5* gene is being downregulated. However, it is important to remember that in the gene expression analysis of *35Spr:MYB75* lines, the *MYB75*^{T131A} and *MYB75*^{T131E} over-expressors were compared to Col-0 WT plants, while in the HPLC analysis conducted in Chapter 3, the biochemical profile of each phosphovariant over-expressor was compared to *35Spr:MYB75*^{WT} plants, in order to get a clear idea of how biochemical profiles change with phosphorylation status. It would therefore be important to determine how the expression of the *UGT71B5* gene is affected in *35Spr:MYB75*^{WT} plants, before looking for correlations between biochemical profiles.

4.5.2 Cell wall-related genes

Genes required for the biosynthesis and remodelling of primary or secondary cell walls, as well as cell wall-associated proteins were classified as "CELL WALL" genes in the pie charts of Fig 4.7 and 4.8. Among cell wall-related genes downregulated in both *35Spr:MYB75*^{T131A} and *35Spr:MYB75*^{T131E} lines, I found two lignin biosynthetic genes, caffeic acid O-methyl transferase (*COMT*, AT1G33030) and cinnamoyl-CoA reductase (*CCR*-like, AT1G76470), as well as laccase 7, (*LAC7*, AT3G09220), which is a member of a gene family implicated in lignin polymerization (Zhao *et al.,* 2013). These findings are congruent with the idea that MYB75 is a negative

regulator of cell wall biosynthesis, as described by Bhargava *et al.,* (2010). These results are preliminary and should be re-examined in detail, particularly because the results reported by Bhargava *et al.,* (2010), showed that *COMT* and *CCR1* (another member of the cinnamoyl-CoA reductase) were among the very few lignin biosynthetic genes whose expression was not significantly affected in either the *myb75*$^{-}$ null mutant or the *MYB75OX* lines, relative to control plants. However, it is important to note that, in the Bhargava *et al.,* (2010) publication, the authors used *PAP1-D* activation tag lines instead of the *35Spr:MYB75* used in the current study. Perhaps more importantly, they used RNA isolated from the lower portion of mature inflorescence stems for their gene expression analysis, whereas I used mature leaf tissue. Interestingly, one lignin-associated gene, Laccase 2 (*LAC2,* AT2G29130), was upregulated uniquely in *35Spr:MYB75*^{T131A}, and was the only cell-wall associated gene upregulated in this genotype. Two cellulose synthase-like genes, cellulose synthase-like A1 (*AtCSLA1,* AT4G16590), and cellulose synthase-like G3 (*CSLG3,* AT4G23990), which have been implicated in hemicellulose biosynthesis, were also downregulated in both *35Spr:MYB75*^{T131A} and *35Spr:MYB75*^{T131E} plants. Although their biochemical function has been well described (Liepman *et al.,* 2005), it is not known to what degree each of these genes participates in secondary verses primary cell wall biosynthesis.

The major class of cell wall-related genes upregulated in *35Spr:MYB75* plants include genes required for cell wall remodelling during cell growth and expansion. Several expansins, including ATEXP1, ATEXP3, ATEXP8, ATEXP11 as well as a cellulase (*GH9B13*, AT4G02290) and pectin lyase (AT3G07010) were upregulated in both *35Spr:MYB75*^{T131A} and 35Spr:*MYB75*^{T131E} plants, and *ATEXP15* was upregulated uniquely in *MYB75*^{T131E} lines. The cellulase and pectin

lyase hydrolyze glycosidic bonds in cellulose and pectic polymers respectively, thus potentially loosening the cell wall and allowing for cellular expansion and growth (reviewed in Cosgrove, 2016). The precise mechanism by which expansins contribute to cell wall loosening is not known, but their mode of action is associated with auxin-driven acidification of the cell wall space (reviewed in Cosgrove, 2016). The genes uniquely upregulated in *35Spr:MYB75^{T131E}* plants include a number of genes required for the biosynthesis, modification and cleavage of carbohydrate components of the cell wall. Examples include a xylogalacturonan xylosyltransferase (AT5G03795), required for pectin biosynthesis, as well as pectin methyltransferase (AT5G20740) and pectinacetylesterase (AT5G26670), which participate in pectin decoration. Apart from cell wall biosynthetic and modifying enzymes, there were three cell wall associated proteins upregulated uniquely in *35Spr:MYB75^{T131E}* lines, which play important roles in growth and development. These includes a growth promoting subtilisin-like serine protease (*ATSBT1*, AT1G01900), required for proteolytic processing of peptide precursors to produce phytosulfokine, a peptide phytohormone which promotes cell proliferation (Srivastava *et al.,* 2008). The other two genes in this category are fasciclin-like arabinogalactans, (*FLA1*, AT5G55730 and FLA13, AT5G44130), which appear to play a role in anchoring the plant cell wall to the plasma membrane. These proteins are thought to be important in maintaining cell matrix integrity and have been implicated in a number of developmental processes (Johnson *et al.,* 2003; 2011).

4.5.3 Development and Differentiation

This category is perhaps the most difficult to describe and discuss, as many genes on this list are implicated in multiple developmental processes, in various biological contexts. In this

section, I will focus on highlighting a few interesting genes that may have a connection to some of the developmental processes which appear to be altered in *35Spr:MYB75* plants.

On the list of genes upregulated in both *35Spr:MYB75*^{T131A} and *35Spr:MYB75*^{T131E} plants, were three transcription factors that are known to participate in flavonoid biosynthesis as well as epidermal cell development. These transcription factors are TT8/bHLH42, TTG2/WRKY44 and LBD38. These transcriptional regulators influence flavonoid and anthocyanin biosynthesis and could have been classified in that category. However, because they have a broader role in development, beyond regulation of phenylpropanoid metabolism, I elected to classify these genes in development and differentiation. The role of TT8 in anthocyanin biosynthesis and epidermal cell fate determination has been discussed in detail earlier in this thesis. Similarly, TTG2/WRKY44 regulates epidermal cell fate, including trichome and root hair development, as well as being a positive regulator for the biosynthesis of proanthocyanidins in the *Arabidopsis* seeds (Verwiej *et al*., 2016, Johnson *et al.*, 2002; Ishida *et al.,* 2007). Expression of both TT8 and TTG2 has been shown to be directly regulated by MYB75 (Baudry *et al.,* 2006; Ishida *et al.,* 2007), but our data suggests that this positive regulation is not impacted by phosphorylation.

The transcription factor LBD38 is known as a global negative regulator of anthocyanin biosynthesis but is also involved in driving changes in expression of developmental genes in a nitrogen status-dependent manner. LBD38 function is therefore required for processes such as nitrogen uptake and assimilation, as well as plant growth and shoot branching (Rubin *et al.,* 2009). Regulation of LBD38 by MYB75 has not been reported previously, and it would be interesting to know if LBD38 is a direct target of MYB75.

Another vascular development-associated gene that is upregulated in both phosphovariants is a xylem cysteine peptidase 2 (AT1G20850, *XCP2).* This gene plays a role in the proteolysis of cellular components during programmed cell death, required for vessel differentiation (Funk *et al*, 2002). This would appear to be pertinent to our observation that *35Spr:MYB75* plants developed ectopic vessels in their mature stems (Fig 4.6). This phenotype was particularly prominent in *35Spr:MYB75*^{T131E} lines where, *XCP2* expression was upregulated 2.7 fold compared to 2.3 fold increase in *35Spr:MYB75*^{T131A} plants.

In an effort to find an explanation for the differences I observed in bolting and flowering time between different phosphovariants, I examined the gene differential expression list for genes that are known to be implicated in regulation of flowering time. MADS (MCM1, Agamous, Deficiens Srf) Affecting Flowering 5 (MAF5, AT5G65080), is upregulated in both *35Spr:MYB75*^{T131A} and *35Spr:MYB75*^{T131E} plants: this transcription factor is a member of a gene family (MAF2-MAF5) of floral repressors in *Arabidopsis.* These genes are part of a regulatory network controlling the transition from vegetative to reproductive stage of the plant life cycle, by integrating signals in response to day length, light, and temperature (Ratcliffe *et al,* 2003). Over-expression of *MAF5* would explain the late flowering phenotype of *35Spr:MYB75*^{T131E} plants, however, since it is upregulated in both *35Spr:MYB75*^{T131E} and *35Spr:MYB75*^{T131A} genotypes, upregulation of *MAF5* is not sufficient to explain the observed phenotypes. The function of these genes is highly dependent on environmental inputs, and it is likely that other genetic factors play an important role in modulating their function. Indeed, in the original report, late flowering phenotype predominated in *35Spr:MAF2* lines, but at the same time, a

significant portion of the transgenic population displayed an early flowering phenotype (Ratcliffe *et al*., 2003).

Within the subset of differentially-expressed genes known to be involved in development I identified several that were uniquely up-or down-regulated in one or the other phosphovariant. Two genes whose expression increased uniquely in *35Spr:MYB75^{T131E}* plants (*Histones H3.1* and *H2A11*), could potentially account for large developmental changes, such as delayed transition from vegetative to reproductive stage. Both of these histone variants are implicated in controlling flowering time. For instance, specific *Histone3* methylation, at lysine 4, has a direct impact on expression of *flowering locus C (FLC)* during vernalization (Tamada *et al.,* 2009), which ultimately controls flowering time. Deposition of histone H2A11 (aka H2A.Z) onto chromatin is required for *FLC* expression (Deal *et al.,* 2007). A detailed discussion of all the ways that histones can impact development is beyond the scope of this thesis; it is sufficient to say that over-expression of these genes in *35Spr:MYB75^{T131E}* lines may be implicated in the developmental changes observed in these plants, and in the differences observed in between *35Spr:MYB75^{T131A}* and *35Spr:MYB75^{T131E}* phosphovariants.

Most of the genes downregulated in one or both phosphovariants were associated with senescence. *Dark inducible 11* (*DIN11*, At3g49620) was downregulated in both *35Spr:MYB75^{T131A}* and *35Spr:MYB75^{T131E}* lines, while *DIN2* (AT3G60140) was downregulated uniquely in *35Spr:MYB75^{T131A}*. These gene products accumulate in senescing leaves and their expression is induced in the dark (Fujiki *et al.,* 2001). Among genes downregulated uniquely in *35Spr:MYB75^{T131E}* lines I found a senescence related gene, *Senescence-Associated and QQS-Related*, (SAQR, AT1G64360), which is involved in integrating senescence related changes and

primary metabolism (Jones *et al.,* 2016), and *ATNAC3/ANAC059* (AT3G29035), a transcription factor which regulates global changes in gene expression associated with leaf senescence (Balazadeh *et al.,* 2011).

4.5.4 Hormones

Among transcripts which show increased expression in both *35Spr:MYB75^{T131A}* and *35Spr:MYB75^{T131E}*, I found genes associated with several plant hormones. The list includes a gene required for ethylene biosynthesis (*ACS4,* AT2G22810), two GASA domain proteins (AT5G14920 and *GASA6*; AT1G74670), which participate in gibberellic acid (GA) signal transduction and response respectively, as well as *gibberellin 3-oxidase 1* (*GA3OX1*, AT1G15550), required for gibberellic acid biosynthesis. A brassinosteroid signalling component, called *BR-enhanced expression 3* (*BEE3*, AT1G73830), which has been implicated in shade avoidance was also on the list of differentially-expressed genes. Of particular interest, however, were those genes whose function is linked to auxin and cytokinin, as these hormones play a critical role in vessel differentiation. An auxin responsive gene, *IAA29* is known to be upregulated in developing vessels, and although the exact biochemical function of this gene is not known, it frequently appears in the literature, pertaining to integration of light and auxin signals in plant growth and development (Wang *et al.,* 2017; reviewed in Halliday *et al.,* 2009). Last but not least, *Target of Monopteros 3*, also known as *Cytokinin Response Factor 2* (TMO3*/CRF2*, AT4G23750), appeared on our list of genes upregulated in both phosphovariant over-expressors. As a downstream target of both cytokinin and auxin (through the auxin responsive global regulator, MONOPTEROS), TOM3/CRF2 plays a vital role in organ

development (both shoots and roots) and in cell fate determination (Ckurshumova *et al.,* 2014; Jeon *et al.,* 2016).

Genes which participate in auxin and cytokinin signalling and response were also found on the list of transcripts upregulated uniquely in *35Spr:MYB75G^{T131E}* lines. These include *Arabidopsis Response Regulator 15* (*ARR15*, AT1G74890), which is involved in auxin and cytokinin crosstalk during cell fate specification (Chandler and Werr, 2015). Another cytokinin responsive gene on this list is *ARR5*; according to GO annotation this gene is implicated in negative feedback regulation of cytokinin signalling, as well as integration of light and circadian clock signals during development. Other hormone-related genes upregulated uniquely in *35Spr:MYB75^{T131E}* lines, were genes required for ethylene biosynthesis (*ACS11*, AT4G08040; *ACS5*, At5G65800) and ethylene response genes (*ATERF6,* At4G17490 and *ERF/AP2,* AT3G60490). Ethylene is a versatile hormone, involved in a broad spectrum of developmental processes and stress responses. Since the effect of this hormone on any particular aspect of plant function largely depends on other hormones and signals present, it is challenging to interpret how changes in the expression of these particular genes might account for any of the observed phosphovariant phenotypes, but their identification in this experimental context may prove to be important in future explorations of MYB75 function, particularly in integration of development and stress responses.

4.5.5 Stress Response and Signalling

Stress response and signalling are arguably the most relevant categories to MAP kinase signal transduction and protein phosphorylation. Biotic and abiotic stress response genes were equally represented in the list of transcripts which were upregulated in both *35Spr:MYB75^{T131A}*

and *35Spr:MYB75^{T131E}* plants. On the other hand, most of the genes upregulated uniquely in *35Spr:MYB75^{T131E}* were associated with defense, plant immunity and other responses to biotic stress. Interestingly, genes downregulated in both phosphovariant over-expressors were also primarily associated with defense and response to pathogen attack, with the exception of two genes associated with osmotic stress, and one drought responsive gene. Three members of the cytochrome P450 gene family were downregulated in both phosphovariants, including CYP82C2, (AT4G31970), CYP71A13 (AT2G30770), and CYP71B15 (AT3G26830). These were classified as stress response genes, as they are required for biosynthesis of camalexin (Klein *et al.,* 2013; Chapman *et al.,* 2016), and a cyanogenic compound, 4-hydroxyindole-3-carbonyl nitrile (4-OH-ICN) (Rajniak *et al.,* 2015), metabolites that are important in plant defense.

Among the genes classified under the "signalling" category*, early flowering 4-like 3* (*ELF4-like 3*, AT2G06255), was downregulated in *35Spr:MYB75^{T131E}* plants. ELF4 plays an important role in transcriptional regulation of genes downstream of PHYB signalling and was shown to be important for seedling de-etiolation under red light (Khanna *et al.,* 2003). ELF4 is also required for the integration of circadian rhythm and flowering time, and *elf4* null mutants flower early under short day conditions (Doyle *et al.,* 2002). This gene might therefore be an interesting candidate for further analysis, when searching for possible explanations for the observed differences in flowering time between *35Spr:MYB75^{T131E}* and *35Spr:MYB75^{T131A}* lines. One gene associated with cell signalling that was uniquely upregulated in *35Spr:MYB75^{T131E}* which I found particularly interesting was *nucleotide diphosphate kinase 2* (*NDPK2*, AT5G63310). This kinase is known to interact physically with phytochromes and plays an important role in photomorphogenic processes such as cotyledon opening and greening during

seedling development. Mutant *ndpk2* seedlings have abnormal cotyledons, smaller rosettes and lower chlorophyll content (Choi *et al.,* 2005). In addition, *ndpk2* mutants display altered polar auxin transport and reduced expression of auxin-responsive genes (Choi *et al.,* 2005). I found this gene interesting because while it connects light and auxin signalling, two processes in which MYB75 is implicated, it does not yet have a defined biochemical. If *NDPK2* were shown to be a direct target of MYB75, and as our data suggests, only a target of the phosphorylated form of MYB75, it would be a direct connection between MYB75 and auxin driven development as well as photomorphogenesis.

4.5.6 Photosynthesis

Development, assembly and maintenance of the chloroplast and photosynthetic machinery is a complex process that is tightly linked to light signalling. Perhaps the most interesting and novel piece of data that came out of my gene expression analysis is the relatively large number of photosynthesis-associated genes which were upregulated uniquely in *35Spr:MYB75^{T131E}*plants. With a total of 16 genes (not counting seven more that barely missed the cutoff, with ~1.9 fold upregulation), this category constitutes about 10% of the genes whose expression increased uniquely in the *35Spr:MYB75^{T131E}* phosphovariant (Fig 4.7B). The genes on this list include those required for chloroplast protein folding, light harvesting complex organization, as well as chloroplast ribosomal proteins. The list also included key components of the photosynthetic machinery, including photosystem I and photosystem II light harvesting proteins, as well as RUBISCO (*RBCS1A*, AT1G67090). The expression of many of these genes is canonically used as a marker of photomorphogenic and developmental processes: for instance, their expression increases with the onset of photosynthesis in germinating seedlings,

and decreases during senescence. Upregulation of photosynthesis-associated genes in *35Spr:MYB75*^{T131E} is particularly relevant since these plants displayed delayed development, and therefore delayed onset of senescence compared to *35Spr:MYB75*^{WT} and *35Spr:MYB75*^{T131A} plants.

4.6 Discussion

The aim of this chapter was to explore several aspects of development in plants over-expressing T131A and T131E phosphovariant forms of MYB75, in an effort to uncover possible new roles of this transcription factor and determine how phosphorylation could potentially influence MYB75 function in a developmental context. This work was primarily undertaken because, according to the data presented in Chapter 3, phosphorylation status did not have a dramatic effect on the ability of MYB75 to drive expression of known and well- defined target genes required for biosynthesis of anthocyanins. However, at the same time, distinct and consistent developmental differences were observed between the various phosphovariant *35Spr:MYB75* lines, which suggested that MYB75 phosphorylation status can influence development.

While I concluded that phosphorylation status of MYB75 has no obvious effect on total anthocyanin levels, I did note that it can influence the types of flavonoid biochemical species that accumulate in transgenic phosphovariant plants. Accumulation of several flavonol glycosides (including three kaempferol and one quercetin derivatives) increased in *35Spr:MYB75*^{T131E}, while *35Spr:MYB75*^{T131A} lines showed a decrease in the levels of two distinct flavonol biochemical species (a quercetin glycoside and an unknown flavonol), when compared to *35Spr:MYB75*^{WT} plants. As discussed in the introduction of this chapter, flavonols can

modulate auxin fluxes and therefore can play a vital role in developmental processes regulated by this hormone. The most conservative explanation for the observed developmental phenotypes is that altered flavonol profiles in *35Spr:MYB75* lines lead to perturbations in auxin flow, which in turn affects germination, flowering time and vascular development. However, I cannot exclude the possibility that MYB75 has additional transcriptional targets that have not been characterized in the literature, and that the developmental phenotypes I observed result from a combination of changes in auxin transport and differential regulation of gene expression in each phosphovariant.

4.6.1 Germination

My analysis of germination rates in *MYB75pr:MYB75 cDNA* lines was performed to test the idea that my failure to isolate lines which express recombinant $MYB75^{T131A}$ or $MYB75^{T131E}$ from the endogenous *MYB75* promoter was caused by lethality at early stages among these phosphovariants. I hypothesized that there was an artificial selection for plants that had reduced or silenced transgene expression, and my data (Fig 4.2) establish that germination rates are, indeed, severely impaired in plants expressing $MYB75^{T131A}$ and $MYB75^{T131E}$. Furthermore, plants expressing $MYB75^{T131A}$ showed significantly lower germination rates than those expressing $MYB75^{T131E}$, suggesting that the phosphorylation status of MYB75 can impact germination rate. Seed dormancy and germination are complex processes regulated by several hormones, including ABA, GA and auxin (reviewed in Shu *et al.,* 2016). The balance between the dormancy promoting ABA and germination-promoting GA hormones ensures that seeds germinate at the appropriate time. Our gene expression analysis suggests that MYB75 can influence (directly or indirectly) the expression of genes which participate in the biosynthesis

and signal transduction of these hormones. However, there is no apparent pattern of transcriptional changes that can easily explain the poor germination rate observed in *MYB75pr:MYB75 cDNA* (T131A and T131E) lines.

From the assay which was conducted to generate the data shown in Fig 4.2 I am unable to assess whether these plants are impaired in germination, or simply fail to germinate because of embryonic arrest or lethality. In order to understand how MYB75 affects these early developmental stages we would need to determine whether plants expressing these MYB75 phosphovariants display embryonic defects, which would require us to dissect a large number of developing seeds and look for abnormalities at different stages of embryogenesis, possibly with the help of embryonic molecular markers. Given the involvement of auxin in early embryo patterning, I suspect that it is aberrant embryo development, rather than failure to germinate, that is the underlying cause for low germination rates in these plant lines. Supporting this conclusion, is the widespread developmental arrest observed among seedlings of these lines: many seedlings derived from the *MYB75pr:MYB75*^{T131A} and *MYB75pr:MYB75*^{T131E} lines remained small (about half the size of *myb75*$^{-}$ and Nossen controls) even 10 days after germination, while some failed to develop leaves, and did not survive when transferred to soil. Since auxin plays a central role in embryogenesis and seedling development, it is possible that perturbations in auxin flow, driven by changes in flavonol profiles, led to developmental abnormalities, and in some cases arrest at these early stages. Although the impact of flavonols on auxin transport is thought to be relatively mild in adult plants, at early stages of development small perturbations in auxin flow can have catastrophic effects (reviewed in Möller and Weijers, 2009).

MYB75 (along with MYB123/TT2) participates in flavonoid biosynthesis during embryogenesis, where proanthocyanidins are the end product (Sharma and Dixon, 2005). Proanthocyanidins (PA's) accumulate in different parts of the developing seed coat, including the micropyle, chalaza and the endothelium (an inner layer of cells in the seed coat, enclosing the developing embryo) (reviewed in Xu *et al*., 2015, Fig 2). Recent evidence suggests that seed coat development can influence cellularization of the endosperm which has a direct impact on embryogenesis (Doughty *et al.,* 2014). The authors suggest that part of this mechanism involves modulation of auxin fluxes in the endosperm by flavonoid accumulation in the endothelium. Among genes which participate in this process, I found TTG2; to be on the list of transcripts upregulated in both *35Spr:MYB75^{T131A}* and *35Spr:MYB75^{T131E}* lines; this transcription factor is associated with increased seed size, as *ttg2* mutants have smaller seeds, and are pale in colour due to their failure to accumulate PA's in the endothelium (Doughty *et al.,* 2014).

4.6.2 Flowering time

The transition from vegetative to flowering stage is an immensely complex process, driven by a vast regulatory network that integrates signals from multiple plant hormones and environmental cues such as light, photoperiod and temperature, as well as the circadian clock. A detailed overview of this subject matter is far beyond the scope of this thesis, so I will limit my discussion to describing some relationships between auxin flow and the floral transition, in the context of possible connections between altered flavonol levels found in *35Spr:MYB75^{T131A}* and *35Spr:MYB75^{T131E}* plants, and the observed differences in flowering time in these lines. Among the developmental changes described in different *transparent testa* (*tt)* mutants were distinct differences in the timing of the transition from vegetative to floral developmental

stages among different mutant genotypes. Lesions in *tt6* and *tt7* genes, for example, resulted in an early flowering phenotype (Buer *et al.,* 2013). Since these gene products are essential for synthesis of kaempferol and quercetin, this observation indicates that the absence of these flavonols may be associated with accelerated flowering (Buer *et al.,* 2013). Our data appears to follow a similar trend, where *MYB75*^{T131E} plants, which show increased levels of certain flavonols, bolt and flower later than *MYB75*^{T131A} plants, which, in turn, display reduced flavonol levels compared to *MYB75*^{WT} over-expressor and have early bolting and flowering times. However, there is one difficulty with this comparison; all *35Spr:MYB75* plants showed increased levels of flavonols compared to Col-0 WT plants (the shifts in flavonol and anthocyanin profiles in *35Spr:MYB75*^{T131A} and *35Spr:MYB75*^{T131E} were described in relation to *35Spr:MYB75*^{WT} plants). Therefore, a simple change in total flavonol levels cannot account for the developmental changes I observed in Fig 4.3. Instead, I would have to postulate that changes in levels of specific flavonol species (as described in the introduction) are responsible for the observed phenotypes.

The fact that *35Spr:MYB75*^{T131E} plants displayed not only delayed bolting and flowering time but also delayed onset of senescence, is consistent with a model of global developmental reprogramming, one which appears to slow down development overall. An example of comparable phenotypes described in the literature includes the *arf2* mutant, defective in an auxin response factor, found upstream of two GA-responsive transcription factors. Mutant *arf2* plants displayed delayed flowering and senescence similar to my *35Spr:MYB75*^{T131E} plants; this mutant phenotype was partially rescued by exogenous application of GA (Richter *et al*., 2013). Unfortunately, our global gene expression profiles did not show any differential expression of

ARFs on the list that might connect the observed phenotypes to this particular pathway. However, there are other genes in the list that could potentially account for global changes in gene expression in *35Spr:MYB75^{T131E}* plants. These include Histones *H3.1* and *H2A.11/H2A.Z,* upregulated in *35Spr:MYB75^{T131E}* plants, and *ATNAC3* (*OSR1/ATNAC3*, AT3G29035), a global regulator of senescence that was downregulated in *35Spr:MYB75^{T131E}*. Decreased expression of the *NAC3* (*OSR1*) transcription factor could account for the increased expression of photosynthetic genes exclusively observed in *35Spr:MYB75^{T131E}* plants, since an inverse correlation has been observed between *OSR1* expression levels and chlorophyll content (Balazadeh *et al.,* 2011), which is dependent on expression of photosynthetic and chloroplast associated genes.

Upregulation of photosynthesis genes, differences in flowering time and phosphorylation of MYB75 have a common theme: light signalling, through phytochromes. Interestingly, Li *et al*., (2016) showed that MPK3, MPK4, and MPK6 were activated by high light in wild type plants but not in *phyAphyB* double mutants. Light therefore appears to be connected to MPK4 activation and subsequent phosphorylation of MYB75 at threonines 126 and 131. The authors also showed that anthocyanin production is reduced in *mpk3/4* double mutants and completely abolished in *phyAphyB* double mutants, as in *myb75^{-}* plants. It is clear that many aspects of MYB75 function, including transcription, turnover and phosphorylation are controlled by light, at least in part through phytochrome signalling, and that this process is an important part of the regulation of anthocyanin biosynthesis. However, my data also suggests that MYB75 has a broader role to play in development, possibly through flavonol-

mediated regulation of auxin flow, or through activation of other, as yet unidentified, target genes under transcriptional regulation by MYB75.

4.6.3 Vascular development

Much like flowering time, vascular development involves massive changes in gene expression, dependent on the integration of multiple environmental and developmental cues. Therefore, the development of ectopic vessels that I observed in *35Spr:MYB75* plants can potentially have many underpinnings. Although polar auxin flow plays a central role in driving vascular differentiation and continuity, there are additional developmental cues required for vessel positioning, which should not be overlooked when trying to understand the observed changes in vascular patterning. One prominent example of such a mechanism is depicted in the analysis of the *COV1* (*continuous vascular ring)* gene. This gene was identified in an EMS mutagenesis screen, where the isolated *cov1* null mutants displayed abnormal vascular patterning in the stem, where vascular tissue development occurred in the interfascicular region (Parker *et al.,* 2003), much as in my *35Spr:MYB75*^{T131E} plants.

Another possible scenario which can account for ectopic vessel development is early onset of cambial activity. As described in the introduction, the onset of cambial activity in later stages of development results in formation of a secondary vasculature which spans the entire circumference of the *Arabidopsis* stem, in a pattern reminiscent of wood formation. A dominant mutant in the *high cambial activity 2* (*HCA2)* transcription factor appears to control the onset of cambial activity. Over-expression of this gene leads to precocious cambium activation, which results in a radial vascular pattern (Gou *et al.,* 2009). The radial distribution of vessel elements seen in *35Spr:MYB75*^{T131E} stems could be a symptom of early cambium

activation in these plants, particularly since *HCA2* (At5g62940) was upregulated slightly (~1.5 fold) in lines *35Spr:MYB75*^{T131E}. Although this level of upregulation failed to meet the 2 fold cutoff, it is worth noting that *CHS*, a known target of MYB75, was also only upregulated ~1.5 fold, in this phosphovariant. A 1.5 fold increase in transcription may, therefore, not be insignificant, and it would probably be worthwhile to examine more closely whether expression of phosphomimic MYB75 has a significant impact on *HCA2* expression.

There is, however, a potentially simpler explanation for the observed vascular phenotypes, one based on auxin transport inhibition by flavonols. The clues can be found in early published work with auxin inhibitors and *pin* mutants. The *pin1pin2* double mutants defective in auxin efflux channels, as well as plants treated with the auxin transport inhibitor NPA, display disorganized vessel positioning, with numerous xylem vessels differentiating in the interfascicular regions, outside their normal vascular bundle positions (Ibañes *et al.,* 2009). Canalization and drainage of auxin is an essential part of vascular differentiation and continuity. The absence or blockage of auxin efflux carriers results in failure to canalize auxin, leading to spilling of auxin into neighboring cells, which can result in their reprogramming and differentiation into vessel elements. Therefore, the phenotypes that I observed can potentially be a result of reduced polar auxin flow, driven by increased intracellular flavonol levels. All *35Spr:MYB75* plants had elevated flavonol levels compared to Col-0 WT plants, and all of these lines also showed some degree of ectopic vessel formation. The phenotype was most severe, and apparent in earlier stages of development only in *35Spr:MYB75*^{T131E} lines, most likely because these plants accumulated more flavonols than the other over-expressor lines. This hypothesis obviously needs further experimental support, such as determining to what degree

auxin flow is affected in stems of each phosphovariant over-expressor. The gene expression analysis should be repeated, using RNA isolated from stems instead of mature leaves, to determine how over-expression and phosphorylation of MYB75 can affect genes required for vascular differentiation and patterning in mature stems.

4.6.4 Global gene expression analysis of 35Spr:MYB75 lines

In retrospect, an experiment that evaluates global changes in gene expression should be done at early stages of a project such as this, particularly when working with a transcription factor such as MYB75. However, my project was framed initially as a question of whether post-translational phosphorylation of MYB75 was possible, and if it were, how this might influence MYB75's ability to regulate anthocyanin biosynthesis, which was the accepted role for this transcription factor. We felt optimistic that, if phosphorylation of MYB75 at threonine 131 had any impact on its function, this would be reflected in the anthocyanin biochemical profiles. However, my results showed that none of the known MYB75 target genes in the anthocyanin biosynthesis pathway were affected by either T131A or T131E mutations, whereas these plants displayed striking developmental changes unique to each phosphovariant. It therefore became imperative to conduct global gene expression analysis, to try to understand how MYB75 (and particularly its phosphorylation status) might be affecting development.

In section 4.5 I discussed a number of differentially expressed genes, in *35Spr:MYB75* lines, as potentially relevant players in the observed developmental changes. However, it is important to note that these results are necessarily still preliminary and specific gene expression changes should be confirmed by real time PCR (qPCR). Nevertheless, several robust and important patterns emerged from this next generation sequencing analysis. First, gene

expression profiling confirmed that the core anthocyanin biosynthesis genes, and many genes encoding anthocyanin-modifying enzymes, were upregulated in both phosphovariant over-expressors. Furthermore, a number of lignin biosynthesis-related genes were downregulated in both *35Spr:MYB75^{T131A}* and *35Spr:MYB75^{T131E}* genotypes, corroborating previously described involvement of MYB75 in this process. Finally, the number of genes whose expression changed as a result of *MYB75^{T131E}* over-expression was substantially larger than the number of genes affected by over-expression of *MYB75^{T131A}*. This is perhaps the most important and robust observation, as it indicates that *MYB75^{T131E}* is a more potent regulator of gene expression than the phospho null *MYB75^{T131A}*, and suggests that MYB75 phosphorylation has a positive impact on its ability to regulate gene expression. Since the ability of a transcription factor to drive gene expression is a function of its affinity for a particular promoter sequence, and of its transcriptional activation/repression strength, either one of those functions could potentially be affected by phosphorylation. However, since anthocyanin biosynthesis genes were similarly upregulated in both phosphovariant genotypes, it is unlikely that general transcriptional activity is enhanced in the *MYB75^{T131E}* phosphovariant. The most likely explanation is that *MYB75^{T131E}* can bind a wider range of target promoters, to either positively or negatively regulate expression of these genes. It is also possible that phosphorylated MYB75 has additional interacting partners that enable phospho-MYB75 to participate in transcriptional activation or repression of a wider range of targets. Finally, the list of genes whose expression is affected by *MYB75^{T131E}* includes several global regulators, such as *ATNAC3* involved in regulating senescence, or histones, which can affect chromatin organization. Therefore, *MYB75^{T131E}* may

affect a much wider range of genes than *MYB75*^{T131A}, through direct or indirect regulation of genes that can in turn lead to global changes in gene expression.

4.7 Materials and Methods

4.7.1 Germination rate in *MYB75pr:MYB75 cDNA* lines

The transgenic *Arabidopsis* plant material used in this assay were seeds from homozygous T3 plants carrying the *MYB75pr:MYB75 cDNA* constructs, in a *myb75*$^{-}$ mutant background (Nossen ecotype). Six independent lines carrying *MYB75pr:MYB75*^{T131A}*cDNA* and four lines carrying *MYB75pr:MYB75*^{T131E}cDNA were used, along with *myb75*$^{-}$ mutant and Nossen WT controls. Seeds were surface sterilized, plated on ½ MS plates and vernalized for 3 days at 4ºC. Plates were put into light and left for 10 days at light fluence of ~30 µmol $m^{-2}s^{-1}$ and 16h light/8h dark photoperiod, at 21ºC. Ten days after exposure to light, the germination percentage was scored for each plate by counting the number of unresponsive seeds and the number of germinated plants. Plants which were counted as germinated included any seed that showed signs of an emerging seedling. The number of seeds used to evaluate the germination rate for each line is depicted in Table 4.1 below.

Table 4.1 Germination score in homozygous *MYB75pr:MYB75 cDNA* plants.

Line	Total number of seeds plated	Number of seeds germinated	Percentage germination
MYB75pr:MYB75^{T131A} L1	580	132	22.7%
MYB75pr:MYB75^{T131A} L2	673	219	32.5%
MYB75pr:MYB75^{T131A} L3	274	73	26.6%
MYB75pr:MYB75^{T131A} L4	584	231	39.6%
MYB75pr:MYB75^{T131A} L5	809	82	10.1%
MYB75pr:MYB75^{T131A} L6	432	127	29.4%
MYB75pr:MYB75^{T131E} L1	669	472	70%
MYB75pr:MYB75^{T131E} L2	820	447	55%
MYB75pr:MYB75^{T131E} L3	724	540	75%
MYB75pr:MYB75^{T131E} L4	720	350	48.6%
Nossen WT	213	209	98%
myb75^{-}	245	240	98%

4.7.2 Plant growth conditions and flowering time

Plants were grown as described in section 3.6.1.3, until the plants were approximately 5 weeks old. Individuals representative of each line were photographed on the same day to demonstrate different flowering times and developmental stages. The plants were photographed again at 7 weeks of age.

4.7.3 Stem sections and histochemical staining

The lower 5cm of the stems of 7 and 8-week-old *Arabidopsis* plants were hand-sectioned. Lignin staining was performed by submerging stem sections in phloroglucinol (Sigma) solution (2% w/v phloroglucinol in 95% ethanol) and adding concentrated HCl dropwise. After 5min incubation, the sections were washed three times in distilled water, mounted in water on slides and imaged immediately. Other stem sections were stained with toluidine blue by submerging the sections in 0.02% toluidine blue solution (in distilled water). After 1-2 min incubation the sections were rinsed in distilled water (at least three times), mounted on a slide in water and imaged immediately. All imaging was performed using a Leica Mecatron Precision DMR compound microscope, with a mounted digital camera, Canon EOS Rebel T5.

4.7.4 Gene expression analysis: next generation sequencing

Arabidopsis plants carrying *35Spr:MYB75^{T131A}gene* and *35Spr:MYB75^{T131E}gene* constructs were grown as described in section 3.6.1.3, alongside Col-0 WT plants. Mature rosette leaves of 5-week-old *Arabidopsis* plants were harvested and total RNA was extracted as described in section 3.6.5 of Chapter 3. Each RNA sample was obtained from two leaves, harvested from two individual plants belonging to the same line. Three separate lines were used for the *35Spr:MYB75^{T131A}* genotype (L1, L22 and L23) and four lines for the *35Spr:MYB75^{T131E}* genotype (L2, L4, L5, L9). Total RNA concentration in each sample was determined using NanoDrop® (Thermo Fischer), and RNA quality (intactness) was evaluated by running 5µl of each sample on a 2% agarose gel. Only RNA samples where the banding pattern appeared intact, with no significant smearing from RNA degradation were used to generate the final samples. The final samples were obtained for each genotype by pooling equal amounts of total RNA from each

line belonging to that genotype: for example MYB75^{T131A}L1, MYB75^{T131A}L22 and MYB75^{T131A}L23 were pooled to obtain the final sample for *35Spr:MYB75^{T131A}*. The final sample for Col-0 WT was generated by pooling four samples from different Col-0 WT plants. RNA sequencing was performed on each final sample using the *Illumina NextSeq500*, at 15-30 million reads, which were trimmed using the Trimmomatic platform (Bolger *et al.,* 2014). Raw data was processed by Dr. Darren Wong (Castellarin lab, UBC wine research centre) as follows: trimmed reads were aligned to the *Arabidopsis thaliana* reference genome (TAIR 10 genome release), using the HISat2 alignment tool. Dr. Wong identified differentially expressed genes whose expression changed in *35Spr:MYB75^{T131A}* and *35Spr:MYB75^{T131E}* plants compared to Col-0 WT control, as determined by GFold software (Feng *et al*, 2012), and performed VENN analysis on the entire dataset, creating six lists: T131A and T131E overlap upregulated, T131A unique upregulated, T131E unique upregulated, T131A and T131E overlap downregulated, T131A unique downregulated, and T131E unique downregulated. To generate the pie charts in Fig 4.7 and Fig 4.8, I eliminated all genes from each list whose expression change was less than twofold, creating a final set of six gene lists. Each gene was functionally categorized based primarily on its predicted function as described in the literature, while GO annotation plus information on related genes, was used to classify genes, in cases where there was insufficient published data on the gene in question. Complete NGS data is available electronically in EXcel format in supplementary materials Table S4.1.

Chapter 5 General Discussion

5.1 Introduction

The biological role of MYB75 has been described in a large number of publications, primarily as a positive regulator of flavonoid and anthocyanin biosynthesis. While accumulation of flavonols and anthocyanins is known to be orchestrated by various environmental and developmental factors, less is known about how these different stimuli are integrated to control anthocyanin production. When our lab decided to explore the possibility that MYB75 is regulated post translationally though phosphorylation by MAP kinases, nothing was known about MYB75 phosphorylation except that the MYB75 amino acid sequence contained, two canonical MPK target sites at threonines 126 and 131. In the early stages of this project the work was divided between myself and two post-doctoral fellows, Dr. Yonge and Dr. Liu: their goal was to determine which of the 20 *Arabidopsis* MPKs can phosphorylate MYB75 recombinant protein, while my job was to describe how MYB75 protein function changes with phosphorylation status and how this affects plant biochemistry and development. My portion of the project included both *in vitro* and *in vivo* approaches, in both cases using point mutants to mimic phosphorylated or unphosphorylated MYB75 protein. In pursuing my project, I encountered several technical setbacks, particularly when trying to express different phosphomimic and phosphonull versions of MYB75 in *Arabidopsis.* On the other hand, many of these setbacks revealed important information about this protein and its possible involvement in plant development. Most crucially, as I was approaching the end of my research, a publication appeared (Li *et al.*, 2016) that confirmed our findings about MYB75 phosphorylation by MPK4 and demonstrated that MYB75 is stabilized by phosphorylation at both threonines 126

and 131, during high light growth conditions. The authors described how this event influences anthocyanin production, in the context of light signalling. Under the circumstances, I needed to emphasize in my thesis aspects of MYB75 phosphorylation that made my findings distinct from the published work by Li *et al*., (2016). Therefore, I chose to build upon my observations of the phenotypes of *35Spr:MYB75 Arabidopsis* lines, observations which had already prompted me to explore other aspects of MYB75 function, particularly developmental changes resulting from phosphorylation. Unfortunately, time and financial constraints did not allow me to develop an in-depth mechanistic explanation for how MYB75 phosphorylation status might be driving the observed developmental changes, leaving this part of the project in its exploratory stages. Nevertheless, I feel that my work does indicate that this transcription factor plays a much broader role in development than previously described, and that MYB75 phosphorylation (presumably by MPKs) plays a pivotal role in this process. In this final chapter I will describe future experiments that should be conducted to refine my findings, to test hypotheses, and to further define the role of MYB75 phosphorylation in regulation of flavonoid biosynthesis and development.

5.2 MYB75 interaction with *Arabidopsis* MAP kinases and phosphorylation

In Chapter 2, I demonstrated that recombinant MYB75 can interact with a relatively large number of *Arabidopsis* MAP kinases *in vitro,* using a yeast two-hybrid system (Clontech). Dr. Yonge and Dr. Liu demonstrated that recombinant MYB75 can be phosphorylated *in vitro* by MPK3, MPK4, MPK6 and MPK11, in the presence of the appropriate CAMKK, and contrary to the data published by Li *et al*., (2016), showed that only threonine 131, and not 126 was

important for this phosphorylation event. These results defined the path of my thesis research, as I subsequently focused on studying plants overexpressing single point mutants, MYB75^{T131A}, MYB75^{T131E} that would mimic modifications to the T131 site. However, these early *in vitro* experiments should be re-visited and extended in order to be able to tell a complete story, delineating a pathway from MPK activation to MYB75 phosphorylation and subsequent change in protein function.

First and foremost, interaction between MYB75 and MAP kinases should be examined *in planta,* using BIFC (bimolecular fluorescence complementation assay) in *N. benthamiana* leaves or *Arabidopsis* protoplasts. Furthermore, we need to demonstrate that MYB75 is phosphorylated *in vivo* by the MPKs which were shown to interact with MYB75 in yeast. A method commonly used to detect phosphorylation of a protein *in vivo* is separation of protein extract by electrophoresis on a Phos-tag™ acrylamide gel, followed by conventional immunodetection by western blot. Phos-tag™ acrylamide slows down the migration of phosphorylated proteins, thus phosphorylation at each site causes an upward shift of the protein on the gel, leading to a distinct banding pattern, with higher degrees of phosphorylation resulting in increasingly greater shifts. This technique was attempted in our lab, first by Dr. Liu using *35Spr:MYB75 cDNA* lines, which unfortunately did not yield sufficient expression levels of recombinant MYB75 protein to effectively conduct this analysis. I later attempted to repeat this assay with my *35Spr:MYB75 gene* lines, which produced significantly more protein, However, I was not successful either, as my western blot results showed a wide range of band sizes, instead of the discrete banding pattern corresponding to MYB75 and its different phosphorylation states. I believe this problem can be amended by using a cleaner

protein extraction protocol. Since recombinant MYB75 was very prone to rapid degradation, I chose not to use conventional protein extraction protocols, but instead I ground plant tissue and directly resuspended it in SDS running buffer, minimizing handling time and therefore reducing protein degradation. It is possible that cellular debris and phosphorylated cell components, contaminating my protein samples caused the high background in the Phos-tag™ acrylamide gel, even though in regular SDS gel electrophoresis there was no significant background signal near the recombinant MYB75 band. Therefore, I believe this experiment would require optimization, in terms of the protein extraction protocol and the Phos-tag™ concentration in the acrylamide gel, in order to detect MYB75 and its phosphorylated forms.

I had originally planned to conduct a number of experiments, together with Dr. Liu, to demonstrate that MYB75 was phosphorylated as a result of activation of MPK3, MPK4 and MPK6 by upstream MKK enzymes *in vivo.* To this end, I crossed my *35Spr:MYB75^{WT}gene* plants, into *DEXpr:CAMKK6* and *DEXpr:CAMKK9*, *Arabidopsis* lines, previously established and characterized in the Ellis lab. These constitutively active but conditionally expressed MKKs have the ability to activate a specific subset of MAP kinases: CAMKK6 can activate MPK4 and MPK6 while CAMKK9 specifically activates MPK6 (Lee *et al*., 2008) My plan was to induce CAMKK expression in successfully crossed progeny (*35Spr:MYB75^{WT}X DEXpr:CAMKK6)* using dexamethasone, and look for a correlation between the activation of specific MAP kinases and increased phosphorylation of MYB75, using phospho-p44/42 antibodies to detect any activated MPKs, and Phos-tag™ acrylamide gel to detect MYB75 phosphorylation. Unfortunately, due to lack of time and resources I never managed to optimize this protocol, as describing the

phenotypes of *35Spr:MYB75 gene* lines became the main focus of my project and took priority over other experiments.

When determining which MPKs can phosphorylate MYB75 *in vitro* our lab chose to focus on the MAP kinases whose function is most widely discussed in the literature and therefore best defined: this includes MPK3, MPK4, and MPK6, as well as MPK11, which is a close homologue of MPK4. Some aspects of development which these MPKs regulate are relevant to the developmental changes I observed in different *35Spr:MYB75* phosphovariant plants, and many of these developmental processes are also regulated by the hormone auxin. MPK3 and MPK6 participate in leaf development through phosphorylation of another MYB transcription factor, ASSYMETRIC LEAVES 1 (AS1), which regulates adaxial cell fate in developing *Arabidopsis* leaves (Park *et al.,* 2013). MPK6 has also been shown to be involved in embryo, floral and inflorescence development. In *mpk6* mutant plants, a large proportion of the embryos were reported to be protruding out of the seed coat (Bush and Krysan, 2007). In the same publication, the authors rescued *mpk6* null mutants from embryonic defects, by complementation experiments using a YFP-MPK6 fusion protein. However, plants carrying this recombinant version of MPK6 also displayed reduced apical dominance, indicating that YFP interferes with MPK6 function with respect to inflorescence development (Bush and Krysan, 2007). These are only a few examples on the growing list of developmental processes regulated by MAP kinases. However, other MAP kinases which I found to interact with MYB75 in yeast may be of interest, particularly in the context of developmental changes I describe in Chapter 4. For instance, MPK13, which interacts strongly with MYB75 in yeast, is involved in lateral root formation, which is an auxin-regulated process (Zeng *et al.,* 2011). MPK14, another strong

binding partner of MYB75, whose function is not well defined in plants, is activated downstream of ABA signalling (Danquah *et al.,* 2015) which is pertinent to seed dormancy and germination. MAP kinases that display moderate interaction strength with recombinant MYB75 in yeast include MPK6, MPK10, MPK18 and MPK19. A recent publication identified MPK10 as another participant in auxin signalling and vascular development (Stanko *et al.,* 2014). Unlike its close relatives, MPK3 and MPK6, which display broadly distributed expression patterns throughout the plant, MPK10 is transiently expressed in developing seedlings at sites of auxin maxima. In addition, MPK10 promoter activity was observed in veins, consistent with the idea that this gene plays a role in vascular development. Accordingly, *mpk10* mutants, as well as mutants defective in *mkk2*, (required for MPK10 activation) displayed altered venation patterns in cotyledons (Stanko *et al.,* 2014, Fig 4). Most importantly, *mpk10* null mutants were delayed in bolting and flowering (Stanko *et al.,* 2014 Fig 3), similar to our *35Spr:MYB75*^{T131E} lines. This seems somewhat counter-intuitive: if MPK10 regulates flowering transition through MYB75 phosphorylation then MYB75^{T131A} might be expected to display a phenotype similar to *mpk10*. However, it is difficult to draw parallels between the Stanko *et al*., (2014) publication and my data, as our approaches were quite different. For instance, the authors in Stanko *et al.,* (2014) used continuous light, whereas we used a 16h light/8h dark photoperiod, which can impact a number of other factors pertinent to the regulation of flowering time. Furthermore, MPK10 has a very specific expression pattern, whereas the 35S promoter used in my work typically leads to ubiquitous protein expression. I also do not know whether MPK10 can phosphorylate T-126, T-131, or both residues, or how phosphorylation status of T-126 might affect MYB75 function with respect to flowering time. Nevertheless, the late onset of bolting and flowering in *mpk10*

mutants is a promising lead potentially connecting MYB75 and development. The authors in Stanko *et al.,* (2014), concluded that MPK10 participates in localized regulation of polar auxin transport, necessary for proper vein patterning in leaves. A possible model connecting MPK10 to control of auxin flow, is that MPK10 phosphorylates MYB75 at threonine 131, which leads to increased accumulation of flavonols, and localized inhibition of polar auxin transport in certain cells, channeling auxin flow through specific cell files. This is just one example of how the phenotypes I described may help build a connection between a particular MAP kinase and the process it regulates, by looking for parallels among phenotypes observed in different MAP kinase mutants and the phosphovariants of MYB75.

The production of anthocyanins under a wide range of stresses and developmentally regulated processes may help explain why MYB75 appears to bind to so many different MPKs. However, there is another explanation for this apparent promiscuity, one that may broaden our horizons in understanding how MYB75 participates in development and plant biochemistry. A large gap in our understanding of MPK signalling is a lack of plant-specific docking proteins that bridge interactions between different components of the MAP kinase signalling cascades. A recent publication describes the role of MYB44 as a scaffold for the interaction between MKK4 and its targets MPK3 and MPK6, in regulation of response to osmotic stress (Persak and Pitzschke, 2013). Interestingly, this function of MYB44 was affected by phosphorylation status of a specific residue on the MYB44 protein, indicating that this docking function, which regulates MPK signalling, is itself regulated by MPK-mediated phosphorylation. The possibility that MYB75 may also have such a docking function is an enticing one, as it would open the doors to a wider number of possible explanations for the phenotypes we observed in plants

expressing different phosphovariant types. Some informative experiments that could explore this idea would include confirming *in vivo* interaction between MYB75 and the MPKs that displayed interaction with MYB75 in yeast (as noted above), and determining if MYB75 can bind any of the components of the MPK signalling cascade upstream of these MPKs, such as MKK, or MKKKs.

5.3 Protein-protein interactions between MYB75 and known binding partners

The yeast two-hybrid assay that I conducted to determine if protein-protein interactions between MYB75 and its known binding partners are affected by phosphorylation status, at either or both threonines 126 and 131, did not yield results that would indicate that phosphorylation is important for this aspect of MYB75 function. I therefore chose not to repeat the assay *in vivo*. The only exception to this interaction pattern was TCP3, which positively regulates MYB-bHLH-WDR complex formation: interaction between MYB75 and TCP3 was slightly reduced by the T131E mutation, according to my yeast two-hybrid data. I designed an experiment to verify this in protoplasts, using multi-colour BIFC to try to confirm preference of TCP3 for $MYB75^{WT}$ over $MYB75^{T131E}$ (see discussion in Chapter 2 for details). Although I thought this approach to be elegant, it proved to be unsuitable for examining quantitative data, such as comparative interaction strength, because protoplast transformation efficiency is typically too low to be amenable to statistical analysis. Examining the interaction dynamics between MYB75 and TCP3 in plants would require a robust expression system, perhaps using FRET (fluorescent resonance energy transfer). Another option is repeating the multi-colour BIFC assay that I used in protoplasts, in tobacco leaves or *Arabidopsis* seedlings, using *Agrobacterium*-mediated

infiltration of plant tissues, which typically results in higher transformation efficiency than do protoplast assays.

It might also be interesting to determine if complex formation between and bHLH and WDR proteins is affected in MYB75^{T131E} compared to MYB75^{WT} (since TCP3 is a positive regulator of this process). This could be done *in vitro* using a yeast three-hybrid system, analogous to the experiment conducted by Li and Zachgo (2011), in which they examined how TCP3 enhances MYB-bHLH-WDR complex formation. However, before embarking on such experiments it is worth considering whether such a putative change in interaction strength justifies further work: I found that total anthocyanin production, and transcription of core anthocyanin biosynthetic genes was not reduced in *35Spr:MYB75^{T131E}* lines compared to other phosphovariants, indicating that, at least in plants overexpressing MYB75, TCP3 is not limiting for this process, or that perhaps the reduced interaction strength between TCP3 and MYB75^{T131E} is not significant enough to affect anthocyanin biosynthesis under the conditions employed in our study.

5.4 MYB75 protein turnover

The data described in Chapter 2 and 3 suggest that phosphomimic MYB75^{T131E} is degraded more rapidly than MYB75^{WT}, and that this susceptibility to degradation is not dependent on the interaction of MYB75 with COP1/SPA ubiquitin ligase complexes. As described in Chapter 2, protein turnover can be a part of a general protein recycling mechanism or be a very target-specific process. Although we cannot exclude the possibility that MYB75^{T131E} is generally less stable than its unmodified progenitor, I suspect that there is a specific degradation pathway that results in turnover of MYB75 when it is phosphorylated at threonine

131. My rationale for this lies in our global gene expression analysis (Chapter 4), that indicate that MYB75^{T131E} is a far more potent regulator of gene expression than MYB75^{T131A} (Fig 4.7 and Fig 4.8), and therefore I hypothesize that more rapid degradation of this phosphovariant is a control measure that prevents phosphorylated MYB75 from driving dramatic changes in gene expression that could be detrimental to the plant. To this end, I believe it would be worthwhile to explore the spatial and temporal distribution of each phosphovariant throughout the plant, as I believe that differential distribution of MYB75 protein, depending on its phosphorylation status could play a part in defining the pattern of MYB75 participation in development. Determining how each MYB75 phosphovariant is distributed throughout the plant would require an *in vivo* approach that allows us to track the protein and its variants through development, across different tissues and organs. An ideal experiment would be to create a *MYB75* promoter-gene cassette, for each phosphovariant of interest, fused to the β-glucuronidase (GUS) reporter (*MYB75pr:MYB75 gene:GUS)*, and transform these constructs into the *myb75*$^{-}$ background in the Col-0 ecotype (recently created by Li *et al.,* 2016). One potential challenge in this approach is low germination rate and early seedling mortality in *MYB75pr:MYB75 cDNA* (T131A and T131E) lines, described in Chapter 4 (Fig 4.2). Therefore, this approach may require the use of a truncated version of each phosphovariant, where the transcriptional activation domain of MYB75 (last 58 amino acids at the C-terminus) is removed, to prevent MYB75 from triggering developmental arrest during early stages of development. This approach would allow me to determine how each phosphovariant is distributed throughout the plant (based on GUS reporter distribution), but could also be used to test the impact of different environmental stimuli on protein accumulation in different tissues and

organs. Importantly, this approach addresses not only protein expression, driven by the endogenous promoter, but MYB75 protein distribution, which is dependent on both protein production and turnover.

It is also important to show that the protein degradation story highlighted in Chapters 2 and 3 applies not only to phosphomimic versions of MYB75 but is also reproducible in the context of genuine phosphorylation events. The crosses which I created between my overexpressor lines and plants carrying CAMKK6 or CAMKK9 under control of a DEX-inducible promoter (*35Spr:MYB75 gene X DEXpr:CAMKK*), could be used for this purpose. I would suggest conducting degradation assays comparable to those performed in Chapter 2, but also using these crosses to show that a genuine (at least from a chemical point of view) phosphorylation event can lead to differences in turnover. Additional crosses may be necessary to use as controls; for instance, crossing *35Spr:MYB75*^{T131A} into the *DEXpr:CAMKK* as a non-phosphorylatable negative control, and perhaps integrating modifications of threonine 126 into the story, in order to relate our results to the published data by Li *et al.,* (2016). I would also cross *35Spr:MYB75*^{T126A} and *35Spr:MYB75*$^{T126A/T131A}$ into *DEXpr:CAMKK* lines to determine how each phosphorylation event affects protein stability; again, to reconcile our data with that of Li *et al.,* (2016). These experiments, however, would have to be conducted in conjunction with Phos-tag™ acrylamide gel shift assays, to demonstrate that activation of *CAMKK* transcription upon addition of DEX actually leads to MYB75 phosphorylation. Therefore, this series of experiments would still require optimization as well as additional genetic crosses.

5.5 Impact of MYB75 phosphorylation on expression of downstream genes

MYB75 transcriptional activity and promoter specificity was not explicitly tested in this thesis, because none of the known target genes appeared to be affected by point mutations mimicking different T-131 phosphorylation states. However, our RNA sequencing data suggests that MYB75^{T131E} is a more potent regulator of gene expression on a global scale than is MYB75^{T131A}. A number of approaches could be used to understand how MYB75^{T131E} affects the expression of a specific subset of genes, and how these expression changes might be connected to the particular developmental changes observed in *35Spr:MYB75^{T131E}* plants. These approaches include transcriptional activation experiments in protoplasts, using either a generic promoter to test transcriptional activity of each phosphovariant, or specific promoters, to test the ability of each phosphovariant to drive the expression of particular genes of interest. However, I believe at this stage additional exploratory experiments are required, to help us define a subset of genes that may be targets of MYB75, whose transcription is dependent on MYB75 phosphorylation status. First, we should repeat the global transcriptome analysis performed on *35Spr:MYB75^{T131A}* and *35Spr:MYB75^{T131E}* lines, to corroborate the results depicted in Fig 4.7, and Fig 4.8. From here, we should focus on a subset of genes that appear consistently up- or down-regulated in a specific phosphovariant, or perform a yeast one-hybrid screen, to identify promoters that each phosphovariant can bind *in vitro,* before conducting transcriptional activation assays in protoplasts. Alternatively, existing *35Spr:3xHA:MYB75 gene* lines described in this thesis can be used to conduct a CHIP (chromatin immunoprecipitation) assay, to identify promoters bound by each phosphovariant *in vivo.*

As previously discussed, when considering the impact of a particular phosphovariant on global changes of gene expression we must consider the possibility that MYB75 can potentially have an indirect influence on a wide spectrum of genes. Modulation of auxin flow, through differential control of flavonol biochemical profiles by each phosphovariant is one possible mechanism by which MYB75 could potentially affect different aspects of development and gene expression. To corroborate this model we must first define the exact perturbations in auxin flow (if any) in *35Spr:MYB75* plants expressing different MYB75 phosphovariants. Relating MYB75 phosphorylation status to auxin flow through control of flavonols would require us to have a better understanding how different biochemical species of flavonols are distributed throughout the plant and how each can affect auxin dynamics. Since this field of study is still in its infancy, relating MYB75 phosphorylation status to the distribution of specific flavonol species and consequent changes in auxin flow still represents a major technical challenge.

Another approach to understanding the role of MYB75 phosphorylation in development, involves connecting a particular MPK to MYB75, by looking for analogous phenotypes, such as the flowering delay observed in *mpk10* mutants and *35Spr:MYB75*^{T131E}. This approach can be useful in delineating a pathway from a specific MPK activation event to changes in gene expression driven by phosphorylated MYB75. It would require re-assessing the phenotypes of *35Spr:MYB75* plants and MPK mutants under the same conditions, and creating crosses between *35Spr:MYB75* lines and the MAP kinase mutants, to demonstrate a connection between the MPK in question and MYB75.

Perhaps the biggest question that still needs to be answered is whether the properties of my phosphomimic and phosphonull lines reflect true phosphorylation-related biological events. Would native phosphorylated MYB75 yield biochemical profiles and developmental changes similar to those that I observed in *35Spr:MYB75*^{T131E} plants? This is perhaps the most challenging undertaking. Phosphorylation is generally considered to be a transient event, whereas the developmental phenotypes observed in *35Spr:MYB75* plants were a result of continuous ectopic expression of a particular phosphovariant. I believe the path to uncovering the role of MYB75 phosphorylation in plant biochemistry and development will require a multifaceted approach, that entails understanding how each phosphovariant is distributed throughout the plant, how phosphorylation affects the MYB75 interaction network, and finally how all of these factors affect the subset of genes that MYB75 can regulate when it is in a particular phosphorylation state. Once target genes of interest are identified, we can look for changes in their expression that result from the activation of a particular MAP kinase, correlating this event with MYB75 phosphorylation, thus delineating a pathway from MPK activation to changes in gene expression, through phosphorylation of MYB75. Many of the tools which I highlighted in the text above will be instrumental to conducting these experiments.

5.6 Conclusions

The complexity of plant development and biochemistry stems from the connectivity of these processes. As sessile organisms, plants are immensely dependent on their ability to adjust to changing environments, in coordination with developmental cues. It is not surprising that as we learn more about plant signalling networks we uncover more and more connections between seemingly unrelated pathways. As our understanding of plant genetics and molecular

biology grows, we learn that some genes participate in multiple processes, in different biological contexts. This universality is apparent when looking at GO annotations in TAIR or NCBI and reading publication abstracts for a particular gene; fewer and fewer genes are defined by a single function. This is particularly true for a global regulator like MYB75, initially thought to be only a positive regulator of anthocyanin, and to some extent flavonol biosynthesis, and more recently shown to be a repressor of secondary cell wall biosynthetic genes, acting in concert with KNAT7. It is very possible that MYB75 has additional roles in plants that have not yet been described. Although many questions remain to be answered and many experiments should be refined, I believe my work has significantly broadened our horizons in understanding the role of this transcription factor in the biochemistry and development of *Arabidopsis*, opening doors to new direction for anyone interested in studying this transcriptional regulator.

Finally, some practical applications that are relevant to this project, revolve around understanding how environmental and developmental cues can be used to obtain a desired biochemical outcome. Most laboratory studies examine each stress or stimulus in isolation. However, I believe that understanding the synergy between different environmental and developmental cues is the key to controlling plant biochemistry. For instance, application of continuous light to seedlings overexpressing MYB75 can boost anthocyanin production on soil or ½ MS agar plates, but not on liquid ½ MS, indicating that immersion in liquid media has a negative effect on anthocyanin biosynthesis. Understanding the relationship between each stimulus and a regulator like MYB75 can potentially help us modify plant biochemistry in a directed manner without the use of genetically modified organisms (GMOs). The field of study of how microenvironmental factors affect plant biochemistry is becoming an active research

topic in sustainable agriculture. These principles are being applied in forest farming of medicinal plants (Gallespie *et al.,* 2006), and other agricultural models that are coming to the forefront with the need for sustainable farming practices (reviewed in Pretty, 2008).

References

1. Abdel-Lateif K., Bogusz D., Hocher V., (2012). The role of flavonoids in establishment of plant root endosymbioses with arbuscular micorrhizal fungi, *rhizobia* and *frankia* bacteria. *Plant Signalling and Behaviour.* 7(6):636-641.

2. Al-Sady B., Ni W., Kircher S., Schafer E., Qual P.H., (2006). Photoactivated phytochrome induces rapid PIF3 phosphorylation prior to proteasome-mediated degradation. *Molecular Cell.*23:439-446.

3. Altamura M.M., Possenti M., Matteucci A., Baima S., Ruberti I., Morelli G., (2001). Development of the vascular system in the inflorescence stem of *Arabidopsis. New Phytologist.* 151:381-389.

4. Andreasson E., Jenkins T., Brodersen P., Thorgrimsen S., Petersen N.H.T., Zhu S., Qiu J-L., Pernille Micheelsen P., Rocher A., Morten Petersen M., Mari-Anne Newman M-A., Nielsen H.B., Hirt H., Somssich I., Mattsson O., Mundy J., (2005). The MAP kinase substrate MKS1 is a regulator of plant defense responses. *The EMBO Journal.* 24:2579-2589.

5. Appella E. and Anderson C.W., (2001). Post-translational modifications and activation of p53 by genotoxic stresses. *European Journal of Biochemistry.* 268:2764–2772.

6. Araújo W.L., Tohge T., Ishizaki K., Leaver C.J., Fernie A.R., (2011). Protein degradation-an alternative respiratory substrate for stressed plants. *Trends in Plant Science.* 16(9):489-498.

7. Arsovski A.A., Galstyan A., Guseman J.M., Nemhauser J.L., (2012). Photomorphogenesis. *The Arabidopsis Book.* January 31. doi: 10.1199/tab.0147

8. Asada K., (2006). Production and scavenging of reactive oxygen species in chloroplasts and their functions. *Plant Physiology.* 141:391-396.

9. Asai T., Tena G., Plotnikova J., Willmann MR., Chiu WL., Gomez-Gomez L., Boller T., Ausubel F.M., Sheen J., (2002). MAP kinase signalling cascade in *Arabidopsis* innate immunity. *Nature.* 415:977–83.

10. Bah A., Vernon R.M., Siddiqui., Krzeminski M., Muhandiran R., Zhao C., Sonenberg N., Kay L.E., Forman-Kay J.D., (2015). Folding of an intrinsically disordered protein by phosphorylation as a regulatory switch. *Nature.* 519:106-109.

11. Barnes S.A., Nishizawa N.K., Quaggio R.B., Whitelam G.C., Chua N-H., (1996). Far-red light blocks greening of *Arabidopsis* seedlings via a phytochrome A-mediated change in plastid development. *The Plant Cell.* 8:601-615.

12. Bailly A., Sovero V., Vincenzetti V., Santelia D., Bartnik D., Koenig B.W., Mancuso S., Martinoia E., Geisler M., (2008). Modulation of P-glycoproteins by auxin transport inhibitors is mediated by interaction with immunophillins. *The Journal of Biological Chemistry.* 283(31):21817-21826.

13. Balazadeh S., Kwasniewski, M., Caldana, C., Mehrnia, M., Zanor, M. I., Xue, G. P., Mueller-Roeber B., (2011). ORS1, an H_2O_2-responsive NAC transcription factor, controls senescence in *Arabidopsis thaliana*. *Molecular Plant.* 4(2):346-360.

14. Baudry A., Heim M.A., Dubreucq B., Caboche M., Weisshar B., Lepiniec L., (2004). TT2, TT8 and TTG1 synergistically specify the expression of BANYULS and proanthocyanidin biosynthesis in *Arabidopsis thaliana. The Plant Journal.* 39:366-380.

15. Baudry A., Caboche M., Lepinec L., (2006). TT8 controls its own expression in a feedback regulation involving TTG1 and homologous MYB and bHLH factors allowing a strong and cell specific accumulation of flavonoids in *Arabidopsis thaliana. The Plant Journal.* 46(5): 768-779.

16. Baudry A., Ito S., Song Y.H., Strait A.A., Kiba T., Lu S., Henriques R., Pruneda-Paz J.L., Chua N.H., Tobin E.M., Kay S.A., Imaizumi T., (2010). F-box protein FKF1 and LPK2 act in concert with ZEITLUPE to control *Arabidopsis* clock progression. *Plant Cell.* 22(3):606-622.

17. Bech-Otschir D. Kraft R., Huang X., Henklein P., Kapelari B., Pollmann C., Dubiel W., (2001). COP9 signalosome specific phosphorylation targets p53 to degradation by the ubiquitin system. *The EMBO Journal.* 20(7):1630–1639.

18. Benjamins R., Quint A., Weijers D., Hooykaas P., Offringa R., (2001). The PINOID protein kinase regulates organ development in *Arabidopsis* by enhancing polar auxin transport. *Development*. 128:4057–4067.

19. Berleth T., and Jürgens G., (1993). The role of the *monopteros* gene in organising the basal region of the *Arabidopsis* embryo. *Development.* 118:575-587.

20. Bessa M., Saville M.K., Watson R.J., (2001). Inhibition of cyclin A/Cdk2 phosphorylation impairs B-Myb transactivation function without affecting interaction with DNA or the CBP coactivator. *Oncogene.* 20:3376-3386.

21. Bhalla U. S., Ram P. T., Iyengar R., (2002). MAP kinase phosphatase as a locus of flexibility in a Mitogen-activated protein kinase signalling network. *Science.* 297:1018-1024.

22. Bhargava A., Mansfield S.D., Hall H.C., Douglas C.J, Ellis B. E., (2010). MYB75 functions in the regulation of secondary cell wall formation in *Arabidopsis* inflorescence stem. *Plant Physiology.* 154:1428-1438.

23. Bhargava A., Ahad A., Wang S., Mansfield D., Haughn G.W., Douglas C.J., Ellis B.E., (2013). The interacting MYB75 and KNAT7 transcription factors modulate secondary cells wall deposition both in stems and seed coat of *Arabidopsis. Planta*. 237:1199-1211.

24. Berendzen K.W., Weiste C., Wanke D., Kilian J., Harter K., Droge-Laser W., (2012). Bioinformatic cis-element analysis performed in *Arabidopsis* and rice disclose bZIP- and MYB-related binding sites in potential AuxRE-coupling elements in auxin-mediated transcription. *BMC Plant Biology.* 12(125). doi: 10.1186/1471-2229-12-125

25. Bernhardt C., Zhao M., Gonzalez A., Lloyd A., Schiefelbein J., (2005). The bHLH genes GL3 and EGL3 participate in an intercellular regulatory circuit that controls cell patterning in the *Arabidopsis* root epidermis. *Development.* 132:291-298.

26. Bolger A.M., Lohse M., Usadel B., (2014). Trimmomatic: a flexible trimmer for illumina sequence data. *Bioinformatics.* 30(15):2114-2120.

27. Boller T., and Felix G., (2009). A renaissance of elicitors: perception of microbe-associated molecular patterns and danger signals by pattern-recognition receptors. *Annual Reviews in Plant Biology.* 60:379–406.

28. Borevitz J.O., Xia Y., Blount J., Dixon R.A., Lamb C., (2000). Activation tagging identifies a conserved MYB regulator of phenylpropanoid biosynthesis. *The Plant Cell.* 12(12):2383 2393.

29. Bouchard R., Bailly A., Blakeslee J. J., Oehring S.C., Vincenzetti V., Lee O. R., Paponov I., Palme K., Mancuso S., Murphy A.S., Schulz B., Geisler M., (2006). Immunophilin-like TWISTED DWARF1 modulates auxin efflux activities of *Arabidopsis* P-glycoproteins. *Journal of Biological Chemistry.* 281:30603-30612.

30. Broekling B.E., Watson R.A., Steinward B., Bush D.R., (2016). Intronic sequence regulates sugar-dependent expression of *Arabidopsis thaliana Production of Anthocyanin Pigment1/MYB75. PLOS One.* 11(6). doi: https://doi.org/10.1371/journal.pone.0156673

31. Brown D.E., Rashotte A.M., Murphy A.S., Normanly J., Tague B.W., Peer W.A., Taiz L., Munday G.L., (2001). Flavonoids act as negative regulators of auxin transport *in vivo* in *Arabidopsis*. *Plant Physiology.* 126:524-535.

32. Buer C.S., Djordjevic M.A., (2009). Architectural phenotypes in the *transparent testa* mutants of *Arabidopsis thaliana. Journal of Experimetnal Botany.* 60(3):751-763.

33. Buer C.S., Kordbacheh F., Truong T.T., Hocart C.H., Djordjevic M.A., (2013). Alterations of flavonoid accumulation patterns in *transparent testa* mutants disturbs auxin transport, gravity responses, and imparts long-term effects on root and shoot architecture. *Planta.* 238:171-189.

34. Bush S.M., and Krysan P.J., (2007). Mutational evidence that the *Arabidopsis* MAP kinase MPK6 is involved in anther, inflorescence, and embryo development. *Journal of Experimental Botany.* 58(8):2181-2191.

35. Carrington J.C., Freed D.D., Leinicke A.J., (1991). Bipartite signal sequence mediates nuclear translocation of the plant potyviral NIa protein. *The Plant Cell.* 3:935-962.

36. Castillon A., Shen H., Huq E., (2007). Phytochrome Interacting Factors: central players in phytochrome-mediated signalling network. *Trends in Plant Science.* 12(11):514-521.

37. Cesi V., Tanno B., Vitali R., Mancini C., Giuffrida M.L., Calabretta B., Raschella G., (2002). Cyclin D1-dependent regulation of B-myb activity in early stages of neuroblastoma differentiation. *Cell Death and Differentiation.* 9:1232-1239.

38. Chandler J.W., and Werr W., (2015). Cytokinin-auxin crosstalk in cell type specification. *Trends in Plant Science.* 20(5):291-300.

39. Chalker-Scott L., (2002). Do Anthocyanins function as osmoregulators in leaf tissues? *Advances in Botanical Research.* 37:104-114.

40. Chang C-S J., Li Y-H., Chen L-T., Chen W-C., Hsieh W-P., Shin J., Jane W-N., Chou S-J., Hu J-M., Somerville S., Wu S-H., (2008). LZF1, a HY5-regulated transcriptional factor, functions in *Arabidopsis* de-etiolation. *The Plant Journal.* 54:205-219.

41. Chapman A., Lindermayr C., Glawisching E., (2016). Expression of antimicrobial peptides under control of camalexin-biosynthetic promoter confers enhanced resistance against *Pseudomonas syringae. Phytochemistry.* 122:76-80.

42. Chapman E.J., and Estelle M., (2009). Mechanism of auxin-regulated gene expression in plants. *Annual Reviews in Genetics.* 43:265-285.

43. Chen D., Xu G., Tang W., Jing Y., Ji Q., Fei Z., Lin R., (2013). Antagonistic basic helix-loop-helix/bZIP transcription factors form transcriptional modules that integrate light and reactive oxygen species signalling in *Arabidopsis. The Plant Cell.* 25:1657-1673.

44. Cheng Y., Dai X., Zhao Y., (2007). Auxin synthesized by the YUCCA flavin monooxygenases is essential for embryogenesis and leaf formation in *Arabidopsis. The Plant Cell.* 19:2430-2439.

45. Chi Y., Yang Y., Zhou Y., Fan B., Yu J-Q., Chen Z., (2013). Protein-protein interactions in the regulation of WRKY transcription factors. 6(2):287-300.

46. Chinchilla D., Zipfel C., Robatzek S., Kemmerling B., Nürnberger T., Jones J.D., Felix G., Boller T., (2007). A flagellin-induced complex of the receptor FLS2 and BAK1 initiates plant defense. *Nature.* 448:497–500.

47. Choi G., Kim J-I., Hong S-W., Shin B., Choi G., Blakeslee J.J., Murphy A.S., Seo Y.W., Kim K., Koh E-J., Song P-S. Lee H., (2005). A possible role for NDPK2 in regulation of auxin-mediated responses for plant growth and development. *Plant Cell Physiology.* 46(8)1246-1254.

48. Christensen S.K., Dagenais N., Chory J., Weigel D., (2000). Regulation of auxin response by the protein kinase PINOID. *Cell*. 100:469–478.

49. Chu B., Zhong R., Soncin F., Stevenson M.A., Calderwood S.K., (1998). Transcriptional activity of heat shock factor 1 at 37°C is repressed through phosphorylation on two distinct serine residues by glycogen synthase kinase 3 and protein kinases Cα and Cζ. *Journal of Biological Chemistry*. 273:18640–18646.

50. Ckurshumova W., Smirnova T., Marcos D., Zayed Y., Berleth T., (2014). Irrepressible *MONOPTEROS/ARF5* promotes *de novo* shoot formation. *New Phytologist.* 204:556-566.

51. Cluis C.P., Mouchel C.F., Hardtke C.S., (2004). The *Arabidopsis* transcription factor HY5 integrates light and hormone signalling pathways. *The Plant Journal.* 38:332-347.

52. Colcombet J., and Hirt H., (2008). Arabidopsis MAPKs: a complex signalling network involved in multiple biological processes. *Biochemistry Journal.* 413:217-226.

53. Cosgrove D.J., (2016). Catalysts of plant cell wall loosening. *F1000 Research.* 5. doi: 10.12688/f1000research.7180.1

54. Craker L.E., and Wetherbee P.J., (1973). Ethylene, light and anthocyanin synthesis. *Plant Physiology.* 51:436-438.

55. Danquah A., Zelicourt A., Boudsocq M., Neubauer J., Frey N.F., Leonhardt N., Pateyron S., Gwinner F., Tamby J-P., Ortiz-Masia D., Marcote M.J., Hirt H., Colcombet J., (2015). Identification and characterization of an ABA-activated MAP kinase cascade in *Arabidopsis thaliana. The Plant Journal.* 82:232-244.

56. Dare.A.P., Schaffer R.J., Lin-Wang K., Allan A.C., Hellens R.P., (2008). Identification of a cis-regulatory element by transient analysis of co-ordinately regulated genes. *Plant Methods*. 4(17). doi: 10.1186/1746-4811-4-17

57. D'Auria J. C., and Gershenzon J., (2005). The secondary metabolism of *Arabidopsis thaliana*: growing like a weed. *Current Opinion in Plant Biology.* 8(3):308-316.

58. Deal R.B., Topp C.N., McKinney E.C., Meagher R.B., (2007). Repression of flowering in *Arabidopsis* requires activation of *FLOWERING LOCUS C* expression by histone variant H2A.Z. *The Plant Cell.* 19:74-83.

59. Del Pozo O., Pedley KF., Martin G.B., (2004). MAPKKK alpha is a positive regulator of cell death associated with both plant immunity and disease. *EMBO Journal.* 23:3072–3082.

60. Deng W., Fang X., Wu J., (1997). Flavonoids function as antioxidants by scavenging reactive oxygen species or by chelating iron? *Radiation Physics and Chemistry.* 50(3):271-276.

61. Doughty J., Aljabri M., Scott R.J., (2014). Flavonoids and the regulation of seed size in *Arabidopsis. Biochemical Society Transactions.* 42(2):364-369.

62. Dubos C., Le Gourrierec J., Baudry A., Huep G., Lanet E., Debeaujon I., Routaboul J.M., Alboresi A, Weisshaar B, Lepiniec L., (2008). MYBL2 is a new regulator of flavonoid biosynthesis in *Arabidopsis thaliana. Plant Journal*. 55:940–53.

63. Doyle M.R.M., Davis S.J., Bastow R.M., McWatters H.G., Kozma-Bognar L., Nagy F., Millar A.J., Amasino M., (2002). The *ELF4* gene controls circadian rhythms and flowering time in *Arabidopsis thaliana. Nature.* 419:74-77.

64. Dubos C., Stracke R., Grotewold E., Weisshaar B., Martin C., Lepiniec L., (2010). MYB transcription factors in *Arabidopsis*. *Trends in Plant Science.* 15(10):573-581.

65. Endt D.V., Kiljne J.W., Memelink J., (2002). Transcription factors controlling plant secondary metabolism: what regulates the regulators? *Phytochemistry.* 61:107-114.

66. Evrard A., Kumar M., Lecourieux D., Lucks J., Koskull-Döring P.V., Hirt H., (2013). Regulation of the heat stress response in *Arabidopsis* by MPK6-targeted phosphorylation of the heat stress factor HsfA2. *Peer Journal.* doi: 10.7717/peerj.59

67. Fabregas N., Foermosa-Jordan P., Confraria A., Siligato R., Alonso J.M., Swarup R., Bennett M.J., Mahönen A.P., Caño-Delgado A.I., Ibañes M., (2015). Auxin influx carriers control vascular patterning and xylem differentiation in *Arabidopsis thaliana. PLOS Genetics.* 11(4). doi: 10.1371/ journal.pgen.1005183

68. Feldbrugge M., Sprenger M., Hahlbrock K., Weisshaar B., (1997). PcMYB1, a novel plant protein containing a DNA-binding domain with one MYB repeat, interacts in-vivo with a light-regulatory promoter. *The Plant Journal.* 11(5):1079-1093.

69. Feng J., Meyer C.A., Wang Q., Liu J.S., Liu X.S., Zhang Y., (2012). GFOLD: a generalized fold change for ranking differentially expressed genes from RNA-seq data. *Bioinformatics.* 28(21):2782-2788.

70. Field S.T., Lee D.W., Holbrook M.N., (2001). Why leaves turn red in autumn. The role of anthocyanins in senescing leaves of red-osier dogwood. *Plant Physiology.* 127: 566-574.

71. Fraser C.M., Thompson M.G., Shirley, A.M., Ralph, J., Schoenherr, J.A., Sinlapadech T., Hall, M.C., Chapple, C., (2007). Related Arabidopsis serine carboxypeptidase-like sinapoylglucose acyltransferases display distinct but overlapping substrate specificities. *Plant Physiology*. 144:1986–1999.

72. Fraser C.M., and Chapple C., (2011). The phenylpropanoid pathway in *Arabidopsis. The Arabidopsis Book.* American society of plant biologists. e0152. doi: 10.1199/tab.0152

73. Friml J., Vieten A., Sauer M., Weijers D., Schwarz H., Hamann T., Offringa R., Jurgens, G., (2003). Efflux-dependent auxin gradients establish the apical-basal axis of Arabidopsis. *Nature*. 426:147–153.

74. Friml J., Yang X., Michniewicz M., Weijers D., Quint A., Tietz O., Benjamins R., Ouwerkerk P.B., Ljung K., Sandberg G., Hooykaas P.J., Palme K., Offringa R., (2004). A PINOID-dependent binary switch in apicalbasal PIN polar targeting directs auxin efflux. *Science.* 306: 862–865.

75. Fujiki Y., Yoshikawa Y., Sato T., Inada N., Ito M., Nishida I., Watanabe A., (2001). Dark-inducible genes from *Arabidopsis* thaliana are associated with leaf senescence and repressed by sugars. *Physiologia Plantarum.* 111(3):345-352.

76. Fukuda H., (2004). Signals that control plant vascular cell differentiation. *Nature Reviews Molecular Cell Biology.* 5:379-391.

77. Galiullina R.A., Kasperkiewicz P., Chechkova N.C., Szalek A., Serebryakova M.V., Poreba M., Drag M., Vartapetian A.B., (2015). Substrate specificity and possible heterologous targets of phytaspase, a plant cell death protease. *The Journal of Biological Chemistry.* 290(41):24806-24815.

78. Gallespie A.R., Yu C.K., Tathfon R., Seifert J.R., (2006). Microenvironments for forest-farming of medicinal herbs in varying forest structures of the Midwestern USA. *Journal of Sustainable Agriculture.* 27(4):71-96.

79. Gangappa S.N., and Botto J.F., (2016). The multifaceted role of HY5 in growth and development. *Molecular Plant.* 9:1353-1369.

80. Gälweiler L., Guan C., Müller A., Wisman E., Mendgen K., Yephpremov A., Palme K., (1998). Regulation of polar auxin transport by AtPIN1 in *Arabidopsis* vascular tissue. *Science.* 282:2226-2230.

81. Gomez-Gomez L., and Boller T., (2000). FLS2: An LRR receptor–like kinase involved in the perception of the bacterial elicitor flagellin in *Arabidopsis*. *Molecular Cell*. 5:1003–1011.

82. González Besteiro M.A., Barterls S., Albert A., Ulm R., (2011). *Arabidopsis* MAP kinase phosphatise1 and its targets MAP kinases 3 and 6 antagonistically determine UV-B stress tolerance, independent of the UVR8 photoreceptor pathway. *The Plant Journal.* 68:727-737.

83. Gonzalez A., Zhao M., Leavitt J.M., Lloyd A.M., (2008). Regulation of the anthocyanin biosynthesis pathway by the TTG1/bHLH/MYB transcriptional complex in *Arabidopsis* seedlings. *The Plant Journal.* 53:814-827.

84. Gou J.Y., Felipes, F.F., Liu, C. J., Weigel, D. and Wang, J.W., (2011) Negative regulation of anthocyanin biosynthesis in *Arabidopsis* by a miR156-targeted SPL transcription factor. *Plant Cell*. 23:1512–1522.

85. Groban E.S., Narayanan A., Jacobson M., (2006). Conformational changes in protein loops and helices induced by post-translational phosphorylation. *PLOS Computational Biology.* 2(4):238-250.

86. Grotewold E., (2006) The genetics and biochemistry of floral pigments. *Annual Review in Plant Biology.* 57:761-780.

87. Gu Y-Q., and Walling L.L., (2000). Specificity of the wound-induced leucine aminopeptidase (LAP-A) of tomato. *European Journal of Biochemistry.* 267:1178-1187.

88. Gyula P., Shafer E., Nagy F., (2003). Light perception and signalling in higher plants. *Current Opinions in Plant Biology.* 6:446-452.

89. Haga, N., Kato K., Murase M., Araki S., Kubo M., Demura T., Müller I., Voss U., Ito M., (2007). R1R2R3-Myb proteins positively regulate cytokinesis through activation of KNOLLE transcription in *Arabidopsis thaliana*. *Development*. 134:1101–1110.

90. Halliday K.J., Martinez-Garcia J.F., Josse E-M., (2009). Integration of light and auxin signalling. *Cold Spring Harbour Perspectives in Biology.* 1(6): a001586. doi: 10.1101/cshperspect.a001586

91. Hardtke C.S., Gohda K., Osterlund M.T., Oyama T., Okada K., Deng X.W., (2000). HY5 activity in *Arabidopsis* is regulated by phosphorylation in its COP1 binding domain. *European Molecular Biology Organization.* 19(18):4997-5006.

92. Hayama R., and Coupland G., (2003). Shedding light on the circadian clock and photoperiodic flowering. *Current Opinion in Plant Biology.* 6:13-19.

93. Heinrich M., Baldwin I.T., Wu J., (2011). Two mitogen-activated protein kinase kinases, MKK1 and MEK2, are involved in wounding- and specialist lepidopteran herbivore *Manduca sexta* induced responses in *Nicotiana attenuata*. *Journal of Experimental Botany.* doi: 10.1093/jxb/err162

94. Heisler M.G., Ohno C., Das P., Sieber P., Reddy G.V., Long J.A., Meyerowitz E.M., (2005). Pattern of auxin transport and gene expression during primordium development revealed by live imaging of the *Arabidopsis* inflorescence meristem. *Current Biology.* 15: 1899-1911.

95. Hicks G.R. and Raikhel N.V., (1993). Specific binding of nuclear localization sequence to plant nuclei. *The Plant Cell.* 5:983-994.

96. Hills A.C., Khan S., Lopez-Juez E., (2015). Chloroplast biogenesis-associated nuclear genes: control by plastid signals evolved prior to their regulation as part of photomorphogenesis. *Frontiers in Plant Sciences.* 6(1078):1-13.

97. Hoch W. A., Zeldin E.L., McCown B.H., (2001). Physiological significance of anthocyanins during autumnal leaf senescence. *Tree Physiology*. 21:1-8.

98. Hoch W.A., Singsaas E.L., McCown B.H., (2003). Resorption protection. Anthocyanins facilitate nutrient recovery in autumn by shielding leaves from potentially damaging light levels. *Plant Physiology.* 133:1296-1305.

99. Holmberg C.I., Hietakangas V., Mikhailov A., Rantanen J.O., Kallio M., Meinander A., Hellman J., Morrice N., MacKintosh C., Morimoto R.I., Eriksson J.E., Sistonen L., (2001). Phosphorylation of serine 230 promotes inducible transcriptional activity of heat shock factor 1. *The EMBO Journal*. 20(14):3800–3810.

100. Holmberg C.I., Tran S.E.F., Eriksson J.E., Sistonen L., (2002). Multisite phosphorylation provides sophisticated regulation of transcription factors. *Trends in Biochemical Sciences.* 27(12):619-627.

101. Hübner S., Smith H.M.S., Hu W., Chan C.K., Rihs H-P., Paschall B.M., Raikhel N.V., Jans D.A., (1999). Plant importin α binds nuclear localization sequences with high affinity and can mediate nuclear import independent of importin ß. *The Journal of Biological Chemistry.* 274(32):22610-22617.

102. Huq E., Al-Sady B., Hudson M., Kim C., Apel K., Quail P.H., (2004). PHYTOCHROME-INTERACTING FACTOR 1 is a critical bHLH regulator of chlorophyll biosynthesis. *Science.* 305(5692):1937-1941.

103. Ibañes M., Fabregas N., Chory J., Caño-Delgado., (2009). Brassinosteroid signalling and auxin transport are required to establish the periodic pattern of *Arabidopsis* shoot vascular bundles. *Proceedings of the National Academy of Science.* 106(32):13630-13635.

104. Ichimura K., Shinozaki K., Tena G., Sheen J., Henry Y., Champion A., Kreis M., Zhang S., Hirt H., Wilson C., Heberle-Bors E., Ellis B.E., Morris P.C., Innes R.W., Ecker J.R., Scheel D., Klessig D.F., Machida Y., Mundy J., Ohashi Y., Walker J.C., (2002). Mitogen-activated protein kinase cascades in plants:a new nomenclature. *Trends in Plant Science.* 7(7):301-308.

105. Ishida T., Hattori S., Sano R., Inoue K., Shirano Y., Hayashi H., Shibata D., Sato S., Kato T., Tabata S., Okada K., Wada T., (2007). *Arabidopsis TRANSPARENT TESTA GLABRA2* is directly regulated by R2R3 MYB transcription factors and is involved in regulation of GLABRA2 transcription in epidermal differentiation. *The Plant Cell.* 19:2531-2543.

106. Ishikura N., (1973). The changes in anthocyanin and chlorophyll content during the autumnal reddening of leaves. *Kumamoto Journal of Science.* 2:43–50.

107. Ishimara N., and Yoshioka H., (2012). Post-translational regulation of WRKY transcription factors in plant immunity. *Current Opinion in Plant Biology.* 15:431-437.

108. Ito M., Araki S., Matsunaga S., Itoh T., Nishihama R., Machida Y., Doonan J.H., Watanabe A., (2001). G2/M-phase-specific transcription during the plant cell cycle is mediated by c-Myb-Like transcription factors. *The Plant Cell.* 13:1891-1905.

109. Izumi M., Hidema J., Makino A., Ishida H., (2013). Autophagy contributes to night time energy availability for growth in *Arabidopsis. Plant Physiology.* 161: 1682-1693.

110. Jeon J., Cho C., Lee M.R., Binh N.V., Kim J., (2016). Cytokinin Response Factor2 (CRF2) and CRF3 regulate lateral root development and response to cold stress in *Arabidopsis. The Plant Cell.* 28:1828–1843.

111. Jeong S-W., Das P.K., Jeoung S. C., Song J-Y., Lee H.K., Kim Y-K., Kim W.J., Park Y.I., Yoo S-D., Choi S-B., Choi G., Park Y-I., (2010). Ethylene suppression of sugar-induced anthocyanin pigmentation in *Arabidopsis. Plant Physiology.* 154:1514-1531.

112. Johnson C.S., Kolevski B., Smyth D.R., (2002). *TRANSPARENT TESTA GLABRA2*, a trichome and seed coat development gene of *Arabidopsis,* encodes a WRKY transcription factor. *The Plant Cell.* 14:1359-1375.

113. Johnson K.L., Jones B.J., Basic A., Schultz C., (2003). The fasciclin-like arabinogalactan proteins of *Arabidopsis.* A multigene family of putative cell adhesion molecules. *Plant Physiology.* 133:1911-1925.

114. Johnson K.L., Kibble N.A.j., Basic A., Schultz C.J., (2011). A fasciclin-like arabinogalactan-protein (FLA) mutant of *Arabidopsis thaliana, fla1,* shows defects in shoot regeneration. *PLOS ONE.* 6(9): e25154. doi: 10.1371/journal.pone.0025154

115. Johnson L.N., (2009). The regulation of protein phosphorylation. *Biochemical Society Transactions.* 37:627-641.

116. Jonak C., Nakagami H., Hirt H., (2004). Heavy metal stress activation of distinct mitogen-activated protein kinase pathways by copper and cadmium1. *Plant Physiology.* 136:3276-3283.

117. Jones D.C., Zheng W., Huang S., Du C., Zhaoe X., Yennamalli R.M., Sen T.Z. Nettleton D., Wurtele E.S., Li L., (2016). A clade-specific Arabidopsis gene connects primary metabolism and senescence. *Frontiers in Plant Science.* doi: https://doi.org/10.3389/fpls.2016.00983

118. Jones J.D, and Dangl J.L., (2006). The plant immune system. *Nature* 444:323–29.

119. Jones P., Messner B., Nakajima J., Schaffner A.R., Saito K., (2003). UGT73C6 and UGT78D1, glycosyltransferases involved in flavonol glycoside biosynthesis in *Arabidopsis thaliana. Journal of Biological Chemistry.* 278:43910-43918.

120. Kanaoka M.M., Pillitteri L.J., Fujii H., Yoshida Y., Bogenschutz N.L., Takabayashi J., Zhu J-K., Torii K.U., (2008). SCREAM/ICE1 and SCREAM2 specify three cell-state transitional steps leading to *Arabidopsis* stomatal differentiation. *Plant Cell.* 20:1775–85.

121. Kato Y., and Sakamoto W., (2014). Phosphorylation of photosystem II core proteins prevents undesirable cleavage of D1 and contributes to the fine-tuned repair of photosystem II. *The Plant Journal.* 79:312-321.

122. Khanna R., Kikis E.A., Quail P.H., (2003). *EARLY FLOWERING* 4 functions in phytochrome B-regulated seedling de-etiolation. *Plant Physiology.* 133:1530-1538.

123. Kim W-Y., Fujiwara S., Suh S-S., Kim J., Kim Y., Han L., Karine D., Putterill J., Nam H.G., Somers D.E., (2007). ZEITLUPE is a circadian photoreceptor stabilized by GIGANTEA in blue light. *Nature.* 499:356-360.

124. Kindren P., Noren L., Lopez J.D.B., Shaikhali J., Strand A., (2012). Interplay between HEAT SHOCK PROTEIN 90 and HY5 controls PhANG expression in response to GUN5 plastid signal. *Molecular Plant.* 5(4):901-913.

125. Kliebenstein D.J., (2004). Secondary metabolites and plant/environment interactions: a view through *Arabidopsis thaliana* tinged glasses. *Plant Cell & Environment.* 27(6):675-684.

126. Klein A.P., Anarat-Cappillino G., Sattely E.S., (2013). Minimum set of cytochromes P450 for reconstituting the biosynthesis of camalexin, a major *Arabidopsis* antibiotic. *Angewandte Chemie.* 52(51):13625-13628.

127. Kohchi T., Mokougawa K., Frankenberg N., Musada M., Yokota A., Lagarias J.C., (2001). The *Arabidopsis* HY2 gene encodes phytochromobilin synthase, a ferredoxin-dependent biliverdin reductase. *The Plant Cell.* 13:425-436.

128. Kosugi S., Hasebe M., Matsumura N., Takashima H., Miyamoto-Sato E., Tomita M., Yanagawa H., (2009). Six classes of nuclear localization signals specific to different binding grooves of importin α. *The Journal of Biological Chemistry.* 284(1):478-485.

129. Kovinich N., Kayanja G., Chanoca A., Riedl K., Ostegui M.S., Grotewold E. (2014). Not all anthocyanins are born equal: distinct patterns induced by stress in *Arabidopsis. Planta.* 240:931-940.

130. Kovtun Y., Chiu W.L., Tena G., Sheen J., (2000). Functional analysis of oxidative stress-activated mitogen activated protein kinase cascade in plants. *Proceeding of National Academy of Science.* 97:2940–45.

131. Krecek P., Skupa P., Libus J., Naramoto S., Tejos R. Friml J., Zazimalova E., (2009). The PIN-formed protein family of auxin transporters. *Genome Biology.* 10(12):249. doi: 10.1186/gb-2009-10-12-249

132. Kubo M., Udagawa M., Nishikubo N., Horiguchi G., Yamaguchi M., Ito J., Mimura T., Fukuda H., Demura T., (2005). Transcription switches for protoxylem and metaxylem vessel formation. *Genes & Development.* 19:1855-1860.

133. Kuhn B.M., Errafi S., Bucher R., Dobrev P., Geisler M., Bigler L., Zazimalova E., Ringli C., (2016). 7-Rhamnosylated flavonols modulate homeostasis of the plant hormone auxin and affect plant development. *The Journal of Biological Chemistry.* 291: 5385-53-95.

134. Kumar S., and Pandey A.K., (2013). Chemistry and biological activities of flavonoids: an overview. *The Scientific World Journal.* doi: http://dx.doi.org/10.1155/2013/162750

135. Lampard G.R., Macalister C.A., Bergmann D.C., (2008). *Arabidopsis* stomatal initiation is controlled by MAPK-mediated regulation of the bHLH SPEECHLESS. *Science.* 322:1113–1116.

136. Lange A., Mills R.E., Lange C.J., Stewart M., Devine S.E., Corbett A.H., (2006). Classical Nuclear Localization Signals: definition, function and interaction with importin-α. *Journal of Biological Chemistry.* 282(8):5101-5105.

137. Laxa M., (2017). Intron-mediated enhancement: a tool for heterologous gene expression in plants? *Frontiers in Plant Science.* 7(1977). doi: 10.3389/fpls.2016.01977

138. Lee H., (2015). Mitogen-activated protein kinase kinase 3 is required for regulation during dark-light transition. *Molecular Cell.* 38(7):651-656.

139. Lee J.S., and Ellis B.E., (2007). *Arabidopsis* MAPK Phosphatase 2 (MPK2) positively regulates oxidative stress tolerance and inactivates MPK3 and MPK6 MAPKs. *Journal of Biological Chemistry.* 282(34):25020-25029.

140. Lee J.S., Huh K.W., Bhargava A., Ellis B.E., (2008). Comprehensive analysis of protein-protein interactions between *Arabidopsis* MAPKs and MAPK kinases helps define potential MAPK signalling modules. *Plant Signaling and Behaviour.* 3(12):1037-1041.

141. Lee K., Song E.H., Kim H.S., Yoo J.H., Han H.J., Jung S.M., Lee S.M., Kim K.E., Kim M.C., Cho M.J., Chung W.S., (2008). Regulation of MAPK phosphatase 1 (AtMKP1) by calmodulin in *Arabidopsis*. *Journal of Biological Chemistry.* 283:23581–23588.

142. Leivar P., and Monte E., (2014). PIFs: systems integrators in plant development. *The Plant Cell.* 26:56–78.

143. Leoni C., Pietrzykowska M., Kiss A. Z., Suorsa M., Ceci L R., Aro E-M., Jansson S., (2013). Very rapid phosphorylation kinetics suggest a unique role for Lhcb2 during state transition in *Arabidopsis. The Plant Journal.* 76:236-246.

144. Li E., Bhargava A., Qiang W., Friedmann M.C., Forniers N., Savidge R.A., Johnson L.A., Mansfield S.D., Ellis B.E., Douglas C.J., (2012). The Class II KNOX gene KNAT7 negatively regulates secondary wall formation in *Arabidopsis* and is functionally conserved in *Populus. New Phytologist.* 194(1):102-115.

145. Li F., and Vierstra R.D., (2012). Autophagy: a multifaceted intracellular system for bulk and selective recycling. *Trends in Plant Science.* 17(9):526-537.

146. Li J., Li G., Wang H., Deng X-W., (2011). Phytochrome signalling mechanisms. *The Arabidopsis Book.* doi: 10.1199/tab.0148

147. Li Q.F., and He J.X., (2016). BZR1 interacts with HY5 to mediate brassinosteroid-and light-regulated cotyledon opening in *Arabidopsis* in darkness. *Molecular Plant.* 4(9)113-125.

148. Li S., and Zachgo S., (2013). TCP3 interacts with R2R3-MYB proteins, promotes flavonoid biosynthesis and negatively regulates the auxin response in *Arabidopsis thaliana*. *The Plant Journal.* 76:901-913.

149. Li S., Wang W., Gao J., Yin K., Wang R., Wang C., Petersen M., Mundy J., Qiu J-L., (2016). MYB75 phosphorylation by MPK4 is required for light-induced anthocyanin accumulation in *Arabidopsis. The Plant Cell.* 28:2866-2883.

150. Liepman A.H., Wilkerson C.G., Keegstra K., (2005). Expression of cellulose synthase-like (Csl) genes in insect cells reveals CslA family members encode mannan synthases. *Proceedings of the National Academy of Science.* 102(6)2221-2226.

151. Liepman A.H., Cavalier D.M., (2012). The CELLULOSE SYNTHASE-LIKE A and CELLULOSE-SYNTHASE-LIKE C families: recent advances and future perspectives. *Frontiers in Plant Sciences.* 3(109). doi: 10.3389/fpls.2012.00109

152. Lim E-K., Ashford D.A., Hou B., Jackson R.G., Bowles D.J., (2004). *Arabidopsis* glycosyltransferases as biocatalysts in fermentation of regioselective synthesis of diverse quercetin glycosides. *Biotechnology and Bioengineering.* 87(5):623-631.

153. Lin C., (2002). Blue light receptors and signal transduction. *The Plant Cell.* S207-S225.

154. Liu H., Liu B., Zhao C., Pepper M., Lin C., (2011). The action mechanisms of plant cryptochromes. *National Institute of Health.* 16(2):684-691.

155. Liu Y., and He C., (2017). A review of redox signalling and the control of MAP kinase pathway in plants. *Redox Biology.* 11:192-204.

156. Luo J., Nishiyama Y., Fuell C., Taguchi G., Elliott K., Hill L., Tanaka Y., Kitayama M., Yamazaki M., Bailey P., Parr A., Michael A.J., Saito K., Martin C., (2007). Convergent evolution of BAHD family of acyl transferases: identification and characterization of anthocyanin acyl transferases from *Arabidopsis thaliana. The Plant Journal.* 50:678-695.

157. MacAlister C.A., Ohashi-Ito K., Bergmann D.C., (2007). Transcription factor control of asymmetric cell divisions that establish the stomatal lineage. *Nature.* 445:537–40.

158. Maier A., Schrader A., Kokkelink L., Flake C., Welter B., Iniesto E., Rubio V., Uhrig J.F., Hulskamp M., Hoeker U., (2013). Light and the E3 ubiquitin ligase COP1/SPA control the protein stability of MYB transcription factors PAP1 and PAP2 involved in anthocyanin accumulation in *Arabidopsis*. *The Plant Journal. 74:638-651.*

159. Mattsson J., Ckurshumova W., Berleth T., (2003). Auxin signalling in *Arabidopsis* leaf vascular development. *Plant Physiology.* 131:1337-1329.

160. McGonigle B., Bouhidel K., Irish V.F., (2017). Nuclear localization of *Arabidopsis* APETALA3 and PISTILLATA homeotic gene products depends on their simultaneous expression. *Genes and Development.* 10:1812-1821

161. Mehrtens F., Kranz H., Bednarek P., Weisshaar B., (2005). The *Arabidopsis* transcription factor MYB12 is a flavonol-specific regulator of phenylpropanoid. *Plant Physiology.* 138:1083-1096.

162. Menke F.L.H., Kang H-G., Chen Z., Park J.M., Kumar D., Klessig D.F., (2005). Tobacco transcription factor WRKY1 is phosphorylated by the MAP kinase SIPK and mediates HR-like cell death in Tobacco. *Molecular Plant-Microbe Interactions.* 18(10):1027-1034.

163. Meshi T., and Iwabuchi M., (1995). Plant transcription factors. *Plant Cell Physiology.* 36(8):1405-1420.

164. Michniewicz M., Zago M.K., Abas L., Weijers D., Schweighofer A., Meskiene I., Heisler, M.G., Ohno C., Zhang J., Huang F., Schwab R., Weigel D., (2007). Antagonistic regulation of PIN phosphorylation by PP2A and PINOID directs auxin flux. *Cell*. 130:1044-1056.

165. Miglarese M.R., Richardson A.F., Aziz N., Bender T.P., (1996). Differential regulation of c-Myb-induced transcription activation by a phosphorylation site in the negative regulatory domain. *The Journal of Biological Chemistry.* 271(37):22697-22705.

166. Miles G.P., Samuel M.A., Ranish J.A., Donohoe S.M., Sperrazzo G.M., Ellis B.E., (2009). Quantitative proteomics identified oxidant-induced AtMPK6-dependednt changes in *Arabidopsis thaliana* protein profiles. *Plant Signalling & Behavior.* 4(6):497-505.

167. Misyura M., Colasanti J., Rothstein S.J., (2013). Physiological and genetic analysis of *Arabidopsis thaliana* anthocyanin biosynthesis mutants under chronic adverse environmental conditions. *Journal of Experimental Botany.* 64(1):229-240.

168. Mitra P.P., and Loqué D., (2014). Histochemical staining of *Arabidopsis thaliana* secondary cell wall elements. *Journal of Visualized Experiments.* 87. doi: 10.3791/51381

169. Miyahara T., Sakiyama R., Ozeki Y., Sasaki N., (2013). Acyl-glucose-dependent glucosyltransferase catalyzes the final step of anthocyanin formation in *Arabidopsis. Journal of Plant Physiology.* 170(6):619-624.

170. Miyashima S., Sebastian J., Lee J-Y., Helariutta Y., (2013). Stem cell function during plant development. *The EMBO Journal.* 32:178-193.

171. Mizoguchi T., Irie K., Hirayama T., Hayashida N., Yamaguchi-Shinozaki K., Matsumoto K., Shinozaki K., (1996). A gene encoding a mitogen-activated protein kinase kinase kinase is induced simultaneously with genes for a mitogen activated protein kinase and an S6 ribosomal protein kinase by touch, cold, and water stress in *Arabidopsis thaliana*. *Proceedings of National Academy of Science.* 93:765-769.

172. Mochizuki N., Brusslan J.A., Larkin R., Nagatani A., Chory J., (2001). *Arabidopsis genomes uncoupled 5 (GUN5)* mutant reveals the involvement of Mg-chelatase H subunit in plastid-to-nucleus signal transduction. *Proceedings of the National Academy of Sciences.* 98(4):2053-2058.

173. Mokaitis K., and Howell S.H., (2000). Auxin induced mitogenic activated protein kinase (MAPK) activation in *Arabidopsis* seedlings. *The Plant Journal.* 24(6):785-796.

174. Möller B., and Weijers D., (2009). Auxin control of embryo patterning. *Cold Spring Harbor Perspectives in Biology.* 1(5): a001545. doi: 10.1101/cshperspect.a001545

175. Moon J., Parry G., Estelle M., (2004). The ubiquitin proteasome pathway and plant development. *Plant Cell.* 16:3181-3195.

176. Morse A.M., Whetten R.W., Dubos C., Campbell M.M., (2009). Post-translational modification of an R2R3-MYB transcription factor by a MAP kinase during xylem development. *New Phytologist.* 183:1001-1013.

177. Murphy A., Peer W.A., Taiz L., (2000). Regulation of auxin transport by aminopeptidases and endogenous flavonoids. *Planta.* 211:315-324

178. Muzac I., Wang J., Anzellotti D., Zhang H., Ibrahim R.K., (2000). Functional expression of an *Arabidopsis* cDNA clone encoding a flavonol-3'-O-methyltransferase and characterization of gene product. *Archives of Biochemistry and Biophysics.* 375:385-388.

179. Nakagami H., Soukupova H., Schikora A., Zarsky V., Hirt H., (2006). A mitogen-activated protein kinase kinase kinase mediates reactive oxygen species homeostasis in *Arabidopsis*. *Journal of Biological Chemistry.* 281:38697-38704.

180. Nanjo Y., Maruyama K., Yasue H., Yamaguchi-Shinozaki K., Shinozaki K., Komatsu S., (2011). Transcriptional response to flooding stress in roots including hypocotyl in soybean seedlings. *Plant Molecular Biology.* 77:129-144

181. Narsai R., Howell K.A., Miller A.H., O'Toole N., Small I., Whelan J., (2007). Genome-wide analysis of mRNA decay rates and their determinants in *Arabidopsis thaliana. The Plant Cell.* 19:3418-3436.

182. Nelson D.C., Lasswell J., Rogg L.E., Cohen M.A., Bartel B., (2000). *FKF1,* a clock-controlled gene that regulates the transition to flowering in *Arabidopsis. Cell.* 101(3):331-340.

183. Nieminen K.A., Kauppinen L., Helariutta Y., (2004). A weed for wood? *Arabidopsis* as a genetic model for xylem development. *Plant Physiology.* 135:653-659.

184. Nishi H., Hashimoto K., Panchencko A., (2011). Phosphorylation in protein-protein binding: effect on stability and function. *Structure.* 19:1807-1815.

185. Ohashi-Ito K., and Bergmann D.C., (2006). *Arabidopsis* FAMA controls the final proliferation/differentiation switch during stomatal development. *Plant Cell.* 18:2493–505.

186. Oh Il-H., and Reddy E.P., (1999). The MYB gene family in cell growth, differentiation and apoptosis. *Oncogene.* 18:3017-3033.

187. Osterlund M.T., Wei N., Deng X.W., (2000). The roles of photoreceptor systems and the COP1-targeted destabilization of HY5 in light control of *Arabidopsis* seedling Development. *Plant Physiology.* 124:1520-1524.

188. Oyama T., Shimura Y., Okada K., (1997). The *Arabidopsis* HY5 gene encodes a bZIP protein that regulates stimulus-induced development of root and hypocotyl. *Genes and Development.* 11:2983-2995.

189. Pan Y., Michael T.P., Hudson M.E., Kay S.A., Chory J., Schuler M.A., (2009). Cytochrome P450 monooxygenases as reporters for circadian-regulated pathways. *Plant Physiology.*150:858-878.

190. Park H.C., Han H.J., Lee S.M., Yun D-J. Chung W.S., (2013). ASYMETRIC LEAVES1 is phosphorylated by MPK3/6 in *Arabidopsis thaliana. Journal of Plant Biology.* 56:208-215.

191. Parker G., Schofield R., Sundberg B., Turner S., (2003). Isolation of *COV1*, a gene involved in the regulation of vascular patterning in the stem of *Arabidopsis. Development.* 130: 2139-2148.

192. Pearce A.K., and Humphrey T.C., (2001). Integrating stress response and cell-cycle checkpoint pathways. *Trends in Cell Biology.* 11(10):426-433.

193. Peck S.C., (2006). Analysis of protein phosphorylation: methods and strategies for studying kinases and their substrates. *The Plant Journal.* 45:512-522.

194. Peer W.A., Brown D.E., Tague B.E., Muday G.K., Taiz L., Murphy A.S., (2001). Flavonoid accumulation pattern in *transparent testa* mutants. *Plant Physiology.* 126(2):536-548.

195. Peer W.A., Bandyopadhyay A., Blakeslee J.J., Makam S.N., Chen R.J., Masson P.H., Murphy A.S., (2004). Variation in expression and protein localization of the PIN family of auxin efflux facilitator proteins in flavonoid mutants with altered auxin transport in *Arabidopsis thaliana. The Plant Cell.* 16:1898-1911.

196. Peer W.A., and Murphy A.S., (2007). Flavonoids and auxin transport: modulators or regulators? *Trends in Plant Science.* 12(12):556-563.

197. Pelletier M.K., and Shirley B.W., (1996). Analysis of flavonone 3-hydroxylase in *Arabidopsis* seedlings. *Plant Physiology.* 111:339-345.

198. Petersen M., Brodersen P., Naested, H., Andreasson E., Lindhart U., Johansen B., Nielson H.B., Lacy M., Austin M.J., Parker J.E., Sharma S.B., Klessig D.F., Martienssen R., Mattsson O., Jensen A.B., Mundy J., (2000) *Arabidopsis* map kinase 4 negatively regulates systemic acquired resistance. *Cell.* 103:1111–1120.

199. Persak H., and Pitzschke A., (2013). Tight interconnection and multi-level control of *Arabidopsis* MYB44 in MAPK cascade signalling. *PLOS ONE.* 8(2): e57547.

200. Piskurewicz U., Tureckova V., Lacombe E., Lopez-Molina L., (2009). Far-red light inhibits germination through DELLA-dependent stimulation of ABA synthesis and ABI3 activity. *European Molecular Biology Organization.* 28:2259–2271.

201. Popescu S.C., Popescu G.V., Bachan S., Zhang Z., Gerstein M., Snyder M., Dinesh-Kumar S.P., (2009). MAPK target networks in *Arabidopsis thaliana* revealed using functional protein microarrays. *Genes and Development.* 23:80-92.

202. Pospisil P., (2009). Production of reactive oxygen species by photosystem II. *Biochimica et Biophysica Acta.* 1787:1151-1160.

203. Pretty J., (2008). Agricultural sustainability: concepts, principles and evidence. *Philosophical Transactions of Royal Society.* 363:447-465.

204. Qi T., Song S., Ren Q., Wu D., Hunag H., Chen Y., Fan M., Peng W., Ren C., Xie D., (2011). The Jasmonate-ZIM-Domain proteins interact with the WD-Repeat/bHLH/Myb complex to regulate Jasmonate-mediated anthocyanin accumulation and trichome initiation in *Arabidopsis thaliana*. *The Plant Cell.* 23:1795-1814.

205. Ragni L., and Greb T., (2017). Secondary growth as a determinant for plant shape and form. *Seminars in Cell and Developmental Biology.* doi: http://dx.doi.org/10.1016/j.semcdb.2017.08.050

206. Rajeevkumar S., Anunanthini P., Sathishkumar R., (2015). Epigenetic silencing in transgenic plants. *Frontiers in Plant Science.* 6(693). doi: 10.3389/fpls.2015.00693

207. Rajniak J., Barco B., Clay N.K., Sattely E.S., (2015). A new cyanogenic metabolite in *Arabidopsis* required for inducible pathogen defence. *Nature.* 525(7569):376-379.

208. Raikhel N., (1992). Nuclear targeting in plants. *Plant Physiology.* 100:1627-1632.

209. Ramsay N.A., and Glover B.J., (2005). MYB-bHLH-WD40 protein complex and the evolution of cellular diversity. *Trends in Plant Science.* 10(2):63-70.

210. Ratcliffe O.J., Kumimoto R.W., Wong B.J., Riechmann J.L., (2003). Analysis of the *Arabidopsis MADS AFFECTING FLOWERING* gene family: MAF2 prevents vernalization by short periods of cold *The Plant Cell*. 15:1159-1169.

211. Ranjeva R., and Boudet A.M., (1987). Phosphorylation of proteins in plants: regulatory effects and potential involvement of stimulus/response coupling. *Annual Reviews in Plant Physiology.* 38:73-93.

212. Richter R., Behringer C., Zourelidou M., Schwechheimer., (2013). Convergence of auxin and gibberellins signalling on the regulation of the GATA transcription factors GNC and GNL in *Arabidopsis thaliana. Proceedings of the National Academy of Science.* 110 (32): 13192-13197.

213. Rizhsky L., Liang H., Shuman J., Shulaev V., Davletova S., Mittler R., (2004). When defense pathways collide. The response of *Arabidopsis* to a combination of drought and heat stress. *Plant Physiol.* 134:1683–96.

214. Rizzini L., Favory J-J., Cloix C., Faggionato D., O'Hara A., Kaiserli E., Beaumeister R., Schafer E., Nagy F., Jenkins G.I., Ulm R., (2011). Perception of UV-B by *Arabidopsis* UVR8 protein. *Science.* 332(6025):103-106.

215. Rodriguez M.C.S., Petersen M., Mundy J., (2010). Mitogen-activated protein kinase signalling in plants. *Annual Reviews in Plant Biology*. 61:621–49.

216. Rogers L., Dubos C., Cullis I.F., Surman C., Poole M., Willment J., Mansfield S., Campbell M.M., (2005). Light, the circadian clock and sugar perception in the control of lignin biosynthesis. *Journal of Experimental Botany.* 56(416):1651-1653.

217. Rowan D.D., Cao M., Lin-Wang K., Cooney J.M., Jensen D.J., Austin P.T., Hunt M.B., Norling C., Hellens R.P., Schaffer R.J., Allan A.C., (2009). Environmental regulation of leaf colour in red 35S:PAP1 *Arabidopsis thaliana. New Phytologist.* 182:102-115.

218. Rubin G., Tohge T., Matsuda F., Saito K., Scheible W-R., (2009). Members of the *LBD* family of transcription factors repress anthocyanin synthesis and affect additional nitrogen responses in *Arabidopsis. The Plant Cell.* 21:3567-3584.

219. Ruckle M.E., and Larkin R., (2009). Plastid signals that affect photomorphogenesis in *Arabidopsis thaliana* are dependent on GENOMES UNCOUPLED1 and cryptochrome1. *New Phytologist.* 182:367-379.

220. Ruckle M.E., Burgoon L.D., Lawrence L.A., Christopher A.S., Larkin R.M., (2012). Plastids are major regulators of light signalling in *Arabidopsis. Plant Physiology.* 159:366-390.

221. Sachs T., (1981). The control of the patterned differentiation of vascular tissues. *Advances in Botanical Res*earch. 9:152–262.

222. Sachs T., (2000). Integrating cellular and organismic aspects of vascular differentiation. *Plant Cell Physiology.* 41:649–656.

223. Saijo Y., Sullivan J.A., Wang H., Yang J., Shen Y., Rubio V., Ma L., Hoecker U., Deng X-W., (2003). The COP1–SPA1 interaction defines a critical step in phytochrome A-mediated regulation of HY5 activity. *Genes and Development.* 17:2642–2647.

224. Saito K., Yonekura-Sakakibara K., Nakabayashi R., Higashi Y., Yamazaki M., Tohge T., Fernie A.R., (2013). The flavonoid biosynthetic pathway in *Arabidopsis*: structural and genetic diversity. *Plant Physiology and Biochemistry.* 72:21-34.

225. Saito, S., Goodarzi A.A., Higashimoto Y., Noda Y., Lees-Miller S.P., Apella E., Andershon C.W., (2002). ATM mediates phosphorylation at multiple p53 sites, including Ser(46), in response to ionizing radiation. *Journal of Biological Chemistry.* 277:12491–12494.

226. Samuel M.A., Chaal B.K., Lampard G., Green B.R., Ellis B.E., (2008). Surviving the passage. Non-canonical stromal targeting of an *Arabidopsis* mitogen-activated protein kinase kinase. *Plant signalling & Behavior.* 3(1):6-12.

227. Sandhar H.K., Bimilesh K., Prasher S., Tiwari P., Slhan M., Sharma P., (2011). A review of phytochemistry and pharmacology of flavonoids. *Internationale Pharmaceutica Sciencia.* 11(1):25-41.

228. Santelia D., Henrichs., Vincenzetti V., Sauer M., Bigler L., Klein M., Bailly A., Lee Y., Friml J., Geisler M., Martinoia E., (2008). Flavonoids redirect PIN-mediated polar auxin fluxes during root gravitropic responses. *Journal of Biological Chemistry.* 283(45):31218-31226.

229. Santner A.A., and Watson J.C., (2006). The WAG1 and WAG2 protein kinases negatively regulate root waving in *Arabidopsis*. *Plant Journal.* 45:752–764.

230. Sasaki N., Nishizaki Y., Ozeki Y., Miyahara T., (2014). The role of acyl-glucose in anthocyanin modifications. *Melocules.* 19:18747-18766.

231. Schaller A., (2004). A cut above the rest: the regulatory function of plant proteases. *Planta.* 220:183-197.

232. Schellmann S., and Hulskamp M., (2005). Epidermal differentiation: trichomes in *Arabidopsis* as a model system. *International Journal of Developmental Biology.* 49:579-584.

233. Schepens I., Duek P., Fankhauser C., (2004). Phytochrome-mediated light signalling in *Arabidopsis. Current Opinions in Plant Biology.* 7:1-6.

234. Schmid M., Davison T.S., Henz S.R., Pape U.J., Demar M., Vingron M., Schölkopf B., Weigel D., Lohmann J.U., (2005). A gene expression map *of Arabidopsis thaliana* development. *Nature Genetics*. 37(5):501–506.

235. Schoenbohm C., Martens S., Eder C., Forkmann G., Wesshaar B., (2005). Identification of the *Arabidopsis thaliana* Flavonoid 3'-hydroxylase gene and functional expression of the encoded P450 enzyme. *Biological Chemistry.* 381(8):749-753.

236. Schuetz M., Smith R., Ellis B., (2013). Xylem tissue specification, patterning and differentiation mechanisms. *Journal of Experimental Botany.* 64(1):11-31.

237. Serna L., (2005). Epidermal cell patterning and differentiation throughout apical-basal axis of the seedling. *Journal of Experimental Botany.* 56:1983-1989.

238. Serna L., and Martin C., (2006). Trichomes: different regulatory networks lead to convergent structures. *Trends in Plant Science.* 11:274-280.

239. Sethi V., Ramghuram B., Sinha A. K., Chattopadhyay S., (2014). A mitogen-activated protein kinase cascade module, MKK3-MPK6 and MYC2, is involved in blue light-mediated seedling development in *Arabidopsis. The Plant Cell.* 26:3343-3357.

240. Shan X., Zhang Y., Peng W., Wang Z., Xie D., (2009). Molecular mechanism for jasmonate-induction of anthocyanin accumulation in *Arabidopsis. Journal of Experimental Botany.* 60(13):3849-3860.

241. Shen Y.H., Godlewski J., Bronisz A., Bronisz A., Zhu J., Comb M.J., Avruch J., Tzivion G., (2003). Significance of 14–3–3 self-dimerization for phosphorylation-dependent target binding. *Molecular Biology of the Cell.* 14:4721-4733.

242. Shi M-Z., and Xie D-Y., (2010). Features of anthocyanin biosynthesis in *PAP1-D* and wild –type *Arabidopsis thaliana* grown in different light intensity and culture conditions. *Planta.* 231:1385-1400.

243. Shi Q-M., Yang X., Song Li., Xue H-W., (2011). *Arabidopsis* MSBP1 is activated by HY5 and HYH and is involved in photomorphogenesis and brassinosteroid sensitivity regulation. *Molecular Plant*. 4(6):1092–1104.

244. Shi M-Z., and Xie D-Y., (2014). Biosynthesis and metabolic engineering of anthocyanins in *Arabidopsis thaliana. Recent Patents on Biotechnology.* 8(1):47-60.

245. Shin D.H., Choi M., Kim K., Bang G., Cho M., Choi S-B., Choi G., Park Y-I., (2013). HY5 regulates anthocyanin biosynthesis by inducing transcriptional activation of the MYB75/PAP1 transcription factor in *Arabidopsis. FEBS Letters.* 587(10):1543-1547.

246. Shin J., Park E., Choi G., (2007). PIF3 regulates anthocyanin biosynthesis in an HY5-dependent manner with both factors directly binding anthocyanin biosynthetic gene promoters in *Arabidopsis. Plant Journal.* 49:981–994.

247. Shin J., Anwar M. U., Davis S.J., (2013). Phytochrome-Interacting Factors (PIFs) as bridges between environmental signals and the circadian clock: diurnal regulation of growth and development. *Molecular Plant.* 6(3):592-595.

248. Shu K., Liu X-D., Xie Q., He Z-H., (2016). Two faces of one seed: hormonal regulation of dormancy and germination. *Molecular Plant.* 9:34-45Schulze B., Mentzel T., Jehle A.K., Mueller K., Beeler S., Boller T., Felix G., (2010). Rapid heteromerization and phosphorylation of ligand-activated plant transmembrane receptors and their associated kinase BAK1. *Journal of Biological Chemistry.* 285(13):9444-9451.

249. Simmonds M.S.J., (2003). Flavonoid-insect interactions: recent advances in our knowledge. *Phytochemistry.* 64:21-30.

250. Smith H.M.S., Hicks G.R., Raikhel N.V., (1997). Importin α from *Arabidopsis thaliana* is a nuclear import receptor that recognizes three classes of import signals. *Plant Physiology.* 114:411-417.

251. Smykowski A., Fischer S.M., Zentgraf U., (2015). Phosphorylation affects DNA-binding of the senescence-regulating bZIP transcription factor GBF1. *Plants (Basel).* 4:691-709.

252. Song S.K., Ryu K.H., Kang Y.H., Song J.H., Choo Y.H., Schiefelbein J., Lee M.M., (2011). Cell fate in *Arabidopsis* root epidermis is determined by competition between WEREWOLF and CAPRICE. *Plant Physiology.* 157(3):1196-1208.

253. Srivastava R., Liu J-X., Howell S.H., (2008). Proteolytic processing of a precursor protein for growth-promoting peptide by subtilisin serine protease in *Arabidopsis. The Plant Journal.* 56:219-227.

254. Stanko V., Guiliani C., Retzer K., Djamei A., Wahl V., Wurzinger B., Wilson C., Heberle-Bors E., Teige M., Kragler F., (2014). Timing is everything: highly specific and transient expression of a MAP kinase determines auxin-induced leaf venation patterns in *Arabidopsis. Molecular Plant.* 7(11):11637-1652.

255. Stephenson P.G., Fankhauser C., Terry M.J., (2009). PIF3 is a repressor of chloroplast development. *Proceedings of the National Academy of Science.* 106(18):7654-7659.

256. Steyn W.J., Wand S.J.E., Holcroft D.M., Jacobs G., (2002). Anthocyanin in vegetative tissues: a proposed unified function in photoprotection. *New Phytologist.* 155:349-361.

257. Stracke R., Werber M., Weisshaar B., (2001). The R2R3 gene family in *Arabidopsis thaliana*. *Current Opinions in Plant Biology.* 4:447-456.

258. Stracke R., Ishihara H., Huep G., Mehrtens F., Niehaus K., Weisshaar B., (2007). Differential regulation of closely related R2R3-MYB transcription factors control flavonol accumulation in different parts of the *Arabidopsis thaliana* seedling. *Plant Journal* 50(4):660-677.

259. Susek R.E., Ausubel F.M., and Chory J., (1993). Signal transduction mutants of *Arabidopsis* uncouple nuclear CAB and RBCS gene expression from chloroplast development. *Cell.* 74:787-799.

260. Tamada Y., Yun J-Y., Woo S.C., Amasino R.M., (2009). *Arabidopsis TRITHORAX-RELATED7* is required for methylation of lysine 4 of Histone3 H3 and for transcriptional activation of *FLOWERING LOCUS C. The Plant Cell.* 21:3257-3269

261. Teige M., Scheikl E., Eulgem T., Doczi R., Ichimura K., Shonozaki K., Dangl J.L., Hirt H., (2004). The MKK2 pathway mediates cold and salt stress signalling in *Arabidopsis*. *Molecular Cell.* 15:141–52.

262. Teng S., Keurentjes J., Bentsink L., Koornneef M., Smeekens S., (2005). Sucrose-specific induction of anthocyanin biosynthesis in *Arabidosis* requires *MYB75/PAP1* gene. *Plant Physiology.* 139:1840-1852

263. Tepperman J.M., Hwang Y.S., Quail P.H., (2006). PhyA dominates in transduction of red-light signals to rapidly responding genes at the initiation of *Arabidopsis* seedling de-etiolation. *Plant Journal.* 48:728-742.

264. Tilbrook K., Arongaus A.B., Binkert M., Heijde M., Yin R., Ulm R., (2013). The UVR8 UV-B photoreceptor:perception, signalling and response. *The Arabidopsis Book.* doi: 10.1199/tab.0164

265. Tipathy B.C., and Oelmüller R., (2012). Reactive oxygen species generation and signalling in plants. *Plant Signalling and Behaviour.* 7(12):1621-1633.

266. Tohge T., Nishiyama Y., Yokota Hirai M., Yano M., Nakajima J-I., Awazuhara M., Inoue E., Takahashi H., Goodenowe D.B., Kitayama M., Noji M., Yamazaki M., Saito K., (2005). Functional genomics by integrated analysis of metabolome and transcriptome of *Arabidopsis* plants over-expressing a MYB transcription factor. *The Plant Journal.* 42:218-235.

267. Tohge T., Watanabe M., Hoefgen R., Fernie A.R., (2013). The evolution of phenylpropanoid metabolism in green lineage. *Critical Reviews in Biochemistry and Molecular Biology.* 48(2):123-152.

268. Van der Hoorn R.A.L., (2008). Plant proteases: from phenotypes to molecular mechanisms. *Annual Reviews in Plant Biology.* 59:191-223.

269. Varagona M.J., Schmidt R.J., Raikhel N.V., (1992). Nuclear localization signal(s) required for nuclear targeting of maize regulator protein Opaque-2. *The Plant Cell.* 4:1213-1227.

270. Verweij W., Spelt C.E., Bliek M., Vries M., Wit N., Faraco M., Koes R., Quattrocchio F.M., (2016). Functionally similar WRKY proteins regulate vacuolar acidification in *Petunia* and hair development in *Arabidopsis. The Plant Cell*. 28:786-803.

271. Vierstra R.D., (2009). The ubiquitin-26S proteasome system at the nexus of plant biology. *Nature Reviews in Molecular and Cell Biology.* 10:385-397.

272. Vogel M.O., Moore M., Könog K., Pecher P., Alsharafa K., Lee J., Dietz K-J., (2014). Fast retrograde signalling in response to high light involves metabolite export, MITOGEN-ACTIVATED PROTEIN KINASE 6 and AP2/ERF transcription factors in *Arabidopsis. The Plant Cell.* 26:1151-1165.

273. Vogt T., (2010). Phenylpropanoid biosynthesis. *Molecular Plant.* 3(1):2-10.

274. Vousden, K.H., (2002) Activation of the p53 tumour suppressor protein. *Biochimica et Biophysica Acta.* 1602:47–59.

275. Wang H-F., Feng L., Niu D-K., (2007). Relationship between mRNA stability and introns presence. *Biochemical and Biophysical Research Communications.* 1(2):203-308.

276. Wang H., Ngwenyama N., Liu Y., Walker J.C., Zhang S., (2007). Stomatal development and patterning are regulated by environmentally responsive mitogen-activated protein kinases in *Arabidopsis*. *Plant Cell.* 19:63–73.

277. Wang H. and Wang H., (2015). Phytochrome signalling: time to tighten up the loose ends. *Molecular Plant.* 8:540-551.

278. Wang L., Wu L.M., Greaves I.K., Zhu A., Dennis E.S., Peacock W.J., (2017). PIF4-controlled auxin pathway contributes to hybrid vigor in *Arabidopsis thaliana. Proceedings of the National Academy of Science.* 114(17): e3555-e3562. doi: https://doi.org/10.1073/pnas. 1703179114

279. Wang, P., Xue, L., Batelli, G., Lee, S., Hou, Y.-J., Van Oosten, M. J., Zhang H., Tao W.A., Zhu J.K., (2013). Quantitative phosphoproteomics identifies SnRK2 protein kinase substrates and reveals the effectors of abscisic acid action. *Proceedings of the National Academy Science U.S.A.* 110(27):11205–11210.

280. Wang Y-H., Garvin D.F., Kochian L.V., (2002). Rapid induction of regulatory and transporter genes in response to phosphorus, potassium, and iron deficiencies in tomato roots. Evidence for cross talk and root/rhizosphere-mediated signals. *Plant Physiology.* 130(3):1361-1370.

281. Wasson A.P., Pellerone F.I., and Mathesius U., (2006). Silencing the flavonoid pathway in *Medicago truncutula* inhibits root nodule formation and prevents auxin transport regulation by Rhizobia. *Plant Cell.* 18:1617-1629.

282. Whitmarsh A.J., and Davis R.J., (2000). Regulation of transcription factor function by phosphorylation. *Cell and Molecular Life Sciences*. 57:1172–1183.

283. Winkel-Shirley B., (2001). Flavonoid biosynthesis, a colourful model for genetics, biochemistry, cell biology and biotechnology. *Plant Physiology.* 126:485-493.

284. Winter D., Vinegar B., Nahal H., Ammar R., Wilson G.V., Provart N.J., (2007). An "Electronic Fluorescent Pictograph" browser for exploring and analyzing large-scale biological data sets. *PLOS One.* 2(8): e718. doi: 10.1371/journal.pone.0000718

285. Xing Y., Jia W.S., Zhang J.H., (2007). AtMEK1 mediates stress-induced gene expression of CAT1 catalase by triggering H_2O_2 production in *Arabidopsis. Journal of Experimental Botany.* 58:2969-2981.

286. Xing Y., Jia W., Zhang J., (2008). AtMKK1 mediates ABA-induced CAT1 expression and H_2O_2 production via AtMPK6-coupled signalling in *Arabidopsis*. *Plant Journal.* 54:440–51.

287. Xing Y., Cao Q., Zhang Q., Qin L., Jia W., Zhang J., (2013). MKK5 regulates high light-induced gene expression of Cu/Zn superoxide dismutase 1 and 2 in *Arabidopsis. Plant Cell Physiology.* 54:1217-1227.

288. Xu W., Dubos C., Lepiniec L., (2015). Transcriptional control of flavonoid biosynthesis by MYB-bHLH-WDR complexes. *Trends in Plant Science.* 20(3):176-185.

289. Yin, R., Han, K., Heller, W., Albert, A., Dobrev, P.I., Zazímalová, E., Schäffner, A.R., (2014) Kaempferol 3-O-rhamnoside-7-O-rhamnoside is an endogenous flavonol inhibitor of polar auxin transport in *Arabidopsis* shoots. *New Phytologist.* 201:466–475.

290. Yonekura-Sakakibara T., Tohge T., Niida R., Saito K., (2007). Identification of a flavonol 7-O-rhamnosyltransferase gene determining flavonoid pattern in *Arabidopsis* by transcriptome coexpression analysis and reverse genetics. *Journal of Biological Chemistry.* 282:14932-14941.

291. Yonekura-Sakakibara T., Tohge T., Matsuda F., Nakabayashi R., Takayama H., Niida R., Watanabe-Takahashi A., Inoue E., Saito K., (2008). Comprehensive profiling and transcription coexpression analysis leading to decoding gene-metabolite correlations in *Arabidopsis. Plant Cell.* 20:2160-2176.

292. Yonekura-Sakakibara K., Fukushima A., Nakabayashi R., Hanada K., Matsuda F., Sugawara S., Inoue E., Kuromori T., Ito T., Shinozaki K., Wangwattana B., Yamazaki M., Saito K., (2012). Two glycosyltransferases involved in anthocyanin modification delineated by transcriptome independent component analysis in *Arabidopsis thaliana. The Plant Journal.* 69:154-167.

293. Yoo S-D., Cho Y., Sheen J., (2009). Emerging connections in the ethylene signalling network. *Trends in Plant Science.* 14(5):270-279.

294. Yu Y., Wang J., Zhang Z., Quan R., Zhang H., Deng X.W., Ma L., Huang R., (2013). Ethylene promotes hypocotyl growth and HY5 degradation by enhancing the movement of COP1 into the nucleus in the light. *PLOS One Genetics.* 9(12):1-13.

295. Yu X., Liu H., Klejnot J., Lin C., (2010). The Cryptochrome blue light receptors. *The Arabidopsis Book.* e0135:1-27

296. Zeng Q., Chen J-G., Ellis B.E., (2011). AtMPK4 is required for male-specific meiotic cytokinesis in *Arabidopsis*. *The Plant Journal*. 67:895-906.

297. Zeng Q., Sritubtim S., Ellis B.E., (2011). AtMKK6 and AtMPK13 are required for lateral root formation in *Arabidopsis. Plant Signaling &Behavior.* 6(10):1436-1439.

298. Zhang J., Subramanian S., Stacey G., and Yu O., (2009). Flavones and flavonols play distinct critical roles during nodulation of *Medicago truncatula* by *Sinorhizobium meliloti. Plant Journal.* 57:171-183.

299. Zhao Q., Nakashima J., Chen F., Yin Y., Fu C., Yun J., Shao H., Wang X., Wang Z-Y., Dixon R.A., (2013). LACCASE is necessary and non redundant with PEROXIDASE for lignin polymerization during vascular development in *Arabidopsis. The Plant Cell.* 25:3976-3987.

300. Zhu L., Bu Q., Xu X., Paik I., Huang X., Hoecker U., Deng X W., Huq E., (2015). CUL4 forms an E3 ligase with COP1 and SPA to promote light-induced degradation of PIF1. *Nature Communications.* 6(7245). doi: 10.1038/ncomms824

301. Zimmermann M.I., Heim M.A., Weisshaar B., Uhrig J.F., (2004). Comprehensive identification of *Arabidopsis thaliana* MYB transcription factors interacting with R/B-like bHLH proteins. *The Plant Journal.* 40:22-34.

302. Zhong R. and Ye Z-H., (2009). Secondary Cell Walls. *Encyclopedia of Life Sciences*. John Wiley & Sons, Ltd. doi: https://doi.org/10.1002/9780470015902.a0021256

APPENDIX

Fig. S2.1

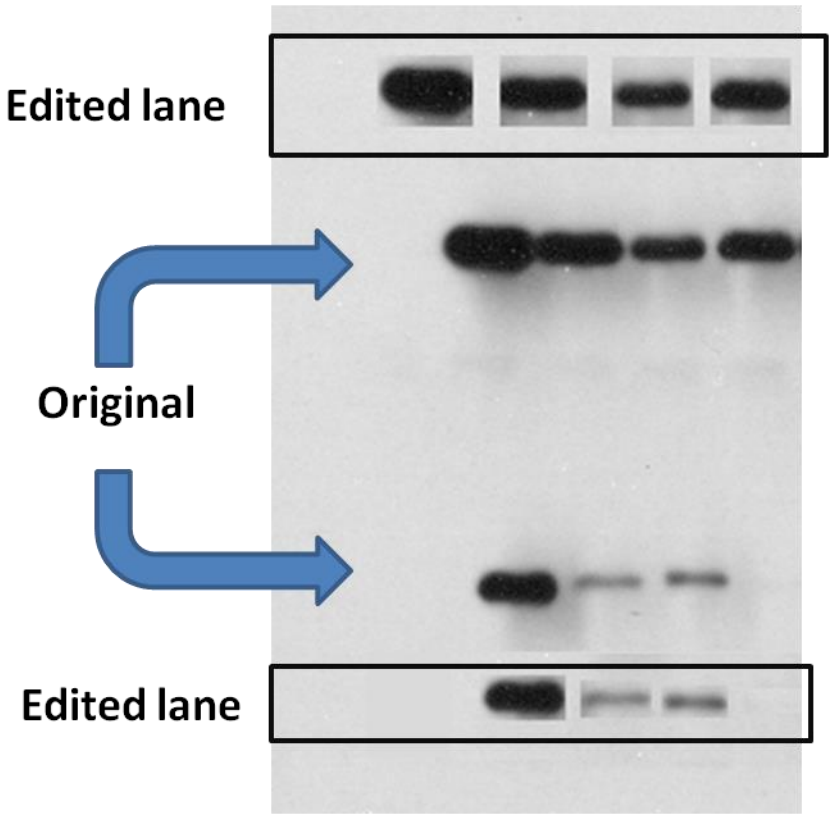

Fig S2.1 Manipulation of western blot images used for quantification of recombinant MYB75 protein by ImageJ in Fig 2.6. SDS PAGE and Western blot analysis was conducted to monitor degradation of recombinant MYB75 protein in *DEXpr:MYB75 gene Arabidopsis* seedlings. The chemiluminescent signal detecting recombinant of MYB75 was captured on photosensitive film and the original image displayed in Fig 2.6 as well as above. Due to signal bleed through between individual lanes, the original image was edited to facilitate ImageJ analysis, as depicted above.

Fig. S2.2

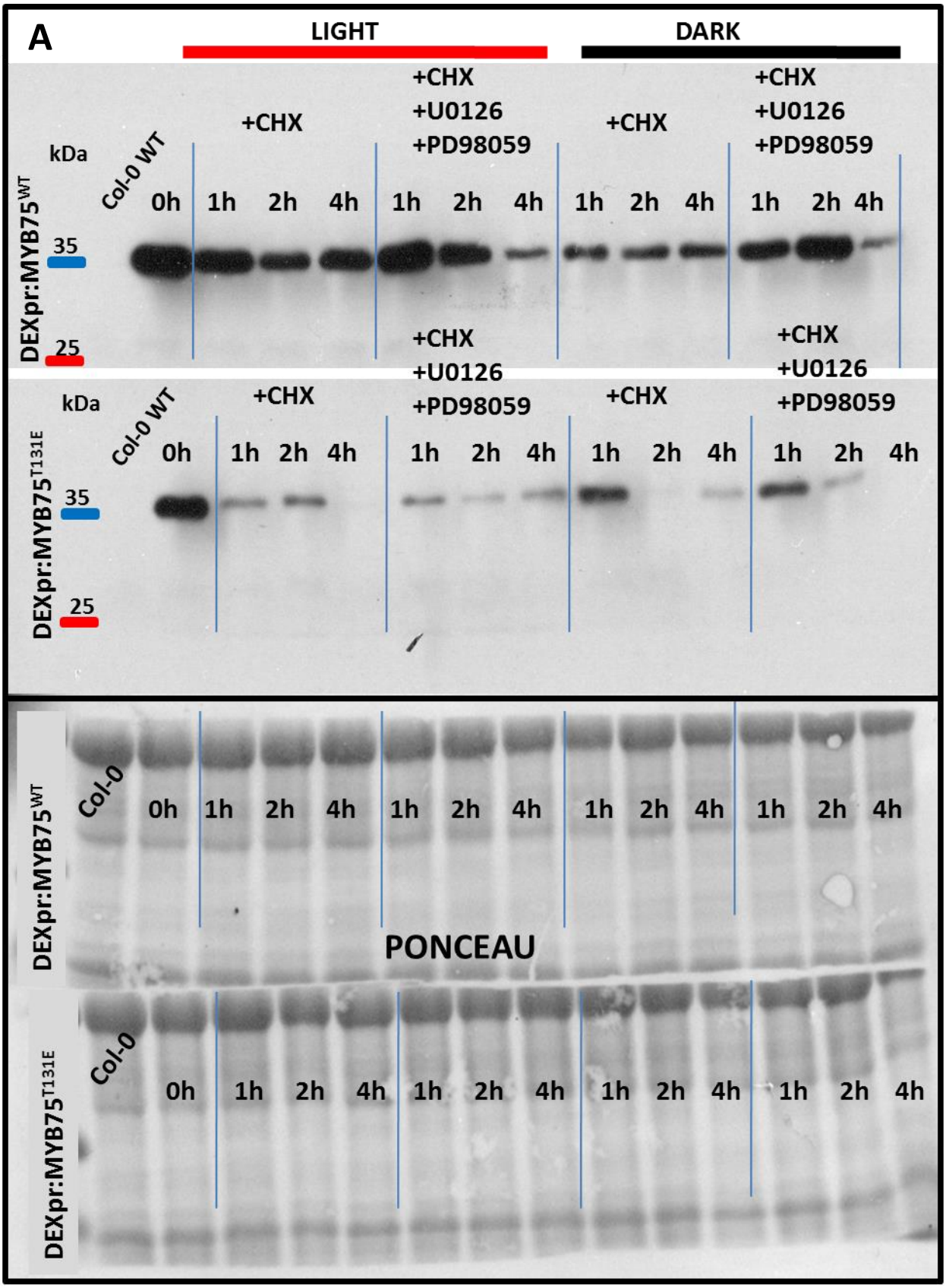
A
LIGHT
DARK
+CHX
+CHX +U0126 +PD98059
kDa
Col-0 WT
0h 1h 2h 4h 1h 2h 4h 1h 2h 4h 1h 2h 4h
DEXpr:MYB75WT
35
25
DEXpr:MYB75T131E
Col-0
PONCEAU

Fig. S2.2 continued

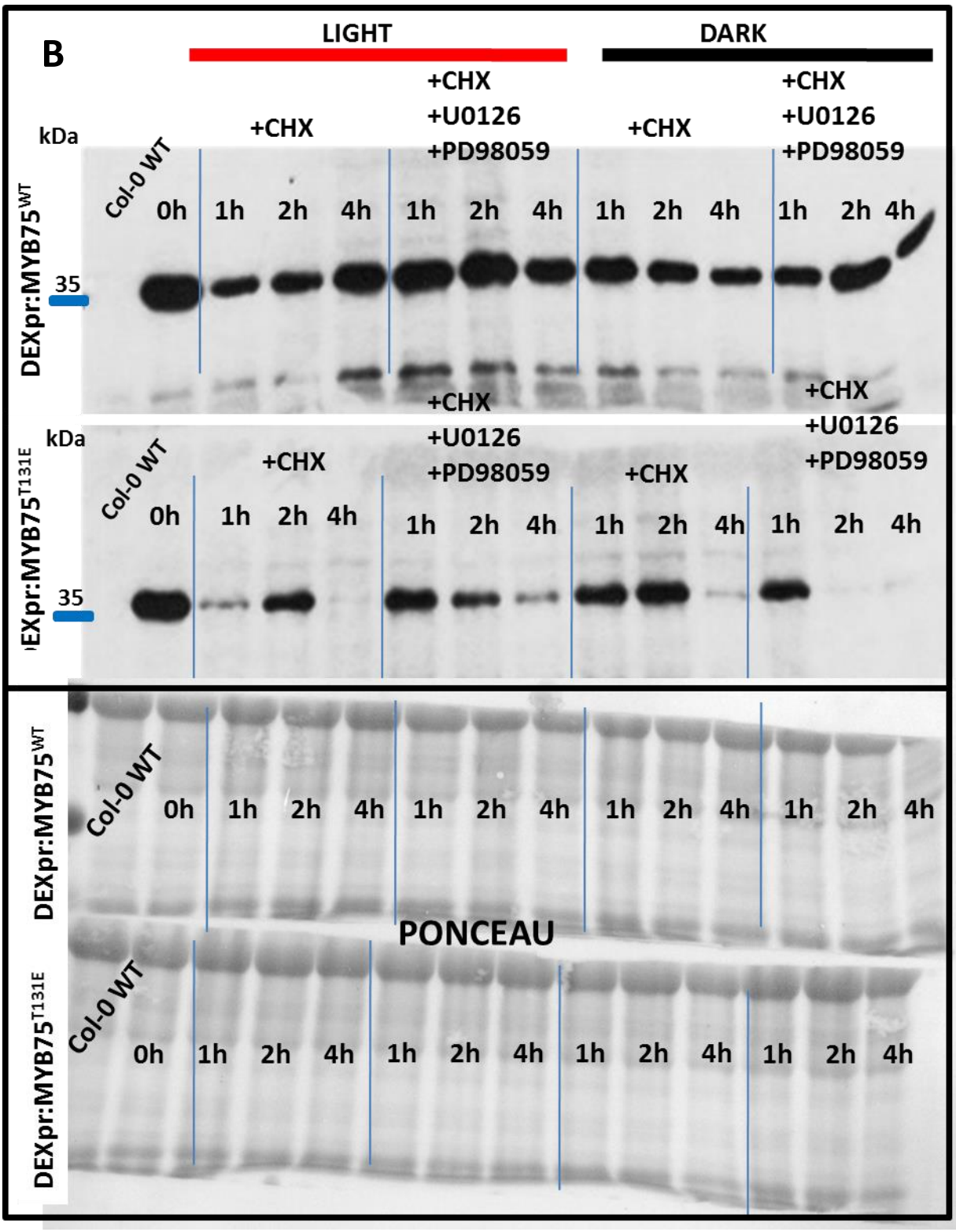

Fig S2.2 Degradation of MYB75^{WT} and MYB75^{T131E} in *Arabidopsis* seedlings: additional results. The western blots above were performed as described in Fig 2.6. Results from Fig 2.6 are displayed here (A; first five lanes) along with additional samples. Ten days after germination, hygromycin-resistant seedlings were transferred to 24 well plates, containing liquid ½MS medium, with ~20-40 seedlings per well. Recombinant MYB75 protein expression was induced by addition of 30µM DEX, with overnight incubation under continuous light, in the presence of 50µM MG132 proteasome inhibitor, to prevent protein degradation. The following day, the DEX/MG132-containing medium was removed and replaced with liquid ½MS containing 1mM CHX with or without phosphorylation inhibitors, 10µM U0126 and 100µM PD98059. The seedlings were subsequently incubated in the light or in the dark, and isolated at different time points, weighed and frozen in liquid nitrogen for subsequent western blot analysis. These results consistently show that MYB75^{T131E} is degraded more rapidly under all treatments than MYB75^{WT}. Phosphorylation inhibitors, 10µM U0126 and 100µM PD98059 appear to have a mild positive effect on the abundance of MYB75^{WT} protein, in the light and in the dark, particularly at earlier time points (1h and 2 h).